FLUX TRANSFER EVENTS: SIGNATURES OF IMPULSIVE RECONNECTION AT THE EARTH'S DAYSIDE MAGNETOPAUSE

by

Richard Philip Rijnbeek

Thesis submitted for the degree of Doctor of Philosophy
of the University of London and for the Diploma
of Membership of Imperial College

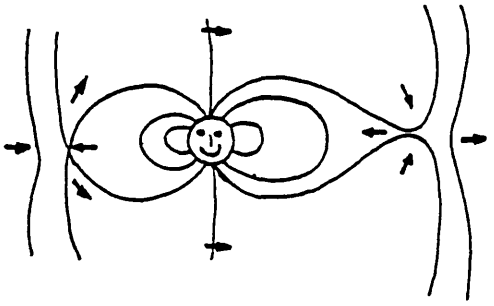
November 1984

Physics Department
Imperial College of Science and Technology
London SW7 2BZ

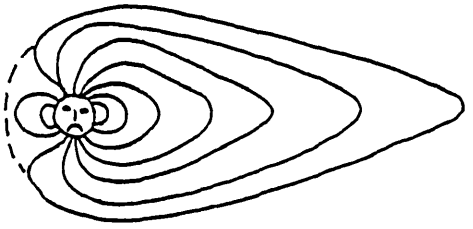
ABSTRACT

A selection of observations (both indirect and in situ) are reviewed which provide strong support for the occurrence and importance of steady (over a time scale of $\gtrsim$ 10 min) reconnection at the Earth's dayside magnetopause, in the manner originally suggested by Dungey (1961). We then consider data from the ISEE 1 and 2 satellites which reveal the occurrence of characteristic signatures at the Earth's magnetopause, called flux transfer events (FTEs), and show how they may be successfully interpreted in terms of an impulsive form of reconnection, with a duration and spatial scale of $\sim$ 2 min and $\sim$ 6400 km, respectively. We show that the FTE phenomenon forms a key element in the solar wind-magnetosphere interaction process whenever the magnetic field external to the magnetopause has a southward component. We also show that FTEs are closely related to the more steady type of reconnection and that high-latitude dayside phenomena previously found in the HEOS 2 data and described as flux erosion events are the same as FTEs. Finally, we look at some questions concerning the process of interaction between the solar wind and the magnetosphere which still remain outstanding.

Much ado about nothing . (William Shakespeare).



FTEs reach parts other flux tubes can't reach.



No FTE,
no comment.

CONTENTS

		Page
TITLE PAGE		1
ABSTRACT		3
ACKNOWLEDGEMENTS		9
LIST OF SYMBOLS AND ABBREVIATIONS		10
LIST OF TABLES		13
LIST OF FIGURES		14
CHAPTER 1	THE RECONNECTION MODEL OF THE MAGNETOSPHERE	19
1.1	Introduction	19
1.2	The solar wind and the magnetosphere	19
1.2.1	The solar wind	19
1.2.2	The magnetosphere	21
1.2.3	Plasma regimes in the magnetosphere	24
1.3	Convection in the magnetosphere	25
1.3.1	Introduction (the frozen-in equation)	25
1.3.2	The reconnection model of the magnetosphere	26
1.3.3	Reconnection for arbitrary IMF	32
1.3.4	The closed model magnetosphere	38
1.4	Control of the magnetosphere by the IMF	39
CHAPTER 2	SOLAR WIND-MAGNETOSPHERE INTERACTION: IN-SITU OBSERVATIONS	49
2.1	Introduction	49
2.2	The boundary layer	50
2.2.1	The magnetotail region	50
2.2.2	The cusp region	53
2.2.3	The frontside magnetosphere	55
2.2.4	Electron observations	57
2.2.5	Boundary layer composition	60

CHAPTER 2 (continued) Page

2.2.6	Low-altitude signature of the boundary layer	61
2.2.7	Location of entry and source mechanisms	61
2.3	In-situ evidence for reconnection	63
2.3.1	The reconnection model	63
2.3.2	Magnetic structure of the magnetopause	65
2.3.3	Plasma flow and reconnection	74
2.3.4	Electric field at the magnetopause	75
2.3.5	Energetic particle signatures	77
CHAPTER 3	FLUX TRANSFER EVENTS	81
3.1	Introduction	81
3.2	Impulsive reconnection: expectations	81
3.2.1	Magnetosheath	81
3.2.2	Magnetosphere	84
3.3	Impulsive reconnection: observations	86
3.3.1	Magnetic field signatures	86
3.3.2	Energetic particle signatures	89
3.3.3	Plasma signatures	92
3.3.4	Modelling of FTE particle distributions	95
3.3.5	Reverse signature FTEs	96
3.3.6	FTEs observed simultaneously outside and inside the magnetopause	101
3.3.7	Re-cap	104
3.3.8	Field twisting inside FTEs	106
CHAPTER 4	FLUX TRANSFER EVENTS: A SURVEY	115
4.1	Introduction	115
4.2	Magnetic field data conversion and display	115
4.3	Coverage, data analysis and results	117
4.3.1	Coverage and magnetosheath field orientation	117
4.3.2	Identification and classification of FTEs	120
4.3.3	Examples of FTE magnetic signatures	122
4.3.4	Location of FTEs	125
4.3.5	Magnetosheath magnetic field and FTEs	125
4.3.6	Coordinate system and FTEs	131
4.3.7	When do FTEs occur?	135

CHAPTER 4 (continued)		Page
4.3.8	Solar wind parameters and FTEs	141
4.3.9	Occurrence rate of FTEs	145
4.3.10	Scale size of FTEs	147
4.4	Discussion	149
4.4.1	FTE magnetic signatures	149
4.4.2	FTEs: reconnection phenomena?	151
4.4.3	Where are FTEs initiated?	152
4.4.4	Mixed FTE crossings	157
4.4.5	FTE flux removal rate	159
CHAPTER 5	FLUX TRANSFER EVENTS AND QUASI-STEADY RECONNECTION	165
5.1	Introduction	165
5.2	Reconnection events and FTEs	167
5.2.1	3 September 1978, outbound pass	168
5.2.2	25 September 1979, inbound pass	170
5.2.3	3 August 1978, outbound pass	172
5.2.4	Conclusion	175
5.3	Plasma properties of FTEs	176
5.3.1	Classification of FTE plasma signatures	176
5.3.2	B_L spikes	180
5.3.3	Discussion	181
CHAPTER 6	FLUX EROSION EVENTS	185
6.1	Introduction	185
6.2	Flux erosion events	185
6.2.1	Observations	185
6.2.2	Interpretation	188
6.3	FTEs: other satellites, other planets	190
CHAPTER 7	QUESTIONS	191
7.1	Introduction	191
7.2	Solar wind-magnetosphere interaction: some remaining questions	191
7.2.1	The boundary layer revisited	191
7.2.2	Flux transfer events (again)	204
7.2.3	Quasi-steady reconnection	213

		Page
REFERENCES		221
APPENDIX A	SATELLITE MISSIONS	237
A.1	The HEOS 2 satellite	237
A.2	The ISEE mission	237
A.3	The GEOS 2 satellite	239
A.4	The AMPTE mission	239
A.5	The ISTP programme	241
APPENDIX B	COORDINATE SYSTEMS	243
B.1	Geocentric Solar Magnetospheric (GSM) coordinates	243
B.2	Geocentric Solar Ecliptic (GSE) coordinates	243
B.3	Solar Magnetic (SM) coordinates	243
B.4	Boundary Normal (LMN) coordinates	245
B.5	Determination of the boundary normal, $\hat{\underline{N}}$	245
APPENDIX C	LIST OF MAGNETOPAUSE CROSSINGS	253

ACKNOWLEDGEMENTS

My thanks are due to the following people:

- Dr. David Southwood, my supervisor, for reading the first draft of this thesis and making many helpful and valuable comments;
- him and Dr. Stan Cowley for introducing me to magnetospheric physics (in particular my research topic) and for advice, guidance, inspiration, discussions and sharing of thoughts which are hopefully reflected in this work;
- all members, past and present, of the Space Physics Group (ex Cosmic Rays and Space Physics) and everyone else who made my period of research so enjoyable;
- Dr. Mark Saunders for many discussions and general help with the work;
- Professor Chris Russell (UCLA) for generously supplying the ISEE 1 and 2 magnetometer data;
- him and Dr. Jean Berchem for discussions which particularly helped to formulate the material in Chapter 4;
- Dr. Götz Paschmann and Dr. Norbert Sckopke (Max Planck Institute, Munich) for providing ISEE plasma data;
- Professor Peter Hedgecock and Mrs. Anne Evans for supplying HEOS 2 magnetometer data;
- Mrs. Diana Beydoun for the excellent job she did in typing this thesis;
- the Science and Engineering Research Council for funding my research;
- and finally my parents who made it all possible and to whom I dedicate this thesis.

LIST OF SYMBOLS AND ABBREVIATIONS

AU	Astronomical unit
$\underline{B}$	Magnetic field
BL	Boundary layer
COSPAR	Committee on Space Research
$\underline{E}$	Electric field
E	Evening, east
EL	Entry layer
ESA	European Space Agency
ESRO	European Space Research Organisation = ESA
FAC	Field-aligned current
FEE	Flux erosion event
FTE	Flux transfer event
GRL	Geophysical Research Letters
GSE	Geocentric Solar Ecliptic
GSM	Geocentric Solar Magnetospheric
$\underline{I}$	Current
IMF	Interplanetary magnetic field
IMS	International Magnetospheric Study (1976-1979)
ISTP	International Solar-Terrestrial Physics programme
L_N	Scale size perpendicular to the magnetopause
LAT	Latitude
LLBL	Low-latitude boundary layer
LMN	Boundary normal components
LT	Local time
M	Morning, west
MHD	Magnetohydrodynamics
MP	Magnetopause
ms	Magnetosheath
msph	Magnetosphere
MV	Minimum variance
N	North
NASA	National Aeronautics and Space Administration

N_E	Electron density
N_{FTE}	Number of FTEs observed on a pass
N_p	Plasma density
N_{SW}	Solar wind density
P	Plasma pressure
$P_{\shortparallel}, P_{\perp}$	Pressure along and perpendicular to $\underline{B}$
PC	Polar cusp
PCR	Polar cap region
PM	Plasma mantle
R	Radial distance
RC	Ring current
R_E	Earth radius ($\sim$ 6400 km)
S	South
S_1, S_2	Outer and inner separatrix
SD	Standard deviation
SM	Solar magnetic
SP	Stagnation point
sw	Solar wind
$T_{\shortparallel}, T_{\perp}$	Temperature along and perpendicular to $\underline{B}$
TB	Trapping boundary
TD	Tangential discontinuity
T_E	Electron temperature
T_p	Plasma temperature
T_R	FTE recurrence time
UCLA	University of California at Los Angeles
UT	Universal time (Hours:minutes)
$\underline{V}$	Velocity
V_{ISEE}	Satellite velocity
V_p	Plasma bulk speed
V_{sw}	Solar wind velocity

AMPTE, CCE, CLUSTER, DE, GEOS, HEOS, IMP, IRM, ISEE, ISIS, OGO, PIONEER, PROGNOZ, SCATHA, TRIAD, UKS, VELA: all names of satellites or satellite missions.

EISCAT, STARE: radar systems

α	Alpha-particles, pressure anisotropy correction

ϕ_p	Azimuth angle of plasma flow
ϕ_{pc}	Cross-polar cap potential
λ_p	Latitude angle of plasma flow
ρ	Density

TABLES

		Page
1.1	Solar Wind Properties	20
1.2	Dayside Magnetosheath Parameters	22
2.1	Minimum Variance Analysis of Magnetopause Crossings	67
4.1	Magnetosheath Field Orientation	118
4.2	Magnetosheath Field Orientation for Crossings with FTEs	128
4.3	Magnetosheath Field Orientation for Magnetosheath FTEs	139
4.4	Magnetosheath Field Orientation for Magnetosphere FTEs	141
4.5	Spatial Distribution of FTEs	146
5.1	Characteristics of Reconnection Passes	166
5.2	Magnetosheath FTE Plasma Signature	178
5.3	Magnetosphere FTE Plasma Signature	178
7.1	Solar Wind-Magnetosphere Interaction: Some Questions	192
B.1	Analysis of 11 August 1979 Magnetopause Crossing	249

FIGURES

		Page
1.1	The solar wind and the IMF (in the equatorial plane)	21
1.2	Plasma regions of the magnetosphere (noon-midnight cross-section)	23
1.3	Reconnection for southward IMF (after Dungey, 1961)	27
1.4	Polar cap convection pattern for southward IMF	29
1.5	Equipotentials ($\underline{E} \times \underline{B}$ flow lines in the equatorial plane	31
1.6	Charged particle populations in the magnetosphere	31
1.7(a)	Reconnection for IMF $B_y > 0$	34
1.7(b)	Reconnection for IMF $B_y < 0$	35
1.8(a)	Reconnection for northward IMF (Dungey, 1963)	36
1.8(b)	Reconnection for northward IMF (Russell, 1972)	36
1.8(c)	Convection pattern for northward IMF	37
1.9	Crooker's (1979) antiparallel reconnection model	37
1.10	Open and closed (hatched) flux tube transport (Cowley, 1982)	39
1.11	TRIAD observations of FACs (Potemra, 1978)	41
1.12	Cusp FACs: response to IMF B_y (Potemra, 1978)	42
1.13	FACs and magnetic field perturbations measured by ISIS 2 (McDiarmid et al., 1978)	43
1.14	Location of polar cusp: response to IMF B_z (Burch, 1972)	46
2.1	Locations of reported boundary layer observations prior to 1978 (Sckopke and Paschmann, 1978)	51
2.2	HEOS 2 pass through the plasma mantle (Rosenbauer et al., 1975)	52
2.3	The polar cusp region (after Sckopke, 1979)	53
2.4	HEOS 2 pass through the entry layer (Paschmann et al., 1976)	54
2.5	HEOS 2 passes through the low-latitude boundary layer (Haerendel et al., 1978)	56
2.6	The boundary layer observed by IMP 6 (Eastman and Hones, 1979)	58

		Page
2.7	ISEE 1 observations of boundary layer pulses (Sckopke et al., 1981)	58
2.8	Dayside reconnection configuration (Sonnerup et al., 1981)	64
2.9	Hodograms for a crossing on 22 November 1979	68
2.10	- ditto -	69
2.11	- ditto -	70
2.12	Hodograms for a crossing on 3 September 1970	71
2.13	- ditto -	72
3.1	Magnetosheath FTE	82
3.2	Particle streaming inside FTEs (from Speiser and Williams, 1982)	84
3.3	Magnetosphere FTE	85
3.4	Boundary normal coordinates	86
3.5	FTEs on 8 November 1977	87
3.6	FTEs on 10 November 1977	89
3.7	Energetic particle data for FTEs (Scholer et al., 1982)	90
3.8	FTE energetic proton distributions (Scholer et al., 1982)	90
3.9	Particle streaming inside FTEs (Daly and Keppler, 1982)	93
3.10	FTE energetic proton distributions (Daly and Keppler, 1982)	93
3.11	Plasma and field data for 8 November 1977 (Paschmann et al., 1982)	94
3.12	Plasma and field data for 10 November 1977, (Paschmann et al., 1982)	94
3.13	Mapping of particle distributions into the magneto-sheath (Speiser et al., 1981)	96
3.14	Reverse FTEs on 9 August 1978	97,98
3.15	Particle streaming for a reverse FTE on 9 August 1978	101
3.16	FTEs on 23 October 1978	103
3.17	FTEs on 9 November 1979	103
3.18	Schematic for FTE encounters on 9 November 1979	105
3.19	Field twist (FAC) inside FTEs (after Saunders, 1983)	107
3.20	FTEs on 23 October 1978	109
3.21	FTEs on 24 October 1979	109
3.22	FTEs on 6 July 1979	110
3.23	Pairs of FACs associated with FTEs (after Southwood, 1984)	112

		Page
4.1	Magnetopause crossing locations and the sign of magnetosheath B_L/B_M	117
4.2	FTEs on 23 January 1978	123
4.3	FTEs on 23 September 1979	123
4.4	FTEs on 24 July 1979	124
4.5	FTEs on 4 July 1978	124
4.6	Magnetopause crossings with magnetosheath/ magnetosphere FTEs and the FTE signature in B_N	126
4.7	Locations of magnetopause crossings with magnetosheath/magnetosphere FTEs and the sign of magnetosheath B_L	127
4.8	Magnetopause crossings with magnetosheath FTEs and the FTE signature in B_N for negative/positive magnetosheath B_M	129
4.9	Magnetopause crossings with magnetosphere FTEs and the FTE signature in B_N for negative/positive magnetosheath B_M	130
4.10	Magnetopause crossings with magnetosheath FTEs in GSE coordinates	132
4.11	Magnetopause crossings with magnetosheath FTEs in SM coordinates	133
4.12	Magnetopause crossings with/without magnetosheath flux transfer events	137
4.13	FTEs on 21 August 1978	138
4.14	FTEs on 30 September 1979	138
4.15	Magnetopause crossings with/without magnetosphere flux transfer events	140
4.16	Occurrence of magnetosheath FTEs vs. orientation of the IMF	143
4.17	Occurrence of magnetosphere FTEs vs. orientation of the IMF	143
4.18	Occurrence of magnetosheath FTEs vs. solar wind velocity	144
4.19	Occurrence of magnetosheath FTEs vs. solar wind density	144
4.20	Estimating the scale size of an FTE	148
4.21	Satellite trajectories relative to an FTE flux tube	148
4.22	FTEs on 28 July 1978	153
4.23	Impulsive reconnection in the cusp regions	154
4.24	Energetic ion streaming inside magnetosheath FTEs (Daly et al., 1984)	156

		Page
4.25	FTEs on 30 October 1978	160
4.26	FTEs on 18 October 1979	161
4.27	FTE flux tubes propagating along the dayside magnetopause	162
5.1	Locations of 17 quasi-steady reconnection events (after Paschmann, 1984)	167
5.2	Quasi-steady reconnection on 3 September 1978	169
5.3	Quasi-steady reconnection on 25 September 1979	171
5.4	Quasi-steady reconnection on 3 August 1978	173
5.5	Possible interpretation of a B_L spike	181
5.6	Possible schematic for reconnection	183
6.1	Flux erosion events on 1 December 1973	187
6.2	Flux erosion events on 10 October 1973	187
6.3	Two possible interpretations for Figure 6.2	189
7.1	Plasma and field data on 27 July 1978	194
7.2	Plasma and field data on 10 January 1978	197
7.3	Plasma and field data on 17 January 1978	199
7.4	Plasma and field data on 26 July 1978	200
7.5	Magnetic field data on 30 October 1979	202
7.6	HEOS 2 field data on 1 October 1972	207
7.7	HEOS 2 field data on 1/2 November 1972	207
7.8	Possible interpretation for Figure 7.7	208
7.9	FTE and pulsations on 31 July 1978	210
7.10	Dayside Northern Hemisphere high-latitude flows for (a) steady reconnection, and (b) impulsive, FTE-like reconnection for positive IMF B_y (Cowley, 1984)	212
7.11	Plasma and field data for 31 July 1978	215
A.1	The HEOS 2 and ISEE 1 and 2 orbits in relation to the magnetosphere	238
A.2	The orbit of GEOS 2	240
A.3	The AMPTE satellites in orbit	240
A.4	The ISTP programme in action	242
B.1	Magnetospheric Coordinate systems	244
B.2	Determination of the magnetopause normal	250

CHAPTER 1

THE RECONNECTION MODEL OF THE MAGNETOSPHERE

1.1 Introduction

This chapter is intended as an introduction to the magnetosphere, specifically the reconnection model, for the reader unfamiliar to the subject. Anyone with a background knowledge of magnetospheric physics can easily skip it. The first half of the chapter outlines the geography and plasma properties of the magnetosphere. Next, a rough description is given of the reconnection model of the magnetosphere in which the importance of convective flows is emphasized. Finally, a selection of observations are reviewed which show the control exerted by the solar wind magnetic field orientation on the magnetosphere, and hence provide indirect support for dayside reconnection.

1.2 The Solar Wind and the Magnetosphere

1.2.1 The solar wind

Two important consequences result from the Sun's high ($\sim 10^6$ °K) coronal temperatures. Firstly, the coronal gas is completely ionised and thus forms a plasma. Secondly, the corona expands radially outward from the Sun to form a continuous stream of plasma, the solar wind. The solar wind fills interplanetary space with plasma of solar origin, streaming past the Earth's orbit at supersonic velocities, i.e., faster than sound or hydromagnetic waves. It thereby forms the connecting link between activity on the Sun and geophysical disturbances associated with the Earth's ionised atmosphere, such as auroras and geomagnetic storms.

Typical solar wind parameter values as measured by spacecraft near the Earth's orbit are shown in Table 1.1. The solar wind consists mainly of protons and electrons, with the most important minor constituent being doubly charged helium, He++. A weak magnetic field

has also been detected in the solar wind. This field is known as the IMF (Interplanetary Magnetic Field) and typically has a strength of $\sim$ 5 nT.

TABLE 1.1

Solar Wind Properties*

Parameter	Value
Proton density	$\sim 5\ cm^{-3}$ (3-10)
Bulk speed	$\sim 350\ km\ s^{-1}$ (200-700)
Kinetic energy flux	$\sim 2 \times 10^{-4}\ W\ m^{-2}$
Proton flux (E > 25 eV)	$\sim 3 \times 10^{8}\ cm^{-2}\ s^{-1}$ (2-7)
Proton temperature	$\sim 5 \times 10^{4}\ °K$
Electron temperature	$\sim 10^{5}\ °K$
Alfvén Mach number	~ 10
Sonic Mach number	~ 10
Mean Mass	$\sim 10^{-27}$ kg
Proton energy	$\sim$ ½ keV
Electron energy	$\sim$ ¼ keV
Magnetic field strength	$\sim$ 5 nT (1-10)
Constituents	H^+, e^-, α (H^+: $\alpha \sim 0.02$ (0.01-0.2))
Mean free path	$\sim$ 1 AU

*Bracketed quantities refer to typical range of variation.

The kinetic energy density in the solar wind is larger than both the thermal and IMF energy densities. As a result, plasma controls the movement in the solar wind and carries magnetic field lines radially outward from the outer layers of the Sun (see also Section 1.3.1). However, the feet of the field lines remain embedded in the Sun and rotate with it. The net result is that the IMF on average takes on the spiral form shown in Figure 1.1, and forms an angle of $\sim 45°$ with the Earth's orbit. Toward and away sectors refer to periods in which the IMF points toward and away from the Sun, respectively.

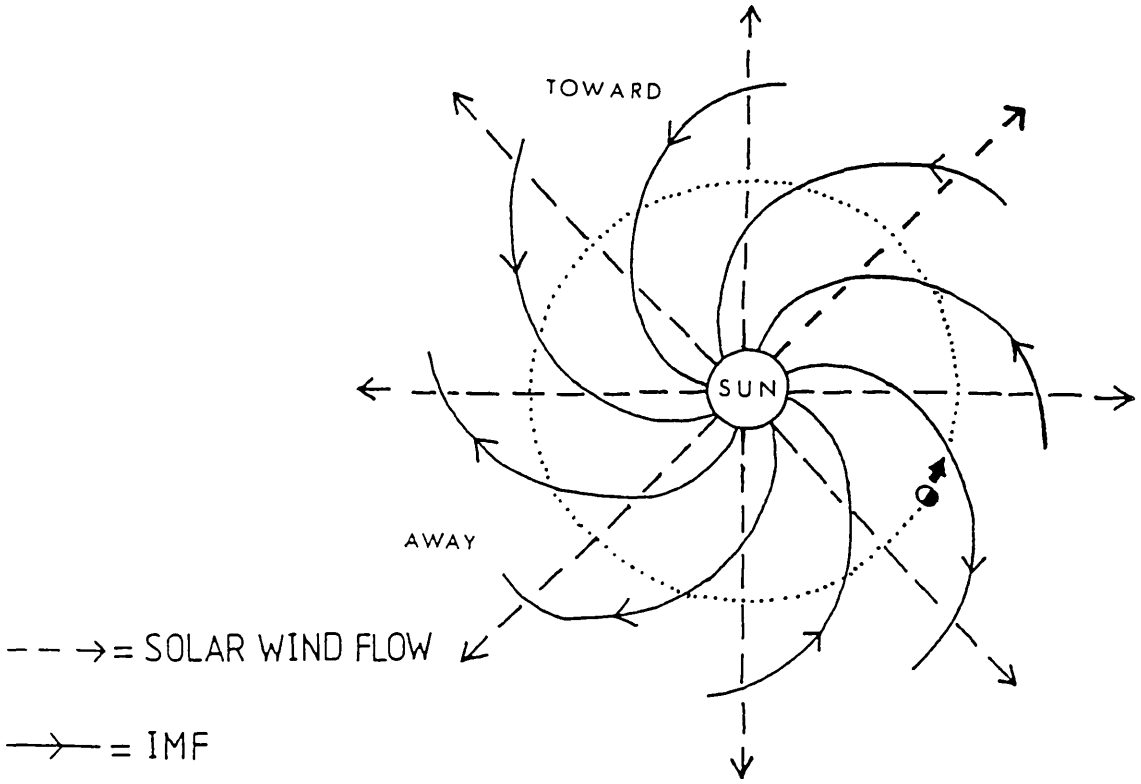


Figure 1.1. The solar wind and the IMF (in the equatorial plane).

1.2.2 The magnetosphere

The magnetosphere is the region in space surrounding the Earth in which the geomagnetic field plays the dominant role in the physical processes which determine the behaviour of plasmas. At its inner boundary it borders on the Earth's ionised upper atmosphere, the ionosphere. Contrary to the situation in the solar wind, the magnetic energy density in the magnetosphere exceeds the plasma energy density in most situations. This explains the dominant influence of the magnetic field. In a vacuum, the terrestrial magnetic field would extend out into infinity, decreasing in field strength in accordance with a dipole field formula. However, the solar wind compresses the geomagnetic field and confines it into a closed, comet-shaped cavity: the magnetosphere.

The magnetosphere presents itself as a blunt-nosed obstacle to the supersonic solar wind flowing past. This results in the formation of a (collisionless) shock wave in front of the magnetosphere, known as the bow shock. As the solar wind crosses the bow shock, it is deflected so as to flow around the magnetosphere. The region between

the bow shock and the magnetosphere is the magnetosheath. Table 1.2 gives some typical parameter values in the magnetosheath near the subsolar point (the nose of the magnetosphere). Comparison with Table 1.1 shows that although the magnetosheath plasma and magnetic field are of solar origin, their properties are distinct from those of the solar wind. Across the bow shock, the solar wind velocity is reduced and the bulk flow randomised so as to heat the plasma. However, further downstream the plasma speeds up to supersonic velocities again. Also, the magnetosheath magnetic field (i.e., the shocked IMF) is compressed and draped over the outer boundary of the magnetosphere, and hence increases in strength.

TABLE 1.2

Dayside Magnetosheath Parameters

Velocity	$\sim$ 150 km s^{-1}
Number density	$\sim$ 10 cm^{-3}
Temperature	$\sim$ 5 x 10^6 °K
Magnetic field strength	$\sim$ 30 nT

The outer boundary of the magnetosphere is called the magnetopause. It separates the external shocked solar wind plasma and IMF (the magnetosheath) from the internal magnetospheric plasma and magnetic field. In satellite data it can be identified from the change in plasma and/or magnetic field properties across it. The magnetopause forms an indentation in the polar cusp regions. The magnetospheric magnetic field lines emanating from the cusp cover the entire magnetopause surface. The cusp region also separates field lines at lower latitudes, which form closed loops across the Earth's dayside, from higher latitude field lines which are swept into the nightside by the external solar wind flow.

The high-latitude geomagnetic field lines which are swept back into the anti-solar direction form the magnetotail (or geomagnetic tail or tail). The outer boundary of the magnetotail is roughly cylindrical in shape, with a radius of $\sim$ 20 R_E. The magnetic field in the

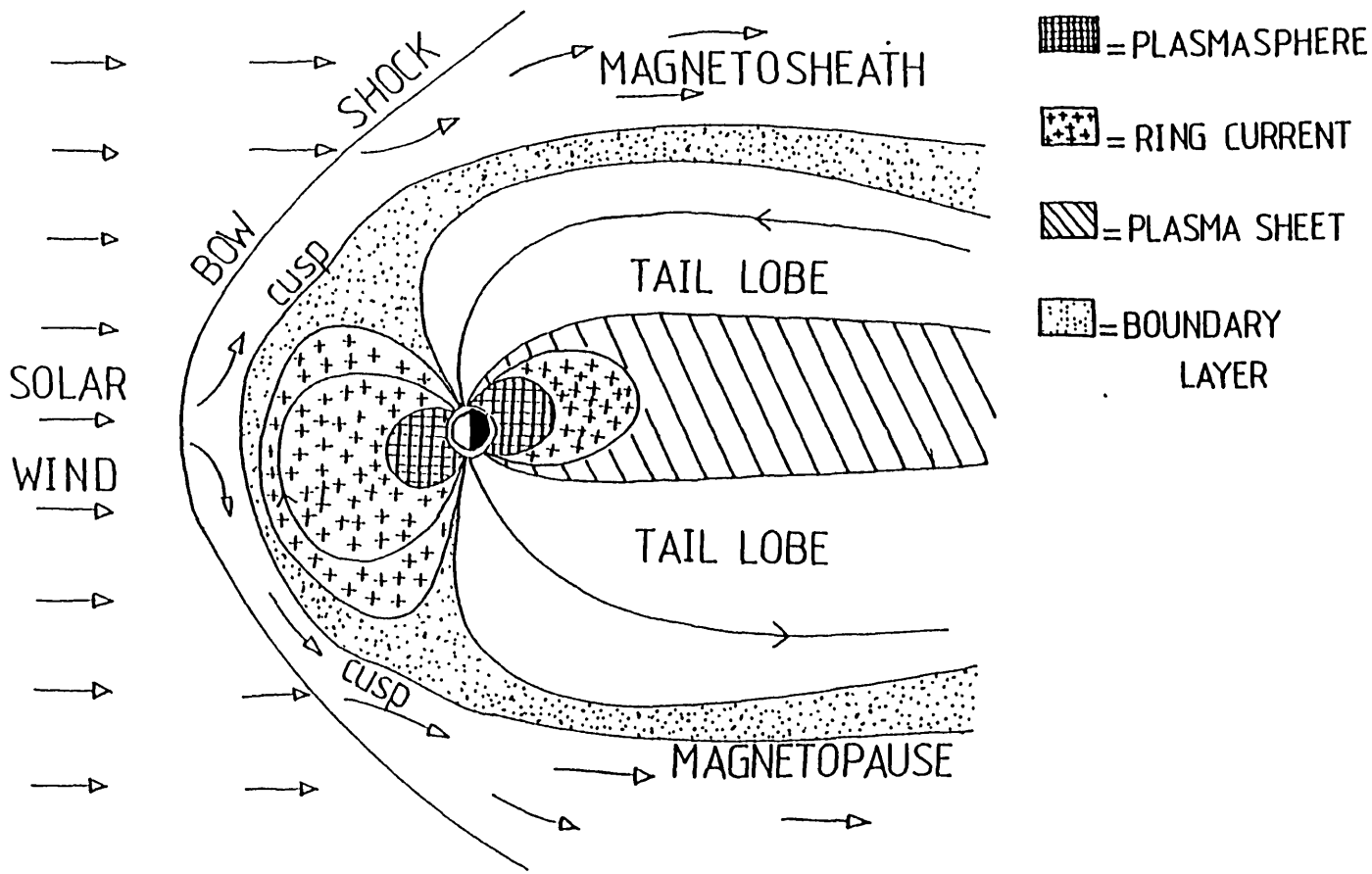


Figure 1.2. Plasma regions of the magnetosphere (noon-midnight cross-section).

northern half of the magnetotail points towards the Earth, while in the southern half it points away from the Earth. The neutral sheet in the centre separates these two regions of oppositely-directed field, and the field strength here may reach very low values (of order a nanotesla). At higher latitudes the field strength is typically $\sim$ 30 nT. The formation of the tail is discussed in section 1.3.2.

1.2.3 Plasma regimes in the magnetosphere

The plasma characteristics in the magnetosphere are not spatially (and to a lesser extent temporally) uniform and it is therefore convenient to identify various regions according to the different plasma populations present. These different regions are shown in Figure 1.2, and they are the plasmasphere, plasmasheet, tail lobes, ring current, radiation belts and the boundary layer.

The plasmasphere is a region of high density, low energy ($\sim$ eV) plasma located at the core of the magnetosphere. At its inner boundary it merges into the ionosphere while its outer boundary is the plasmapause, typically situated $\sim$ 5 R_E from the Earth in the equatorial plane. At the plasmapause, the density of the low energy plasma drops very sharply from $\sim 10^3$ cm^{-3} to $\sim$ 1 cm^{-3}. Bordering on the plasmapause on the nightside of the Earth is the plasmasheet, so named because it occupies the central part of the tail as a sheet-like region. It contains plasma with energies considerably higher ($\sim$ keV) than in the plasmasphere, although its density is much lower. At high latitudes the plasmasheet borders on a region with extremely low densities, known as the tail lobe. The ring current is located outside the plasmasphere, and at its tailward edge it merges into the plasmasheet. The ring current plasma is even hotter than the plasmasheet plasma. However, even the ring current particles may be considered low in energy compared to the radiation (Van Allen) belt populations. The radiation belts occupy the inner part of the magnetosphere, overlapping both the plasmasphere and ring current regions. The radiation belt particles are extremely energetic, reaching energies up to MeV in the inner zones. Finally, satellites have detected a layer of magnetosheath-like plasma inside the outer boundary of the magnetosphere. The properties of this layer are not spatially uniform over the whole of the magnetopause surface, but collectively we shall call this region the boundary layer (see Chapter 2).

1.3 Convection in the Magnetosphere

1.3.1 Introduction (the frozen-in equation)

Ultimately, the properties and behaviour of a plasma would have to be described in terms of the motions of all the individual particles subject to external forces as well as the interactions between the individual particles. However, to make the problem soluble in practice some simplifying assumptions and approximations are necessary. In much of plasma physics it is reasonable to discuss the behaviour of a plasma in terms of magnetohydrodynamics (MHD), which describes the plasma as a fluid. Such a treatment usually relies on the plasma being collision-dominated, so that the individual particles have short mean free paths. The solar wind and magnetospheric plasmas are, however, essentially collision-free and individual particles have exceedingly long mean free paths. Remarkably, MHD can still provide a useful first order approximation to describe their behaviour. The reason for their fluid-like behaviour is the presence of a magnetic field, which shortens the effective controlling distance to a scale length of order the gyroradius of the individual particles. Thus, MHD provides a reasonably valid description of a magnetized, collision-free plasma, provided the individual particle gyroradius and gyroperiod are short compared to the distance and time over which any macroscopic quantities (e.g., the magnetic field itself) change appreciably.

Another frequently-used approximation in the solar wind as well as in the magnetosphere is to neglect the electrical conductivity of the plasma. The assumption of infinite conductivity enables Ohm's law (for steady state conditions and in the absence of pressure gradients) to be expressed in the form:

$$\underline{E} + \underline{V} \times \underline{B} = 0 \qquad (1)$$

where $\underline{E}$, $\underline{V}$ and $\underline{B}$ are respectively the electric field, the plasma fluid velocity and the magnetic field. Equation (1) states that motion of a plasma is equivalent to an electric field, i.e., in the plasma frame of reference the large-scale electric field is zero. Combining this equation with one of Maxwell's equations ($\nabla \times \underline{E} = - \frac{\partial \underline{B}}{\partial t}$) results in the frozen-in equation:

$$\frac{\partial \underline{B}}{\partial t} = \nabla \times (\underline{V} \times \underline{B}) \qquad (2)$$

Equation (2) implies that the magnetic flux through a closed loop moving with the fluid (plasma) is constant (e.g., Cowling, 1976, Chapter 1). We are therefore justified in picturing the magnetic field and plasma as moving together as a fluid with a drift velocity given by:

$$\underline{V} = \frac{\underline{\underline{E}} \times \underline{\underline{B}}}{B^2} \tag{3}$$

This drift motion is often referred to as convection.

The moving-field-line picture provides an intuitive insight into many space physics problems. For example, as a consequence of its larger energy density the plasma in the solar wind controls the IMF, leading to the garden-hose effect as shown in Figure 1.1. In the magnetosphere the situation is reversed and hence the magnetic field has the dominant control. The frozen-in concept also allows a surprisingly accurate specification of the characteristic magnetopause shape (e.g., Spreiter and Alksne, 1969): to first order, the solar wind cannot penetrate the geomagnetic field because the solar wind plasma is frozen-out of the geomagnetic field, just as the IMF is frozen-in to the solar wind. Finally, convection of plasma and magnetic flux tubes provides a very convenient concept to describe the large-scale structure and dynamics of charged particle populations in the magnetosphere.

Before applying convection to the magnetosphere, however, two words of warning are in order. For particles of high energies ($\gtrsim$ 100 keV), the motions are dominated by the particles' natural drift velocities (e.g., the magnetic gradient and curvature drifts) and the convective motion acts only as a small perturbation. Also, in several regions of the magnetosphere the fluid approximation breaks down because the magnetic field changes over spatial scales of order or smaller than the particle gyroradii (e.g., the magnetopause and neutral sheet).

1.3.2 The reconnection model of the magnetosphere

In 1961, Axford and Hines (1961) and Dungey (1961) independently published papers proposing the existence and indicating the important consequences of solar wind-driven large-scale convective flows in the Earth's magnetosphere, in which plasma and magnetic flux tubes are

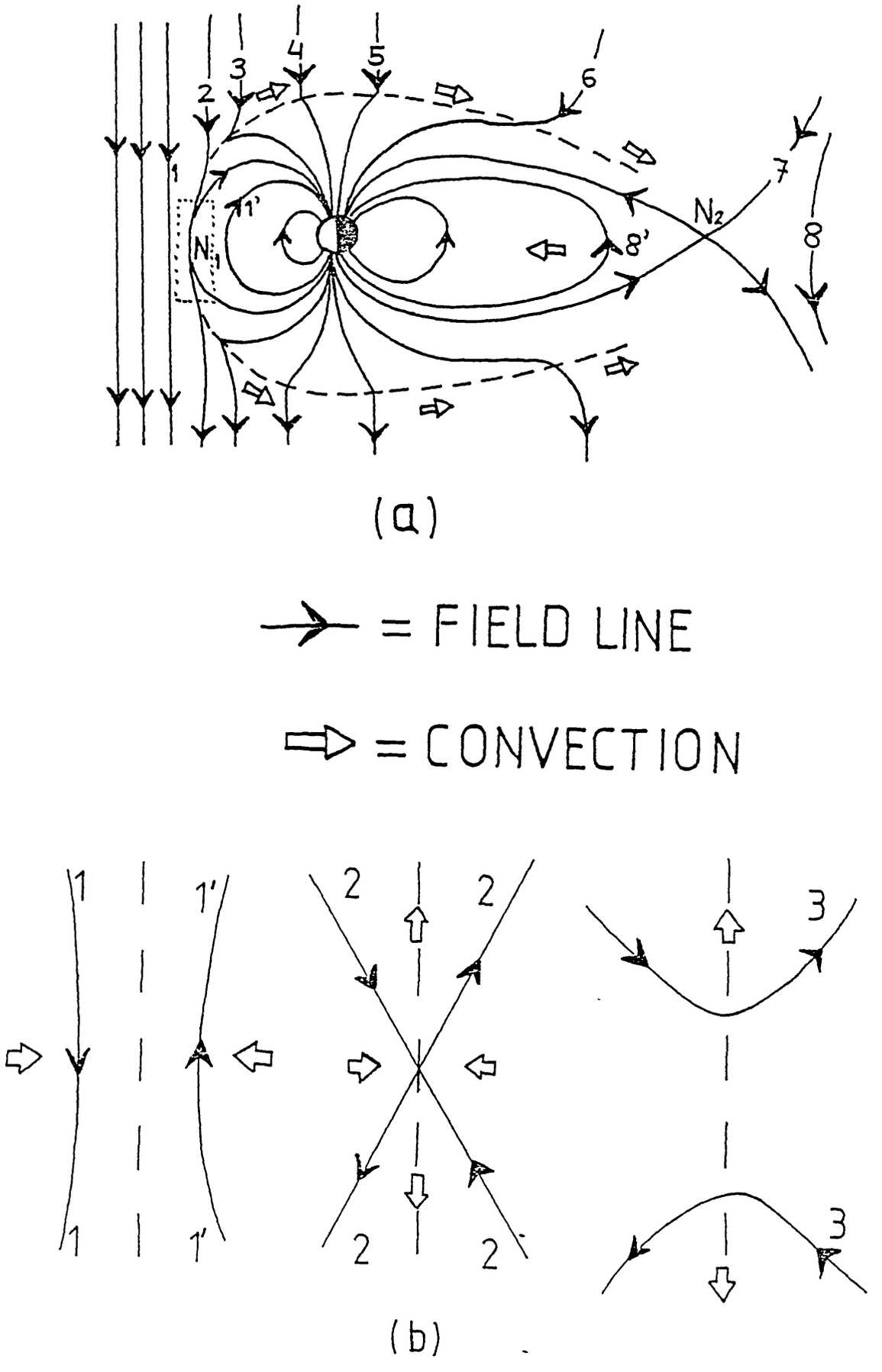


Figure 1.3. Reconnection for southward IMF (after Dungey, 1961).

transported from the dayside to the nightside along the outer parts of the magnetosphere and subsequently returned to the dayside in the inner part. Dungey (1961) proposed reconnection as the primary mechanism to achieve the coupling between the solar wind and the Earth's outer magnetosphere. The classic picture of reconnection is shown in Figure 1.3(a), in which a purely southward IMF reconnects with the oppositely-directed magnetospheric field at the subsolar point. A southward interplanetary field line (1) and a northward geomagnetic field line (1') are brought into contact at the nose of the magnetosphere (N_1). Here a break-down of the frozen-in equation within a finite but small volume (the diffusion region) allows the field lines to be broken and reconnected to each other across the boundary. This is shown in more detail in Figure 1.3(b). A pair of open field lines are formed (3), each of which has just one foot attached to the Earth. The field line attached to the Northern Hemisphere and the one attached to the Southern Hemisphere travel respectively northward and southward over the poles to reach the downstream magnetotail region (3-6). In the central tail region, the pair of open field lines reconnect again at N_2. After reconnection at N_2, the outer field line (8) escapes downstream into interplanetary space while the inner field line (8') moves back to the dayside magnetosphere, where the whole process is repeated.

Reconnection results in three regions of topologically different magnetic field lines, which are:

(a) interplanetary field lines (1,8);

(b) open field lines - field lines which are attached to the Earth at one end and extend into interplanetary space at the other end (2-7);

(c) closed field lines - field lines which are attached to the Earth at both ends (1',8').

The existence of open field lines is a necessary feature of the reconnection model of the magnetosphere and hence this model is often referred to as the open model.

A natural feature of the reconnection model is the existence of large-scale plasma circulation inside the magnetosphere, as shown in Figure 1.3 in the noon-midnight meridian plane. Plasma and embedded magnetic flux tubes are transported from the dayside and over the poles into the tail, where they convect inward and subsequently return to the

dayside at lower latitudes. Figure 1.4 shows the reconnection-driven convection cycle as viewed from above the North Pole and mapped onto the Earth's Northern Hemisphere. The dashed circular line shows the dividing line between open field lines at high latitudes and closed field lines at lower latitudes. This boundary is called the polar cap boundary and in the reconnection model also forms the dividing line across which the convective flow direction reverses from antisunward at high latitudes to sunward at low latitudes.

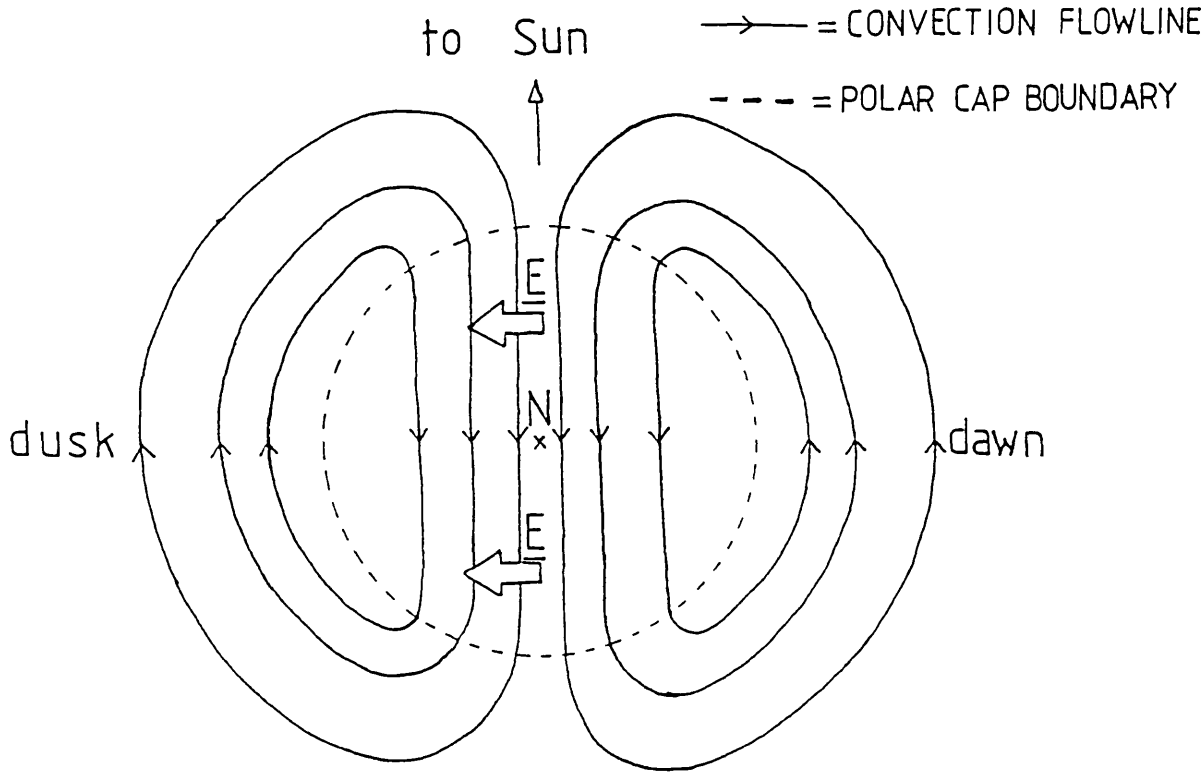


Figure 1.4. Polar cap convection pattern for southward IMF.

Figure 1.4 also shows the direction of the large-scale magnetospheric electric field across the polar cap which is associated with the polar cap convective flows. The source of the large-scale electric field is the solar wind. For a southward IMF, the electric field is in a dawn-dusk direction. The high electrical conductivity along the open field lines allows the electric field to penetrate right down to the ionosphere, where it maps to a dawn-dusk cross polar cap electric field, consistent with the antisunward plasma convection. For typical values of the solar wind velocity ($\sim$ 400 km/s) and IMF strength ($\sim$ 5 nT), the voltage across the width of the magnetosphere

($\sim$ 30 R_E) is $\sim$ 380 kV, which is more than ample to account for potential differences observed across the polar cap ($\sim$ 50-100 kV).

The geomagnetic tail is also a natural feature of the reconnection model. The outer portion of the open field lines lies outside the bow shock in the solar wind and moves much faster than the portion close to Earth. The portion of the field lines embedded in the ionosphere is pulled across the polar cap from its dayside to its nightside boundary at a slower velocity which is determined by the ionospheric conductivity. The open field lines are therefore bent back and stretched antisunward to form an elongated tail. Theoretical estimates (e.g., Dungey, 1965) place its closure at a downstream distance of $\sim$ 1000 R_E. Observational data (e.g., Fairfield, 1968) confirm that the tail can be detected at such large distances.

The formation of the plasmasphere also arises naturally from the reconnection model. As well as taking part in the solar wind induced convection, the magnetosphere also corotates with the Earth. The Earthward-pointing corotational electrical field associated with this motion dominates in the inner magnetosphere, while the dawn-dusk electric field dominates in the outer regions. Figure 1.5 shows in the equatorial plane the streamlines of magnetospheric plasma motion obtained by superimposing the motion due to the Earth's rotation onto the reconnection-driven circulation. On the dusk side there is a stagnation point and the streamline through this point separates two different regions of plasma flow. The inner region may be identified with the plasmasphere and the field lines in this region circulate round the Earth and never come into contact with the outer boundary of the magnetosphere. The field lines in the outer region all take part in the magnetospheric convection cycle and become open at some stage in their history, allowing the ionospheric plasma to escape.

The reconnection model also qualitatively explains many of the aspects of charged particle populations in the magnetosphere (see Cowley, 1980, for a detailed review). The two principal source regions for magnetospheric plasma are the magnetosheath (ex-solar wind) and the ionosphere. Magnetosheath plasma can enter the outer magnetosphere along open field lines (Figure 1.6). A magnetosheath particle entering on the dayside will travel down an open field line into the cusp region. Here it will mirror and convect antisunward along field lines which now extend deep into the magnetotail. The altitude of the mirroring point and its subsequent trajectory will

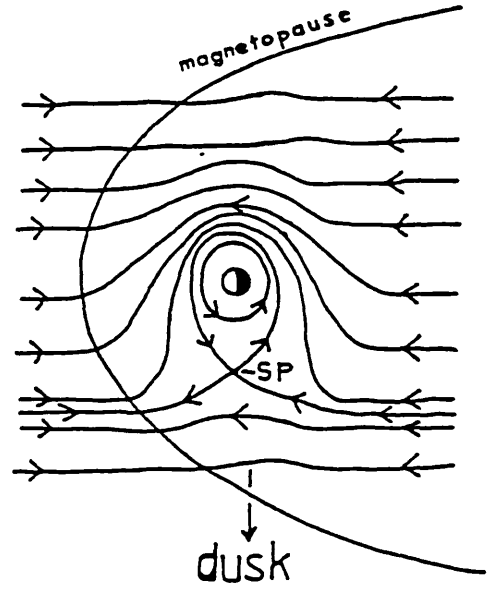


Fig. 1.5. Equipotentials ($\underline{E}$ x $\underline{B}$ flow lines) in the equatorial plane.

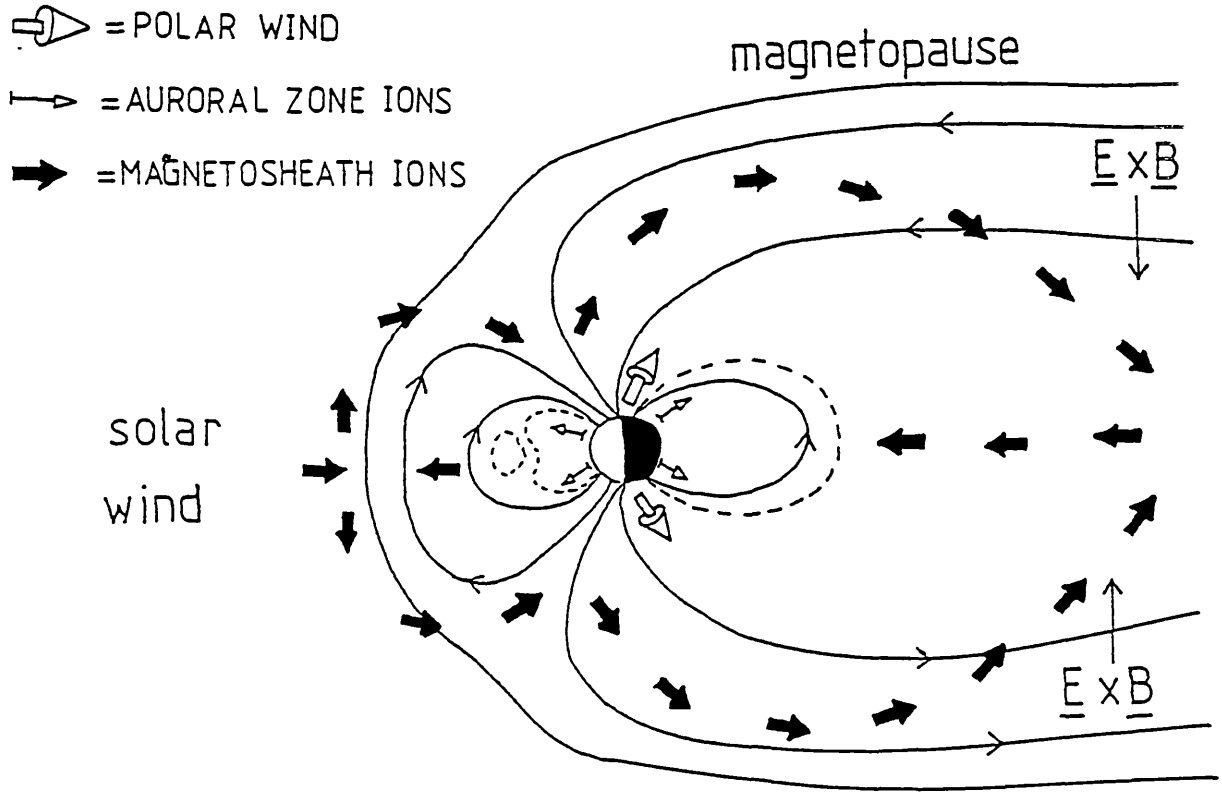


Fig. 1.6. Charged particle populations in the magnetosphere.

depend on its initial energy. A fast particle will mirror earlier and arrive back at the magnetopause, where it may get transmitted back into the magnetosheath. If the particle is slower than the local convection speed of field lines, however, it will not reach the magnetopause. Instead, it travels antisunward along the tail field lines while at the same time $\underline{E} \times \underline{B}$ drifting towards the neutral sheet. If it reaches the neutral sheet sunward of the tail reconnection site (N_2 in Figure 1.3) it gets trapped onto closed magnetic field lines convecting earthward and gets energised in the process. Thus the magnetosheath provides a likely major source for the hot ($\sim$ few keV) plasma sheet population. Unless the magnetosheath particle gets trapped in a ring current orbit or precipitated into the atmosphere, it will eventually reach the dayside boundary again. The whole cycle is then repeated until the particle is energised enough to escape into the magnetosheath.

There are various possible ways in which ionospheric plasma can get caught up in the magnetospheric circulation system. Ionospheric plasma may be transmitted directly into the magnetosphere at high latitudes. The resulting stream of low energy ($\sim$ eV) charged particles is known as the polar wind (e.g., Axford, 1968). Ionospheric plasma may also be accelerated directly into the magnetosphere as high energy ($\sim$ keV) particles as a result of low-altitude ionospheric energisation processes. Plasmaspheric ions can also enter the magnetospheric circulation system as a result of variations of the dawn-dusk convection electric field. An enhancement in the electric field causes a shrinking of the plasmasphere and the formation of detached plasmasphere regions (e.g., Chappell, 1974). The detached plasmasphere regions convect to the dayside magnetopause and are then caught in the reconnection flows along the magnetopause (e.g., Freeman et al., 1977).

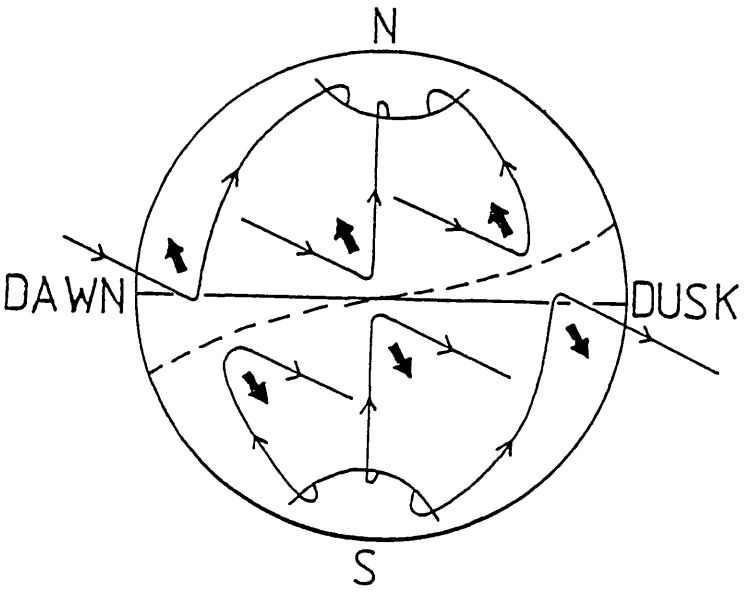
1.3.3 Reconnection for arbitrary IMF

Dungey's (1961) reconnection picture (Figure 1.3) is a singular case since the IMF can have arbitrary orientation in general. In the 2-D picture for southward IMF in Figure 1.3, the reconnection sites N_1 and N_2 are also neutral points, i.e., points at which the magnetic field strength goes to zero. In 3-D, N_1 and N_2 are joined by a line, the reconnection line, the trace of which coincides with the

intersection between the magnetopause and the ecliptic plane. Attempts have been made to generalise this picture to allow reconnection to occur for other orientations of the IMF (e.g., the vacuum models of Cowley, 1973; Stern, 1973). In order for reconnection to be a viable driving mechanism for convection, it should occur along a line of finite longitudinal extent (e.g., Nishida, 1971): the reconnection line. The rate at which IMF lines are reconnected depends on the extent of the reconnection line and there are a variety of reconnection models in existence which assume different locations and geometries for the reconnection line.

In most models of dayside reconnection the reconnection line passes through the subsolar (stagnation) point. A second assumption also frequently used to specify the orientation of the reconnection line is that it should lie parallel to the current separating the two field regions, i.e., the magnetopause current (e.g., Gonzalez and Mozer, 1974; Sonnerup, 1974; Hill, 1975). In such models, reconnection can operate for arbitrary IMF, provided the IMF is not strongly northward. However, Cowley (1976) has brought the general validity of the second assumption into question. A different approach has been made by Crooker (1979). She assumes that reconnection occurs only for strictly antiparallel field orientations. In this model the reconnection line passes through the subsolar point only for a purely southward IMF and the major site of reconnection is shifted to the dayside cusp regions for other orientations. Dungey (1963) proposed that reconnection can also occur for a purely northward IMF. In this case the reconnection site is located on the tail magnetopause poleward of the polar cusp boundary. In principle it is therefore feasible that reconnection can occur for any IMF orientation.

To illustrate the various models discussed above, Figures 1.7 to 1.9 show the reconnection configurations qualitatively derived from these models. The case for due southward IMF has been illustrated in Figures 1.3 and 1.4. Figure 1.7 shows the case where the IMF has an additional B_y component (e.g., Gonzalez and Mozer, 1974). The effect of IMF B_y is the asymmetric addition of open flux tubes to the dawn (dusk) side for positive (negative) B_y in the Northern Hemisphere and vice versa in the Southern Hemisphere. This results in asymmetric convective flows in the polar cap regions and a displacement of the polar cap towards dawn or dusk. As in the case of due southward IMF,



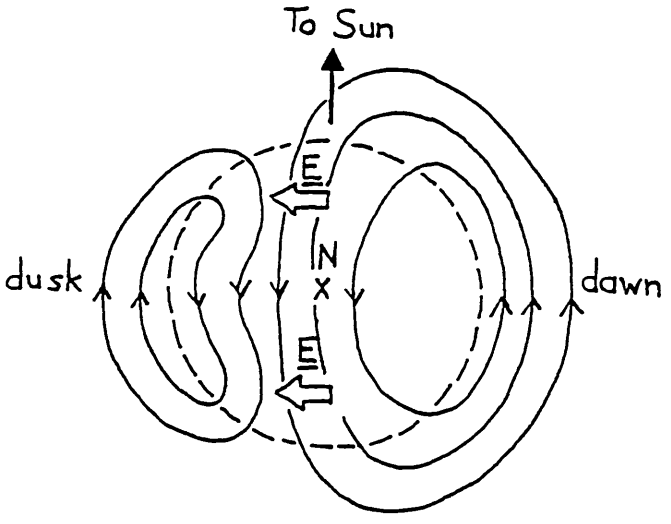
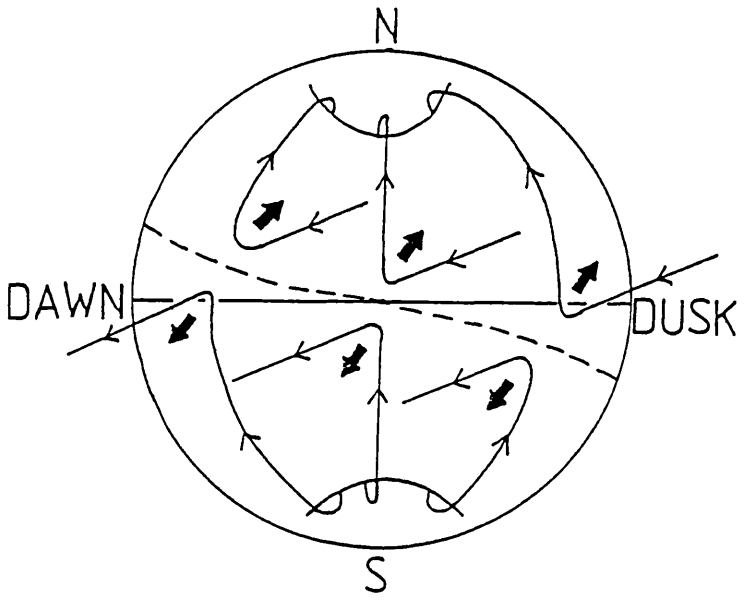


Fig. 1.7(a). Reconnection for IMF $B_y > 0$.



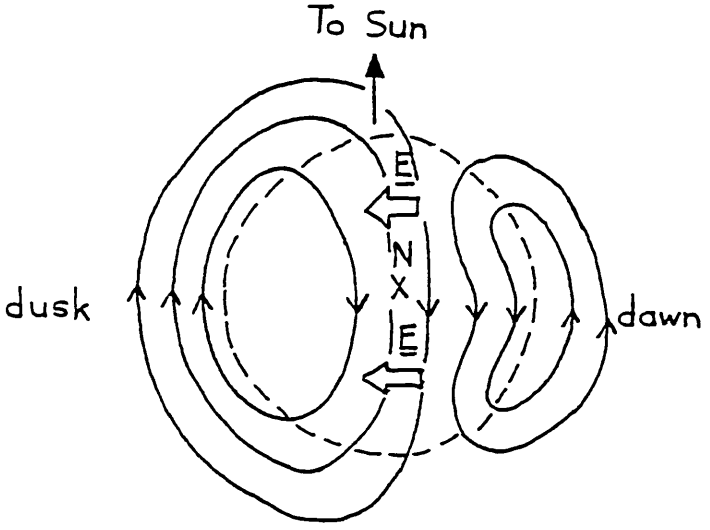


Fig. 1.7(b). Reconnection for IMF $B_y < 0$.

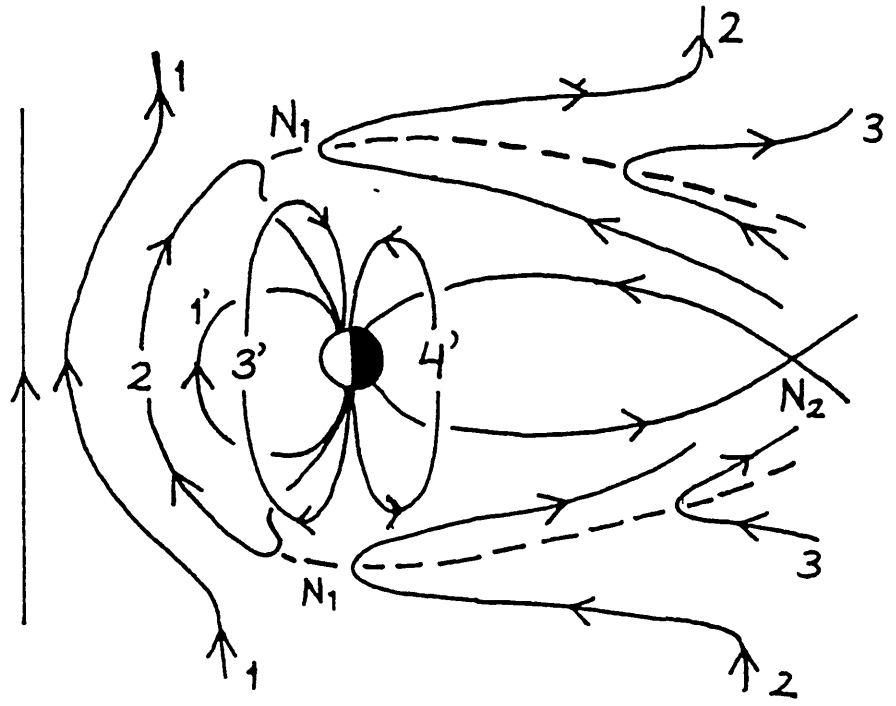


Fig. 1.8(a). Reconnection for northward IMF (Dungey, 1963).

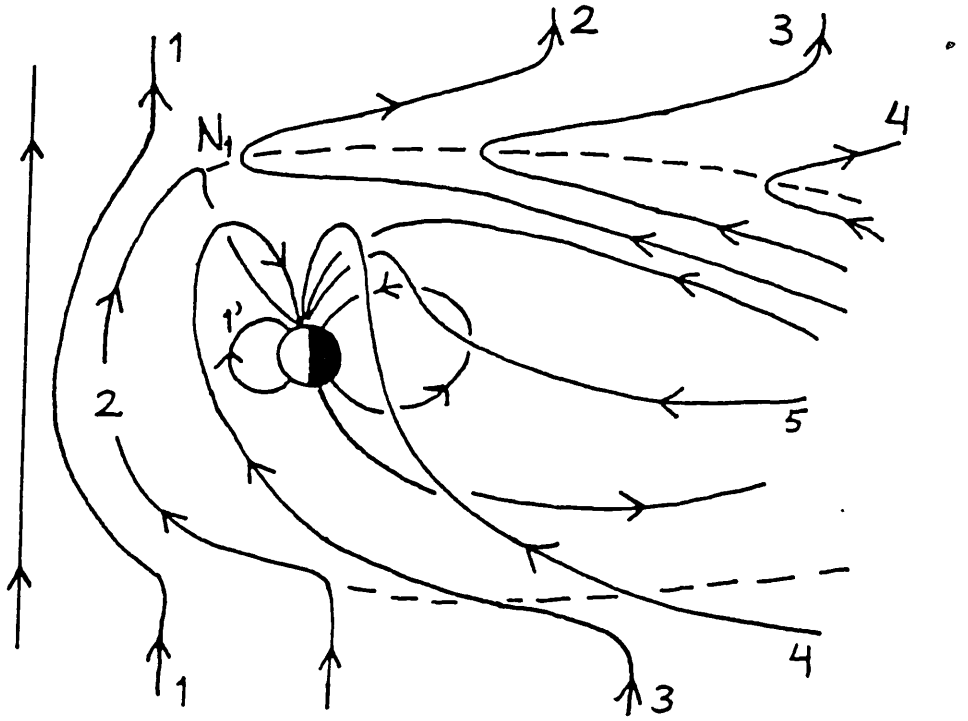


Fig. 1.8(b). Reconnection for northward IMF (Russell, 1972).

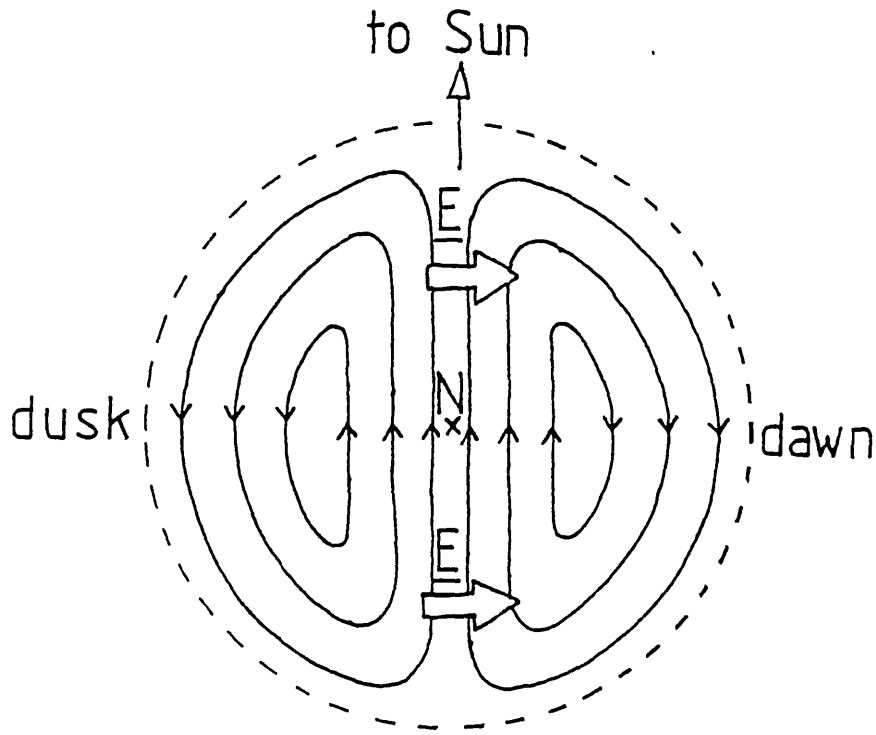


Fig. 1.8(c). Convection pattern for northward IMF.

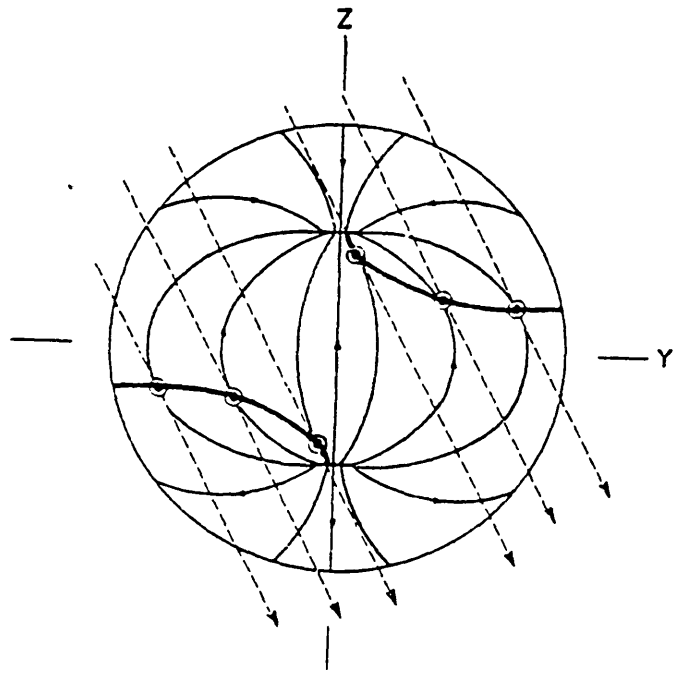


Fig. 1.9. Crooker's (1979) antiparallel reconnection model.

the solar wind electric field maps to a dawn-dusk electric field across the polar cap. Figure 1.8 shows two possible magnetic field topologies for reconnection when the IMF is strongly northward (Dungey, 1963; Russell, 1972). Note that the convective flow in the central polar cap region is sunward. Finally, Figure 1.9 shows the orientation of the reconnection line based on Crooker's (1979) antiparallel reconnection model. The convective flow patterns are similar to those of the other reconnection models.

1.3.4 The closed model magnetosphere

Mechanisms other than reconnection which could act as driving forces for magnetospheric convection have also been suggested at various times in the past. Axford and Hines (1961) proposed that solar wind energy and momentum is transferred to the outer layers of the magnetosphere through some process(es) equivalent to friction. Such transfer processes (e.g., cross-field diffusion) do not require the presence of open field lines and hence the Axford and Hines (1961) model is often referred to as the closed model. In this model closed magnetic flux tubes and plasma are transported from the dayside along the flanks of the magnetosphere into the tail and subsequently return to the dayside again, possibly after reconnection in the tail. There is no reason to suggest that reconnection and closed flux tube transport processes cannot exist simultaneously and in fact observational data (Chapter 2) indicate that it is highly likely to occur. The effect of both processes operating simultaneously is shown in Figure 1.10 (from Cowley, 1982). Figure 1.10(a) shows an open flux tube and a closed flux tube in the process of being transported into the tail. The resulting convective flow patterns, in the equatorial plane and mapped on to the north polar region, is shown in Figures 1.10(b) and 1.10(c), respectively. The hatched region indicates the flow associated with closed flux tube transport. Note that the convection reversal region (Figure 1.10(c)) no longer coincides with the polar cap boundary. Both reconnection and closed model processes can be expected to play a significant part in magnetospheric convection. However, in terms of the total cross-magnetosphere potential the former process is the more significant. In-situ observations at the magnetopause suggest that closed model processes can only account for $\lesssim$ 10% of the typical cross-magnetosphere voltage (e.g., Cowley, 1982; Mozer, 1984).

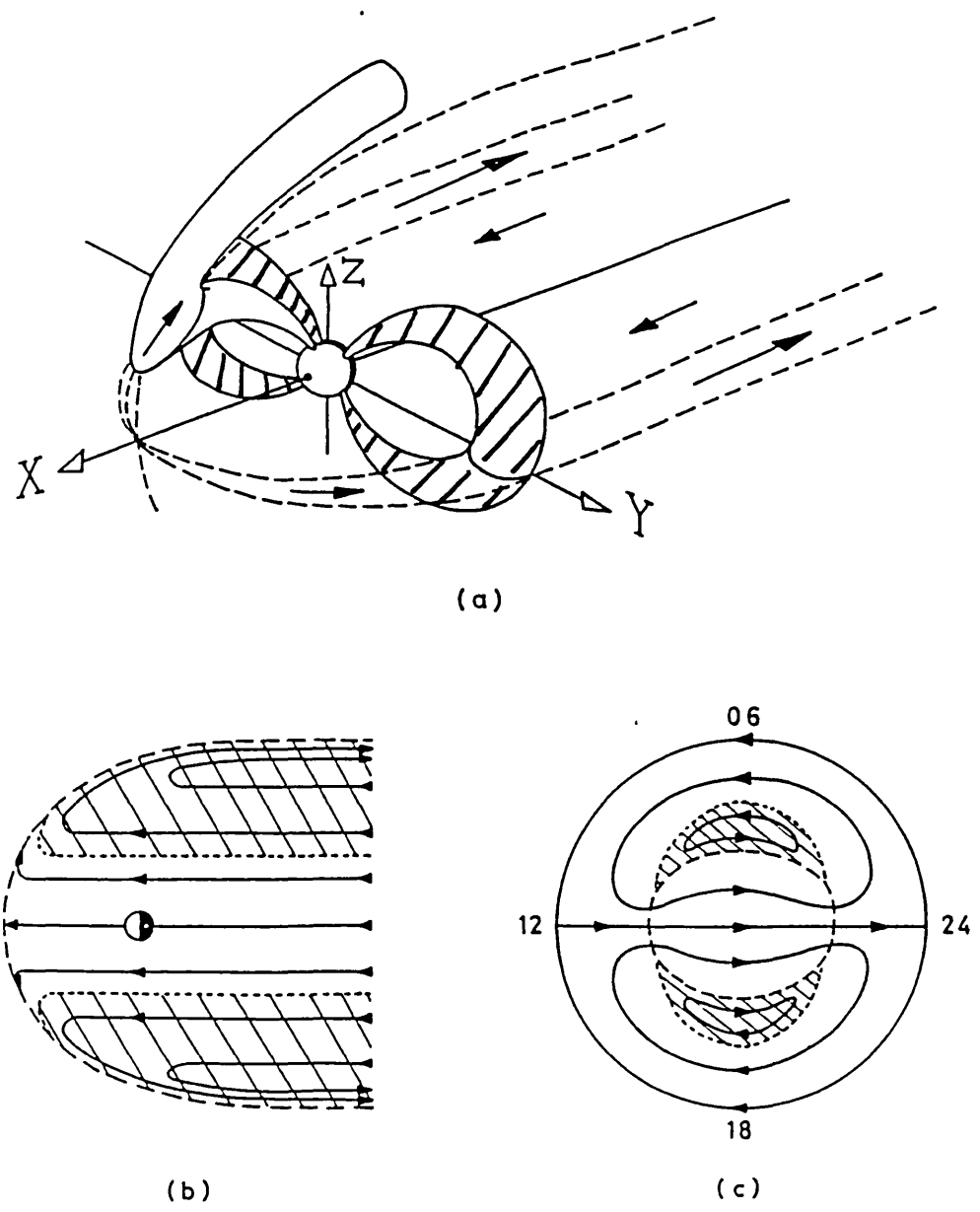


Figure 1.10. Open and closed (hatched) flux tube transport (Cowley, 1982).

1.4 Control of the Magnetosphere by the IMF

At the Earth's orbit the average flux of solar wind energy ($\sim 10^{12}$ W) incident on the dayside magnetosphere is more than enough to drive continuously all known magnetospheric disturbance phenomena. The amount of solar wind energy transferred to the magnetosphere is, however, determined by the nature and efficiency of the interaction mechanism(s) between the solar wind and the magnetosphere. The outer

boundary of the magnetosphere suggests itself as the most obvious place to study the interaction, since it is here that the actual coupling takes place. However, a discussion of in-situ observations of interaction signatures will be deferred to later chapters. Instead, we shall conclude this chapter by reviewing a selection of magnetospheric phenomena and examine their correlation with variations in the solar wind parameters in order to assess indirectly the nature of the solar wind-magnetosphere interaction.

Geomagnetic activity. Geomagnetic activity is monitored in terms of geomagnetic index values, which are derived from the level of disturbances in the geomagnetic field as observed by ground-based chains of magnetometers (e.g., Rostoker, 1972). A number of publications have established that of all the measured solar wind parameters it is the southward IMF component which shows the most significant correlation with the level of geomagnetic activity (Fairfield and Cahill, 1966; Rostoker and Fälthammar, 1967; Wilcox et al., 1967; Hirshberg and Colburn, 1969). Therefore, the emphasis has shifted instead to finding the most appropriate combination(s) of solar wind parameters which show the best correlation with various magnetic indices (e.g., Arnoldy et al., 1971; Burton et al., 1975; Perreault and Akasofu, 1978).

Ionospheric current systems. Electrical coupling between the ionosphere and the magnetosphere is achieved through a system of field-aligned currents (FACs) which flow to and from the ionosphere along magnetic field lines. Their existence has been deduced and their properties studied from the magnetic perturbations ΔB they produce in and about the ionosphere. The magnitude and direction of the FACs can be determined from the magnetic perturbations ΔB by applying Ampere's law: $\nabla \times \underline{B} = \mu_0 \underline{J}$ (e.g., Zmuda and Armstrong, 1974). The most significant advances in the study of FACs have been made with the low-altitude ($\sim$ 1000 km) polar orbiting TRIAD and ISIS 2 satellites.

Figure 1.11 shows the large-scale distribution and flow directions of FACs as deduced from TRIAD observations (e.g., Iijima and Potemra, 1976a,b; Iijima et al., 1978; Potemra et al., 1980). The main FAC regions are as follows. Region 1 FACs consist of current sheets which approximately follow the auroral oval, i.e., the locus where the

maximum auroral intensity occurs (magnetic latitude of $\sim$ 70° - 80°). Region 1 FACs flow into the ionosphere in the dawn sector and away from the ionosphere in the dusk sector and have an average current intensity of $\sim$ 2 $\mu A\ m^{-2}$. Adjacent and equatorward of Region 1 are the Region 2 FACs, which at any given local time flow in the opposite direction and on average have an intensity of $\sim$ 1 $\mu A\ m^{-2}$. As shown in Figure 1.11, Region 1 and Region 2 overlap near local midnight to form three adjoining regions of FACs (the Harang discontinuity).

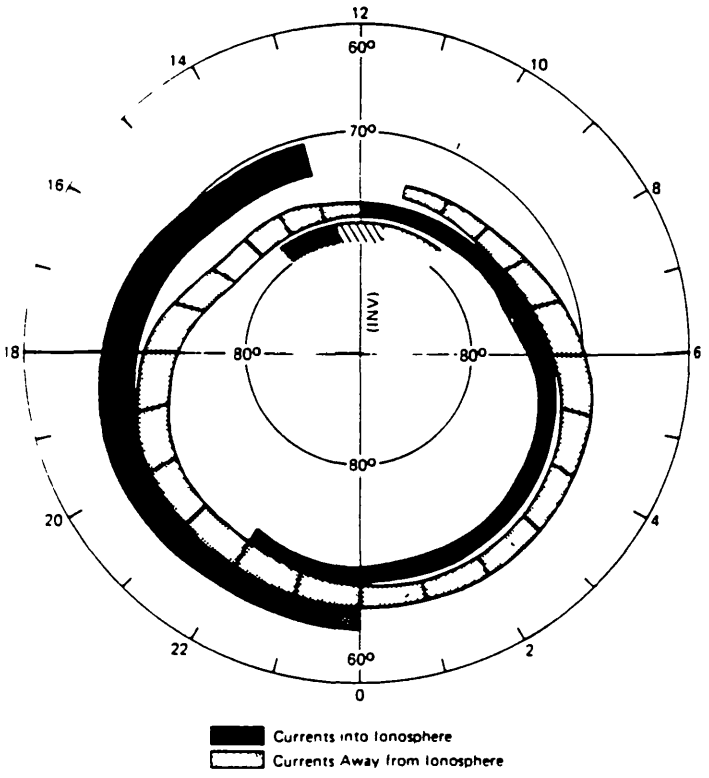


Figure 1.11. TRIAD observations of FACs (Potemra, 1978).

Figure 1.11 also shows another current system poleward of Region 1 near local noon. This region is referred to as the cusp region FAC (Iijima and Potemra, 1976b; Iijima et al., 1978). The behaviour of these FACs is intimately related to the orientation of the IMF. Their intensities are usually larger during periods of southward IMF. Figure 1.12 shows the relationship of cusp FACs relative to the polarity of IMF B_y in the Northern Hemisphere; these relationships are systematically reversed in the Southern Hemisphere.

The prenoon upward flowing cusp currents are preferentially observed when IMF B_y is positive and the postnoon currents are more frequently observed when B_y is negative. The ionospheric closure current (DPY, see later) between Region 1 and cusp FACs is mainly directed eastward for IMF $B_y > 0$, and westward for $B_y < 0$ (Wilhjelm et al., 1978). Regions 1 and 2 are contained within the region of sunward convection and are not affected by IMF B_y (Saflekos et al., 1979), while the cusp FACs are located in the region of antisunward convection. Inspection of Figure 1.12 will also show that the electric field at low latitudes associated with sunward convection is in the proper direction to couple Regions 1 and 2 by Pedersen currents. The field associated with convection at the throat, i.e., the region of flow reversal in the cusp near local noon, is in the correct direction to couple Region 1 and the dominant cusp FAC region. All these observations are consistent with Figure 1.7.

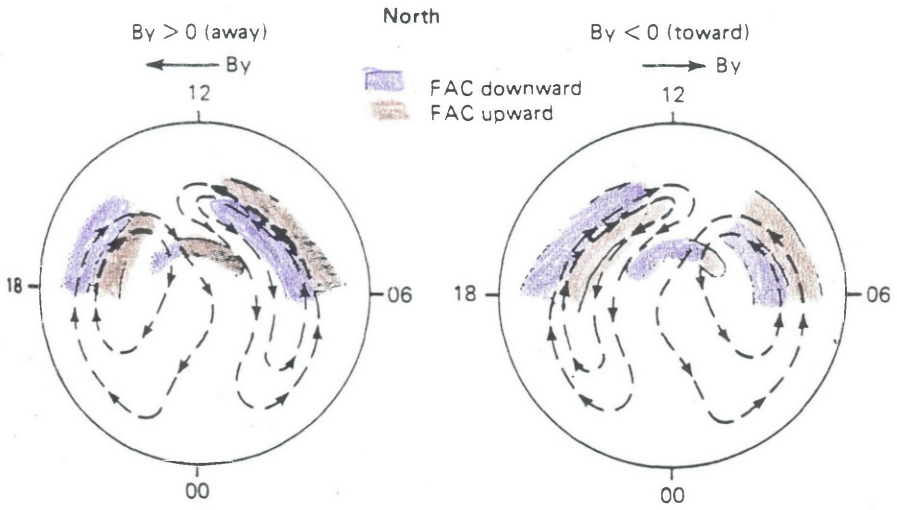


Figure 1.12. Cusp FACs: response to IMF B_y (Potemra, 1978).

Data from ISIS 2 have also provided results similar to those of TRIAD (McDiarmid et al., 1978a,b, 1979). The direction of the convective flow deduced from the measurements of ΔB are consistent with the 2-cell system in Figure 1.4, and in the presence of IMF B_y with those in Figure 1.7. Figure 1.13 summarises the ISIS 2 findings. Figure 1.13(a) shows the FACs inferred from ΔB measurements.

Comparison with Figure 1.11 shows slight disagreement with TRIAD data near local noon. However, this is likely the result of the way in which cusp FACs are defined in the TRIAD data. Figure 1.13(b) shows the schematic plot of ΔB measurements; reversing the arrows gives the convective flow pattern. The polar cap boundary (dashed line) is identified with the location of maximum ΔB. Along this boundary the region of largest ΔB occurs in the dayside cusp region near local noon and its sense (eastward or westward) is controlled by the IMF polarity (B_y > 0 or < 0). The latitude of the peak ΔB also moves equatorward as IMF B_z goes increasingly negative. The location where ΔB changes sign, i.e., the convective flow reversal boundary, is indicated by the dotted line in Figure 1.13(b). It extends slightly equatorward of the polar cap boundary, and thus indicates evidence for closed model transfer processes in addition to reconnection, as shown in Figure 1.10. Finally, note that evidence for ΔB consistent with sunward convection at high latitudes when the IMF is strongly northward (see Figure 1.8) has also been obtained from both ISIS 2 (McDiarmid et al., 1978a, 1980) and TRIAD (Zanetti et al., 1982) data.

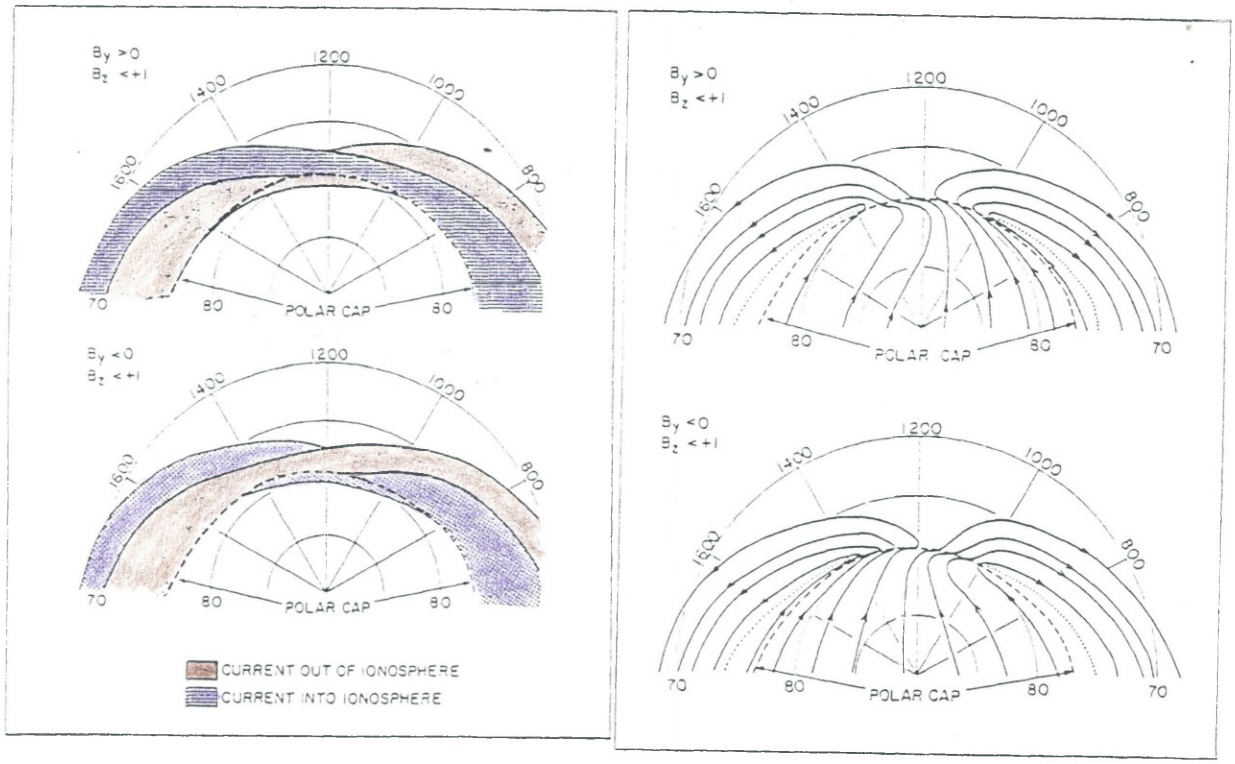


Fig. 1.13. FACs and magnetic field perturbations measured by ISIS 2 (McDiarmid et al., 1978).

FACs transfer energy and momentum and transmit magnetic stress from the outer magnetosphere to the ionosphere. Here the FACs spread out horizontally into current flows which electrically connect and close oppositely directed FAC regions and dissipate the external solar wind flow energy, mainly as heat. These horizontal currents may be separated into Hall currents and Pedersen currents, which flow respectively along the - $\underline{E} \times \underline{B}$ direction and along $\underline{E}$. These currents arise from the difference in heights at which the ion and electron gyrofrequencies become comparable to or smaller than the charged-neutral particle collisions. All currents give rise to geomagnetic perturbations which should be observable from the ground. However, most of the geomagnetic variations on the ground which are of external origin may be attributable to Hall currents since the effect of Pedersen currents and FACs tend to cancel each other (e.g., Fukushima, 1969, 1976). Current systems which are constructed on the assumption that Hall currents are responsible for geomagnetic variations are known as equivalent current systems.

Polar cap disturbances are usually thought to comprise at least two distinct current systems, DP1 and DP2 (e.g., Nishida, 1968). Of these, DP2 shows the clearest correlation with the southward IMF component, and it intensifies as IMF B_z goes increasingly negative. Hall currents flow in the opposite direction to convective flows and thus the magnetospheric convection pattern can be inferred from equivalent current systems by simple inversion. It is found that the convection pattern deduced from DP2 then bears a close resemblance to Figure 1.4 (e.g. Maezewa, 1976) when the IMF field is southward. During periods of strongly northward IMF the 2-cell system disappears. The region of strongest magnetic variations is then confined to high latitudes (> 70°) and sunward convection is then observed in the central polar cap, consistent with Figure 1.8 (e.g., Friis-Christensen and Wilhjelm, 1975; Maezewa, 1976). DP1 is not controlled directly by the north-south IMF component and is associated with the main phase of a substorm, i.e., the period of enhanced tail reconnection.

In addition to showing a dependence on IMF B_z, polar cap magnetic variations are also affected by IMF B_y. This correlation is often referred to as the Svalgaard-Mansurov effect, although Friis-Christensen and Wilhjelm (1975) refer to IMF B_y dependent variations as DPY. The convection patterns inferred from DPY agree closely with those drawn in Figure 1.7.

Motion of magnetospheric boundaries

Magnetopause. A feature of all reconnection models is an enhancement in the dayside reconnection rate as the IMF turns increasingly southward. An increase in reconnection leads to increased erosion, i.e., removal of magnetic flux from the dayside magnetosphere. The dayside flux content is then built up again following reconnection in the tail, with subsequent sunward transport of magnetic flux. However, there is a finite time delay before a self-consistent convection return rate is established to balance the dayside reconnection rate (e.g., Coroniti and Kennel, 1973; Holzer and Reid, 1975). Therefore, following a southward turning of the IMF there is a net flux loss from the dayside magnetosphere and it may be expected to shrink, provided the solar wind dynamic pressure stays constant. This shrinkage is observable as both an inward motion of the magnetopause and as an increased flaring of the tail. The inward motion of the dayside magnetopause has been observed in single case event studies (e.g., Aubry et al., 1970) and from statistical studies (e.g., Fairfield, 1971; Maezewa, 1974; Formisano et al., 1979), which show the magnetopause displaced inward by $\sim 1\ R_E$ during periods of southward IMF. The amount of flux transferred to and from the dayside as a result of imbalances in the dayside and nightside reconnection rates has been estimated as $\sim 10^8$ Wb by Holzer and Slavin (1978,1979).

Polar cusp. In addition to an inward motion of the dayside magnetopause an enhanced reconnection rate also leads to an increase in size of the polar cap, i.e., the amount of open flux. Russell et al. (1971) first established that the high-altitude polar cusp moves equatorward or poleward according to whether the IMF turns southward or northward. This behaviour was later confirmed in a statistical study by Burch (1972, 1973, 1974). Figure 1.14 shows the latitudes of the equatorward (solid circles) and poleward (open circles) boundaries of the cusp (determined from electron precipitation measurements) plotted against the 45 min. average IMF B_Z component. As the IMF goes increasingly southward, both boundaries move equatorward at about the same rate. For strongly northward IMF the equatorward boundary stays virtually stationary while the poleward boundary moves poleward, the result of which is that the latitudinal cusp width increases from $\sim 4°$ to $\sim 7°$. This widening of the cusp is consistent with tail field lines reconnecting with northward IMF (Figure 1.8) since this allows a

deeper penetration of magnetosheath plasma into the cusp at the poleward cusp edge.

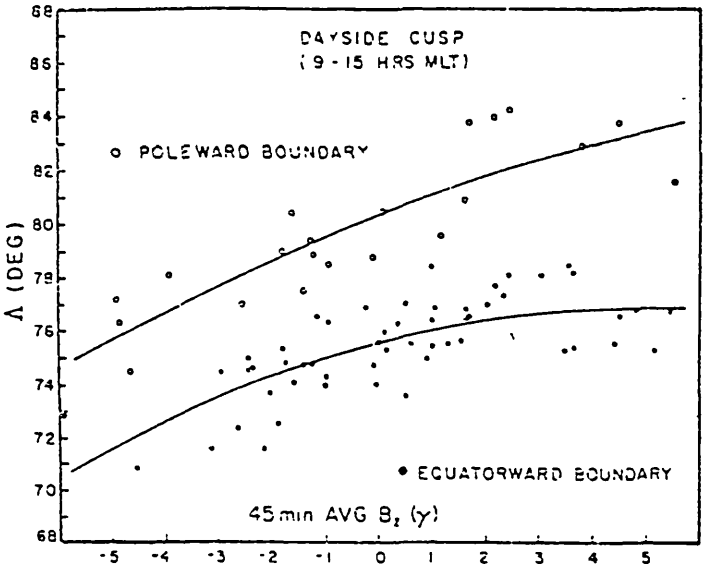


Figure 1.14. Location of polar cusp: response to IMF B_Z (Burch, 1972).

Convection electric field. There are a large number of techniques available to measure magnetospheric electric fields (e.g. Mozer, 1973; Stern, 1977). The earliest successful measurements of large-scale electric fields were made with low-altitude ($\sim$ 1000 km) polar orbiting spacecraft (e.g., Caufmann and Gurnett, 1971, 1972; Heppner, 1972, 1973). The convection patterns inferred from these measurements confirm the basic patterns established earlier from ground-based magnetometer observations. The satellite data showed the frequent occurrence of electric field reversals at auroral latitudes ($\sim$ 70-80°), with sunward convection on the equatorward side of the reversal boundary and antisunward convection poleward of it. Frank and Gurnett (1971) also found that the reversal region is closely related to the high-latitude termination of energetic ($\gtrsim$ 45 keV) electrons, thus suggesting that the reversals are closely related to the polar cap boundary.

The large-scale polar cap electric field intensity and distribution show close correlation with the IMF. Heppner (1972)

showed that for IMF B_y positive, the dawn-dusk electric field component shows a maximum in the dawn (dusk) sector in the Northern (Southern) Hemisphere, while the reverse is true for IMF B_y negative. The resulting shift in the basic convection pattern towards either the dawn or dusk sector, depending on the IMF B_y polarity and the hemisphere, is consistent with that shown in Figure 1.7. The polar cap electric field also intensifies in response to an increase in the southward IMF component (e.g. Mozer et al., 1974). Finally, during periods of strongly northward IMF an oppositely directed dusk-dawn electric field has been found in the central (high-latitude) polar cap region (e.g., Burke et al., 1979). Such an electric field is consistent with sunward plasma flows across the polar cap resulting from reconnection with northward IMF, tailward of the polar cusp boundary (Figure 1.8).

Convective plasma flows. Direct measurements of convective plasma flows have also been made. Heelis et al. (1976) presented satellite measurements of ion vector velocities in the Southern Hemisphere. Their results confirm the general appearance of the convection pattern shown in Figure 1.4. However, they observe that the throat region is somewhat narrow, suggesting that the reconnection line may be limited in longitudinal extent.

Polar cap potential. The potential drop across the polar cap ϕ_{pc} gives a measure of the strength of the convective plasma flows in the magnetosphere and hence the strength of the solar wind-magnetosphere interaction. Reiff et al. (1981) measured the potential drop across the region of antisunward convection in the high-latitude ionosphere under a variety of IMF orientations. They found a mean value of $\sim$ 70 kV and they also showed that the measured potential drops correlate well with the predictions from various empirically and theoretically derived reconnection models. A background voltage of $\sim$ 30 kV not accounted for by the models was attributed to closed model transfer processes.

Wygant et al. (1983) did a similar survey and showed that the bulk of the background voltage results from a time response of ϕ_{pc} to variations in IMF B_z. This time response may result from a fly-wheel effect between neutral winds in the upper atmosphere and the solar wind-induced ionospheric convection. An upper limit of $\sim$ 16 kV was quoted for closed model transfer processes.

CHAPTER 2

SOLAR WIND - MAGNETOSPHERE INTERACTION: IN-SITU OBSERVATIONS

2.1 Introduction

In the previous chapter we looked at some of the large-scale features expected to be present in an open model of the magnetosphere. Subsequently, we briefly considered some observational results which showed that the orientation of the IMF exerts a controlling influence on a host of magnetospheric phenomena, a result which may be regarded as providing indirect evidence for the occurrence of dayside reconnection as originally proposed by Dungey (1961). In this chapter we will consider in-situ satellite observations at the site of interaction between the solar wind and magnetosphere, i.e., the magnetopause boundary, principally in order to establish whether reconnection does occur in the manner envisaged originally (e.g., Levy et al., 1964) and as indirect observations seem to suggest.

Observations have established that there is a temporally and spatially varying layer of magnetosheath-like plasma inside of and adjacent to the magnetopause. This layer has been observed over the entire known magnetopause and its presence provides direct evidence for the interaction between the solar wind and the magnetosphere and the entry of solar wind plasma into the magnetosphere. We shall use the term boundary layer as a general reference to this layer. In the first half of this chapter the properties of the boundary layer as measured by various satellite plasma and magnetic field instruments are reviewed. Depending on its location in the magnetosphere (and also to a small degree on the particular investigator(s)) the boundary layer has been given various names, the most frequently used of which are the magnetotail boundary layer, the plasma mantle, the (tail) lobe plasma, the entry layer and the low latitude boundary layer (in order of their discovery). In considering boundary layer observations we shall start

off in the magnetotail region and work our way forwards toward the frontside magnetopause.

Before results from the ISEE 1 and 2 satellite mission (see Appendix A) became available, the results obtained from plasma and magnetic field data at and near the dayside magnetopause aroused considerable controversy as to whether reconnection in the subsolar region ever occurs as a large-scale, stationary process or even whether it occurs at all. The high-time resolution plasma and field data from ISEE 1 and 2 resolved this question and confirmed that quasi-steady reconnection at the dayside magnetopause does indeed occur, at least at times. In the second part of this chapter we will consider a set of signatures using ISEE 1 and 2 data which give in-situ evidence for the occurrence of dayside reconnection.

2.2 The Boundary Layer

2.2.1 The magnetotail region

The first regular encounters of the boundary layer were made from satellite observations inside the magnetotail region. Figure 2.1 shows the regions explored by a number of satellites in which such a boundary layer was found inside of and adjacent to the magnetopause. Intrilligator and Wolfe (1972), using Pioneer 8 plasma data obtained during a magnetopause crossing approximately 40 R_E down-tail, reported a diffuse boundary region. In the same year, Hones et al. (1972), and subsequently Akasofu et al. (1973) established the properties of the boundary layer region observed along the dawn and dusk flanks of the magnetopause at down-tail distances of $\sim$ 18 R_E using the electrostatic analyzers on board the Vela 4 and 5 satellites. The boundary layer region, which they termed the magnetotail boundary layer, was identified as a layer of relatively cool, antisunward flowing plasma in between the inner magnetotail (plasma sheet at low latitudes, tail lobe at higher latitudes) and the magnetosheath, with energy spectra similar to and density levels and flow speeds reduced in comparison with the adjacent magnetosheath. The thickness of the boundary layer was found to correlate with latitude, being thicker at higher latitudes ($\sim$ 1-2 R_E) and thin ($\sim$ 100s of km) or even non-detectable near the equatorial plane.

The HEOS 2 plasma and magnetic field data extended the boundary layer observations to the distant polar magnetosphere region. Here, the

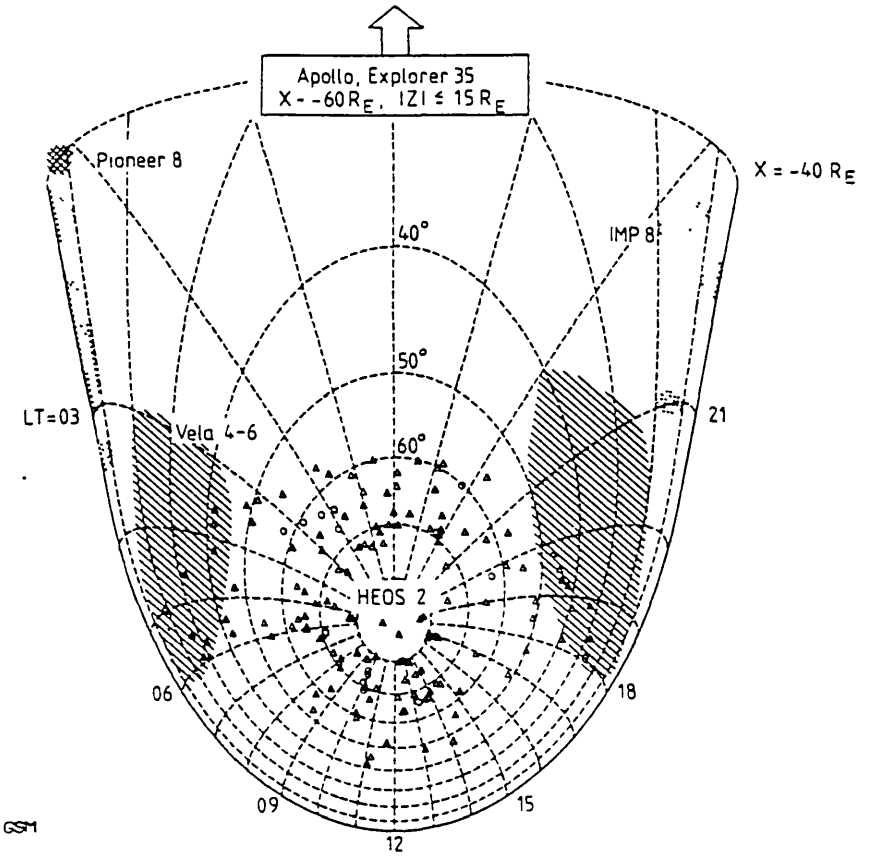


Figure 2.1. Locations of reported boundary layer observations prior to 1978 (Sckopke and Paschmann, 1978).

boundary layer region poleward of the cusp was called the plasma mantle (Haerendel and Paschmann, 1975). HEOS 2 data from a fairly typical pass through this region are shown in Figure 2.2. On this outbound pass, HEOS 2 travelled from the mid-altitude polar cusp (PC) on the dayside, across the polar cap (PCR), through the plasma mantle (PM) and into the magnetosheath (MS). In moving towards the magnetopause, the plasma density gradually increases and the bulk flow velocity in the plasma mantle is directed tailward, approximately along the local geomagnetic field, with a magnitude less than that observed in the adjacent magnetosheath. A survey of many such crossings revealed the following properties of the plasma mantle (Rosenbauer et al., 1975; Sckopke et al., 1976; Sckopke and Paschmann, 1978). It is a permanent feature of the polar magnetosphere tailward of the cusp. Generally, the plasma number density, flow speed and temperature all decrease with depth inside the mantle, although on individual passes magnetopause motions or temporal fluctuations of the plasma source may obscure this

trend (e.g., at $\sim$ 11:00 and 11:30 UT in Figure 2.2). The plasma velocity is directed tailward and is generally less than but positively correlated with the velocity in the adjacent magnetosheath and in the solar wind. The proton temperature shows a significant temperature anisotropy, with $T_{\parallel} < T_{\perp}$. The thickness of the plasma mantle is variable, ranging from $\lesssim$ 0.5 R_E to larger than 4 R_E. The thickness and occurrence of the mantle is positively correlated with the southward IMF component.

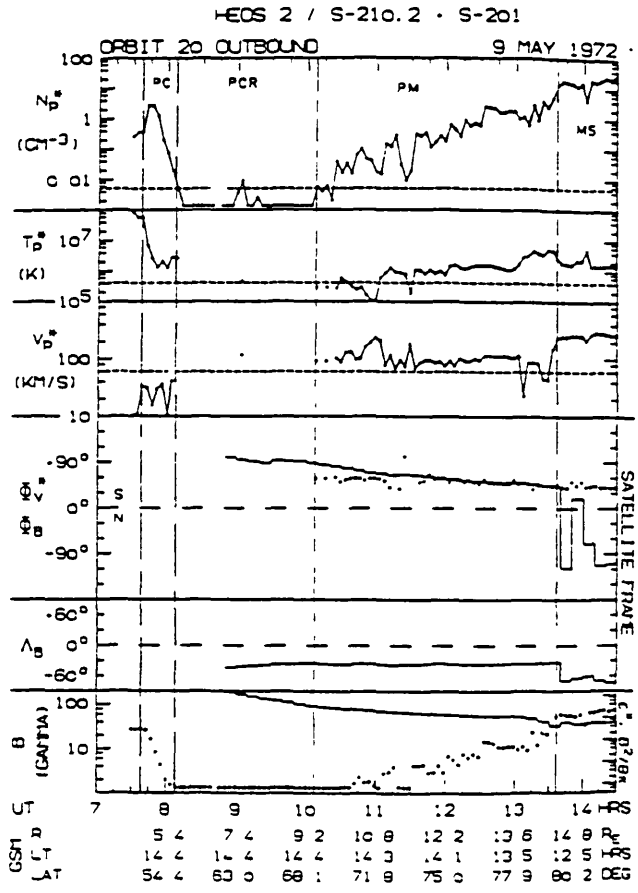


Figure 2.2. HEOS 2 pass through the plasma mantle (Rosenbauer et al., 1975).

Plasma detectors on the moon have also observed a boundary layer region outside the plasma sheet (Hardy et al., 1975, 1976, 1979). At these lunar distances ($\sim$ 60 R_E) it is known as the lobe plasma. Its bulk velocity and number density is similar to that of the plasma mantle but it is somewhat cooler. It extends $\sim$ 8-10 R_E inward from the

magnetopause and at times may be observed right across the tail. Its thickness is strongly correlated with the sign of IMF B_y, while the probability of it being observed is also larger when the IMF has a southward component.

2.2.2 The cusp region

In the early 1970s low-altitude satellite measurements established the presence of magnetosheath-like plasma inside the dayside polar cusp regions, right down to ionospheric altitudes (e.g., Heikilla and Winningham, 1971; Frank, 1971; Frank and Ackerson, 1971). Figure 2.3, which is a noon-midnight cross-section of the high latitude magnetosphere, shows schematically various plasma regions identified in the polar cusp region. The exterior cusp is a region of stagnant magnetosheath plasma just outside the magnetopause, which results from the indentation of the magnetopause in the cusp region (e.g., Sckopke, 1979).

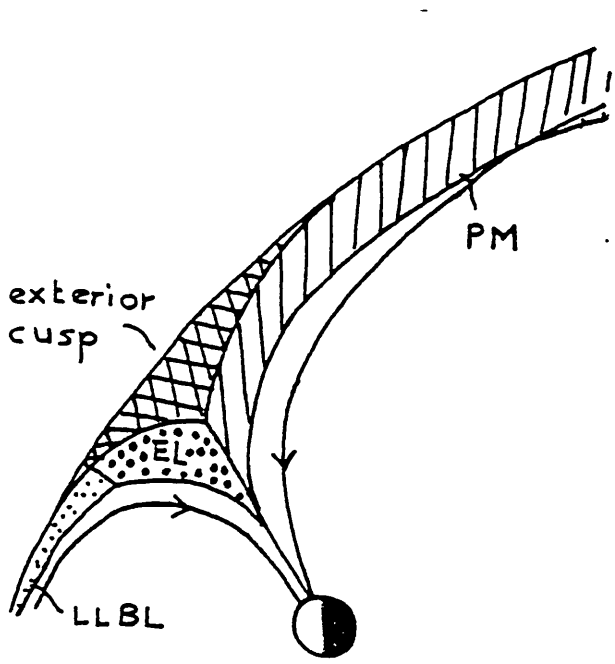


Figure 2.3. The polar cusp region (after Sckopke, 1979).

Inside the magnetopause, HEOS 2 data revealed a boundary layer region of irregularly flowing, magnetosheath-like plasma: the entry

layer (e.g., Haerendel and Paschmann, 1975; Paschmann et al., 1976; Hansen et al., 1976). Figure 2.4 shows HEOS 2 plasma and magnetic field data obtained during an outward bound pass through the polar magnetosphere. RC, EL and MS refer respectively to the hot ring current, entry layer and magnetosheath regions. In the entry layer, the number density and temperature reach magnetosheath levels shortly after its inner edge is crossed, while the plasma velocity is variable in both magnitude and direction. The thickness is variable, but is generally $\sim$ 1-2 R_E (Paschmann et al., 1976). The magnetic field in the entry layer shows large-amplitude fluctuations, similar in magnitude to those in the magnetosheath, and also shows a gradual tailward bending (i.e., Λ_B goes increasingly negative in Figure 2.4).

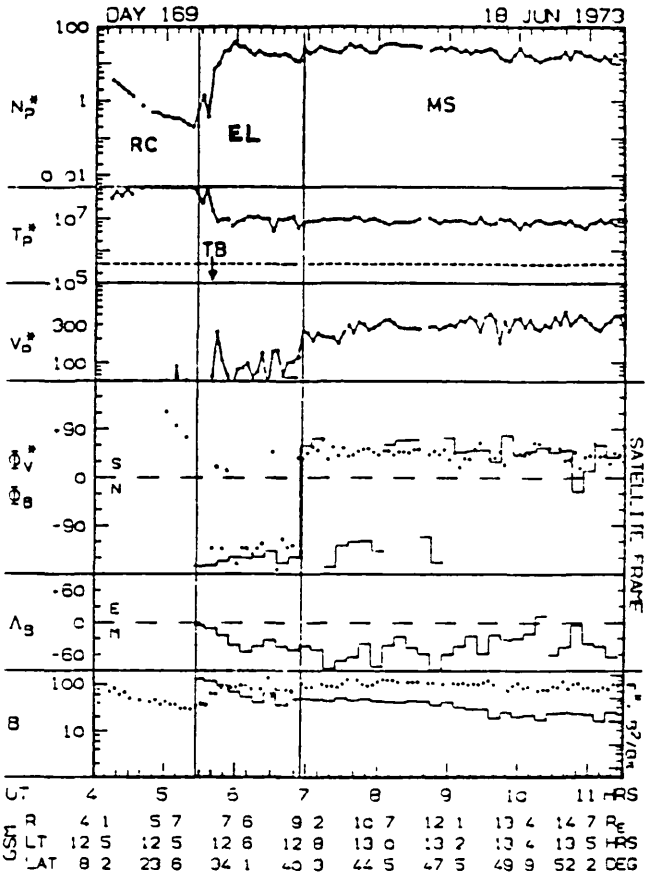


Figure 2.4. HEOS 2 pass through the entry layer (Paschmann et al., 1976).

IMP 6 has also observed the distant polar cusp at times of disturbed magnetic activity (Fairfield and Hones, 1978). The properties

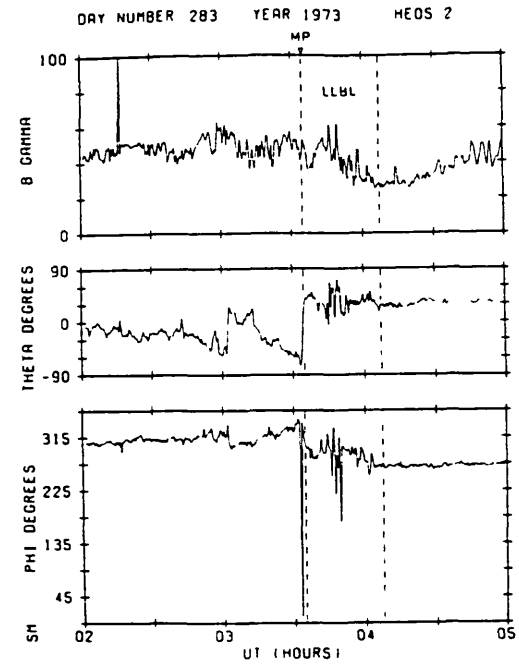
of the flow in this region suggested turbulence and an examination of the plasma flow down the cusp field lines at its low-latitude edge also revealed flows which were accelerated in comparison with the magnetosheath.

2.2.3 The frontside magnetosphere

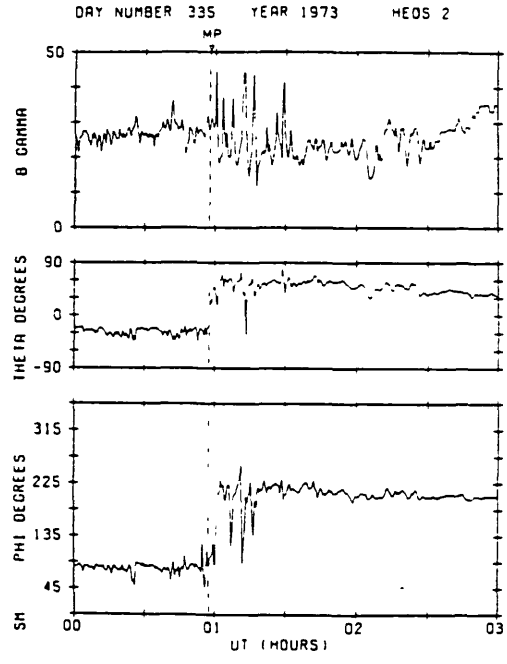
At lower dayside latitudes, the characteristics of the boundary layer differ from those of the entry layer, and therefore a new name was introduced for this region: the low latitude boundary layer. HEOS 2 sampled this region at relatively high (GSM) latitudes and a survey revealed the following general characteristics (Haerendel et al., 1978). It contains a mixture of magnetosheath and magnetospheric plasma. Frequently, the density jumps abruptly at its inner and outer edge, so that the density remains at a level intermediate to that observed in the adjacent magnetosheath and magnetosphere regions. The plasma flow is more ordered than in the entry layer, and is often in the same direction as the external magnetosheath flow but always at a reduced magnitude. Its thickness is variable, but on average it is less than that of the entry layer and it does not show any pronounced correlation with IMF B_z. An interesting discovery made by Haerendel et al. (1978) was the occurrence of transient (of order a minute), large-amplitude magnetic field perturbations in the layer. Many such events showed substantial increases in field strength and an orientation unlike that found in either the magnetosheath or the magnetosphere. Figure 2.5 shows an example illustrating these features. We will discuss and interpret these events more fully in Chapter 6.

Crooker (1977) presented Explorer 33 plasma and magnetic field data obtained in the dayside boundary layer. She confirmed that it is a permanent feature of the frontside magnetosphere for all IMF orientations, with a thickness $\lesssim 1\ R_E$. She also found that the pressure anisotropy observed in the magnetosheath ($p_\perp > p_\parallel$) is only preserved in the boundary layer if the IMF has a southward orientation.

Eastman et al. (1976) and Eastman and Hones (1979) presented results from a survey of IMP 6 traverses through the low latitude boundary layer region. They found a more gradual transition of plasma parameters (density, temperature and flow velocity) across the boundary layer than was evident in the HEOS 2 data set. However, sharp density drops at the magnetopause suggestive of a detached boundary layer region were



(a)



(b)

Fig. 2.5. HEOS 2 passes through the low-latitude boundary layer (Haerendel et al., 1978).

seen on occasion. The boundary layer thickness was found to be variable, but generally in the range $\sim$ 0.1-0.5 R_E with a tendency for larger thicknesses at higher latitude. Again, no correlation was apparent with the IMF B_z component. Figure 2.6 shows a typical example of a crossing made by IMP 6 to illustrate the above features.

The most recent observations of the low latitude boundary layer have been made with the high time resolution instrumentation on board the ISEE 1 and 2 spacecraft (e.g., Paschmann et al., 1978; Frank et al., 1978; Sckopke et al., 1981; Cowley, 1982; Hones et al., 1982; Hones, 1983; Saunders, 1983; Eastman et al., 1982). Paschmann et al. (1978) found that it is often characterized by a sharp drop in density and temperature both at the magnetopause and at its inner edge. Its extent is highly variable, partly resulting from non-uniform motions of the magnetopause, partly from temporal and/or spatial fluctuations. During periods of southward magnetosheath field, isolated pulses of magnetosheath-like plasma are commonly observed inside the magnetopause, features referred to as "inclusion events" by Paschmann et al. (1978). Also, brief bursts of enhanced plasma flows may be observed at times at the magnetopause. Sckopke et al. (1981) made an extensive study of one particular crossing which occurred on the dawn flank. Plasma and field data from this crossing are reproduced in Figure 2.7. They identified four plasma regions on this pass: the magnetosheath (region 4), the hot and dilute ring current (region 1) and two regions with densities and temperatures intermediate to these two regions, the boundary layer proper (region 3) and the halo (region 2). The latter two regions recur quasi-periodically in the data, with a duration of a few minutes.

Hones et al. (1982) and Hones (1983) investigated the magnetic structure of the boundary layer on the flanks of the magnetosphere. They reported several instances of tailward draping of the magnetic field in the boundary layer, an orientation which suggests that the high-latitude segments of the boundary layer field lines are pulled tailward faster than their equatorial segments. They refer to this feature as reverse draping. Tailward draping of the field was also observed during some of the boundary layer pulses observed by Sckopke et al. (1981) (Figure 2.7).

2.2.4 Electron observations

The discussion above of boundary layer properties was mainly in the

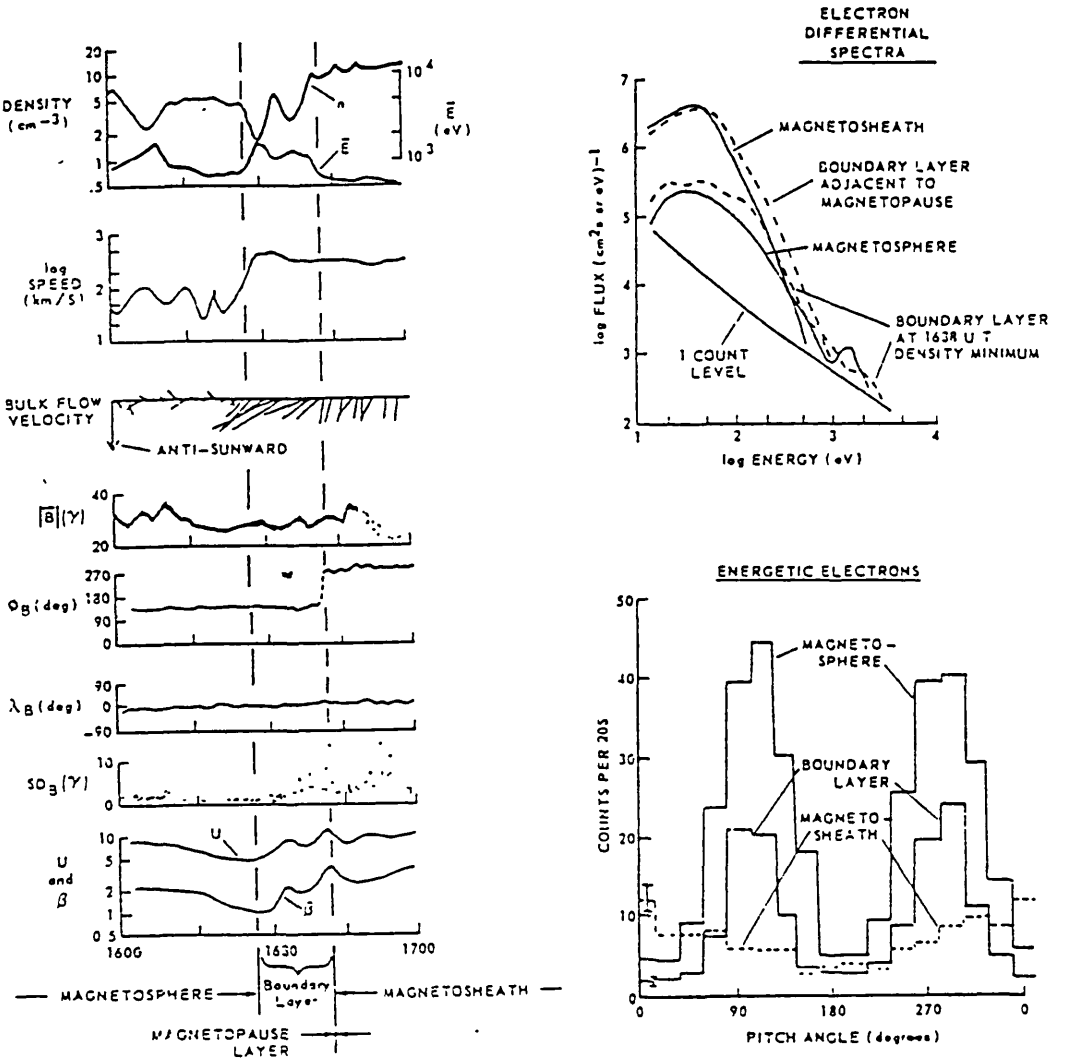


Fig. 2.6. The boundary layer observed by IMP 6 (Eastman and Hones, 1979).

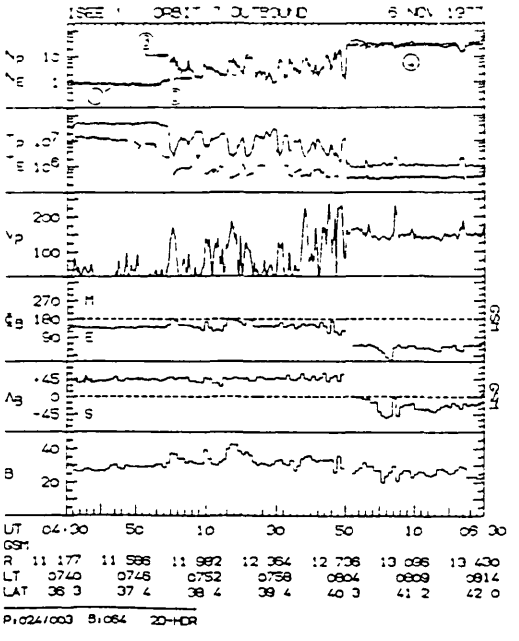


Fig. 2.7. ISEE 1 observations of boundary layer pulses (Sckopke et al., 1981).

light of observations of plasma parameters dominated by the contribution of protons. The existence of a transition region between the outer magnetosphere and the magnetosheath has been confirmed on the basis of electron data. Observational data have established that there is a layer of energetic electrons (E > 20 keV) over most of the magnetospheric surface, which lies primarily outside the magnetopause (e.g., Meng and Anderson, 1970, 1975; Baker and Stone, 1977a, b, 1978; Domingo et al., 1978). Energetic electrons have also been observed inside the magnetopause, in association with the boundary layer. Palmer and Hones (1978) studied the characteristics of energetic electrons in the magnetotail boundary layer at the Vela orbit. They used the directional anisotropy of the electron fluxes to infer whether the boundary layer is on closed or open field lines, and found evidence for both. Lundin et al. (1982) report that the electron spectra in the plasma mantle are generally similar to those in the adjacent magnetosheath, although locally a higher energy component may be found. Along the flanks, however, the spectra deviate significantly, possibly as a result of electrons being accelerated out of the ionosphere.

HEOS 2 low energy (10 eV - 4 keV) electron data have been used to study the high latitude boundary layer (Bavassano-Cattaneo and Formisano, 1978; Formisano and Bavassano-Cattaneo, 1978; Formisano, 1980). Electron spectra throughout the cusp (down to $\sim$ 2-3 R_E), and in the entry layer and plasma mantle are found to be similar to those in the magnetosheath (i.e., cool electrons, with E $\lesssim$ 100 eV). At lower latitudes, a somewhat warmer (E $\sim$ 100-300 eV) electron population was found, in a layer of variable thickness close to the magnetopause which tended to be thicker (up to $\sim$ 1 R_E) towards the flanks. Paschmann et al. (1976) used energetic electron (E > few keV) observations to infer that part of the entry layer is on closed field lines (see Figure 2.4).

Haerendel et al. (1978) reported that the electron spectra in the low latitude boundary layer are intermediate to those in the magnetosheath and magnetosphere, but closer to the former. Eastman et al. (1976) and Eastman and Hones (1979) confirmed from IMP 6 data that the electron spectra in the dayside boundary layer and on the flanks of the magnetosphere are similar to those in the magnetosheath (see Figure 2.6). They argued that this similarity indicates that the magnetosheath is the source of the boundary layer plasma and that the entry point is close to the point of observation. They also inferred from the pancake-shaped (i.e.,

trapped) electron distributions that the boundary layer is normally on closed field lines. Recent observations from ISEE 1 and 2 and from GEOS 2 have also shown the presence of energetic electrons, both inside and outside the magnetopause (see section 2.3.5 and Chapter 3).

2.2.5 Boundary layer composition

From its thermal properties it has long been inferred that the plasma in the boundary layer contains a component of both solar wind and of magnetospheric origin. Plasma composition experiments have since confirmed this picture. They have also shown that there is strong evidence for processes (e.g., in the ionosphere and at the magnetopause) leading to heating and/or acceleration of the cold component of magnetospheric/ionospheric plasma and that consequently plasma of internal origin makes a bigger contribution than was originally thought.

In the solar wind, the dominant ion species are H^+ and He^{++}, while the magnetospheric plasma consists primarily of H^+, He^+ and O^+, with He^+ denser than O^+ in the plasmasphere and polar wind and O^+ denser than He^+ in most other magnetospheric regions (e.g., plasma sheet, ring current, tail lobes, auroral acceleration regions). The presence of either He^+ or O^+ in the boundary layer in substantial quantities therefore indicates plasma of magnetospheric/ionospheric origin. Hardy et al. (1977) tentatively identified the presence of O^+ in the lobe plasma. Lundin et al. (1982) have reported PROGNOZ 7 ion composition measurements obtained in the plasma mantle. They report unusually high O^+ flux levels on the flanks and their results indicate a substantial ionospheric contribution. Ion composition measurements have also been obtained in the low latitude boundary layer near local noon (Lundin et al., 1982; Shelley et al., 1978; Peterson et al., 1982; Sonnerup et al., 1981). These data show the presence of a solar wind and magnetospheric ion component at the magnetopause and in the adjacent magnetosheath and boundary layer, with He^+ dominant over O^+, suggesting a plasmasphere source for the magnetospheric component (e.g., Freeman et al., 1977; Cowley, 1980). All these observations serve to illustrate that the boundary layer may be fed by keV ions of magnetospheric/ionospheric origin, e.g., directly from the ionosphere or as a result of acceleration processes in the magnetopause layer.

2.2.6 Low-altitude signature of the boundary layer

Proton measurements in the low-altitude cusp are found to show an energy-latitude dispersion (e.g., Reiff et al., 1977) and several types of signature have been distinguished. The signatures are consistent with reconnection and diffusion as the principal source mechanisms for the dayside boundary layer (e.g., Shelley et al., 1976; Reiff et al., 1977; Reiff, 1979; Burch et al., 1980). The former may be more important in terms of the instantaneous injection rate of plasma during southward IMF (Reiff et al., 1977) and evidence for the energization expected to accompany reconnection (section 2.3) has also been inferred from the observed proton distributions (Hill and Reiff, 1979). However, the exact location of the reconnection site has not been pinned down from these measurements (Burch et al., 1982; Reiff, 1984).

2.2.7 Location of entry and source mechanisms

The boundary layer has been investigated in different locations and with different instrumentation (with different time resolution) and it is therefore not surprising that its properties are found to vary. This in turn has led to a variety of source mechanisms and locations of entry being postulated for the boundary layer, which may be briefly summarised as follows.

Magnetotail boundary layer. Various authors have suggested that this boundary layer region results from diffusive penetration of magnetosheath plasma across the magnetopause, with a subsequent tailward transport of closed flux tubes along the flanks in a manner similar to that originally suggested by Axford and Hines (1961) (e.g., Hones et al., 1972; Eastman and Hones, 1979; Palmer and Hones, 1978).

Plasma mantle and lobe plasma. It is generally agreed that the plasma mantle is on open field lines. In the reconnection model, the primary source of the plasma mantle is the magnetosheath, entering the magnetosphere on the dayside and subsequently being mirrored and transported across the cusps into the tail by a convection electric field. The convection electric field is a function of the IMF orientation, which explains the correlation of thickness with the IMF (e.g., Cowley, 1980 and refs. therein). Direct entry across the tail magnetopause may also play a part, although density gaps at the magnetopause (Rosenbauer et al., 1975) show that at times the boundary forms an effective barrier locally,

preventing penetration. The observations of Lundin et al. (1982) show also that ions accelerated out of the ionosphere play a major part in the formation of the mantle.

The correlation of the lobe plasma thickness with the IMF has led to the suggestion that it is the tailward extension of the plasma mantle, and hence on open field lines (e.g., Hardy et al., 1975). It may also partly be the result of closed flux tubes transported downtail (e.g., Palmer and Hones, 1978).

Entry layer. Initially it was thought that magnetosheath plasma could enter directly into the cusps, but subsequently this idea has been replaced with more complicated entry mechanisms. Some cusp observations have been interpreted in terms of a closed model magnetosphere, in which magnetosheath plasma populates the entry layer by diffusing across the magnetopause, e.g., as the result of the Kelvin-Helmholtz instability (Hansen et al., 1976; Paschmann et al., 1976). Other authors have preferred an interpretation in terms of a combination of diffusion and reconnection (either in the cusp region or in the subsolar region), although different emphasis is placed on the relative importance of the two processes (e.g., Fairfield and Hones, 1978; Reiff et al., 1977; Haerendel et al., 1978; Crooker, 1977).

Low-latitude boundary layer. Observations in this region have aroused the most controversy in terms of both the source mechanism and location of entry. The HEOS 2 observations suggest that it is located on closed field lines (Haerendel et al., 1978). Although the entry mechanism was left unspecified, the plateaued densities suggested a non-local entry process. The cusp region was suggested as the main point of entry of magnetosheath plasma, the entry mechanism being a turbulent diffusion process with transient reconnection in the cusps as a possible by-product (e.g., Paschmann et al., 1976; Haerendel, 1978; Haerendel et al., 1978). On the basis of IMP 6 data, it was suggested that the dayside boundary layer is populated primarily by magnetosheath plasma, and that it is located predominantly on closed field lines. Entry occurs via (sporadic) local diffusion across the entire frontside magnetosphere, with the tailward transport of closed flux tubes along the flanks leading to the formation of the magnetotail boundary layer (e.g., Eastman et al., 1976; Eastman and Hones, 1979). The substantial cross-field component of the boundary layer plasma on the flanks led Eastman et al. (1976) to postulate the boundary layer as the

generator of the cusp and Region 1 field-aligned current systems (see also Sonnerup, 1980).

ISEE observations of the low-latitude boundary layer have also been interpreted in terms of a closed model magnetosphere (e.g., Eastman et al., 1982). Sckopke et al. (1981) explained the pulsed appearance of the boundary layer for the pass they examined in terms of the Kelvin-Helmholtz instability operating at the inner edge of the boundary layer. Finally, Hones et al. (1982) argued that their reverse draping signatures are consistent with high-latitude, diffusive entry of plasma and also a high-latitude boundary layer source for the Region 1 FAC (see also Paschmann et al., 1976).

Prior to the ISEE mission, the in-situ observational evidence for dayside reconnection could at best be considered somewhat ambiguous. The high-time resolution instrumentation of the ISEE 1 and 2 satellites has, however, changed this situation as will be discussed in the next part of this chapter.

2.3 In-situ Evidence for Reconnection

2.3.1 The reconnection model

Reconnection has two important consequences. Firstly, it changes the topology of the magnetic field and, secondly, it results in a conversion of electromagnetic field energy into plasma energy (usually a combination of increased thermal energy and accelerated flows). As yet, there is no general reconnection model which predicts and treats all aspects of the magnetic field structure and plasma properties existing at the boundary between two magnetized, collision-free plasmas, i.e., the dayside magnetopause in the magnetospheric context (see, e.g., reviews by Sonnerup, 1979a,b; Vasyliunas, 1975; Cowley, 1980,1982). However, following work done by Petscheck (1964), Levy et al. (1964) described a reconnection model which qualitatively treats the asymmetric plasma conditions at the dayside magnetopause, i.e., a cool, dense plasma on the one side (the magnetosheath) and a hot, dilute plasma on the other side (the magnetosphere). This model, which is the one usually adopted to compare satellite observations with (e.g., Sonnerup, 1981), is pictured schematically in Figure 2.8. This figure shows the two-dimensional geometry and time-independent electromagnetic field configuration expected for reconnection occurring in the subsolar

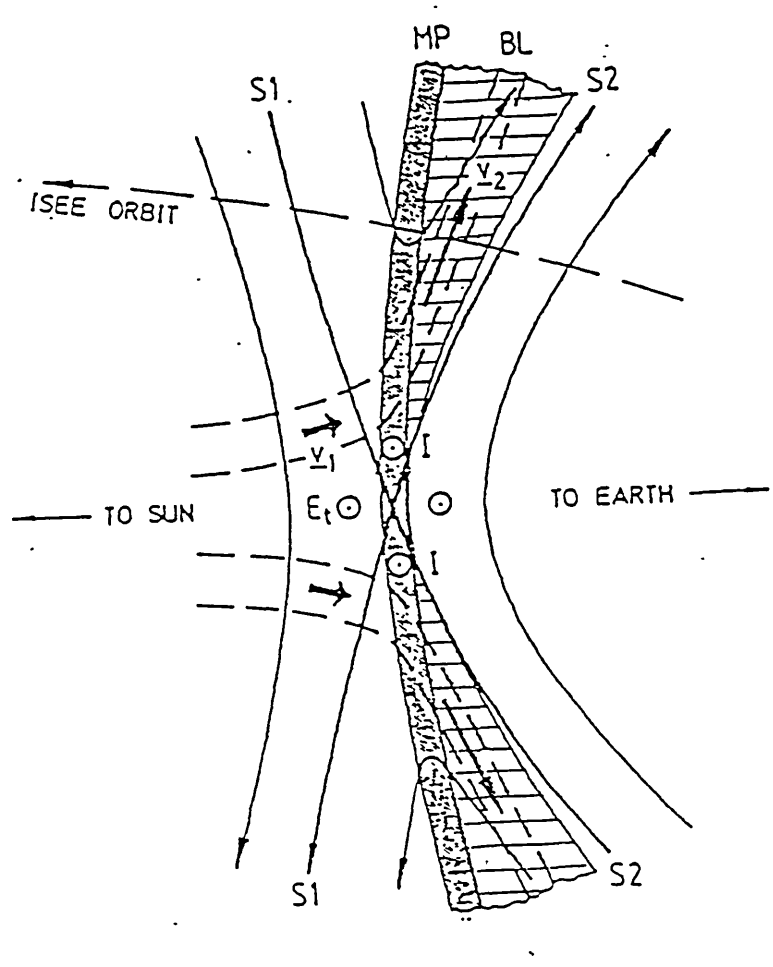


Figure 2.8. Dayside reconnection configuration (Sonnerup et al., 1981).

region, with the external (magnetosheath) and internal (magnetospheric) fields antiparallel to each other, i.e., due south and north respectively. As a result of reconnection, the magnetosheath and magnetospheric field lines are connected to each other across the magnetopause layer (shown shaded). The lines S_1 and S_2 (which form surfaces in 3-D) separate the resulting open field lines from the external and internal unreconnected field lines and are referred to as separatrices. The point (line in 3-D) of intersection between the two separatrices S_1 and S_2 forms the actual reconnection site and is known as the reconnection line (or separator or X-line). The region surrounding the reconnection line in which the break-down of the frozen-in condition occurs (i.e., where resistive effects become important) is termed the diffusion region. The diffusion region, which in the magnetospheric context is expected to be small ($\lesssim$ 1000 km), is surrounded by the much larger convection region in which the frozen-in

equation is applicable. Also in the model, two standing waves emerge from the diffusion region. The external standing wave is an intermediate (large-scale Alfvén) wave and is identified with the magnetopause. The internal standing wave is a slow mode expansion wave and is expected to coincide approximately with the inner edge of the boundary layer. The boundary layer in this model is located entirely on open field lines.

We shall now look at some ISEE observations which illustrate various features of the model in Figure 2.8 and which provide strong evidence for the occurrence of quasi-steady dayside reconnection in the subsolar region in the manner originally envisaged by Dungey (1961) and Levy et al. (1964).

2.3.2 Magnetic structure of the magnetopause

Simple MHD theory predicts that the magnetopause in an open field model magnetosphere should have the structure of a rotational discontinuity, for the simple reason that this is the only MHD discontinuity which allows a finite normal field component as well as an arbitrary change in angle of the tangential field component across it (e.g., Landau and Lifshitz, 1960). In the magnetic field data, a rotational discontinuity is characterized by the following features:

(1) the magnetic field component perpendicularly outward from the magnetopause, B_N, has a finite, non-zero value. Inspection of Figure 2.8 will show that B_N has a negative (positive) value for a satellite crossing which occurs above (below) the reconnection line;

(2) provided the pressure remains isotropic (e.g., Hudson, 1970), the magnitude of the tangential field component stays constant as the magnetic field reverses in direction across the magnetopause.

For reasonable reconnection rates the magnitude of B_N is expected to be a few nanoteslas, i.e., an order of magnitude smaller than the tangential component (e.g., Yang and Sonnerup, 1977; Cowley, 1982). This small value of B_N therefore requires an accurate determination of the direction of the outward normal to the magnetopause, $\hat{\underline{N}}$. For a 1-D magnetopause model (i.e., no large attitude variations), the relation $\nabla.\underline{B} = 0$ requires that B_N should remain constant across the magnetopause. However, in practice it is not possible to determine a direction which allows for a strictly constant B_N, so that the direction which yields

minimum variance for B_N, $\hat{\underline{N}}_3$, is used as an approximation to the actual magnetopause normal, $\hat{\underline{N}}$. The direction of $\hat{\underline{N}}_3$ is determined by a technique known as minimum variance analysis (see Appendix B for more details).

Table 1 summarises the results obtained by applying the minimum variance analysis technique to five magnetopause crossings identified as reconnection events on the basis of magnetic field and plasma data by Gosling et al. (1982) and Sonnerup et al. (1981). Minimum variance analysis determines the mutually perpendicular unit vector directions of the minimum ($\hat{\underline{N}}_3$), intermediate ($\hat{\underline{N}}_2$) and maximum ($\hat{\underline{N}}_1$) variance of the magnetic field vectors across the magnetopause, as well as their associated eigenvalues λ_3, λ_2 and λ_1. For accurate determination of $\hat{\underline{N}}_3$, the ratio λ_2/λ_3 should be as large as possible. The unit vectors $\underline{N}_1$ and $\underline{N}_2$ are approximately tangential to the local magnetopause surface and for typical field conditions on the dayside point approximately northward and dawnward (westward), respectively. The quantities tabulated in Table 1 are explained in the footnotes (see also Appendix B for details of their derivation). The time interval corresponds to the maximum interval over which the analysis was performed; within this interval several attempts to determine $\hat{\underline{N}}_3$ were made and the results of the most accurate determination are tabulated. The intervals include data points from the whole of the magnetopause current layer, as well as measurements obtained adjacent to it. Medium resolution magnetic field data from ISEE 1 and 2 were used, which are obtained as 12-sec averages overlapped by two-thirds, i.e., one data point every 4 secs. The quantity s, first introduced by Sonnerup and Cahill (1968) is given by $s = \sigma/\overline{B}$, where $\overline{B}$ is the average field magnitude and σ is the standard deviation of individual B measurements from $\overline{B}$. It gives a measure of the variation in field magnitude across the magnetopause current layer and is zero if B stays constant.

Figures 2.9 - 2.13 show magnetic field data from the five magnetopause crossings, displayed in the form of hodograms. Alongside each set of hodograms, the time variation of the B_3 component is also plotted. A hodogram is a projection of the magnetic field onto a plane, and Figures 2.9 - 2.13 show the locus traced out by the tip of the field vector in that plane. The left hand panels show the field trace in the N_1N_2 plane. For constant field magnitude the B_1B_2 trace should

TABLE 2.1

Minimum Variance Analysis of Magnetopause Crossings

[1]Date and Time	Satellite	[2]λ_1/λ_2; λ_2/λ_3	[3]$\hat{\underline{N}}_3$(GSM)	[4]$\Delta\hat{\underline{N}}_3.\hat{\underline{N}}_2$	[5]No. of Points	[6]$\overline{B}_3 \pm \Delta\overline{B}_3$	[7]S
22 Nov. 1979 22:00-22:13	ISEE 1	33.0; 3.2	0.559, -0.800, -0.217	4°	60	-4.8±2.2 (-4.2±2.0)	0.03
22 Nov. 1979 23:43-23:53	ISEE 1	27.4; 64.6	0.794, -0.608, -0.020	1°	45	-1.6±0.4 (-1.9±0.3)	0.04
22 Nov. 1979 22:19-22:32	ISEE 1	28.2; 3.2	0.888, -0.459, 0.036	4°	194	-0.3±2.8 (-0.9±1.3)	0.03
3 Sept. 1978 7:06 -7:14	ISEE 2	10.0; 3.0	0.910, 0.011, 0.415	5°	120	-1.4±2.3	0.5
3 Sept. 1978 7:17 -7:23	ISEE 1	16.3; 1.9	0.904, 0.018, 0.428	11°	90	-3.9±2.5	0.4

[1] Maximum interval used for analysis
[2] Ratio of eigenvalues
[3] Direction of minimum variance in GSM
[4] Estimated error in $\hat{\underline{N}}_3$
[5] Number of data points used in analysis
[6] Average value of B_3 and its estimated error
(Average of B_3 over all ($\sim$ 4) attempts and corresponding standard deviation)
[7] Variance in field magnitude (see text)

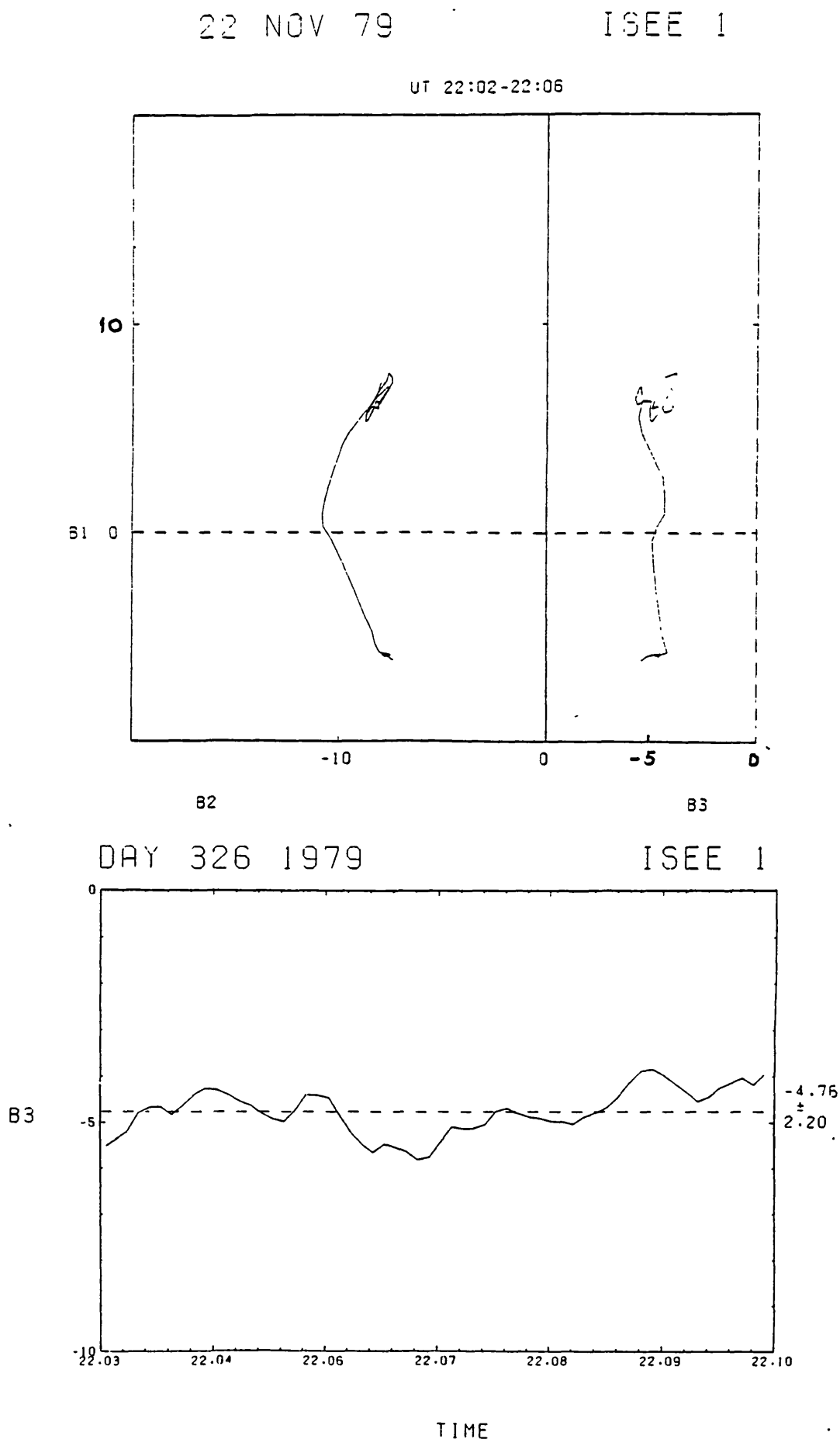


Fig. 2.9. Hodograms for a crossing on 22 November 1979.

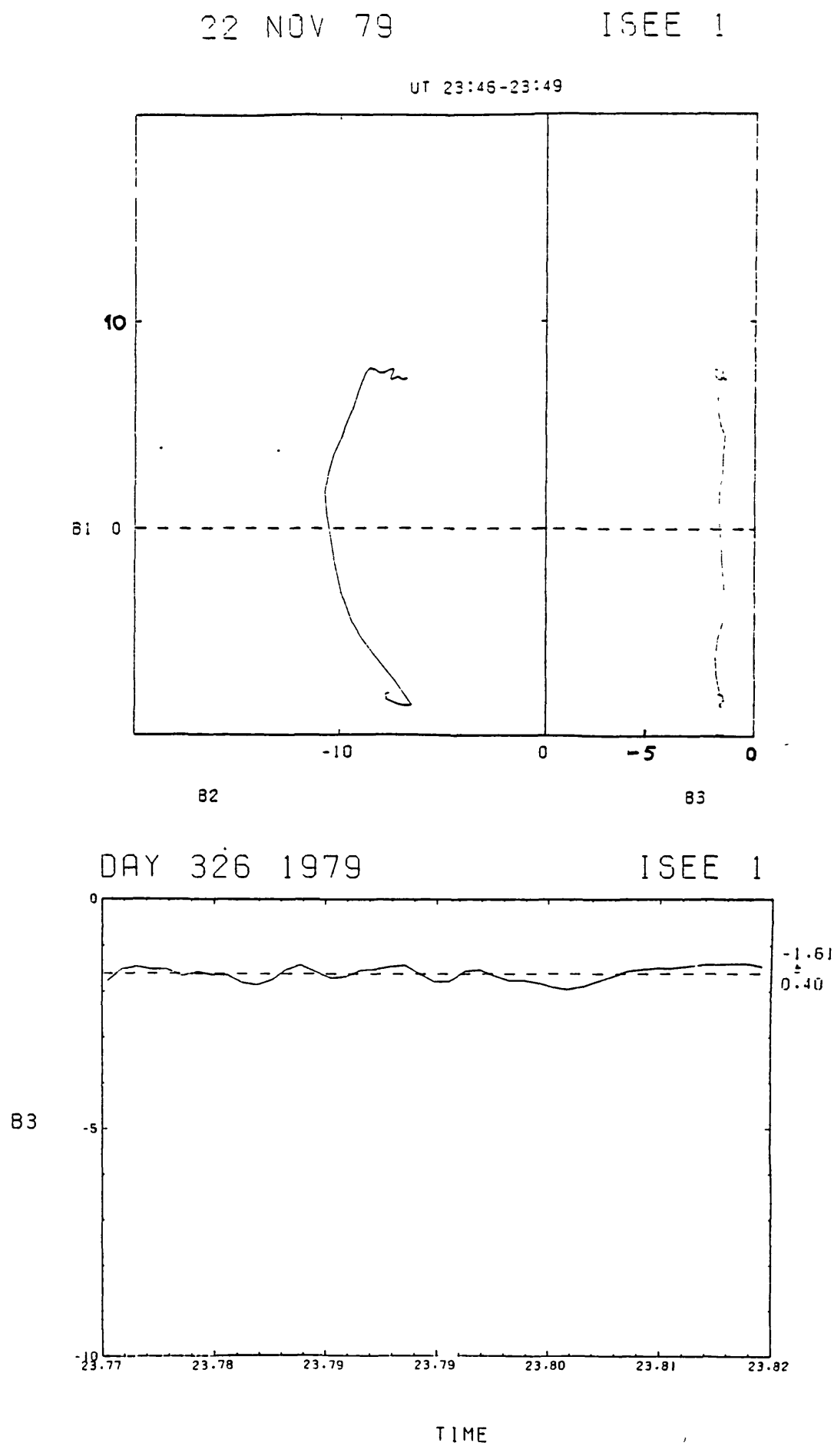


Fig. 2.10. Hodograms for a crossing on 22 November 1979.

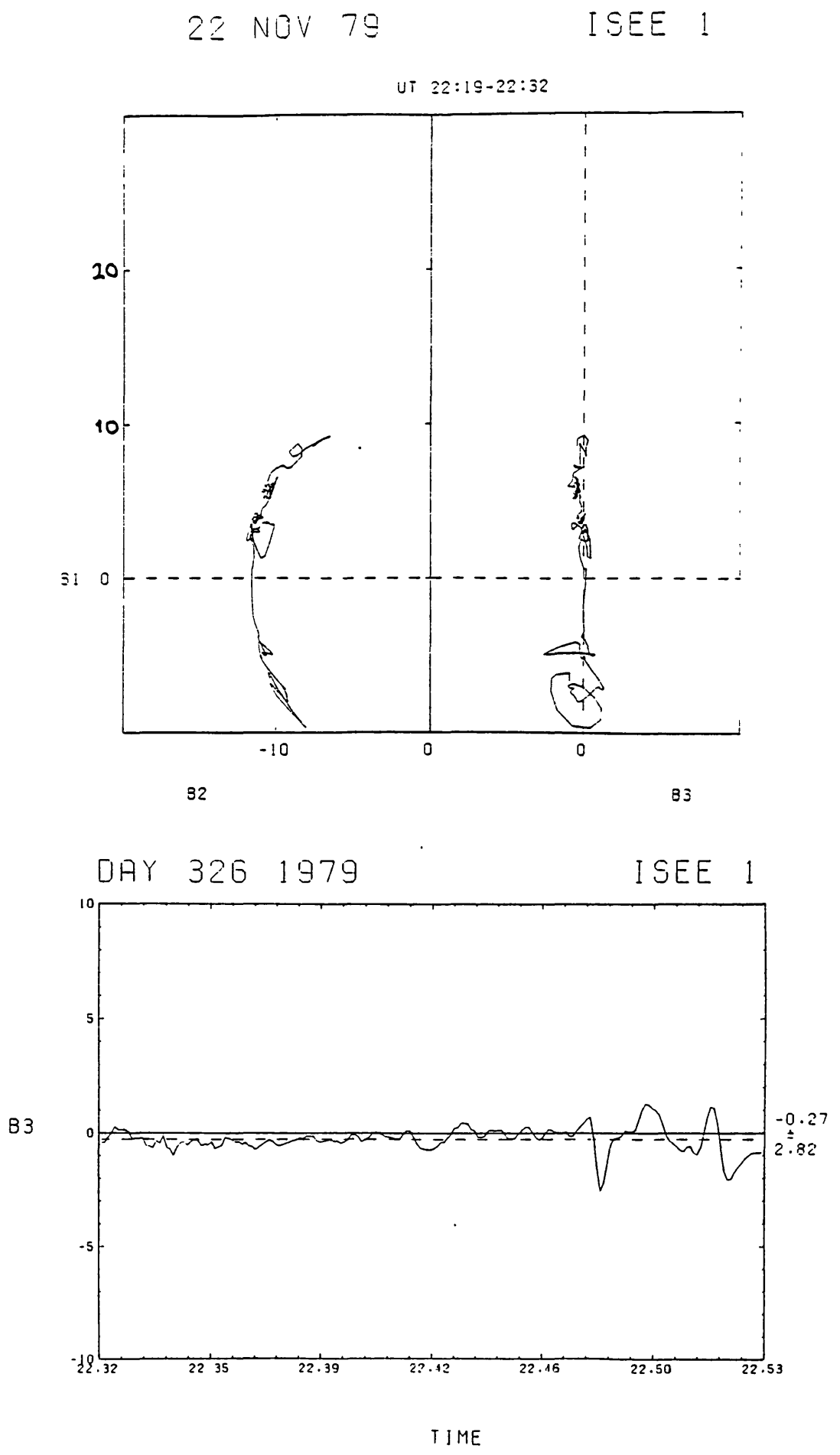


Fig. 2.11. Hodograms for a crossing on 22 November 1979.

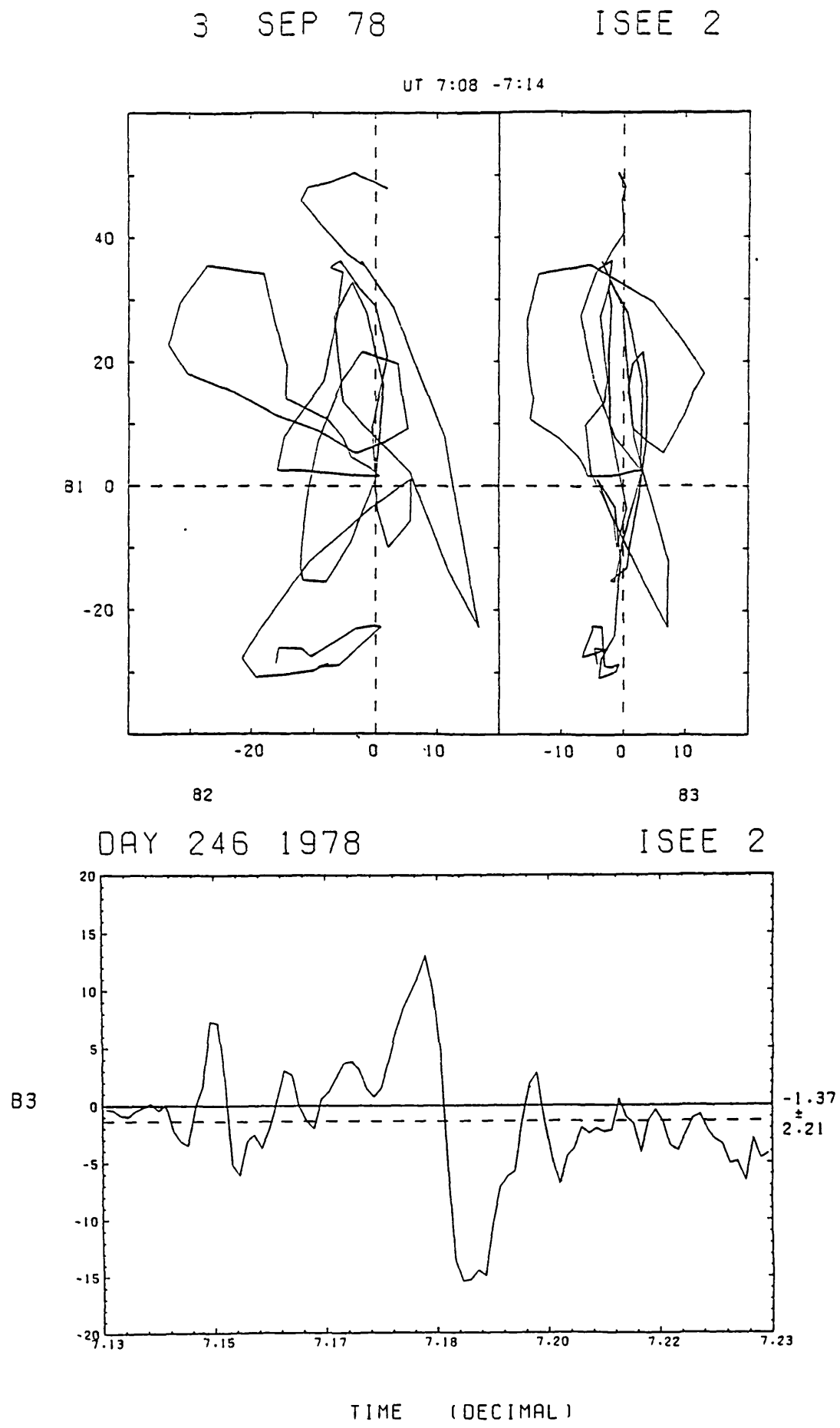


Fig. 2.12. Hodograms for a crossing on 3 September 1978.

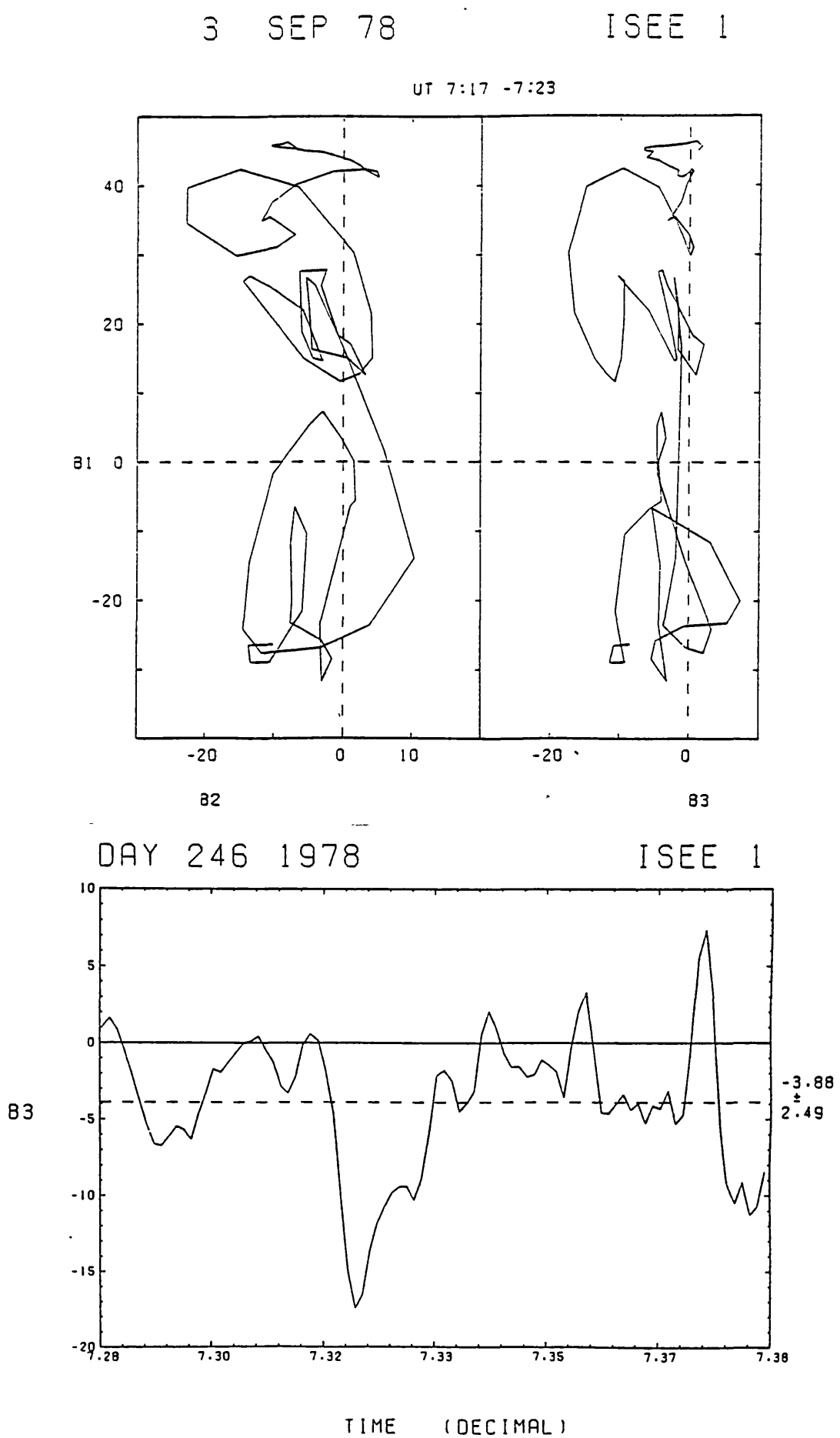


Fig. 2.13. Hodograms for a crossing on 3 September 1978.

describe an arc of a circle centred at the origin, while for constant B_N the B_1B_3 trace should approximately be a straight line parallel to the B_1 axis if $\hat{\underline{N}}$ is well determined. The two crossings in Figures 2.9 and 2.10 show good agreement with this picture. The value of B_3 and its error estimate indicates that there is a significant B_N component during these crossings. The negative value for B_N implies a crossing north of the reconnection line, a location which is also consistent with the plasma flow data (Gosling et al., 1982). Also, the magnetic field strength stays approximately constant; hence the small value for s.

The other crossings do not show such good agreement. The crossing in Figure 2.11 has a small value for s, implying a nearly constant field magnitude. However, the error estimate for B_3 is significantly larger than B_3 itself and thus a zero value for B_N is not inconsistent with these results. The situation is still worse for the crossings in Figures 2.12 and 2.13; here neither B_3 nor the field magnitude stay constant. These two crossings occurred within a short time of each other. ISEE 2, which was $\sim$ 1400 km further out along N_3, crossed the magnetopause first, and was followed $\sim$ 10 mins later by ISEE 1. The crossings in Figures 2.11 - 2.13 are all inferred to be north of the reconnection line from the plasma data and in this sense the negative values of B_3 are consistent.

The observations above illustrate that identifying the magnetopause as a rotational discontinuity on the basis of magnetic field data alone is not an easy task. Undoubtedly, part of the problem is that the magnetopause is dynamic over short time scales when conditions expected to be suitable for reconnection occur (compare Figures 2.12 and 2.13; see also Russell and Elphic, 1978; Berchem and Russell, 1983). Non-MHD effects, time and attitude variations all contribute to the difficulties in determining reliably the direction of the magnetopause normal, $\hat{\underline{N}}$. However, it is interesting to note that the normal directions obtained in Figures 2.12 and 2.13 agree closely (to within $\lesssim 0.5°$), in spite of the different time intervals and appearance of the magnetic field traces. Also apparent in Figures 2.11 - 2.13 are loop-like structures in the hodograms, which are especially evident in the B_1B_3 trace. This feature has also been noted by Gosling et al. (1982) for the crossing in Figure 2.11 and they comment that it is not caused by simple oscillation of the magnetopause. The loop-like structures

in the B_1B_3 trace show up as large-amplitude bipolar perturbations in the ~~right hand~~ bottom plots. These bipolar perturbations have a time scale of order a minute and are probably the significant reason why the value of B_N is not well-determined. An interpretation of such field perturbations is discussed in subsequent chapters.

2.3.3 Plasma flow and reconnection

Referring to Figure 2.8, the finite B_N component allows the inflowing magnetosheath plasma to cross the magnetopause to form a boundary layer region on open field lines. MHD theory for a rotational discontinuity predicts that in the frame of the magnetopause the magnitude of the plasma flow along the inward normal to the magnetopause is given by the Alfvén speed based on B_N (e.g., Hudson, 1970; Sonnerup et al., 1981):

$$V_N = \pm B_N \left[(1 - \alpha)/\mu_0\rho \right]^{\frac{1}{2}} \qquad (1)$$

Here V_N is the inflow speed, ρ is the density and α is the pressure anisotropy correction given by

$$\alpha = (p_{\parallel} - p_{\perp}) \; / \; (B^2/\mu_0) \; .$$

Assuming that the net flux of plasma is inward, as it should be because of the higher magnetosheath density, the $\pm$ corresponds to $B_N < 0$ and $B_N > 0$ respectively, i.e., V_N is always negative. The value of V_N is proportional to B_N and is therefore small compared to the tangential flow. As we saw in the previous section, the direction of the magnetopause normal is difficult to determine and therefore V_N cannot usually be determined to the required degree of accuracy to predict the flow of plasma across the magnetopause.

Reconnection also results in a conversion of electromagnetic energy into plasma energy and the effects of this energy conversion process should be much easier to observe in practice. As plasma crosses the magnetopause its momentum is suddenly changed under the action of stresses in the open field lines. If the sharply curved field lines at the magnetopause in Figure 2.8 are pictured as elastic bands, then they can be imagined to act as magnetic slingshots which catapult the plasma poleward in a narrow layer in and adjacent to the

magnetopause region. The acceleration required to produce the plasma jets is given by the $\underline{I} \times \underline{B}_N$ force, where $\underline{I}$ is the magnetopause current. Conservation of momentum requires the following relation to be satisfied (Hudson, 1970) for a rotational discontinuity:

$$\Delta \underline{V} = \pm (1 - \alpha) \Delta \underline{B} / \sqrt{\mu_0 \rho} \qquad (2)$$

where Δ refers to the change in parameter across the discontinuity. Again, the $\pm$ refers to $B_N < 0$ and $B_N > 0$ respectively. The left hand side expresses the rate at which the tangential plasma momentum changes. The right hand side gives the sum of the tangential Maxwell stresses and the stresses due to pressure anisotropy. The latter is found observationally to be small compared to the former (Sonnerup et al., 1981).

To detect observationally the jets of plasma requires 3-D plasma and magnetic field data with high time-resolution since the jets are expected to be small and highly directional (e.g., Yang and Sonnerup, 1977). The ISEE mission provided the first opportunity to test the applicability of equation (2) in detail. Paschmann et al. (1979), Sonnerup et al. (1981) and Gosling et al. (1982) have used this equation as the prime basis for testing the reconnection model with observational data at the magnetopause. They published data for twelve events in which accelerated plasma flows observed in the magnetopause and boundary layer are quantitatively consistent with tangential stress balance. The reconnection flows were observed over relatively long time scales ($\gtrsim$ 10 mins) and consequently they are commonly referred to as quasi-steady reconnection events.

2.3.4 Electric field at the magnetopause

An essential requirement for reconnection to occur is the presence of a tangential electric field $\underline{E}_t$ at the magnetopause. In fact, reconnection may be defined as occurring when a non-zero value of $\underline{E}_t$ (either electrostatic or induced) exists along the reconnection line (Dungey, 1978; Sonnerup, 1979a; Sonnerup et al., 1981; Cowley, 1984). The presence of a reconnection electric field $\underline{E}_t$ has the effect of $\underline{E} \times \underline{B}$ drifting plasma into the magnetopause layer from the adjacent regions. It also results in a conversion of electromagnetic energy into plasma energy at a rate given by $\underline{I} \cdot \underline{E}_t$, where $\underline{I}$ is the magnetopause current

(also sometimes referred to as the Chapman-Ferraro current). Referring to Figure 2.8 it can be seen that $\underline{E}_t$ is parallel to $\underline{I}$, so that $\underline{E}_t \cdot \underline{I} > 0$, which implies that reconnection results in a gain in plasma energy. It was the lack of observational evidence for such a gain in plasma energy which led some people (e.g., Heikilla, 1978) to conclude that the magnetopause is at all times an approximately equi-potential surface, and hence that reconnection does not occur. As shown in the previous section, however, the ISEE mission has resolved this question in favour of reconnection.

In the steady-state 2-D situation in Figure 2.8 the relation $\nabla \times \underline{E} = 0$ implies that $\underline{E}_t$ is constant across the magnetopause layer. The detection of $\underline{E}_t$ is difficult. Firstly it is expected to be small (proportional to B_N), with a value of order mV/m. Secondly, it needs to be measured in the frame of reference of the magnetopause since only in this frame is it required to be constant. Since the magnetopause is often dynamic on short time scales it is not always easy to find the appropriate reference frame. However, in spite of these difficulties the electric field instruments on board the ISEE 1 and GEOS 2 satellites have provided us with direct, in-situ electric field measurements at the magnetopause, which conclusively show the existence of a significant large-scale $\underline{E}_t$.

Mozer et al. (1978) established the existence of a significant ($\sim$ 2 mV/m) large-scale value of $\underline{E}_t$ for an ISEE 1 magnetopause crossing which occurred during the 20 November 1977 inbound pass while the magnetosheath field had a southward component. In combination with the magnetic field data a local power dissipation $\underline{I} \cdot \underline{E}$ of order 100 $\mu W/m^2$ was inferred (the electric field instrument only makes measurements in the satellite spin plane, essentially GSE X-Y). Also, it was found that the convection electric field drift $\frac{\underline{E} \times \underline{B}}{B^2}$ had a component towards the magnetopause from both sides, as required for reconnection. Similar results were obtained for ten out of the eleven magnetopause crossings occurring on this pass (Mozer et al., 1979). Grard et al. (1978) also obtained similar results for the magnetopause encounters observed by GEOS 2 at geostationary orbit on 28 August 1978. Fahleson et al. (1979) estimated $\underline{E}_t$ for several low latitude ISEE 1 magnetopause crossings, which occurred for different local times and magnetosheath field directions. They found the largest power dissipation ($\sim$ 200 $\mu W/m^2$) for a crossing occurring on the frontside with southward external field (10 November 1977, inbound pass). No power dissipation

was found for a corresponding crossing with northward external field.

Values of $\underline{E}_t$ similar to those above ($\sim$ 1 mV/m) were also indirectly determined from plasma and magnetic field data for the events discussed by Sonnerup et al. (1981). Finally, Aggson et al. (1983) used ISEE 1 electric field measurements to measure large magnitude convective flow changes at the magnetopause (in analogy with the plasma flow measurements discussed in the previous section) and identified several magnetopause crossings as rotational discontinuities. Their results also indicate that the reconnection rate may vary significantly over short time scales, so that the process may be regarded as impulsive.

Few comparisons have been made between the results obtained from electric field, magnetic field, wave and plasma data so that the question is not yet resolved what forms of energy the electromagnetic energy is converted into. However, possible sources of electromagnetic power dissipation include the following:

- plasma acceleration at the magnetopause and in the boundary layer (e.g., Sonnerup et al., 1981; Gosling et al., 1982);
- heating of plasma, either of magnetospheric or magnetosheath origin (e.g., Petersson et al., 1982; see also discussion by Cowley, 1980, 1982);
- production of layers of streaming, energetic electrons observed outside the magnetopause (e.g., Baker and Stone, 1977).

Ogilvie and Scudder (1979) report observing a significant electron heat flux during the 20 November 1977 crossings. Finally, Paschmann et al. (1983) have checked the energy balance for the 9 August 1978 and 8 September 1978 reconnection events and their results confirm the conclusions based on tangential momentum balance considerations. They also find that the enthalpy (random heating) energy increase and the kinetic energy increase of the plasma are of comparable importance.

2.3.5 Energetic particle signatures

Energetic ($\gtrsim$ 20 keV) particles have been used both to remote sense various magnetospheric boundaries, such as the magnetopause, the plasma-sheet, the outer separatrix and the trapping boundary (usually identified with the last closed field line), and also to probe the topology of magnetic fields (e.g., Daly, 1982; Scholer, 1983). In particular, energetic particle signatures have been used successfully to confirm that magnetopause crossings identified as reconnection events on the

basis of plasma, magnetic and electric field data have the required magnetic topology shown in Figure 2.8. As shown in Figure 2.8, the incoming magnetosheath particles interact with the magnetopause and then accelerate poleward in the region between the two separatrices. A fraction of the particles are transmitted across the magnetopause to form the boundary layer (on open field lines), while the rest will be reflected back into the region between the magnetopause and the outer separatrix S_2. For crossings north (south) of the reconnection line, the transmitted magnetosheath particles stream parallel (anti-parallel) and the reflected particles stream anti-parallel (parallel) to the local field direction. The magnetospheric (hot ring current or cold plasmaspheric) particles drift towards the magnetopause from the inside and are also accelerated in their interaction with the magnetopause. Again, an individual particle may either be transmitted across the magnetopause or reflected back into the magnetosphere. The magnetospheric particles leaking out into the magnetosheath stream anti-parallel (parallel) to the field direction, while reflected particles stream parallel (anti-parallel) to the magnetospheric field direction for a crossing north (south) of the reconnection line. The conditions which determine the exact fraction of magnetosheath or magnetospheric particles being transmitted or reflected are as yet unknown.

Scholer et al. (1981) and Sonnerup et al. (1981) have presented energetic ion data obtained outside the magnetopause during several of the crossings identified as reconnection events on the basis of tangential stress balance conditions. Their observations are consistent with the picture in Figure 2.8. In particular, ions which were inferred to be of magnetospheric origin because of the similarity of their spectra to those found inside the magnetosphere were found in the magnetosheath and were used to define the outer separatrix. These ions were also found to stream anti-parallel to the field for the crossings inferred to be north of the reconnection line from the plasma and field data, and parallel to the field for the one case observed south of the reconnection line. Sonnerup et al. (1981) also found one instance of a significant reflected magnetosheath ion component. This reflected component constituted 20% of the total number density and 20% of the converted electromagnetic energy (Paschmann et al., 1983). It also showed a streaming direction anti-parallel to the magnetic field, consistent with the inferred northward location of the crossing

relative to the reconnection line.

Energetic particle signatures inside the magnetopause have also been reported. Williams and Frank (1980) used observations of 3-D ion and electron distributions from ISEE 1 to infer the magnetic field geometry inside and close to the magnetopause during the 20 November 1977 inbound pass. Their data showed instances where ISEE 1 encountered field-aligned energetic ion asymmetries in association with marked changes in the plasma flow. They explained their results in terms of encounters with open field lines, albeit with a spatially and/or temporally varying geometry in view of the variability of the observed signatures. The direction of ion streaming was consistent with a satellite location south of the reconnection line. Scholer et al. (1982) and Eastman and Frank (1982) extensively studied the high-speed flow region of the boundary layer during the 8 September 1978 reconnection event. The ions in this region streamed anti-parallel to the field, consistent with the satellite location north of the reconnection line. The energetic electron data, however, displayed trapped distributions throughout most of the boundary layer and a sharp intensity cut-off at the magnetopause. Eastman and Frank (1982) interpreted the trapped electron observations as indicating closed field lines, and consequently placed the high-speed flow region on closed field lines. They suggested that the ion streaming is a result of ions which travel along field lines from the Southern Hemisphere having to travel a larger distance to the satellite observation point. The longer path length then increases the likelihood of these ions escaping across the magnetopause at some point in their trajectory, e.g., as a result of boundary motions. The observed ion azimuthal distributions are not consistent with this interpretation, however. Instead, Daly and Fritz (1982) showed that the electron observations are consistent with Figure 2.8 if it is assumed that the electrons are trapped as a result of adiabatic mirroring. Indeed, a field strength minimum was observed at the magnetopause. The ions are not similarly trapped because they do not satisfy the requirements of adiabaticity: their gyroradius (of order the magnetopause thickness) and bounce period are much larger than that of the electrons. Scholer and Ipavich (1983) have presented observations from the 5 July 1978 reconnection event which show the acceleration of magnetospheric particles at the magnetopause and subsequent reflection back of a

fraction (∿ 10-50%) of the incident particles. Finally, Korth et al. (1983) reported measurements of energetic ion and electron distributions obtained from GEOS 2 during the strong compression of the magnetosphere on 28 August 1978. They found field-aligned, anti-parallel streaming of the energetic electrons and ions (of magnetospheric origin), both inside and outside the magnetopause. Such a streaming direction is consistent with an inflow and outflow of magnetospheric particles along a northerly connected open field line, i.e., a satellite crossing north of the reconnection line (Fig. 2.8).

A question which is still not fully resolved is why the energetic particles should be observed at all. For typical conditions at the magnetopause, the bounce period of an energetic ion and electron is of order ∿ 1 min and 1 sec, respectively. They should therefore be lost quickly. In order to explain why they are observed over longer time scales various resupply mechanisms have been suggested (e.g., Scholer et al., 1981; Daly and Fritz, 1982; Korth et al., 1983). For example, if the reconnection rate is fast enough the spacecraft continuously samples newly opened flux tubes which resupply the energetic particle reservoir.

CHAPTER 3

FLUX TRANSFER EVENTS

3.1 Introduction

In the previous chapters we have seen that Dungey's reconnection model of the magnetosphere provides a unifying concept for many features of the magnetosphere. Theoretically, magnetic reconnection was first considered as a large-scale, quasi-stationary process (e.g., Levy et al., 1964; Vasyliunas, 1975). In-situ observations at the dayside magnetopause using high time resolution, 3-D plasma and magnetic field data from ISEE 1 and 2 have given us convincing experimental confirmation of the signatures expected from such a process.

The suggestion that reconnection might occur as a transient and patchy process at the magnetopause was first made observationally on the basis of HEOS 2 data by Haerendel et al. (1978, see Figure 2.5). These observations will be discussed in more detail in Chapter 6. Other evidence for such a process can be found in the large fluctuations which occur in the normal field component B_N during magnetopause crossings (e.g., Figures 2.12 and 2.13). In this chapter we shall consider the expected signatures of an impulsive and small-scale reconnection process based on a very simple model. We shall then compare the resulting picture with observations obtained from ISEE 1 and 2 and make some suitable modifications in the light of these observations. We shall only consider case event studies. A statistical survey of such impulsive reconnection signatures will be the subject of the next chapter.

3.2 Impulsive Reconnection: Expectations

3.2.1 Magnetosheath

Figure 3.1 shows a section of the Earth's frontside magnetopause as viewed by an observer on the Sun. The diagonal (red) arrowed lines

are the magnetosheath magnetic field lines overlying the plane of the paper, i.e., the magnetopause, and they have a southward and duskward (eastward) orientation in this instance. The vertical (black) arrowed lines show the northerly directed magnetospheric magnetic field lines underlying the magnetopause. The two tubes show sections of two isolated open flux tubes, which are the result of a localised burst of reconnection somewhere in the subsolar region, roughly in the middle of the diagram. A satellite encountering either of these open flux tubes can expect to see some characteristic magnetic field and plasma signatures.

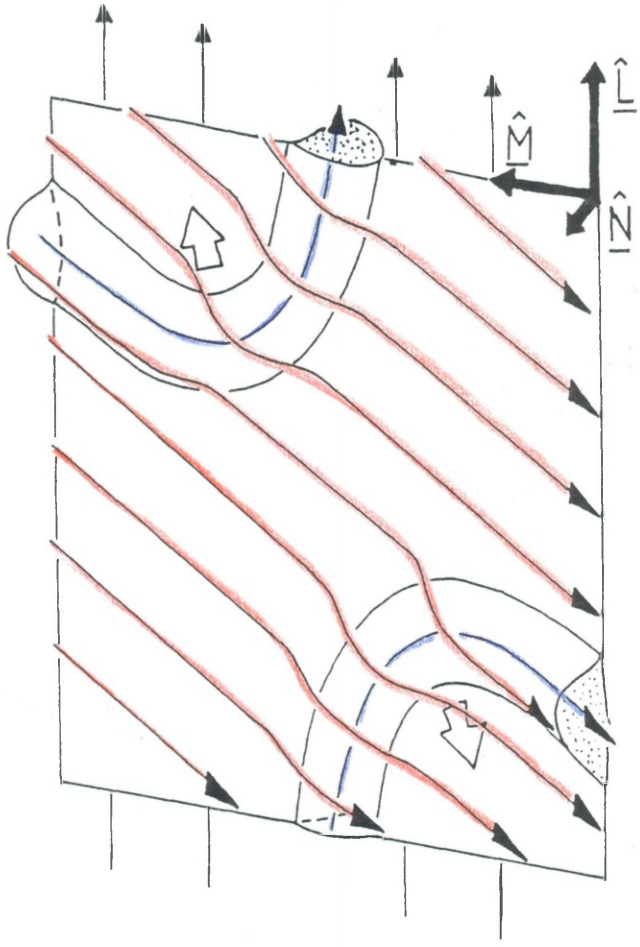


Figure 3.1. Magnetosheath FTE.

In the initial stages of reconnection the two bundles of open field lines have a very sharp kink where the tubes cross the magnetopause. Magnetic tension in the open field lines will try to blunt the kink with the result that the two open flux tubes try to move away from

their initial reconnection site, roughly in the direction indicated by the two broad open arrows. The speed at which the flux tubes shorten is of order the Alfvén speed (cf. section 2.3.3). For conditions at the magnetopause, this speed ($\sim$ 100 km s^{-1}) is much larger than the satellite velocity ($\sim$ 2 km s^{-1}), and the satellite can therefore be considered a stationary observing point. However, the ambient magnetosheath plasma flows at a speed comparable to the rate of shortening of the flux tubes. The satellite will therefore see a flux tube move past at a velocity determined by the vector addition of the magnetosheath plasma flow and the magnetic tension release.

If we consider a reconnection site in the subsolar region, then we can see in Figure 3.1 that the flux tube connected to the Earth's Northern Hemisphere will move northward, while the southerly connected tube will move southward. As the flux tubes move poleward, the surrounding unreconnected magnetic field lines are swept out of the way and drape over the bulges formed by the tubes. A satellite in the magnetosheath which encounters the northward moving, northerly connected flux tube will see the draped field lines tilt out of the plane of the magnetopause (i.e., out of the plane of the paper in Figure 3.1) as the tube approaches, while in the wake of the tube it will see the draped magnetosheath field lines tilt into the plane of the magnetopause, towards the Earth. Conversely, a satellite which encounters the southward moving, southerly connected flux tube will sense field perturbations in the opposite sense, i.e., a field tilt towards the Earth on approach of the tube, and a tilt away from the Earth as it recedes. Also, in the arm of the flux tubes which juts out into the magnetosheath (i.e., the part which is approximately aligned with the magnetosheath field direction) the open field lines are pulled from their magnetosheath orientation to a more northerly, magnetospheric orientation. A satellite entering one of these flux tube arms will therefore observe such a field rotation.

The open field lines inside the two flux tubes provide a path which enables magnetosheath plasma to enter the magnetosphere while at the same time allowing magnetospheric plasma to leak out into the magnetosheath. A satellite entering a flux tube should therefore detect a mixture of particle populations of magnetosheath and magnetospheric origin. The direction of motion of the tube should be a good indicator of the bulk velocity of the plasma inside, which in general

may be different from the ambient magnetosheath velocity as a result of magnetic tension release in the flux tube. Energetic particles of magnetospheric origin may be used to trace the open field line topology in a way similar to that discussed in section 2.3.5. The particles should stream antiparallel to the local field direction inside the flux tube connected to the Northern Hemisphere and parallel to the field inside the southerly connected tube (Figure 3.2).

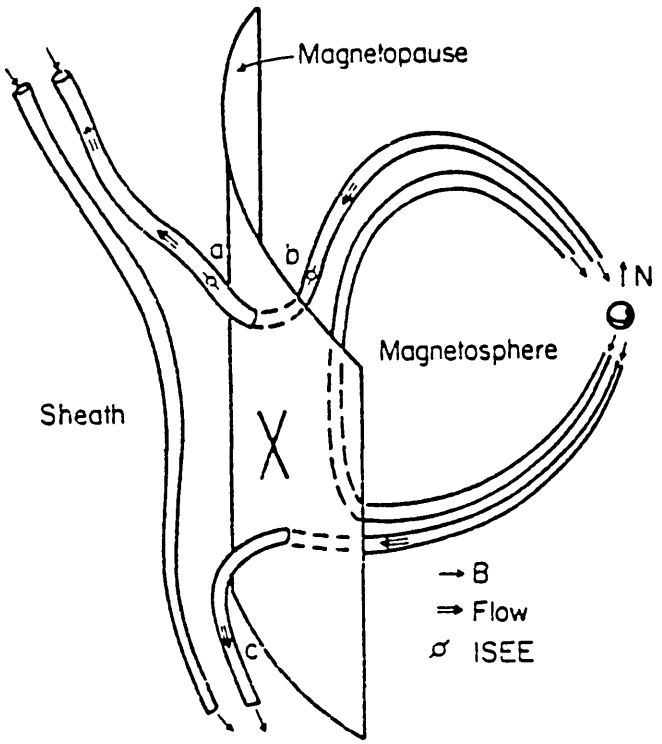


Figure 3.2. Particle streaming inside FTEs (from Speiser and Williams, 1982).

3.2.2 Magnetosphere

Figure 3.3 shows the view of the magnetopause corresponding to that shown in Figure 3.1, but this time as seen by an observer on the Earth facing the Sun. This time the magnetospheric field lines overlie the plane of the Figure (i.e., the magnetopause) while the

magnetosheath field lines underlie it. Inspection of this figure will show that a satellite located in the magnetosphere sees qualitatively the same signatures as one located outside, in the magnetosheath. The field perturbations caused by unreconnected magnetospheric field lines draping over the moving flux tubes are in the same sense as those observed in the magnetosheath, i.e., a tilt away and then toward the Earth for a northward moving tube and tilts in the opposite sense for a southward moving tube. Inside the magnetospheric arm of the flux tubes (i.e., the part approximately aligned with the magnetospheric field direction) the field is pulled towards the field orientation in the magnetosheath. Inside the magnetospheric arm of the flux tubes we should also see evidence for plasma mixing and particle streaming, as before.

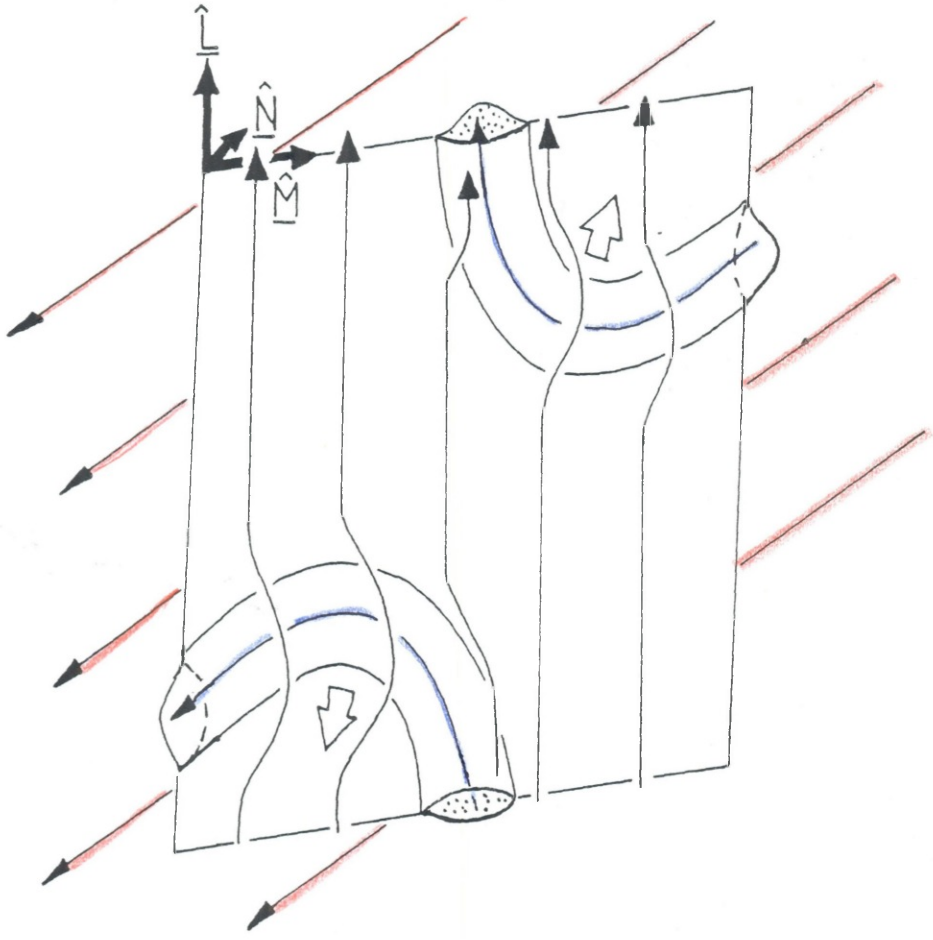


Figure 3.3. Magnetosphere FTE.

3.3 Impulsive Reconnection: Observations

3.3.1 Magnetic field signature

A requirement for the successful identification of the magnetic field signature discussed in the previous section is the use of a special coordinate system to plot the data in. The boundary normal coordinate system, first introduced by Russell and Elphic (1978), consists of three mutually orthogonal components L, M and N, as illustrated in Figure 3.4. This coordinate system is referenced to the local magnetopause surface and it hinges on a successful determination of the direction of the normal to the magnetopause at the satellite location (see Appendix B). The N-component is perpendicular to the magnetopause and points outward, away from the Earth. The L- and M-components are tangential to the magnetopause surface in such a way that the L-N plane contains the GSM Z-axis. $\hat{L}$ and $\hat{M}$ point roughly northward and dawnward, respectively, along the frontside magnetopause.

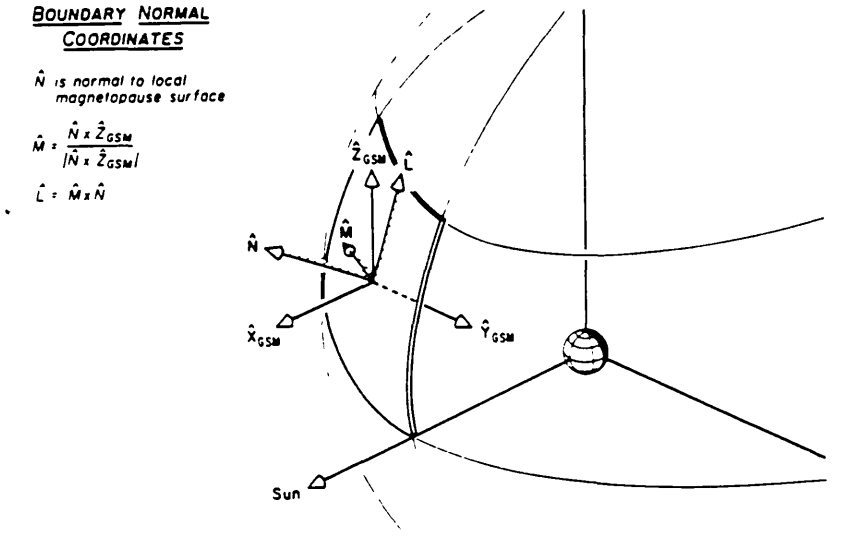


Figure 3.4. Boundary normal coordinates.

Figure 3.5 shows a sixty-minute plot of medium resolution magnetic field data (12 sec averages overlapped by two thirds and plotted every 4 sec) obtained from ISEE 1 (heavy line) and ISEE 2 (thin line) during an inbound pass of the dayside magnetopause region on 8 November 1977. The four panels show from top to bottom the L, M and N components of the magnetic field and the total field strength B, all in units of a nanotesla. The horizontal axis gives the Universal Time (UT) in hours and minutes. Below it, the spacecraft location is given as the radial distance R (units of an Earth-radius), the local time LT (hours and minutes) and northerly latitude LAT (degrees) in GSM coordinates.

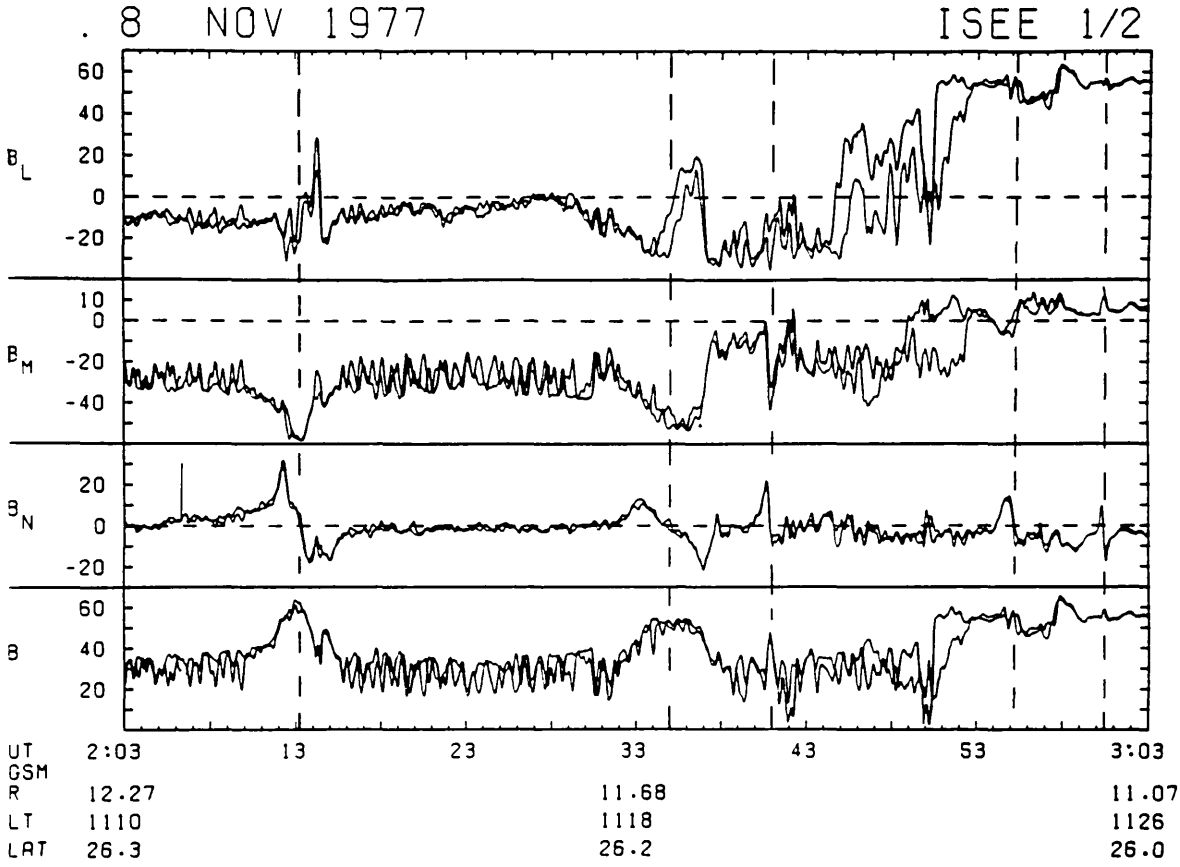


Figure 3.5. FTEs on 8 November 1977.

At the start of the interval both ISEE 1 and 2 are in the magnetosheath, where the magnetic field points southward and duskward, i.e., B_L and B_M are both negative. At the end of the interval both

satellites are inside the magnetosphere, where the magnetic field has its expected northward orientation, i.e., B_L is positive. The main magnetopause crossing occurs at ∿ 2:50 and at ∿ 2:53 UT for ISEE 1 and 2 respectively, which at this time are separated by ∿ 300 km along the boundary normal $\hat{N}$. The crossing occurs close to noon at a northerly latitude of ∿ 26°. Prior to the magnetopause crossing there are two prominent events in the magnetosheath at ∿ 2:13 and ∿ 2:35 UT which are seen by both ISEE 1 and 2 and which in some respects look like partial magnetopause crossings: the B_L component goes positive and the field strength B reaches magnetospheric values during the events. However, the B_N component shows a characteristic bipolar signature, increasing first to large positive values and then decreasing to large negative values before returning to zero again. In other words, the field tilts first away from the Earth and then towards it. The B_M component, in contrast to its behaviour during the later magnetopause crossing, becomes more strongly negative during the events. The net result of the B_L and B_M deflections is that the tangential field component rotates to a direction intermediate to that observed in the magnetosheath and in the magnetosphere. This set of magnetic field signatures is therefore consistent with an interpretation in terms of an encounter with a northward moving open flux tube as discussed in the previous section. Magnetosheath magnetic field signatures such as are observed at 2:13 and 2:35 UT were termed flux transfer events (FTEs) by Russell and Elphic (1978), who were the first to discover them in the ISEE data. Note in Figure 3.5 that other FTEs also occur at ∿ 2:41 UT in the magnetosheath and at 2:55 and 3:00 UT in the magnetosphere. The magnetospheric FTEs show the same positive-negative B_N signatures as the magnetosheath FTEs.

Figure 3.6 shows a one-hour plot of magnetic field data obtained during an inbound pass on 10 November 1977. As a result of boundary motions the magnetopause is crossed three times at 14:39, 14:47 and 14:58 UT during this pass. The magnetopause encounters occur close to noon at a northerly latitude of ∿ 20°. The magnetosheath magnetic field again has a southward and duskward orientation. Characteristic FTE signatures consisting of positive-negative B_N perturbations can be identified in the magnetosheath at ∿ 14:36, 14:38 and 14:55 UT, at the magnetopause at ∿ 14:47 and 14:58 UT and in the magnetosphere at ∿ 15:03 and 15:16 UT. All the FTE B_N signatures are accompanied by an

enhancement in field strength over ambient values as well as a deflection in the tangential field components B_L and B_M. However, note that the tangential field tilt is not always such as to cause a rotation of the field towards the direction of the field on the opposite side of the magnetopause, e.g., at 14:36, 15:03 and 15:16 UT. This is contrary to expectations based on the model described in the previous section.

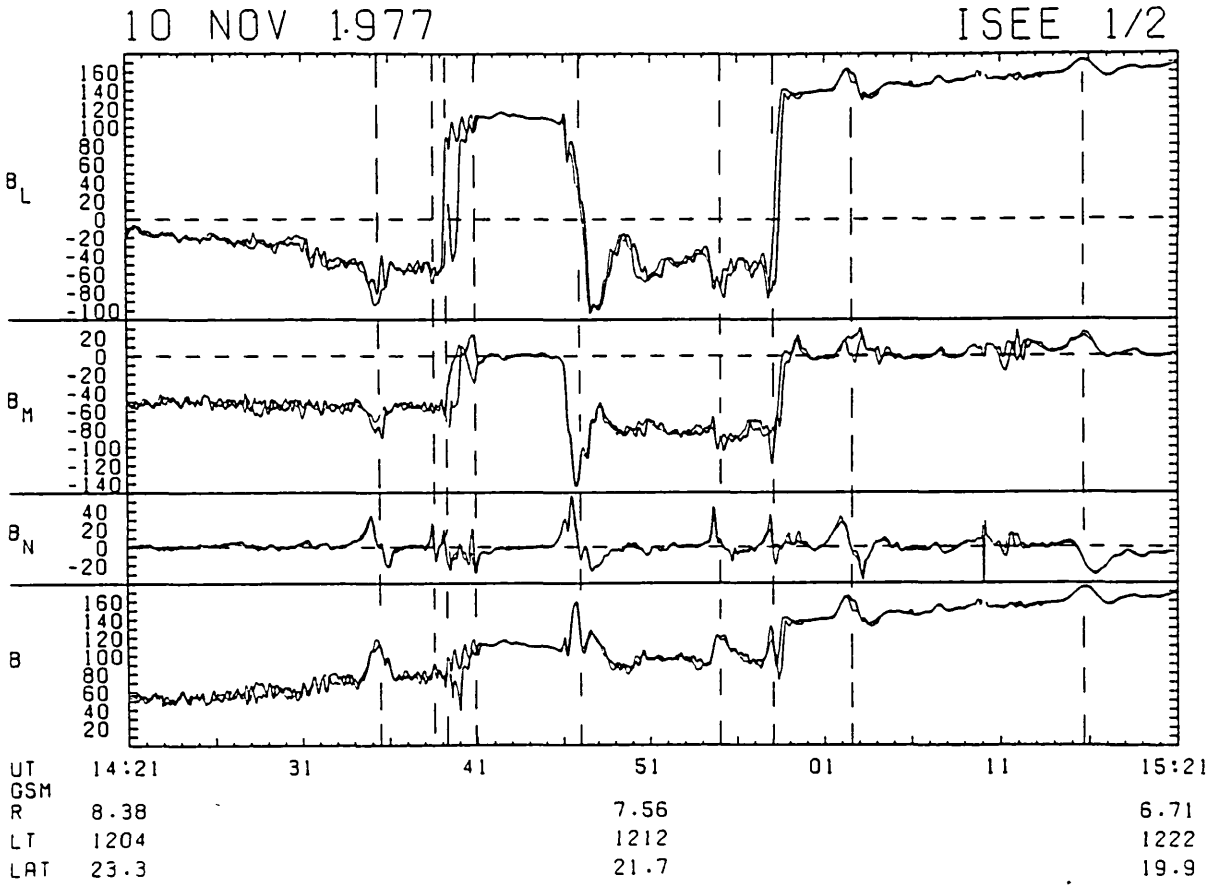


Figure 3.6. FTEs on 10 November 1977.

3.3.2 Energetic particle signatures

Scholer et al. (1982) analysed the energetic particle behaviour during the FTEs observed on 8 November 1977 (Figure 3.7). The top four panels show the plasma density N_p in cm^{-3} (obtained over the total instrumental energy range) and the magnetic field data in boundary normal (LMN) coordinates, all obtained from ISEE 1. The bottom two

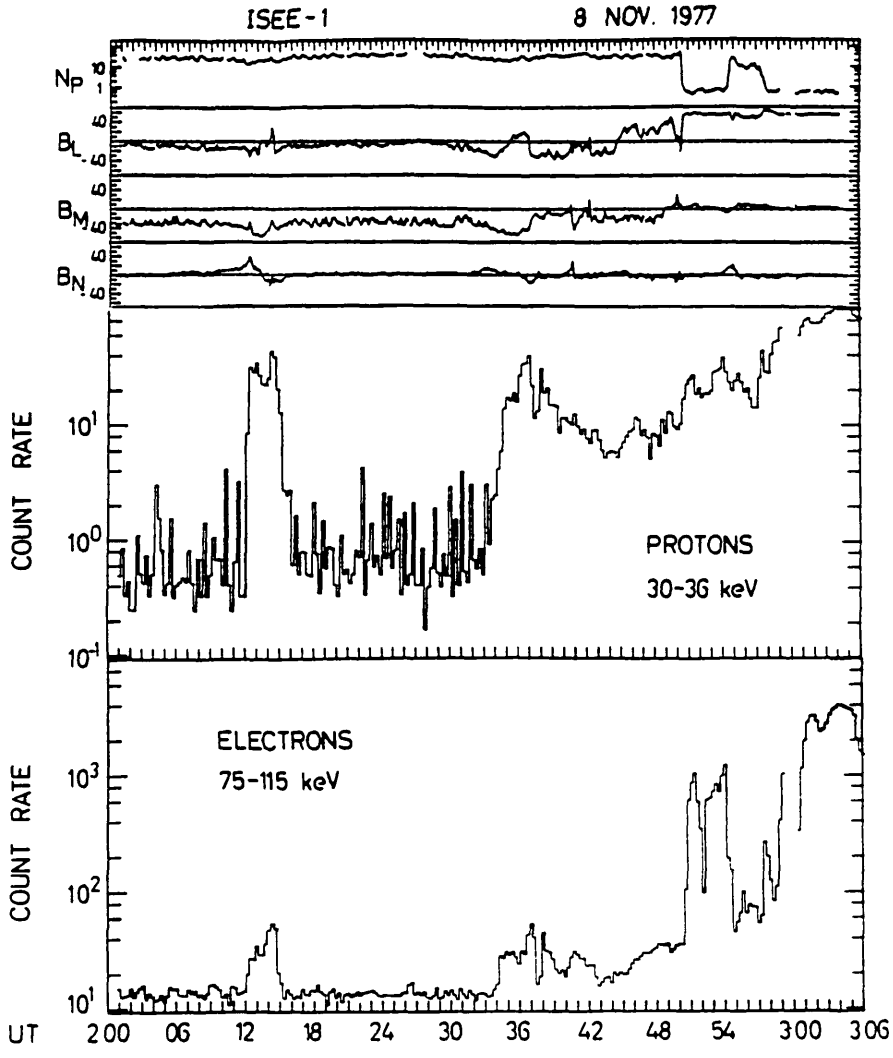


Fig. 3.7. Energetic particle data for FTEs (Scholer et al., 1982).

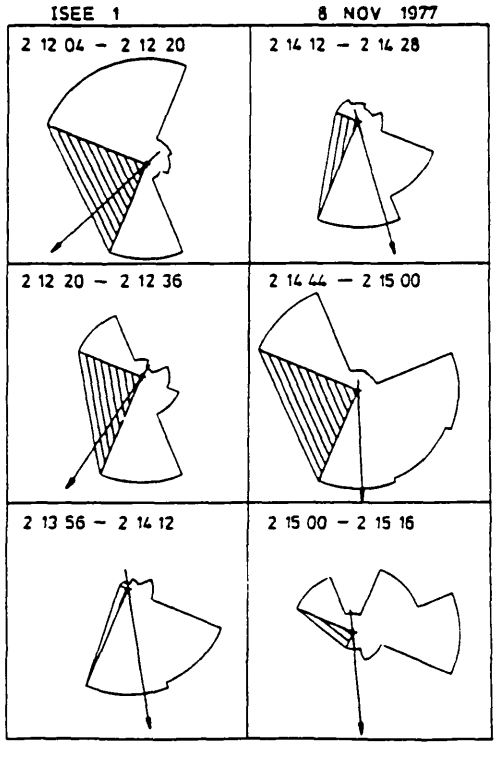


Fig. 3.8. FTE energetic proton distributions (Scholer et al., 1982).

panels show the energetic components of the spin-averaged count rates of protons (30-35 keV) and electrons (75-115 keV). The density of magnetosheath plasma ($\sim$ 1 keV) is higher than the magnetospheric plasma so that the magnetopause can be identified from the reduction in N_p at $\sim$ 2:50 UT as well as from the change in field direction. The high ($\gtrsim$ 20 keV) energy plasma density is, however, higher in the magnetosphere (ring current) than in the magnetosheath, as can be seen from the bottom panels.

Inspection of Figure 3.7 will show that clear enhancements in the energetic proton and electron intensities occur during the two prominent FTE magnetic field signatures observed in the magnetosheath at 2:12 - 2:15 UT and at 2:34 - 2:38 UT. Comparison with the N_p panel then indicates that during the FTEs a mixture of magnetosheath and magnetospheric charged particle populations is observed. This is confirmed from an examination of the proton, alpha particle and electron spectra as shown by Scholer et al. (1982, their Figure 4). The ion and electron spectra are similar to those observed later in the ring current, although the ion fluxes are slightly, and the electron fluxes substantially reduced compared to the values in the magnetosphere (Figure 3.7).

A detailed sequence of the energetic proton distributions during the 2:13 UT FTE is shown in Figure 3.8. The count rate obtained in the satellite spin plane (approximately the ecliptic plane) has been divided into six sectors corresponding to the instrument look directions. The shaded area has been eliminated to allow for sensitivity of the sensors to the Sun, which is to the left of the figure. The arrowed line shows the projection of the magnetic field onto the ecliptic plane. It can be clearly seen that in the centre of the FTE (2:13:56 - 2:14:12 and 2:14:12 - 2:14:28 UT invervals) the protons stream antiparallel to the magnetic field. Such a streaming direction is consistent with an interpretation in terms of energetic ions escaping from the magnetosphere into the magnetosheath along newly opened field lines connected to the Northern Hemisphere. In contrast to the energetic ion behaviour, however, the energetic electron distributions during the two magnetosheath FTEs are approximately isotropic (not shown).

Energetic particle data for the 10 November 1977 crossings (Figure 3.6) were presented by Daly et al. (1981) and Daly and Keppler (1982). Figure 3.9 shows the energetic particle data and (for

reference) the magnetic field data in boundary normal coordinates obtained from ISEE 2. The top two panels show respectively the energetic ion ($\gtrsim$ 25 keV) and electron ($\gtrsim$ 20 keV) data sorted into three pitch angle bins with a range of 60° each. Pitch angles of 0° and 180° show respectively streaming parallel and antiparallel to the local field direction. As shown in Figure 3.9, the energetic particle intensities during the FTEs observed in the magnetosheath, at the magnetopause and in the magnetosphere are intermediate to those observed in the magnetosheath and magnetosphere proper. In particular, the electron intensities are an order of magnitude below magnetospheric values. Also evident is the streaming of the ions antiparallel to the magnetic field (highest intensity in the 180° pitch angle bin) during the magnetosheath FTEs, consistent with encounters of open flux tubes connected to the Northern Hemisphere. However, note that the electron distributions are more isotropic and even show a slight anisotropy parallel to the local field direction. Confirmation of the similarity in particle populations during the magnetospheric and magnetosheath FTEs is given in Figure 3.10. This figure shows the ion distributions during a magnetosheath FTE (crosses), a magnetospheric FTE (solid circles) and a reference interval in the magnetosphere (open triangles). Both types of FTE show distributions peaked toward 180°, i.e., anti-parallel streaming. A final point worth noting in Figure 3.9 is that the energetic particle intensity enhancements during the magnetosheath FTEs is of longer duration for the ions, while during the magnetosphere FTEs the intensity decreases last longer for the electrons (Daly and Keppler, 1982). This behaviour eliminates the possibility that the FTEs are caused by close encounters of the magnetopause (see Daly, 1982, Figure 3).

3.3.3 Plasma signatures

Paschmann et al. (1982) made an extensive investigation of the plasma signatures of FTE magnetic signatures. Figure 3.11 shows plasma and magnetic field data obtained from ISEE 1 during the 8 November 1977 pass. The top three panels show the total plasma density N_p, the energetic components of the plasma densities of ions $\overline{N}_p$ (8-40 keV) and electrons $\overline{N}_E$ (1.7-20 keV, dotted line), and the plasma flow speed V_p (km s^{-1}). All plasma parameters are obtained from 3-D measurements (Bame et al., 1978). The bottom four panels again show the magnetic field in LMN coordinates and the field strength P_B (nanoteslas) and

plasma pressure P_p (10^{-8} dyne cm^{-2}). The magnetosheath FTEs show clear enhancements in the energetic particle densities as also reported by Scholer et al. (1982). The plasma bulk speed V_p is perturbed and during the latter part of the magnetosheath FTEs it is enhanced compared to ambient magnetosheath values. The plasma velocity during these events has a northward and dawnward component (Paschmann et al., 1982, Figure 7) in accord with the positive-negative sense of the B_N perturbation. The plasma and magnetic field data are therefore consistent with an encounter of a northerly connected flux tube as drawn in Figure 3.1. Note finally that the total (plasma and field) pressure is enhanced during the FTEs.

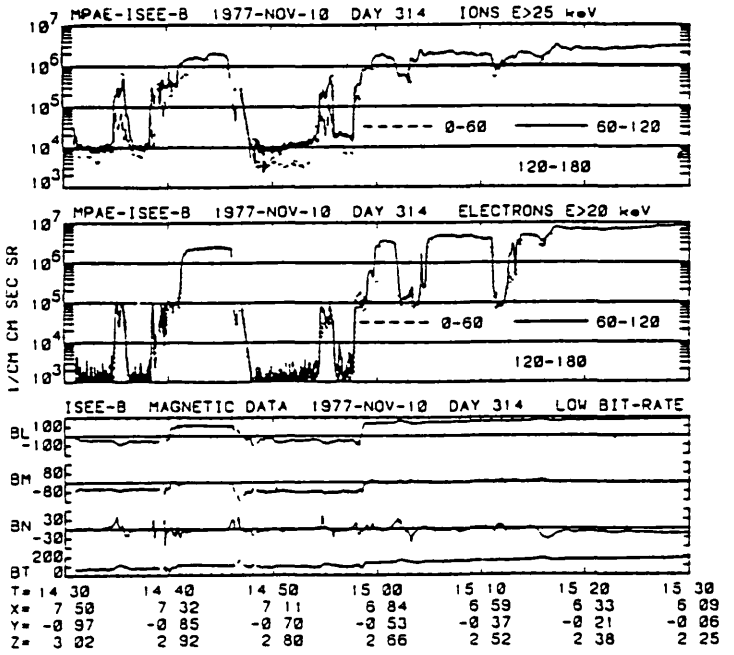


Fig. 3.9. Particle streaming inside FTEs (Daly and Keppler, 1982).

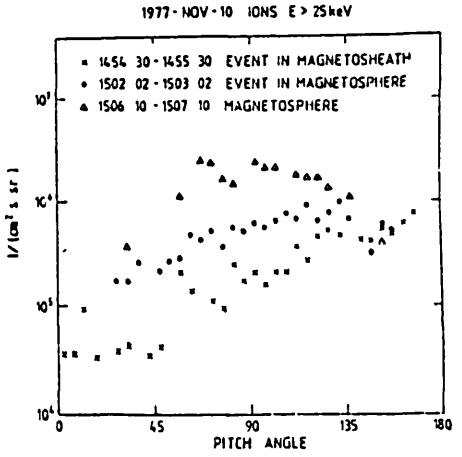


Fig. 3.10. FTE energetic proton distributions (Daly and Keppler, 1982).

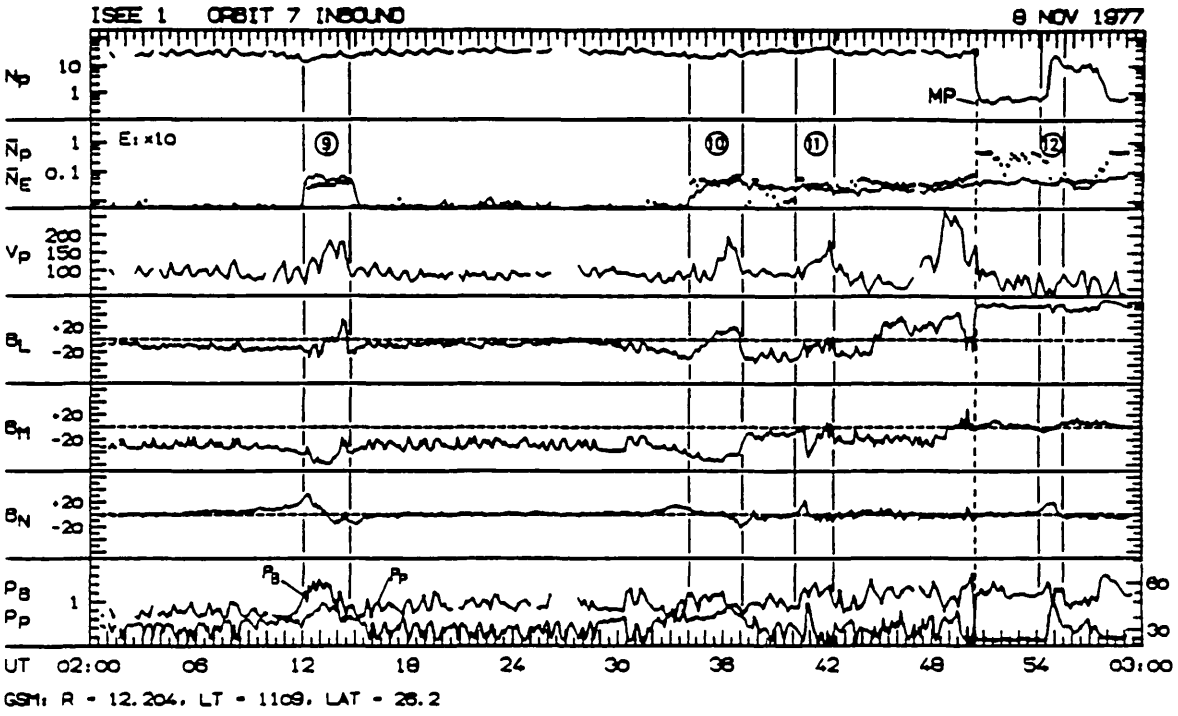


Fig. 3.11. Plasma and field data for 8 November 1977 (Paschmann et al., 1982).

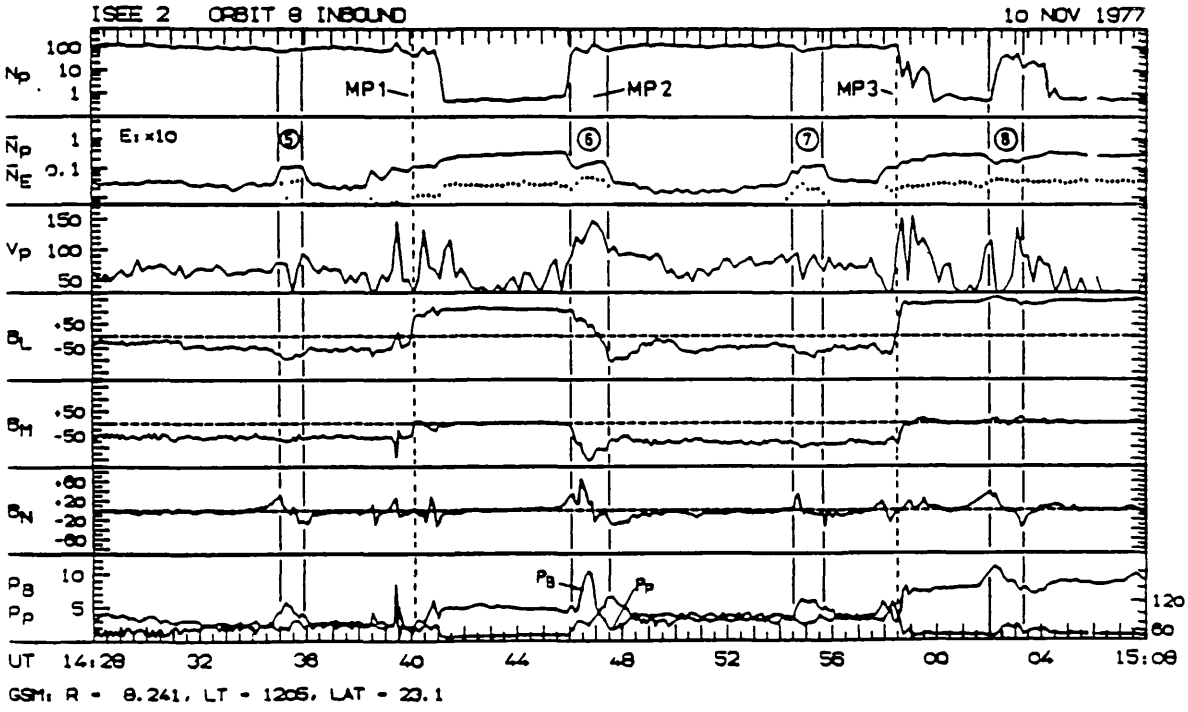


Fig. 3.12. Plasma and field data for 10 November 1977 (Paschmann et al., 1982).

Figure 3.12 shows the plasma and field data during the 10 November 1977 pass, in the same format as Figure 3.11. Note again the energetic particle enhancements during the magnetosheath FTEs, as well as the enhanced flow speeds for the FTEs at the magnetopause. The magnetospheric FTE at 15:03 UT occurs in close association with an isolated pulse of boundary layer plasma, as does the FTE at 2:55 UT in Figure 3.11. This shows that magnetospheric FTEs also contain a mixture of magnetosheath and magnetospheric plasma.

Electron plasma data for a total of 31 FTEs have been analysed by Ogilvie and Scudder (1984). The electron plasma component observations confirm the mixture of plasmas described above. The authors also report evidence for field-aligned ionospheric electrons during some events.

3.3.4 Modelling of FTE particle distributions

In order to test whether the energetic ions observed during FTEs in the magnetosheath result from leakage of magnetospheric particles through the magnetopause, Speiser et al. (1981) and Speiser and Williams (1982) used a simple model of the near subsolar boundary to follow computationally particle orbits from the magnetosphere into the magnetosheath. The model they considered is one-dimensional, with linear variations only along the normal to the boundary, and quasi-static. The latter condition in effect means that the boundary as seen by the particles is time-stationary or is in a series of nearly steady states. Artificial mirroring is also imposed inside the magnetosphere. As input to the model, data from the ISEE satellites during the 10 November 1977 inbound pass (Figure 3.6) were used to find the average magnetosheath and magnetospheric magnetic fields and also the 3-D distributions for magnetospherically trapped energetic (> 24 keV) ions. The ion orbits are then followed computationally through the model magnetopause into the magnetosheath, where model magnetosheath distribution functions are set up using Liouville's theorem under the assumption that scattering processes are not important for the energetic ions (see Figure 3.13). The authors compared the model magnetosheath distribution functions with the actual ones observed during several FTEs. They found good agreement if they used an inward pointing normal field component (estimated to be a few nT) and a tangential electric field not greater than $\sim$ 0.5 mV m^{-1} for the mapping process. They concluded

therefore that the energetic ions observed during magnetosheath FTEs are indeed consistent with direct leakage of previously trapped magnetospheric protons through the magnetopause along northerly connected open field lines. The tangential electric field value is somewhat lower than electric field measurements observed at the magnetopause seem to suggest (section 2.3.4). Fahleson et al. (1979) report a value of $\sim$ 2 mV m^{-1} for the 10 November 1977 crossings. These values are not inconsistent, however, since an FTE flux tube may be sampled by ISEE at a considerable distance away from the magnetopause and the flux tube may have detached itself and moved away from the reconnection site sometime in the past.

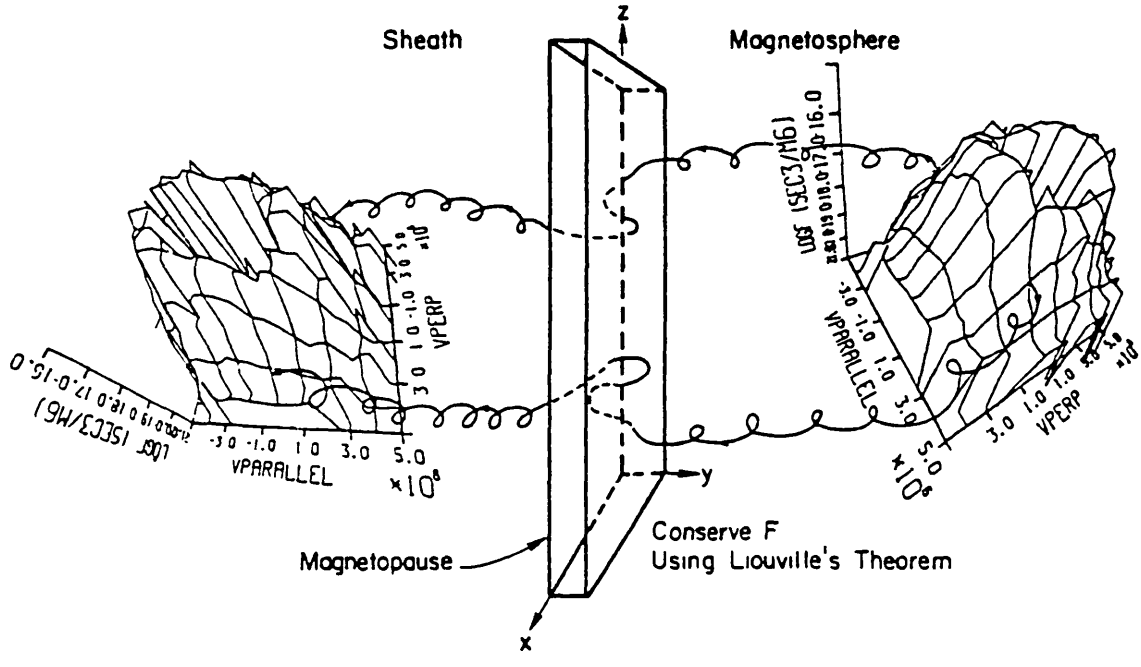


Figure 3.13. Mapping of particle distributions into the magnetosheath (Speiser et al., 1981).

3.3.5 Reverse signature FTEs

The initial reports of FTEs were confined mainly to observations made during the early part of the ISEE mission, i.e., late Autumn 1977. During this period the ISEE 1 and 2 satellites crossed the dayside magnetopause region on the dawn side of the Earth at relatively high northern magnetic latitudes: $\sim$ 20-40° in GSM coordinates. If FTE reconnection occurs near the geomagnetic equator as postulated in

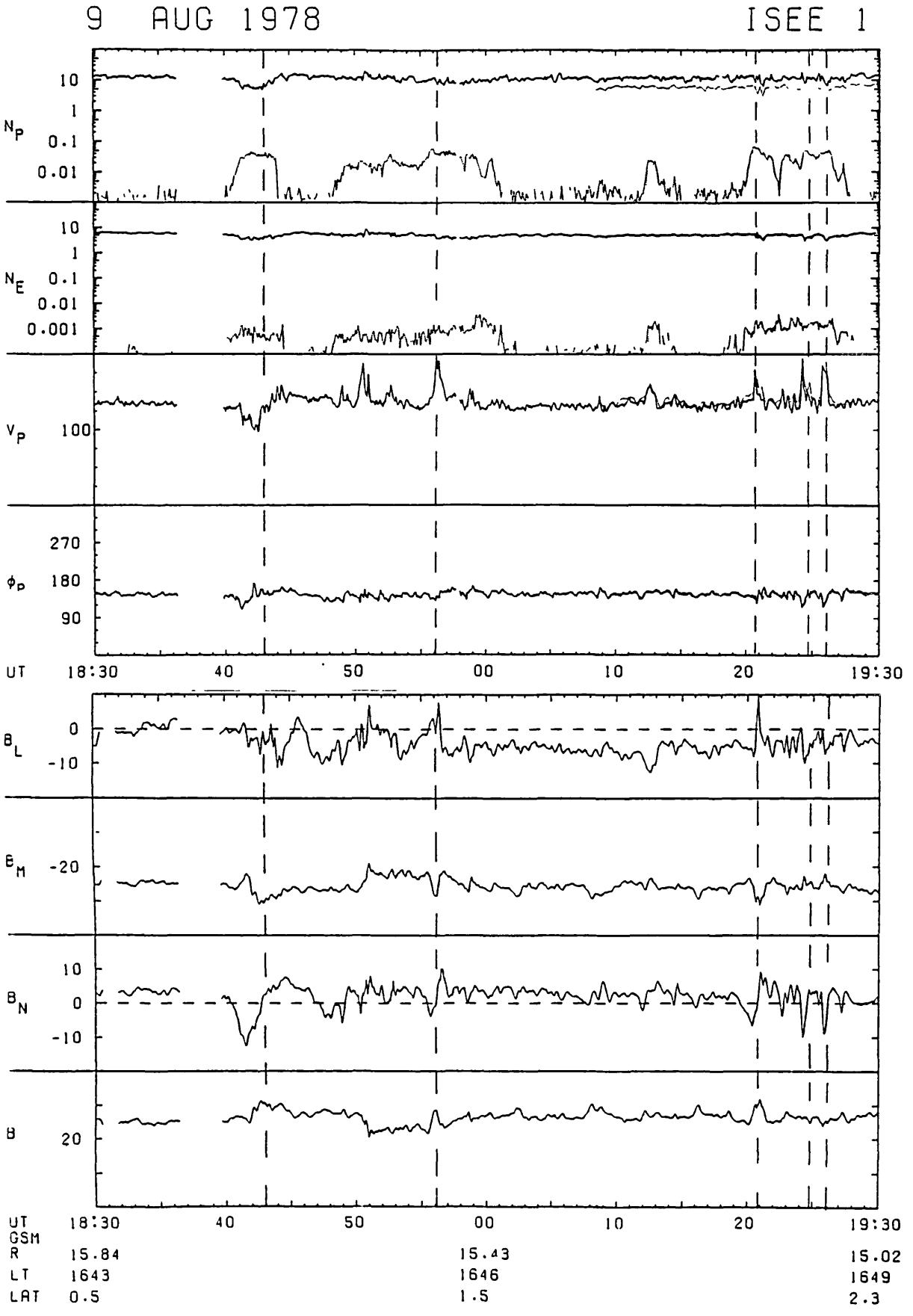


Fig. 3.14. Reverse FTEs on 9 August 1978.

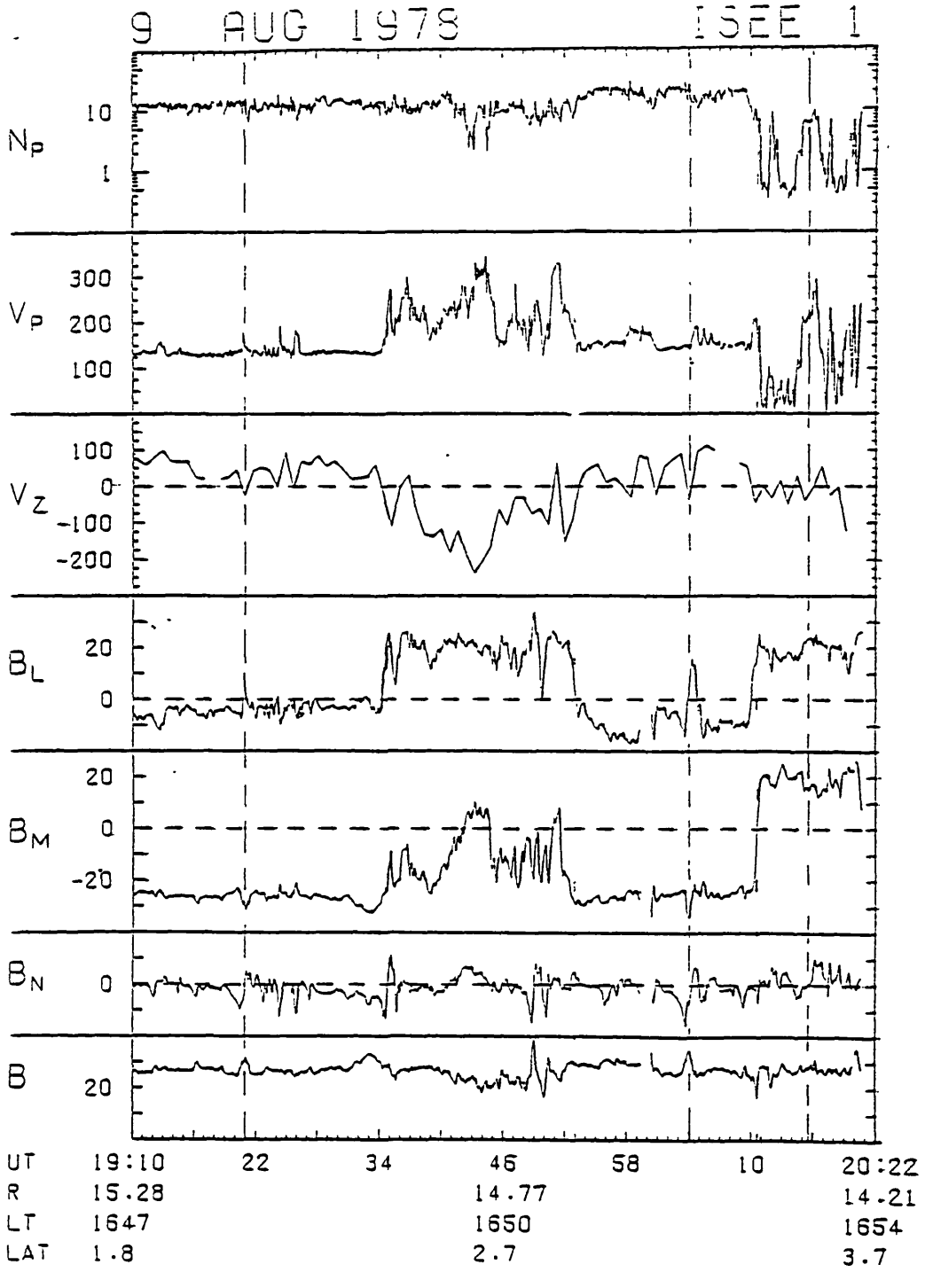


Fig. 3.14. Reverse FTEs on 9 August 1978.

section 3.2, then we should expect the FTEs to show signatures consistent with a satellite location north of the reconnection site, i.e., a positive-negative B_N deflection indicating northward motion as well as northward plasma flows and anti-parallel energetic particle streaming inside the FTE flux tubes. The two case event studies we have considered (Figures 3.5 and 3.6) satisfy these criteria. Later on in the mission the ISEE satellites were able to sample the magnetopause at lower latitudes, and one such crossing we shall now select for a detailed discussion.

Figure 3.14 shows two 1-hour plots of plasma and magnetic field data obtained from ISEE 1 during the inbound pass on 9 August 1978. The panels show respectively from top to bottom the plasma density N_p, the plasma flow speed V_p, azimuthal angle ϕ_p (180° is antisunward, 270° is dawnward), north-south GSM component V_z of the flow, and the magnetic field in boundary normal coordinates. All plasma parameters are from 2-D measurements (obtained in the satellite spin plane $\sim$ ecliptic plane) at 12 sec resolution, except V_z which is obtained from 3-D measurements at a resolution of one data point every 48 sec. Referring to Figure 3.14 we can see that ISEE 1 is initially in the magnetosheath, where the field is southward and duskward (B_L and B_M both negative). The magnetopause is then crossed three times at 19:34, 19:53 and 20:11 UT as a result of boundary motions. The magnetopause crossings occur in the dusk local time sector slightly northward of the geomagnetic equator. This location is consistent with the magnetosheath plasma flow direction (duskward and slightly northward, i.e., $\phi_p \sim 150°$ and $V_z \sim 100$ km s^{-1} positive) and the magnetospheric field direction, which is northward (B_L positive) and dawnward (B_M positive). From the number density and B_M behaviour we can deduce that the magnetopause is only partially crossed during the 19:34 - 19:53 UT interval. This interval is one of the quasi-steady reconnection events reported by Sonnerup et al. (1981) and they interpret this region to be located on open field lines southward of the reconnection line. Evidence for this may be found in the form of accelerated flows directed southward (negative V_z) during this interval. Sonnerup et al. (1981) also report observing energetic particles streaming parallel to the field, in the magnetosheath, consistent with the escape of magnetospheric particles along southerly connected open field lines.

FTE signatures occur throughout the interval plotted in Figure 3.14.

Three of the most prominent FTE magnetic signatures occur at 19:21 and 20:04 UT in the magnetosheath and at 20:15 UT in the magnetosphere. All three FTEs show a rotation of the tangential field towards the direction of the field on the opposite side of the magnetopause, in particular the B_L component goes positive during the two magnetosheath FTEs. In addition, the magnetic field strength increases substantially during the two magnetosheath FTEs in agreement with observations reported earlier (see, e.g., Figures 3.5 and 3.6). The novel magnetic feature of the present events is the B_N signature. The B_N signature is bipolar, but instead of being positive-negative it goes in the reverse sense, i.e., negative-positive. Such a signature we postulated as being caused by the southward motion of a southerly connected FTE open flux tube in section 3.2. We shall now seek confirmation of this from the plasma data.

Plasma data show that all three FTEs contain a mixture of magnetosheath and magnetospheric particle populations. They are also accompanied by plasma flows which are (slightly) enhanced in comparison with the magnetosheath plasma flow. The plasma flow during the FTEs is also directed southward, as may be seen from the negative V_z values. This latter feature is perhaps not so clearly evident as one would wish because of the low time-resolution of the 3-D plasma data. The time-resolution is in fact of the same order as the duration of the FTEs. However, the fact that we do see a southward flow deflection at one data point indicates that we are encountering southward moving open flux tubes, an interpretation which is in agreement with the reverse B_N signatures. The matter is finally clinched by energetic ion data, which provide clear evidence that the flux tubes are connected to the Southern Hemisphere. Figure 3.15 shows energetic ion data during the 19:21 UT magnetosheath FTE (supplied by Daly, 1982). These data were obtained from the medium energy particle spectrometer on board ISEE 2 (Williams et al., 1978). The energetic ($\gtrsim$ 45 keV) ion count rates are divided into four pitch angle bins with a range of 45° each. However, the 45-90° pitch angle range (not shown) was contaminated by sunlight and these data are therefore unreliable. During the 19:21 UT FTE there is a significant anisotropy along the magnetic field such that the ions are streaming predominantly parallel to the local field direction, i.e., the 0-45° pitch angle range has the highest intensity. This feature is consistent with energetic ions of magnetospheric origin leaking into the

magnetosheath along southerly connected open field lines.

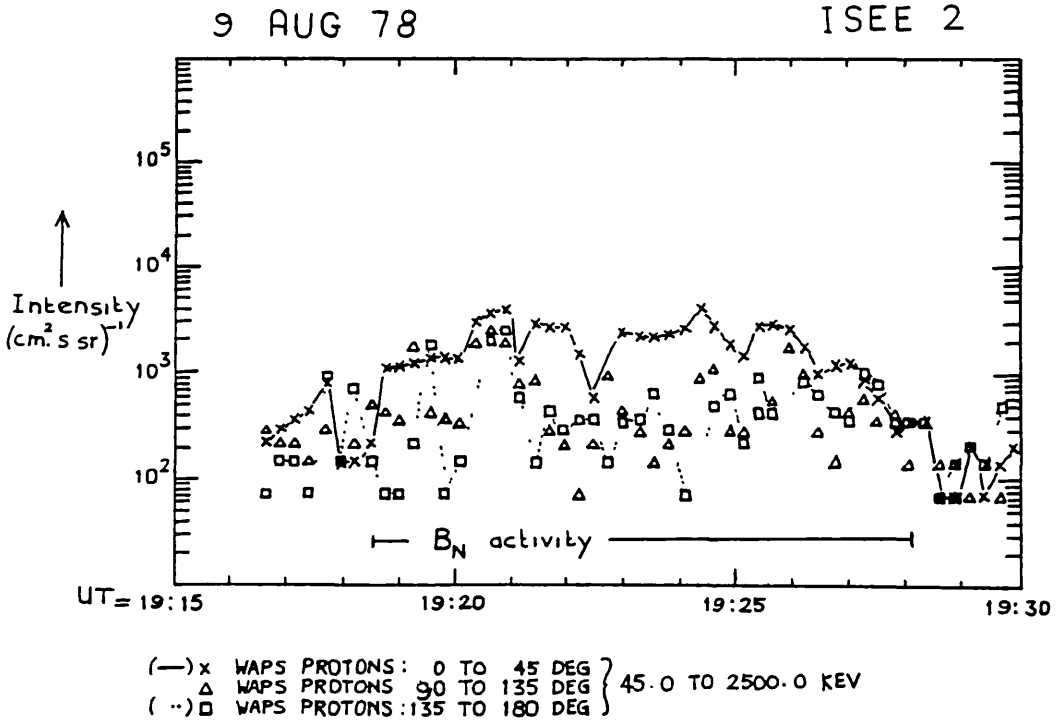


Figure 3.15. Particle streaming for a reverse FTE on 9 August 1978.

A final point of interest to note in Figure 3.14 is that FTEs occur in close association with an interval of quasi-steady reconnection. Both the FTE observations and the reconnected plasma flows are consistent with a satellite location south of the reconnection site. This suggests that there may be a close physical connection between the two types of reconnection and we shall explore this in more detail in Chapter 5.

3.3.6 FTEs observed simultaneously outside and inside the magnetopause

The case events we have considered so far were obtained when the ISEE 1 and 2 satellite separation across the magnetopause was relatively small, of order 100 km. The magnetic signatures of the FTEs observed

by ISEE 1 and 2 at these separations are virtually identical, indicating that the spatial scale of the FTE signatures exceeds the satellite separation. The ISEE 1 and 2 satellite separation is varied throughout the mission, so that at times it is of order an Earth-radius ($\sim$ 6400 km). At such times it is possible for ISEE 1 and 2 to sample different field regions, i.e., magnetosheath or magnetosphere, for prolonged intervals of time. Two such instances will now be discussed.

Figure 3.16 shows a 1-hour plot of magnetic field data (LMN co-ordinates) obtained from ISEE 2 (heavy trace) and ISEE 1 (light trace) during an outbound pass on 23 October 1978. At the time the satellite separation in LMN components is (708, 1164, -6115) km, with ISEE 2 leading. The magnetopause region is encountered in the dawn sector at a northerly GSM latitude of $\sim 40°$. Note that there is a data gap in the ISEE 1 data in the interval 12:12 - 12:32 UT. At the start of the interval both satellites are inside the magnetosphere, where the field has a northward and duskward orientation consistent with the ISEE locations. The magnetosheath field is southward and duskward. ISEE 2 crosses the magnetopause layer (as defined by the change in field direction) once at 12:15 UT, but as a result of boundary motions ISEE 1 crosses it several times. FTE magnetic signatures occur throughout this interval, but the FTE deserving special attention occurs at 12:36 UT. Prior to and after this event ISEE 1 is inside the magnetopause, while ISEE 2 is located in the magnetosheath. This event therefore represents a simultaneous observation of a magnetospheric and magnetosheath FTE.

Other occurrences such as the one above are shown in Figure 3.17. This plot of data is taken from an inbound pass on 9 November 1979 when the satellite separation was (2565, 2423, 3787) km in LMN components, with ISEE 2 leading. The magnetopause region was encountered south of the magnetic equator close to local noon. Reverse polarity FTEs which are observed in both the magnetosheath and magnetosphere regions occur at 13:52, 13:59 and 14:02 UT. Note that the latter two signatures are seen slightly displaced in time by ISEE 1 and 2, with ISEE 1 being the first satellite to observe the FTEs.

The observations above show that magnetosheath and magnetospheric FTEs are not magnetic structures which are detached from the magnetopause: they are coupled to and penetrate through the magnetopause layer. Also, FTEs cannot be caused by surface waves propagating along the magnetopause unless the inner edge of the boundary layer oscillates in antiphase,

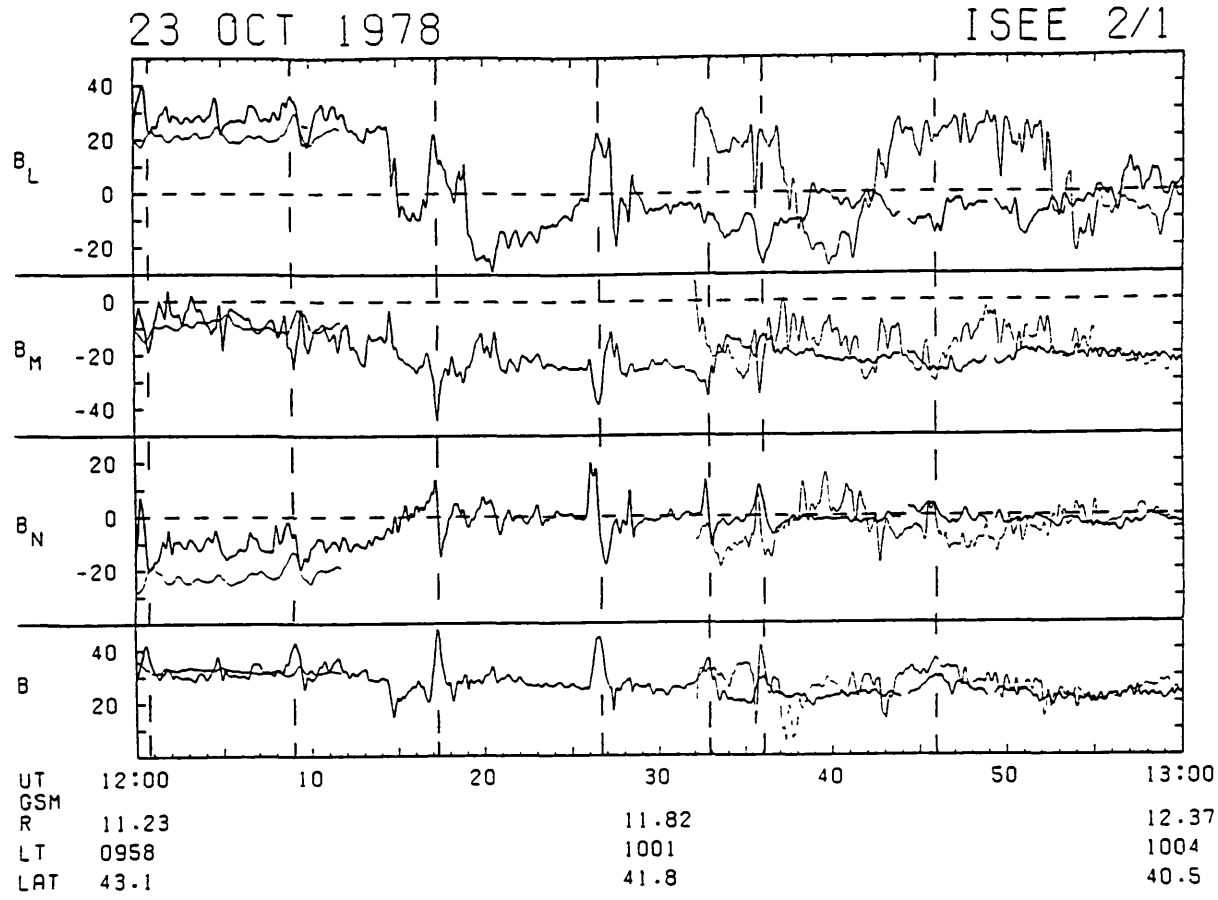


Fig. 3.16. FTEs on 23 October 1978.

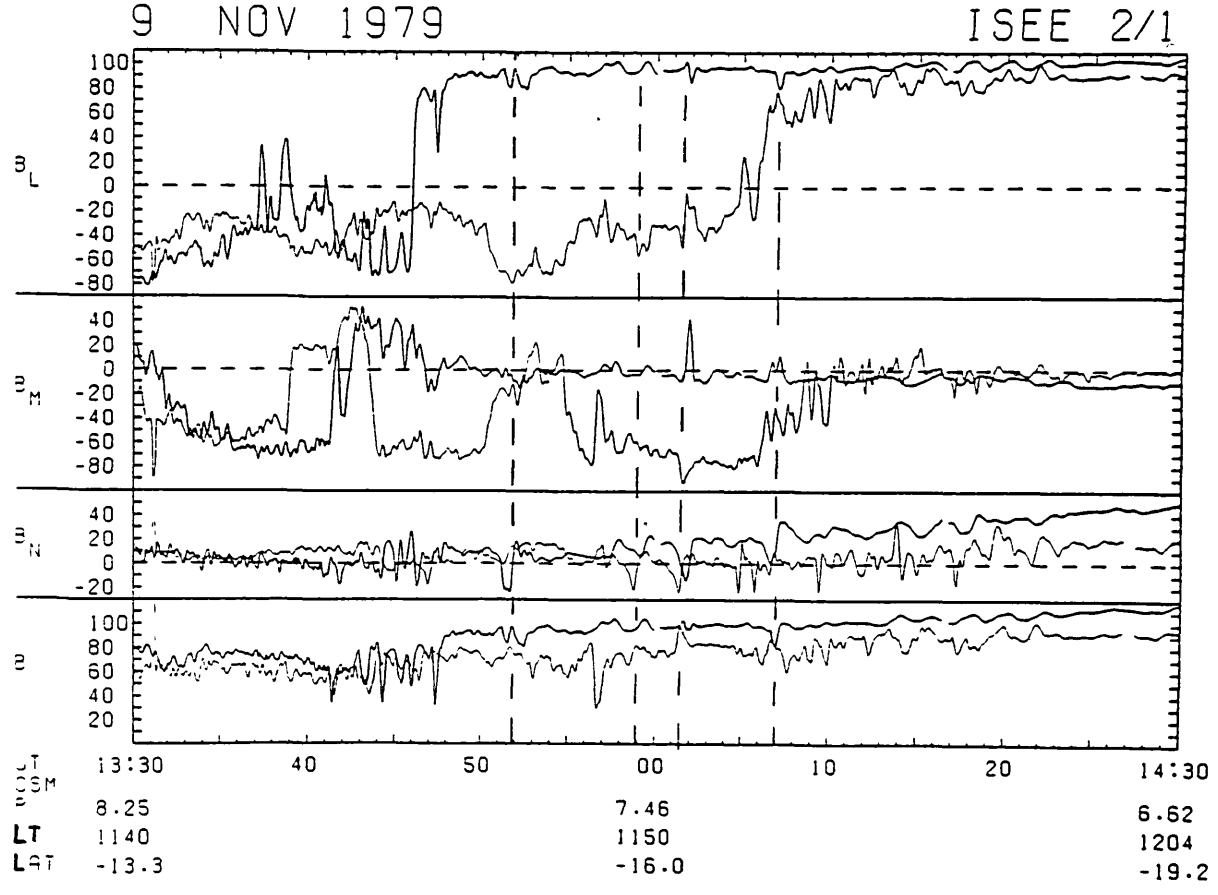


Fig. 3.17. FTEs on 9 November 1979.

which seems unlikely. Separately, the models described by Sckopke et al. (1981, their Figure 7) also do not provide an adequate explanation. In fact, the simplest explanation is in terms of an encounter with an open flux tube as described in section 3.2.

It is significant to note that the sense of the B_N signature is the same for the magnetosheath FTEs as it is for the simultaneously observed magnetospheric FTEs. This supports the contention that magnetosheath and magnetospheric FTEs are part of the same phenomenon. Also, the time lag in the ISEE 1 and 2 observations in Figure 3.17 suggests that we are dealing with propagating structures. Figure 3.18 shows the situation which may correspond to the FTE encounters in Figure 3.17. A southerly connected flux tube travels southward with a velocity V_{FTE}. The solid symbol shows ISEE 1 and ΔM and ΔL refer to the satellite separations along $\hat{M}$ and $\hat{L}$, respectively. The flux tube has to travel a longer distance before it engulfs ISEE 2. The exact distance depends on the geometry of the flux tube, the path followed by it relative to the satellites and the satellite separation. For want of a better value we may estimate it as the satellite separation in the L-M plane, $\sim$ 3500 km. If we take V_{FTE} to be $\sim$ 100 km s^{-1}, then the expected time lag is 35 secs. This value is in rough agreement with the observations.

3.3.7 Recap

Most of the plasma and magnetic field observations of FTEs fit in well with expectations based on the model outlined in section 3.2. In particular, the model can account for bipolar B_N signatures, some of the observed tangential field rotations, plasma mixing, plasma flow signatures and energetic ion streaming directions. Magnetospheric FTEs are observed in association with detached boundary layer pulses inside the magnetosphere and thus provide an explanation for the origin of the inclusion events reported by Paschmann et al. (1978). The case events presented so far are also in agreement with a reconnection site in the subsolar region. Even the 9 August 1978 pass fits in with this picture since the reconnection line may tilt away from the equator in response to IMF B_y (Figure 1.7). However, there are several questions arising from the observations which are worthy of further consideration.

One feature which is not immediately explained from the model in section 3.2 is the continuous B_N signature of FTEs: once inside an

FTE flux tube we should expect it to go to zero. Other features are the magnetic field strength increases accompanying FTEs and the anomalous tangential field rotations, in which the field rotates away from the field direction on the opposite side of the magnetopause. In the next subsection we shall consider an explanation for these features in terms of field aligned currents (FACs) associated with FTEs.

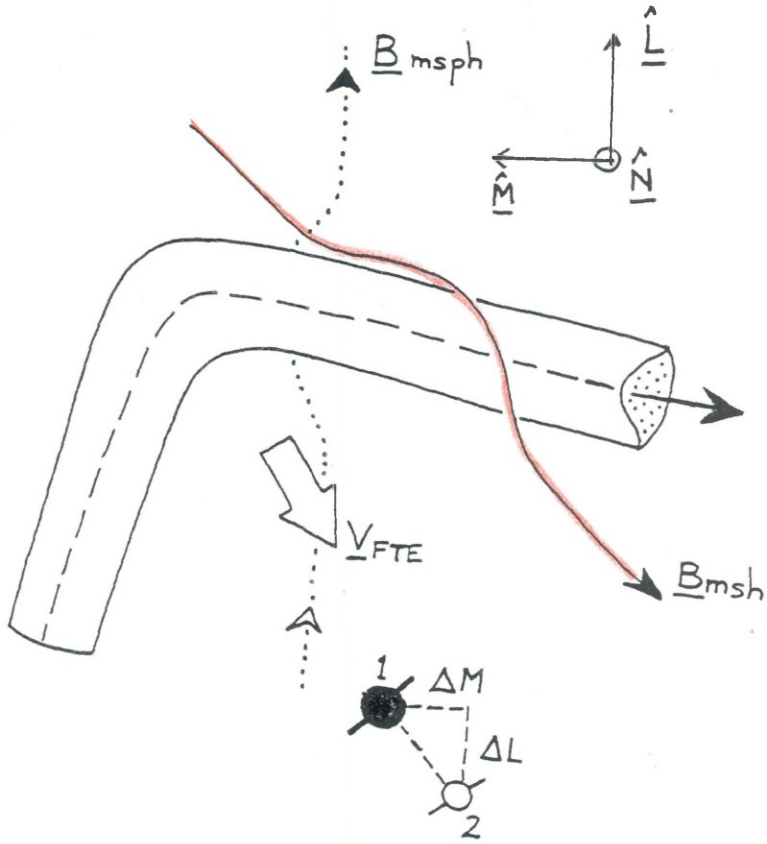


Figure 3.18. Schematic for FTE encounters on 9 November 1979.

As pointed out in the previous chapter (2.3.5), we need a resupply mechanism(s) in order to explain the presence of energetic particles on open field lines. The loss times of energetic protons (∿ 1 min) and electrons (∿ 1 sec) are shorter than the time during which FTEs are observed (∿ 2 min). Only along field lines still attached to the reconnection site (i.e., the separatrices in Figure 2.8) do we expect to observe energetic particles, and in general the particle fluxes should

be low, contrary to what is observed. The resupply question for FTEs has been addressed by, e.g., Scholer et al. (1982), Daly and Keppler (1982) and Scholer (1983). One possible resupply mechanism is that magnetic gradient drifts cause energetic particles to drift onto open field lines from surrounding closed magnetospheric field lines. Another possibility is that reconnection is still in progress while the FTE is being observed. If the resupply rate is faster than $\sim$ 1 min, then energetic ions are supplied fast enough for them to be observed continuously streaming out along open field lines. If the resupply rate is slower than the electron loss rate, i.e., $\sim$ 1 sec, then this may explain why we observe electrons at much reduced and isotropic intensities. In fact, Scholer et al. (1982) reported a small electron component streaming counter to the ions. This may be explained in terms of scattering of the electrons off the strong electric and magnetic field wave turbulence observed during FTEs (Gurnett et al., 1979; Anderson et al., 1982).

A number of other observations also indicate that reconnection may still be in progress during FTEs, contrary to the situation depicted in Figure 3.1. Speiser and Williams (1982) observed quasi-trapped (Q-T) distributions on entry and exit of FTEs. They interpret the Q-T distributions as the slower outward moving particles that get left behind by more field-aligned particles which make a faster exit along the open field lines. This implies that older and newer open field lines are sequentially sampled as the FTE tube is crossed. Paschmann et al. (1982) noted that the accelerated flows observed during some FTEs (e.g., in Figure 3.11) may result from reconnection continuing at lower latitudes inside the FTE flux tubes, rather than the contraction velocity of the flux tubes as a whole. Further evidence is provided by the electron plasma observations of Scudder et al. (1984). Many FTEs are accompanied by a narrow region of intense electron heat flux at their boundaries. Such heat dissipation is expected to occur in the diffusion region and if an FTE flux tube is still connected to the reconnection site at lower latitudes, then we may expect a heat flow layer along the outer separatrix S_1 for magnetosheath FTEs and along the inner separatrix S_2 for magnetospheric FTEs (Figure 2.8).

3.3.8 Field-twisting inside FTEs

In an attempt to explain the continuous sinusoidal B_N signatures

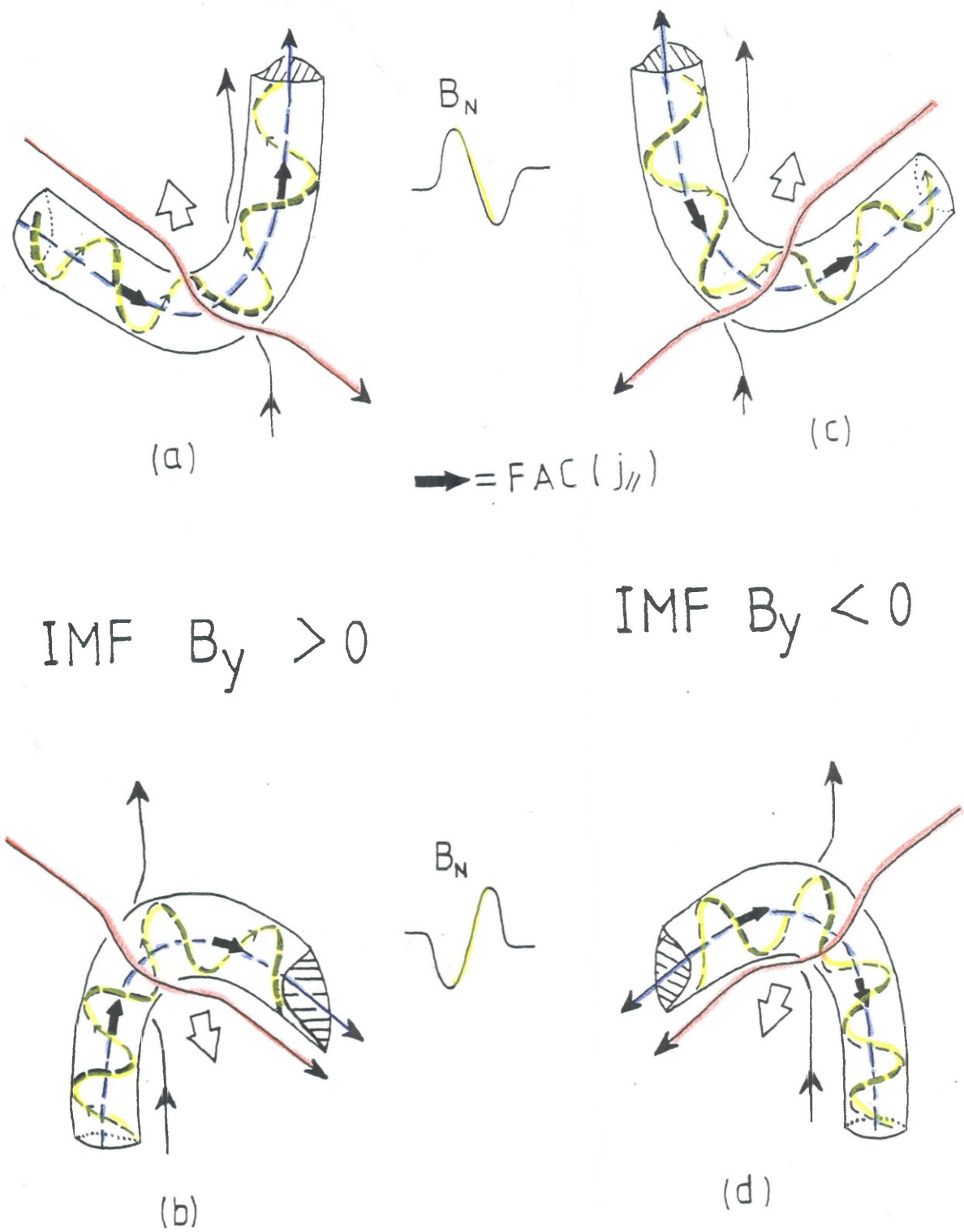


Fig. 3.19. Field twist (FAC) inside FTEs (after Saunders, 1983).

(i.e., B_N continues to vary throughout the interval in which open field lines are encountered) and the anomalous tangential field tilts (i.e., tilts away from the field direction on the opposite side of the magnetopause) observed inside FTE flux tubes, Cowley (1982) and Paschmann et al. (1982) independently suggested that there is a distributed field-aligned current (FAC) associated with FTEs. By Ampère's law this FAC is associated with a twisting of the field lines, as illustrated in Figure 3.19. This figure shows segments of FTE open flux tubes as viewed from the magnetosheath, which are connected to the Northern (a,c) or Southern (b,d) Hemisphere for IMF $B_y > 0$ (a,b) or IMF $B_y < 0$ (c,d). For the sake of argument, we shall assume that the northerly connected tubes move northwards across the observation point and give rise to bipolar, positive-negative B_N signatures, while the southerly connected tubes give rise to reverse polarity B_N signatures, as shown. The blue-arrowed lines show the magnetic field line along the central axis of the tubes. The broad solid arrows inside the flux tubes show the FAC, the direction of which is such as to be consistent with the appropriate B_N signature. The FAC causes a twisting of the field around the central tube axis, as indicated by the yellow dotted lines. Note that the sense of the twist of the field is continuous across the magnetopause. Figure 3.19 also shows that if the twisting is tight enough (as is the case in this figure), the field in the outer sections of the flux tubes (i.e., the regions furthest away from the magnetopause) may tilt away from the orientation of the field on the opposite side of the magnetopause.

The suggestion that FTEs have an associated FAC inside them has been used to argue that the boundary layer encounters observed during the 6 November 1977 pass (Figure 2.7) are consistent with observations of magnetospheric FTEs (Cowley, 1982; Saunders, 1983), rather than diffusive processes (Sckopke et al., 1981). The interpretation in terms of FTEs is further strengthened by observations of magnetosheath FTEs during the same pass (e.g., Paschmann et al., 1982). Direct evidence for the occurrence of field twisting has now also been found from dual-satellite observations of FTEs at times when the ISEE 1 and 2 satellite separation was large (Saunders et al., 1984a,b). Figures 3.20, 3.21 and 3.22 show three such instances. Figure 3.20 shows a 1-hour plot of magnetosheath field data during an outbound pass on 23 October 1978, with a satellite separation of 5485 km along the estimated boundary normal direction (ISEE 2 leading). At 13:25 UT both satellites observe an FTE,

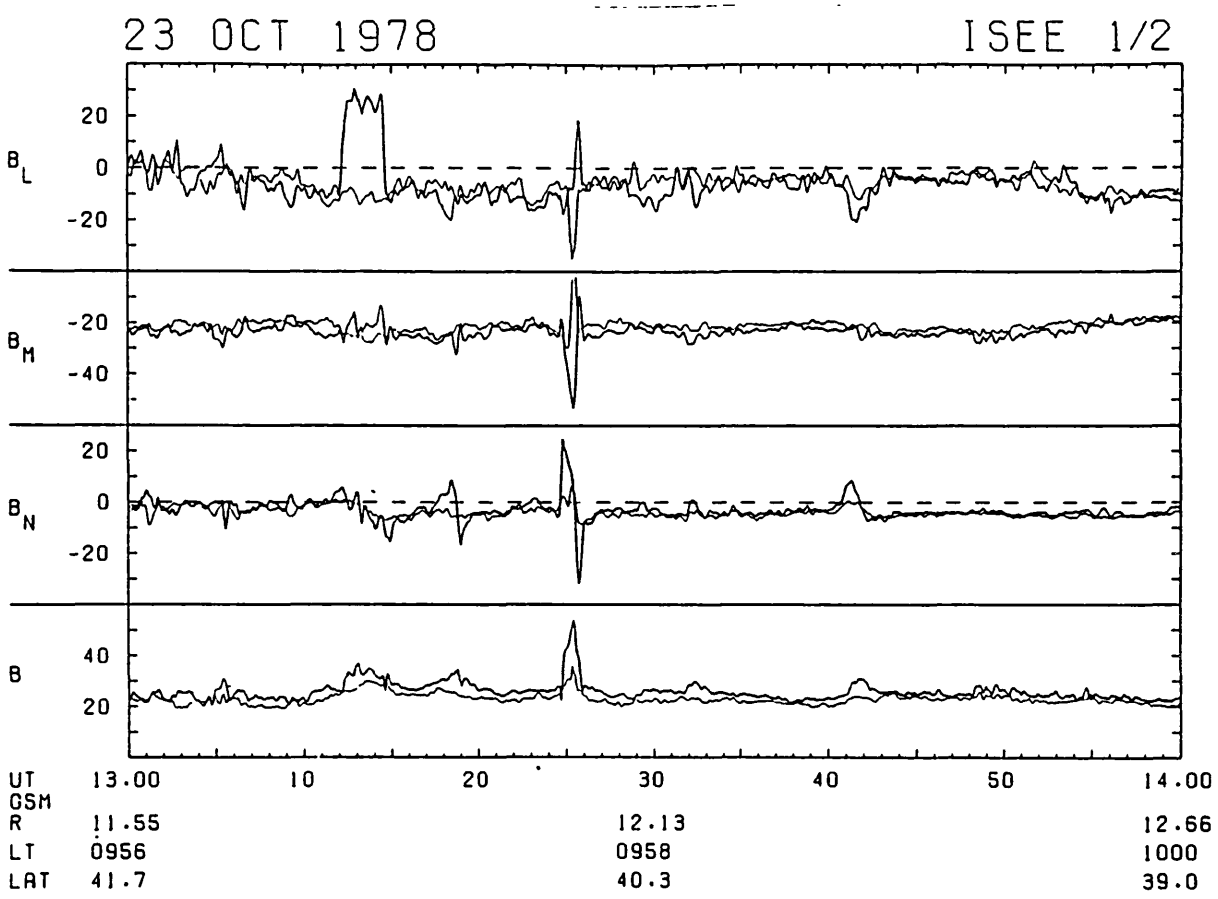


Fig. 3.20. FTEs on 23 October 1978.

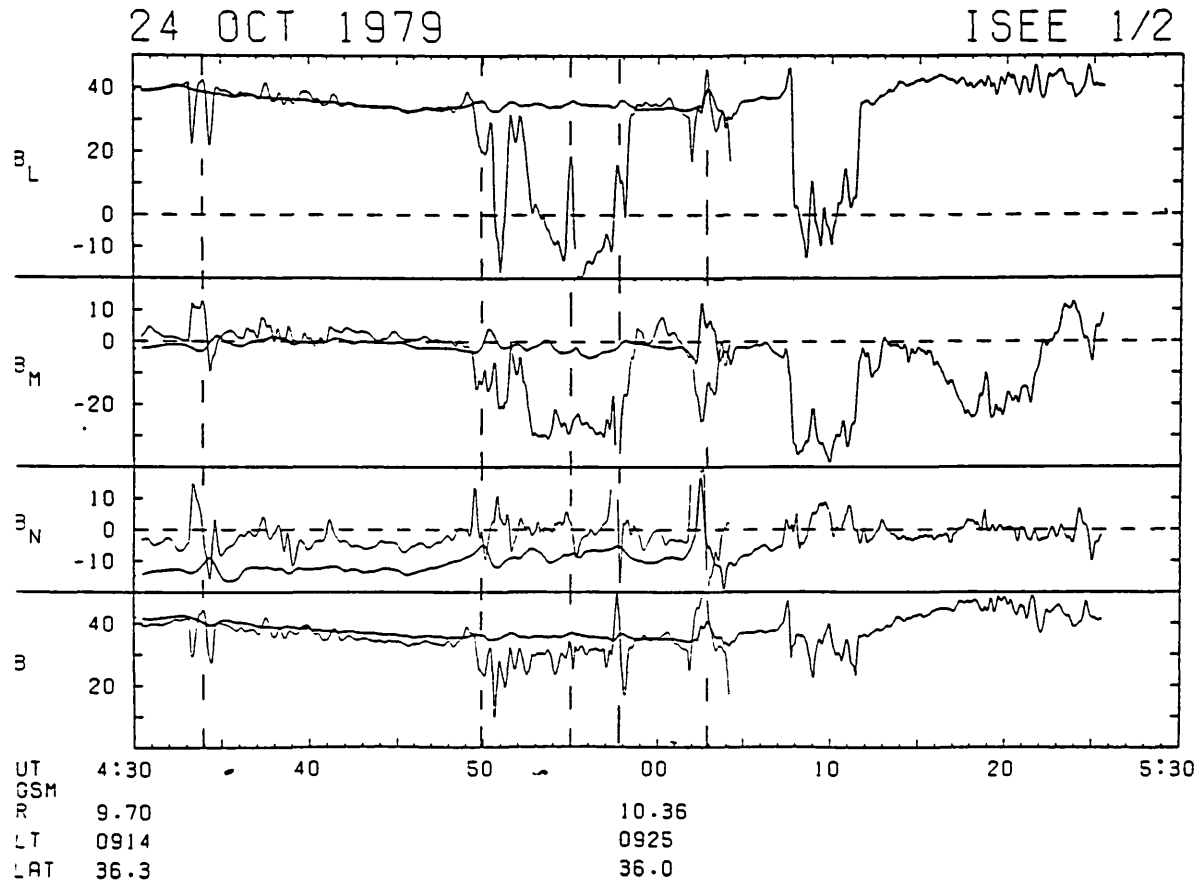


Fig. 3.21. FTEs on 24 October 1979.

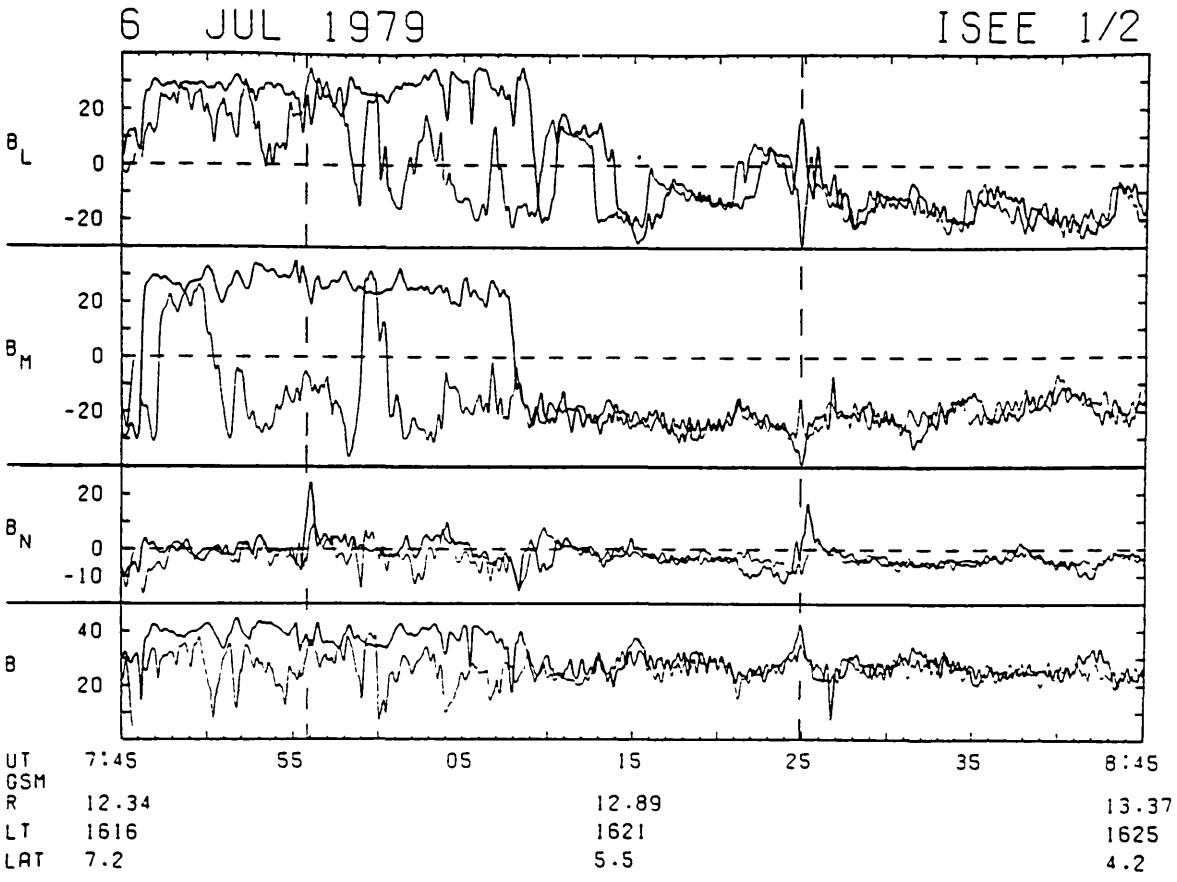


Fig. 3.22. FTEs on 6 July 1979.

but while the field tilts towards the magnetospheric field orientation (northward and duskward) in the ISEE 1 data, ISEE 2 observes a simultaneous away tilt. Figure 3.21 shows data from an outbound pass on 24 October 1979, during which the satellite separation was 5680 km along $\hat{N}$, with ISEE 2 leading. At 5:03 UT both satellites observe a magnetospheric FTE. During this event, ISEE 2 observes the tangential field to rotate towards the field orientation in the magnetosheath, while ISEE 1 observes an away tilt. Our final example in Figure 3.22 shows data from an outbound pass on 6 July 1979. Here ISEE 2 leads ISEE 1 by $\sim$ 2000 km along the boundary normal. At 8:25 UT both satellites observe a reverse magnetosheath FTE (note that there is some fine structure in the B_N signature). As before, the two satellites observe field tilts which are in opposite directions with ISEE 2 observing the away tilt.

Saunders et al. (1984a,b) have studied a large number of FTEs using simultaneous ISEE 1 and 2 observations when the separation was large. They find that tangential field tilts which rotate away from the field direction on the opposite side of the boundary are generally observed by the satellite furthest away from the magnetopause, in

agreement with Figure 3.19. They also show that there is vortical plasma flow during the FTEs in Figure 3.20, and that the plasma flow and magnetic field perturbations during the events approximately satisfy the properties of a propagating Alfvén wave. They also estimate the pitch (wave) length of the field twist about the FTE axis to be $\sim 6\ R_E$.

Inspection of Figure 3.19 shows that the direction of the FAC inside FTEs changes sign in response to the sign of IMF B_y. Similar behaviour has also been reported for the high-latitude, large-scale ionospheric FAC systems, discussed in section 1.4. This suggests that there is some relationship between the ionospheric and FTE FACs. It remains to be determined whether the low-altitude FACs result from straightforward mapping of the FTE FACs into the ionosphere, as suggested, e.g., by Cowley (1982). Figure 3.19 shows that the direction of the FAC inside FTEs is compatible with the region 1 FACs which lie at the equatorward boundary of the polar cusp regions (Figures 1.11 and 1.13). Saunders et al. (1984a) show that the magnitude of the FTE FAC ($\sim$ 1 to 2 x 10^5 Amps) is more than ample to account for values observed in the ionosphere.

Although observations imply the existence of a FAC(s) inside an FTE, this still does not explain the underlying cause of the FTE field twist. In fact, without detailed knowledge of the generating mechanism of the FAC there is no reason to suppose that the FAC produces B_N perturbations in the same sense as those produced by the draping of exterior field lines. In principle it is therefore possible that the sense of the B_N perturbations inside and outside an open flux tube are different, unlike the situation drawn in Figure 3.19. This may then lead to more complex B_N signatures than the bipolar signatures we have considered so far. The exact form of such signatures depends on the relative contributions of the FAC and draping effects. One suggestion which has been made to explain the FTE FAC is that the field twist results from the velocity shear at the magnetopause surface as the FTE propagates along it (e.g., Russell, 1984). It has also been suggested from data obtained from the thermal electron instrument on board ISEE 1 (Ogilvie et al., 1978) that low energy electrons act as the charge carriers for the FAC (J. D. Scudder, reported in a question to Russell, 1984).

Recently, a new suggestion has been put forward by Southwood (1984)

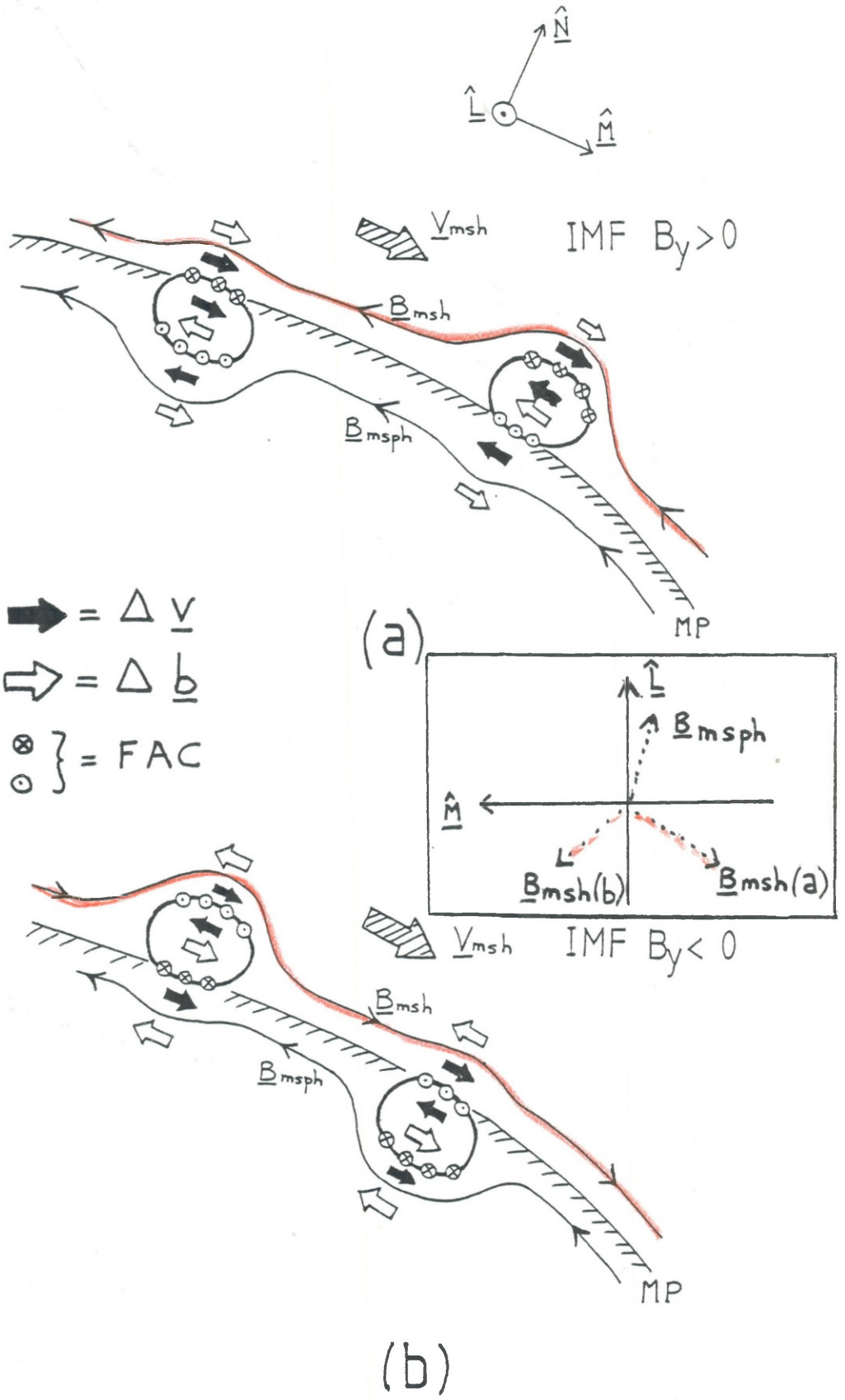


Fig. 3.23. Pairs of FACs associated with FTEs (after Southwood, 1984).

to explain the observed field twist inside FTEs. Figure 3.23 illustrates this latest model. It shows a cut through the magnetosphere along a plane parallel to and north of the equator, and is viewed from above the North Pole. The two blue structures attached to the magnetopause show the magnetosheath and magnetospheric arms of a single FTE open flux tube, which is connected to the Earth's Northern Hemisphere (similar diagrams can be drawn for southerly connected tubes). Figure 3.23(a) shows the situation for IMF $B_y > 0$, and Figure 3.23(b) that for IMF $B_y < 0$. The FTEs produce bulges in the magnetopause surface and the external plasma will have to move out and over these bulges. The directions of the plasma flow perturbations ($\Delta\underline{v}$) and the corresponding magnetic field perturbations ($\Delta\underline{b}$) are indicated in Figure 3.23. Note that the main components of the magnetospheric and magnetosheath fields (along the north-south axis) are out of the plane of this 2-D diagram and that the magnetospheric field is assumed to have a small duskward component, in agreement with the dawn magnetopause location of the drawing.

The new feature of the Southwood (1984) model is the presence of a pair of oppositely directed FACs, one of which flows on the outer edge (furthest away from the magnetopause) of the flux tube, and the other of which flows along the magnetopause edge of the tube. The former FAC flows into (out of) the magnetosphere for the northerly connected flux tube drawn in Figure 3.23(a) (3.23(b)) when IMF B_y is > 0 (< 0). The direction of this FAC is therefore compatible with ionospheric region 1 FACs observed equatorward of the cusp. The FAC along the magnetopause edge of the tube flows in the opposite direction. It should map to higher latitudes and its direction is in fact consistent with ionospheric FACs observed in the dayside cusp region (Figure 1.13).

According to Figure 3.23, the region in which the magnetic field tilts in a direction away from the magnetic field orientation on the opposite side of the boundary is located outside the open flux tube region. In the Southwood (1984) model FTE signatures with away tilts probably do not represent actual encounters with open field lines, but rather the FTE signatures result from the magnetic perturbations produced outside the open flux tubes.

CHAPTER 4

FLUX TRANSFER EVENTS: A SURVEY

4.1 Introduction

The early published studies of FTEs all concentrated on a small number of magnetopause crossings, occurring mostly during the latter part of 1977. During this period the ISEE satellite coverage of the dayside magnetopause was limited to the dawn sector at northern latitudes. In subsequent years the ISEE 1 and 2 orbit has enabled a much larger portion of the magnetopause to be investigated, with additional coverage on the dusk side and at southerly magnetic latitudes. The improved coverage and the larger data set of crossings have given rise to the first surveys on FTEs (Berchem and Russell, 1984; Daly et al., 1984; Rijnbeek et al., 1984; Saunders et al., 1984). These studies have given us important information concerning the spatial distribution of FTEs, the factors which control their occurrence, the site(s) where they originate from and finally, and perhaps most importantly, the role which FTEs play in driving the large-scale convective flows inside the magnetosphere. It turns out that the FTE phenomenon is not just a curiosity, but that FTEs are of global importance and that they are a key element in the solar wind-magnetosphere interaction process.

In this chapter we shall extend the survey of Rijnbeek et al. (1984) whilst also referring to results from the other FTE surveys. In the first part of this chapter we shall consider the results of the survey and then we shall discuss and try to interpret these results.

4.2 Magnetic Field Data Conversion and Display

The magnetic field data used in this survey to identify FTEs are obtained from the ISEE 1 and 2 flux gate magnetometers (Russell, 1978) and are supplied to Imperial College on a routine basis by Professor C. T. Russell at UCLA (see Saunders (1982) for details).

The data are supplied at two time resolutions. The low resolution data (64 sec averages) are used to produce 24-hour microfilm plots from which the magnetopause crossings can easily be identified provided there is a change in field direction and/or magnitude across them. The medium resolution data (one data point every 4 sec) are used to identify FTEs, after conversion into the boundary normal (LMN) coordinate system (Appendix B). In this survey ISEE data from 1977, 1978 and 1979 are included. The conversion procedure into LMN coordinates for the 1977 and 1978 data is described in Rijnbeek et al. (1984). For the 1979 data a more elaborate procedure has been adopted, as follows. All magnetopause crossings occurring on a particular satellite pass are identified using medium resolution magnetic field data. For each full crossing (this term is explained in the next section) an interval is then selected which includes the magnetopause layer as well as data points over an interval of a few minutes in the adjacent magnetosheath and magnetosphere regions. This data interval is then used as input to a programme which determines the normal direction $\hat{\underline{N}}$ to the magnetopause using minimum variance analysis, a conic section model of the magnetopause (Fairfield (1971); Formisano et al. (1979)) and the tangential discontinuity technique (Appendix B). Two tangential discontinuity normals are obtained, one based on the end data points of the interval, and the other based on a field average determined during the first and last ½-minute of the interval. Using the minimum variance, model and tangential discontinuity normals in turn the medium resolution field data are then converted into boundary normal coordinates and plots of 1-2 hours length and centred on the magnetopause crossing are produced. The plot which orders the data best, i.e., which gives least variance in the B_N component, is then selected as having the direction $\hat{\underline{N}}$ which most closely approximates the local magnetopause normal. This direction $\hat{\underline{N}}$ is then used to produce one hour plots of data, over an interval extending normally from the bow shock to well within ($\sim$ 3-4 hours away from the crossing) the magnetosphere.

Although the procedure outlined in the paragraph above for the 1979 data is likely to lead to a more accurate approximation to the magnetopause normal than that described in Rijnbeek et al. (1984), an examination of plots produced using different determinations of $\hat{\underline{N}}$ shows that the identification of FTEs (see next section) is not sensitively dependent on $\hat{\underline{N}}$. In fact, for the prominent FTEs angular deviations of $\sim 30°$ are found not to alter the signature appreciably.

Finally, note that although data from only one of the ISEE satellites are used to determine $\hat{N}$, the final field plots are produced using superposed ISEE 1 and 2 data whenever both are available.

4.3 Coverage, Data Analysis and Results

4.3.1 Coverage and magnetosheath field orientation

The magnetic field data in this survey cover the periods 24 October 1977 to 23 January 1978; 2 July 1978 to 26 December 1978 and 29 June 1979 to 23 November 1979. During this time the ISEE satellites made $\sim$ 350 inbound and outbound passes through the magnetopause region. For each pass the magnetopause region was identified from the magnetic field data. In addition, for many of the 1977 and 1978 passes low resolution plasma data plots were available and these were used as confirmation of the magnetopause identification. On any particular outbound or inbound pass the magnetopause may be encountered more than once as a result of boundary motions. We shall therefore restrict general use of the words magnetopause crossing to full crossings and only distinguish between different crossings on the same pass if they are separated by over half an hour. Full crossing refers to a full penetration of the magnetopause layer, i.e., as the satellite travels directly from the magnetosheath through the magnetopause into the magnetosphere or vice versa.

Figure 4.1 shows the locations of 326 magnetopause crossings which are used in this survey and they represent 141 inbound and 138 outbound passes. Not all of the passes in the periods mentioned above are represented; this is the result of large data gaps in the magnetopause region, unprocessed data, or because the magnetopause cannot be reliably identified without the additional use of plasma data. Table 4.1 summarises the magnetosheath field orientation determined immediately adjacent to the magnetopause.

Figure 4.1(a) shows the magnetopause crossing locations after rotation into the GSM equatorial plane. For reference the solid curve shows the Fairfield (1971) model curve of the magnetopause and it can be seen that the curve is a good approximation to the average boundary shape. Figure 4.1(a) also shows that there is a good and fairly uniform coverage of the frontside magnetopause. The GSM local time coverage ranges from 0347 to 1859 in hours and minutes. Crossing locations

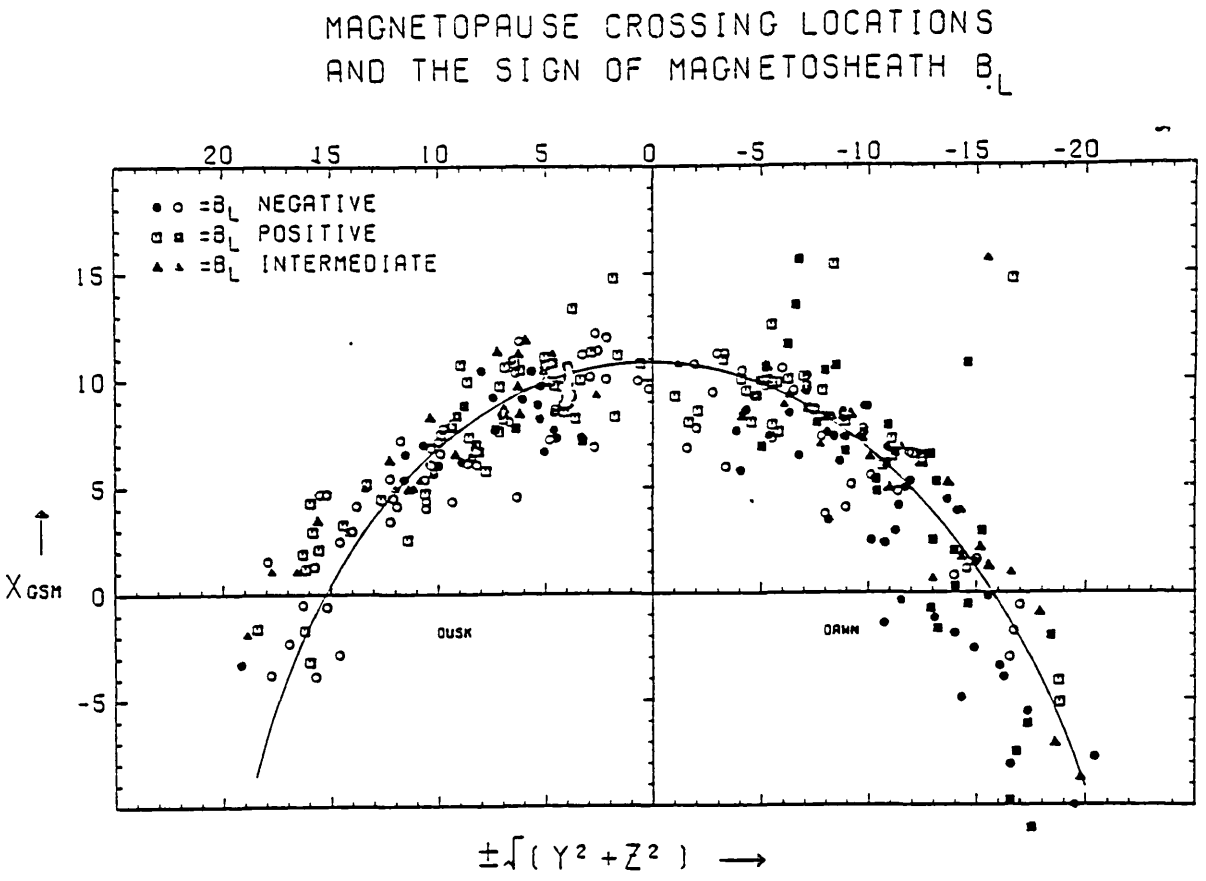


Fig. 4.1(a).

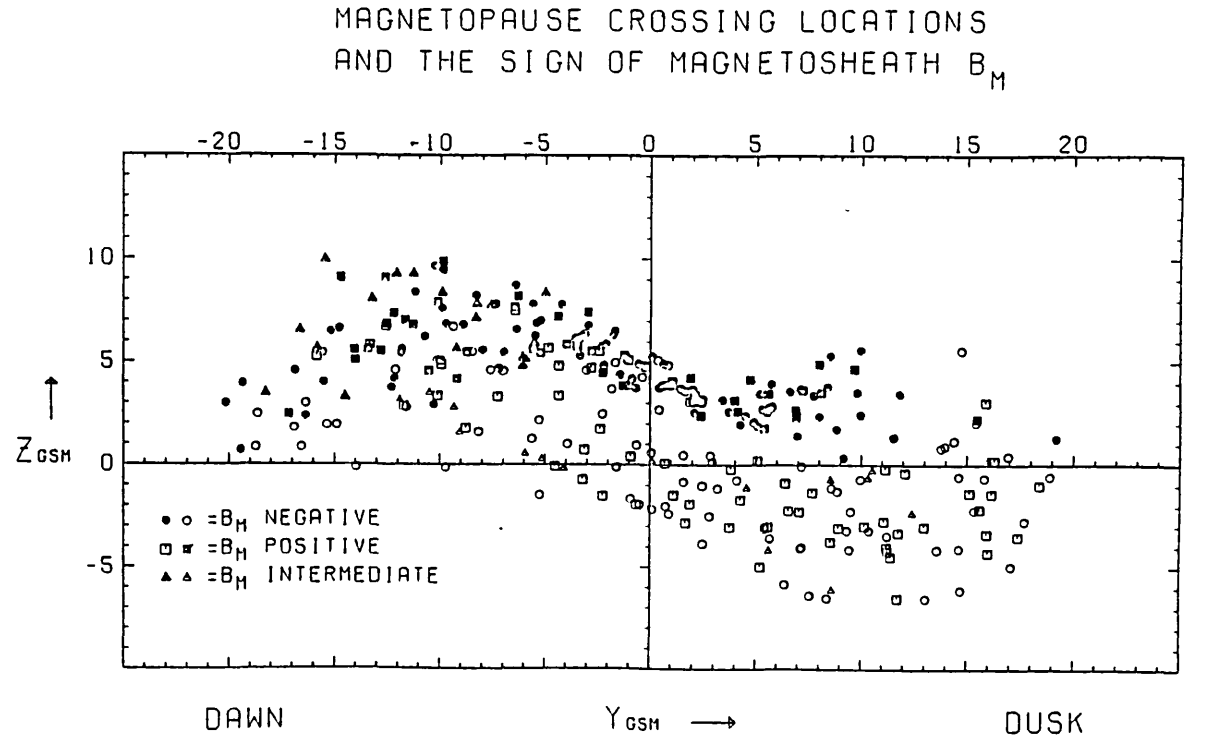


Fig. 4.1(b).

associated with inbound and outbound passes are represented by open and solid symbols, respectively. Different types of symbol refer to the magnetosheath B_L polarity just outside the magnetopause. If the B_L component is smaller than $\sim$ 5 nT in magnitude or if it fluctuates about the zero level then it is referred to as intermediate. Figure 4.1(b) shows the crossings plotted in the Y-Z GSM plane and this time the different types of symbol refer to the magnetosheath B_M polarity. This plot shows that the ISEE orbit does not produce such a uniform distribution of crossings in latitude. Crossings at northerly latitudes occur predominantly in the dawn sector, while southerly crossings occur predominantly in the dusk sector. The GSM latitude coverage ranges from 46.0° N to 33.5° S. Finally, it should be mentioned that to avoid too much overlap of the symbols only the innermost and outermost crossing locations have been plotted in Figure 4.1 in cases where more than two crossings occur on a particular outbound or inbound pass.

Table 4.1

Magnetosheath Field Orientation*

B_M \ B_L	Negative	Positive	Intermediate	Sub-Total B_M
Negative	95	53	29	177
Positive	45	47	18	110
Intermediate	17	15	7	39
Sub-Total B_L	157	115	54	

* determined immediately adjacent to the magnetopause

Table 4.1 shows the orientation distribution of the magnetosheath field in the L-M plane as determined immediately adjacent to the magnetopause crossings plotted in Figure 4.1. This Table shows that the crossings with negative B_L slightly exceed those with positive B_L, probably resulting from a more variable boundary motion and hence larger

number of crossings on a particular pass for southward fields. Also, the magnetopause is easier to identify when a large change in field direction occurs. However, the main feature to note is the discrepancy between the number of crossings with positive and negative B_M. The crossings with negative B_M outweigh those with positive B_M by almost a factor of two, and this is mainly because of the disparity when B_L is negative. Ordinarily one would expect different polarities of B_L or B_M to occur with equal probability, and hence it is surprising to see that the magnetosheath field prefers to lie along the negative B_M axis when B_L is negative while there is no reverse feature when B_L is positive. This feature has also been noted in the 1977-1978 data by Rijnbeek et al. (1984). The reason for it is unclear, but it could be a seasonal effect since most of the data are taken from the latter half of each year and no data from the spring season are included, during which ISEE 1 and 2 traverse the magnetotail region.

4.3.2 Identification and classification of FTEs

As described in Chapter 3, in Russell and Elphic's (1978) original description the magnetic signature of a magnetosheath FTE consists of an almost symmetric bipolar positive-negative deflection in the normal component B_N. The B_N signature is coupled with a rotation of the tangential field component towards the magnetospheric field orientation and also a substantial increase in field magnitude which reaches or even exceeds the magnetospheric level. FTEs with B_N signatures in the reverse, negative-positive sense have now also been found. This set of magnetosheath FTE signatures forms the basis of the selection criteria adopted by Berchem and Russell (1984). In publications subsequent to Russell and Elphic's (1978) discovery paper the definition of the FTE signature has been extended to include: events observed inside the magnetopause and magnetosphere regions; events which do not show a smooth rotation in the tangential field component but rather large-scale oscillatory changes; events with tangential field tilts away from the field direction on the opposite side of the magnetopause (see Chapter 3). In order to assess the importance of FTEs in driving magnetospheric convection and also to provide a more exhaustive survey we shall therefore adopt a more liberal interpretation of the FTE magnetic signature than that used by Berchem and Russell (1984). We shall justify this decision more fully in the discussion section.

The identification criteria for FTE magnetic signatures we shall adopt are as follows. An FTE needs to show a clear signature in the B_N component as well as a simultaneous deflection in the tangential field component. These signatures need to stand out from the general level of ambient magnetic field fluctuations. Also, in order to make allowance for the limited resolution available from the one hour plots of medium resolution field data, events with peak-to-peak B_N variations of less than $\sim$ 10 nT and events with a duration shorter than $\sim$ 1 min are not included in this survey. In one case the ambient field strength was low enough to enable the B_N amplitude limit to be lowered to $\sim$ 5 nT. In a number of other cases, when the ambient field strength is high, the B_N amplitude limit was raised to 20 nT or even higher. However, the B_N amplitude and FTE duration limits have no physical justification and are merely cut-offs designed to ensure the correct identification of FTEs. The possibility of FTE signatures occurring below these limits is not precluded and is in fact very likely, as careful examination of the data plots throughout this work will show.

In contrast to Berchem and Russell (1984), who only use magnetosheath FTEs in their statistics, we shall include FTEs observed in the magnetopause and magnetosphere regions in this survey although treating them on a separate basis. We shall also refrain from using a substantial field strength increase as an FTE identification criterion and rather use it as a guide to identify FTEs. There are occasions when FTEs are accompanied by oscillations in field magnitude or even substantial reductions in field strength (e.g., Figure 2 of Rijnbeek et al., 1984). Plasma data are also used whenever available to confirm that FTEs observed interior to the magnetopause are accompanied by boundary layer encounters, i.e., pulses of increased total number density and velocity compared to the ambient magnetospheric level (see Chapter 3). These checks generally confirm the FTE identification, but not all boundary layer plasma encounters are associated with magnetic signatures identified as FTEs for the purposes of this survey.

We shall refer to events observed interior and exterior to the magnetopause as magnetosphere and magnetosheath FTEs, respectively. We shall also classify FTEs according to their B_N signatures using the following scheme:

(1) standard FTEs show an outward followed by an inward (positive-negative) B_N signature (not necessarily symmetric);

(2) reverse FTEs show an inward followed by an outward (negative-positive) B_N signature (not necessarily symmetric);

(3) irregular FTEs show a single inward (negative) or outward (positive) signature or show a more complex B_N signature, such as inward-outward-inward.

Note that in the Berchem and Russell (1984) survey events falling under category (1) are referred to as direct FTEs.

4.3.3 Examples of FTE magnetic signatures

Figures 4.2 to 4.5 show examples of magnetosheath and magnetosphere FTE magnetic signatures. These figures are intended to complement other examples occurring in this work as well as the figures published in Rijnbeek et al. (1984) and they serve to illustrate some typical FTE magnetic signatures over a wide range of locations on the frontside magnetopause.

Figure 4.2 shows magnetic field data from ISEE 1 in LMN coordinates during an inbound pass of the magnetopause region on 23 January 1978. The magnetopause is crossed at $\sim$ 8:29 UT on the dawn flank at a northerly GSM latitude of $\sim$ 18°. Shortly after the start of the interval plotted the magnetosheath assumes a southward and duskward orientation and two standard FTEs can be seen at 8:09 and 8:15 UT, the latter apparently followed by a partial magnetopause penetration. Three standard FTEs occur in the magnetosphere at 8:36, 8:43 and 8:51 UT. The event at 8:43 UT has a pronounced tilt away from the magnetosheath field orientation.

Figure 4.3 shows field data from the inbound pass on 3 September 1979. The magnetopause is crossed at $\sim$ 12:30 UT at a duskward and southerly location. A number of reverse FTEs occur in the magnetosheath as indicated by the dashed vertical lines. Figure 4.4 shows data from the 24 July 1979 inbound pass, which occurred on the dusk flank at southerly latitudes. The magnetopause is crossed at $\sim$ 16:07 UT. The magnetosheath field has a mainly dawnward and sunward orientation. Several standard FTEs can be seen during this interval, both in the magnetosheath and magnetosphere regions. Figure 4.5 shows the final example, an inbound pass on 4 July 1978 which occurred on the dusk flank and above the magnetic equator. The magnetopause is crossed at 21:52 UT and the magnetosheath field has a southward and duskward orientation. Reverse and irregular FTEs occur over a three-hour interval during this

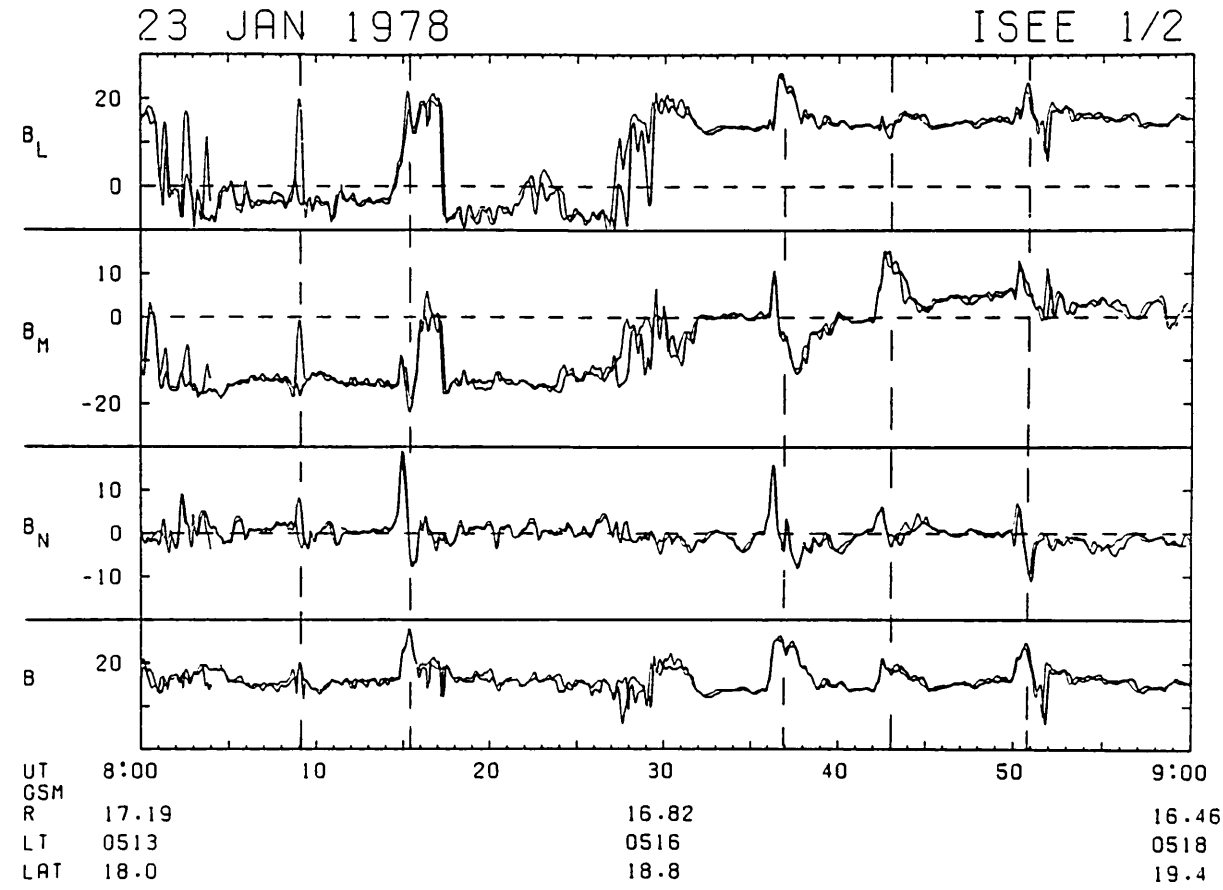


Fig. 4.2. FTEs on 23 January 1978.

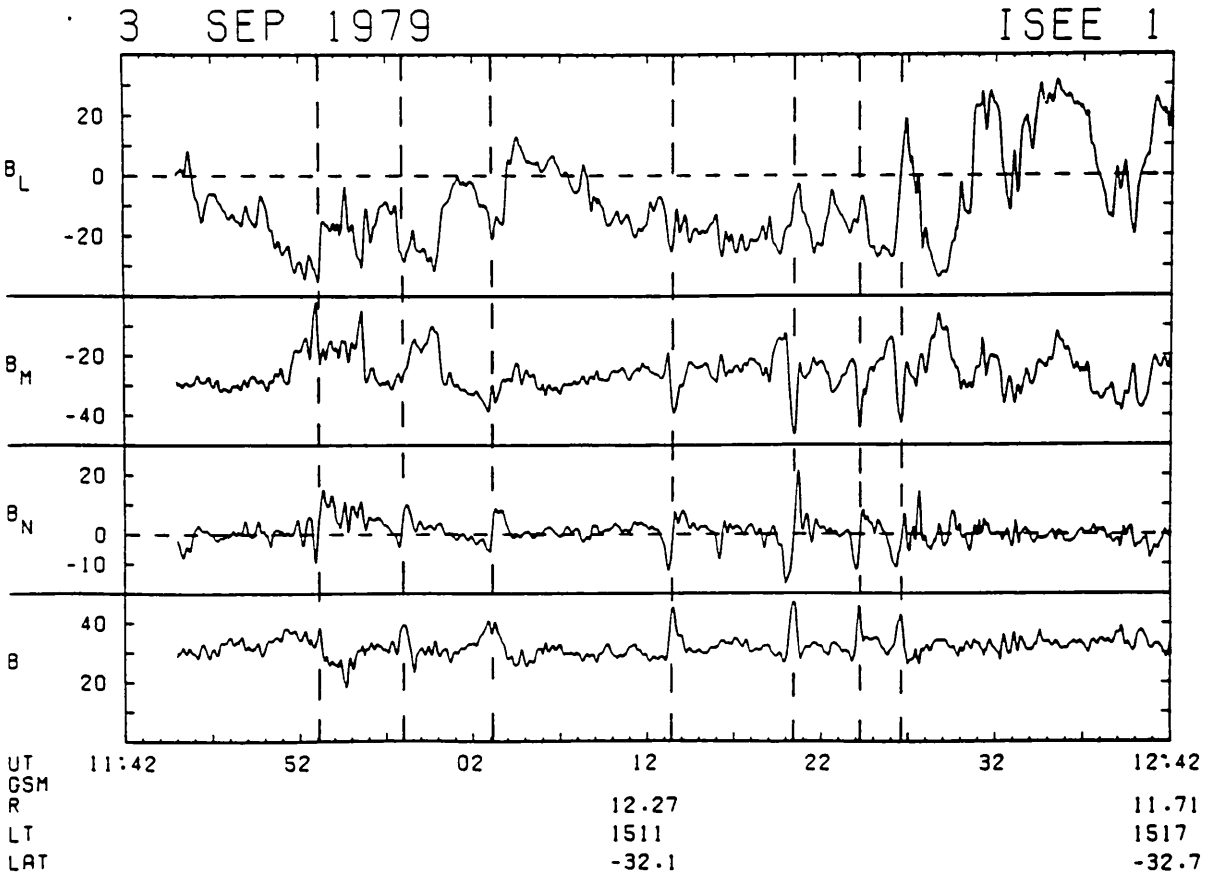


Fig. 4.3. FTEs on 23 September 1979.

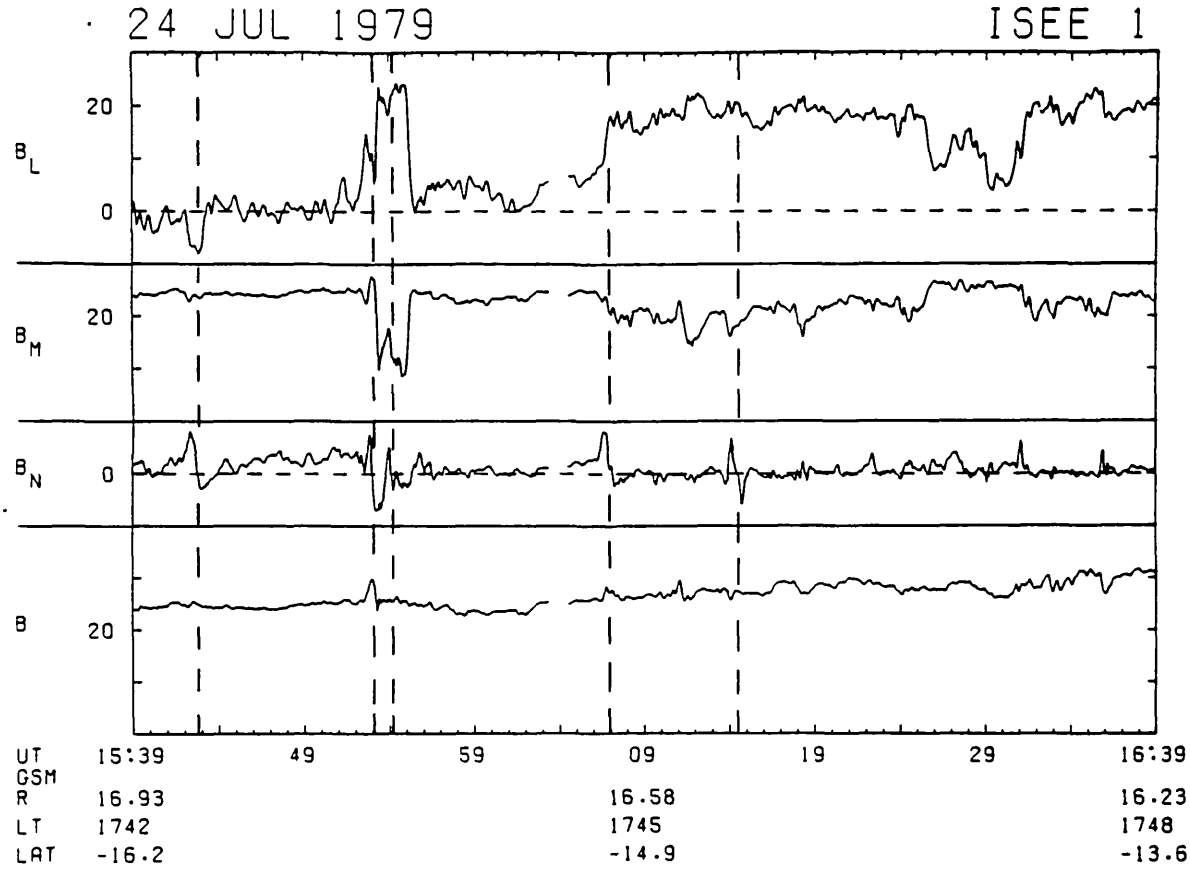


Fig. 4.4. FTEs on 24 July 1979.

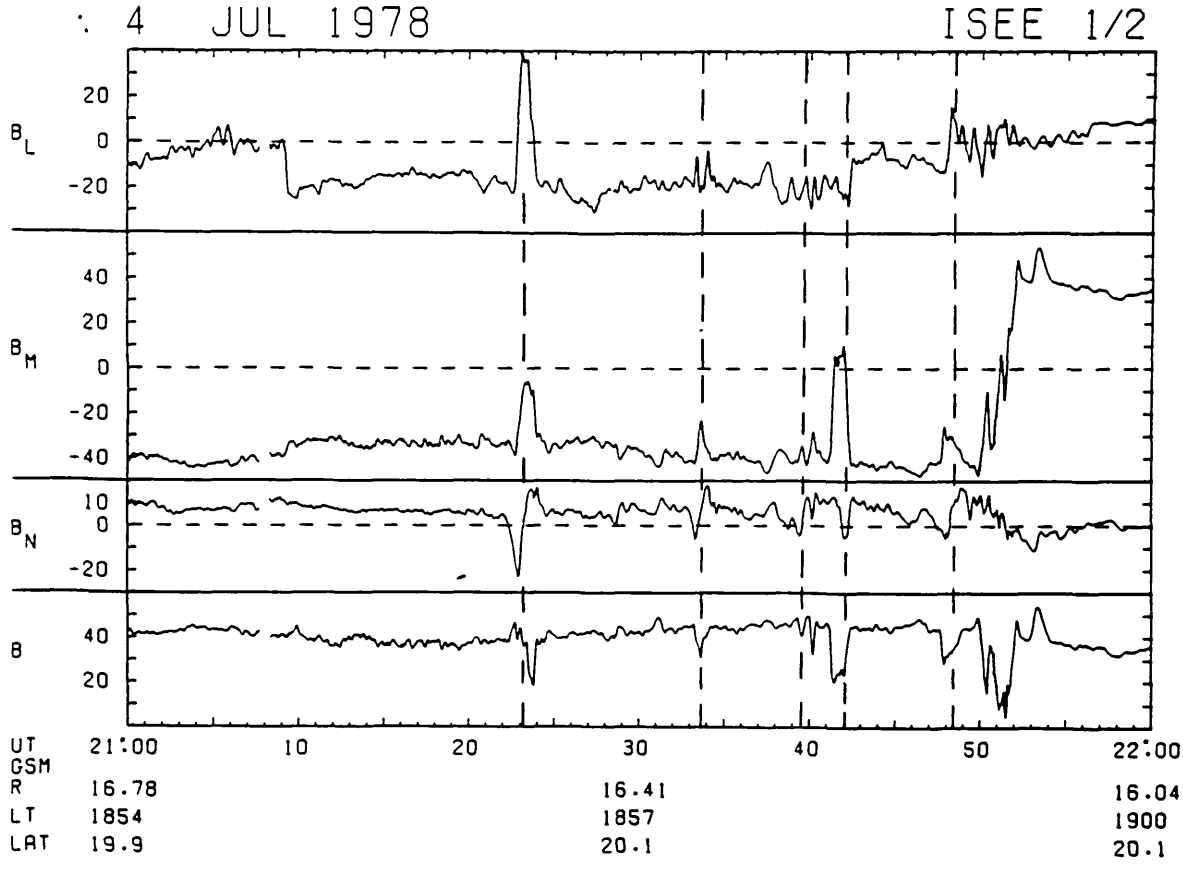


Fig. 4.5. FTEs on 4 July 1978.

pass and although most of them are accompanied by field strength increases, there are large field strength decreases during several events, e.g., at 21:42 UT in Figure 4.5.

Having defined our procedure for identifying FTEs we shall now concentrate on determining the properties of FTEs and the factors which control their occurrence.

4.3.4 Location of FTEs

Figure 4.6 shows the shows the locations in the Y-Z GSM plane of all the magnetopause crossings with which FTEs are associated. Figure 4.6(a) shows the locations of 165 magnetopause crossings spread over 88 inbound and 73 outbound passes which have magnetosheath FTEs associated with them. Figure 4.6(b) is the corresponding plot for 152 magnetopause crossings with magnetosphere FTEs, spread over 75 inbound and 70 outbound passes. The crossing symbols in both plots show a similar diagonally banded distribution to that in Figure 4.2, implying that there is no obvious FTE spatial dependence within the area covered by ISEE 1 and 2. The different symbols in the plots of Figure 4.6 show the type of B_N signature displayed by the FTEs for each particular crossing. If both irregular and standard (reverse) FTEs are observed in association with a specific crossing, then only the standard (reverse) FTE symbol is plotted. The mixed FTE symbol refers to crossings with observations of both standard and reverse FTEs. Examination of Figure 4.6 shows that the majority of the crossings occur either in association with standard FTEs or with reverse FTEs, the former occurring predominantly at northerly latitudes while the latter occur mostly at southerly latitudes. These features are evident for both the magnetosheath and magnetosphere FTEs. Also, the number of crossings in Figure 4.6 shows that FTEs are a common feature of the frontside magnetopause region covered by ISEE 1 and 2. Finally, note that on the scale of the plot the FTE observation locations do not differ for our purposes from the magnetopause locations with which they are associated.

4.3.5 Magnetosheath magnetic field and FTEs

In Figure 4.7 the same crossings which are plotted in Figure 4.6 are plotted in the GSM equatorial plane. Figure 4.7(a) shows the crossings with magnetosheath FTEs and Figure 4.7(b) is the corresponding plot for crossings with magnetosphere FTEs. In each plot the symbols

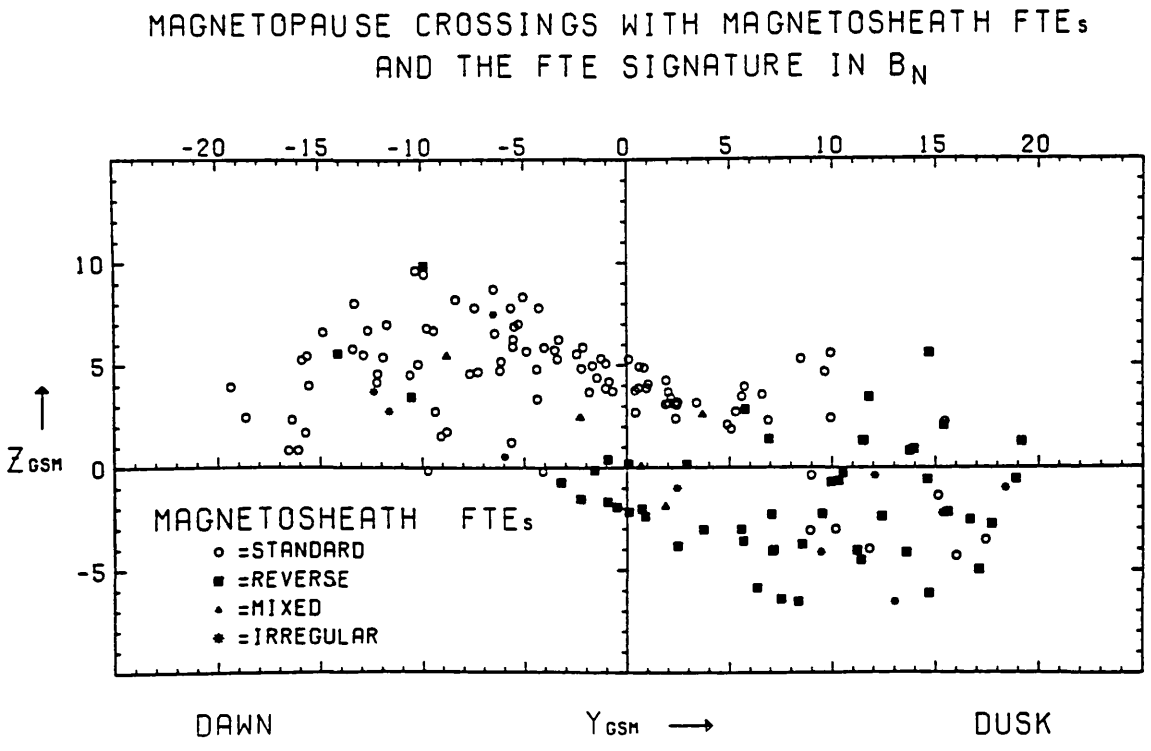


Fig. 4.6(a).

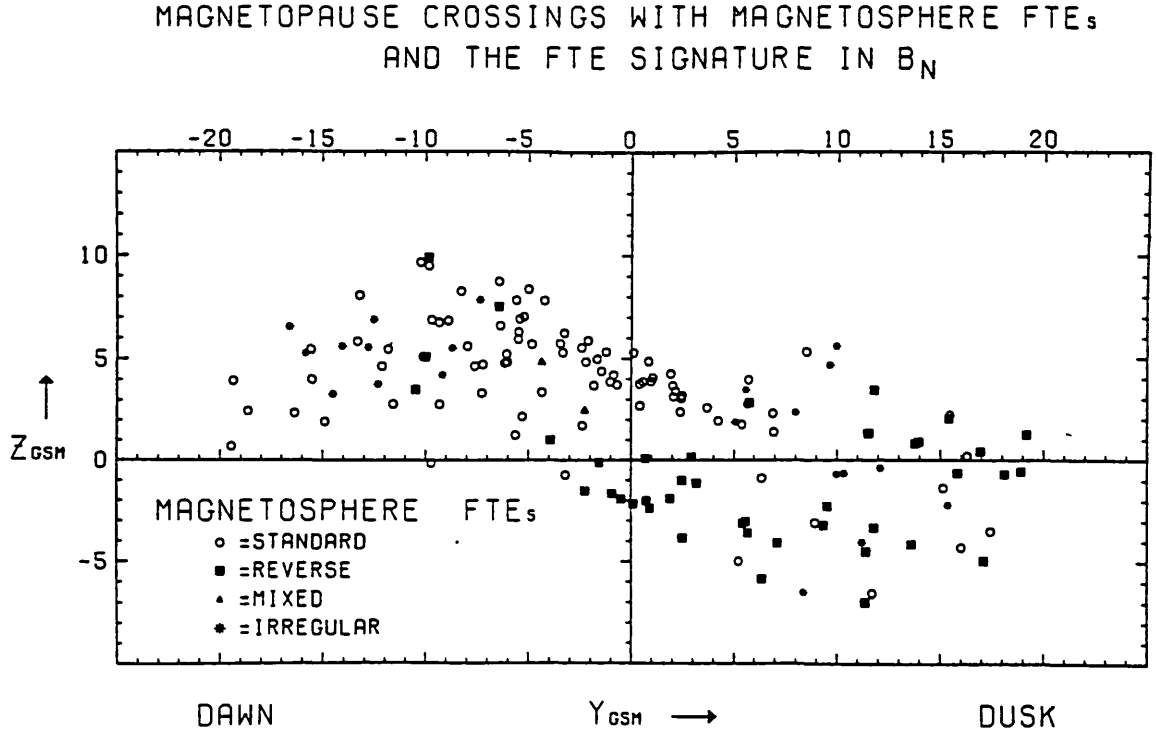


Fig. 4.6(b)

LOCATIONS OF MAGNETOPAUSE CROSSINGS WITH MAGNETO-SHEATH FTEs AND THE SIGN OF MAGNETOSHEATH B_L

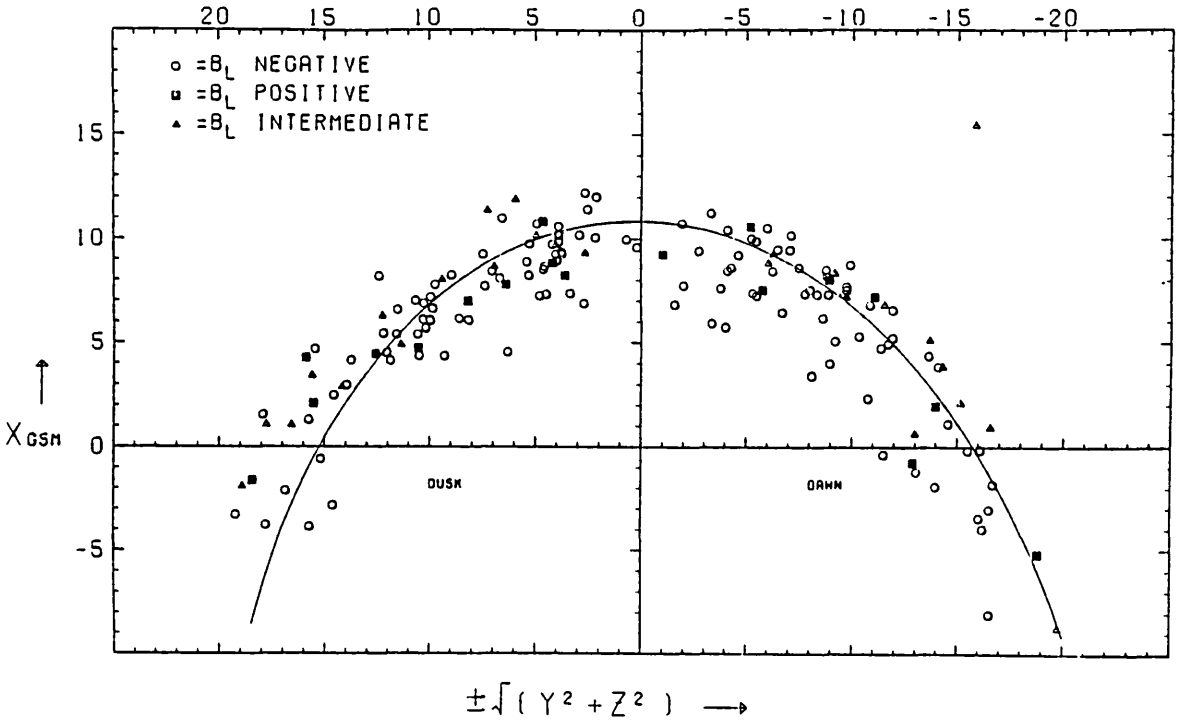


Fig. 4.7(a).

LOCATIONS OF MAGNETOPAUSE CROSSINGS WITH MAGNETO-SPHERE FTEs AND THE SIGN OF MAGNETOSHEATH B_L

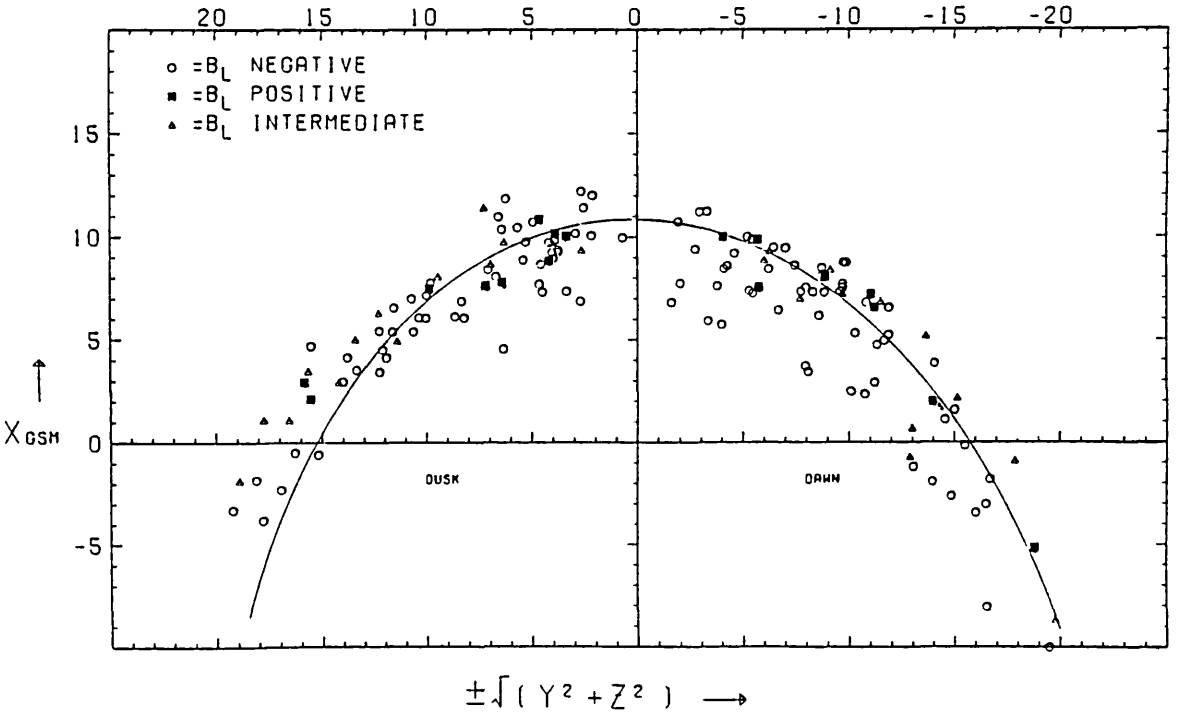


Fig. 4.7(b).

refer to the polarity of the magnetosheath B_L component, determined immediately adjacent to the magnetopause. Figure 4.7 should therefore be compared with Figure 4.1. This comparison will show that the subsets of crossings with magnetosheath FTEs and those with magnetosphere FTEs both have a distribution which is very similar to the total number of crossings, in agreement with the conclusion in 4.3.4. Another feature which is apparent in Figure 4.7 is that most of the crossings with a northward (positive B_L) magnetosheath field component have been filtered out, while most of the crossings with negative B_L polarity remain. Table 4.2 demonstrates this also. Here the crossings of Figure 4.7 are subdivided according to the polarity of the magnetosheath B_L and B_M components. The figures show the number of crossings with magnetosheath FTEs associated with a particular combination of B_L and B_M polarity, while the numbers in parentheses refer to crossings with magnetosphere FTEs. The table shows that almost three-quarters of the crossings with magnetosheath or magnetosphere FTEs are associated with a negative B_L component, while only about one tenth have a positive B_L polarity. This result suggests that the magnetosheath B_L polarity is the primary factor controlling FTE occurrence.

Table 4.2

Magnetosheath Field Orientation* for Crossings with FTEs**

B_M \ B_L	Negative	Positive	Intermediate	Subtotal B_L
Negative	73(70)	9(11)	19(15)	101(96)
Positive	33(30)	8(5)	8(10)	49(45)
Intermediate	13(8)	2(1)	0(2)	15(11)
Subtotal B_M	119(108)	19(17)	27(27)	

* determined immediately adjacent to the magnetopause

** parentheses refer to magnetosphere FTEs

Table 4.2 also shows that most of the crossings with FTEs are

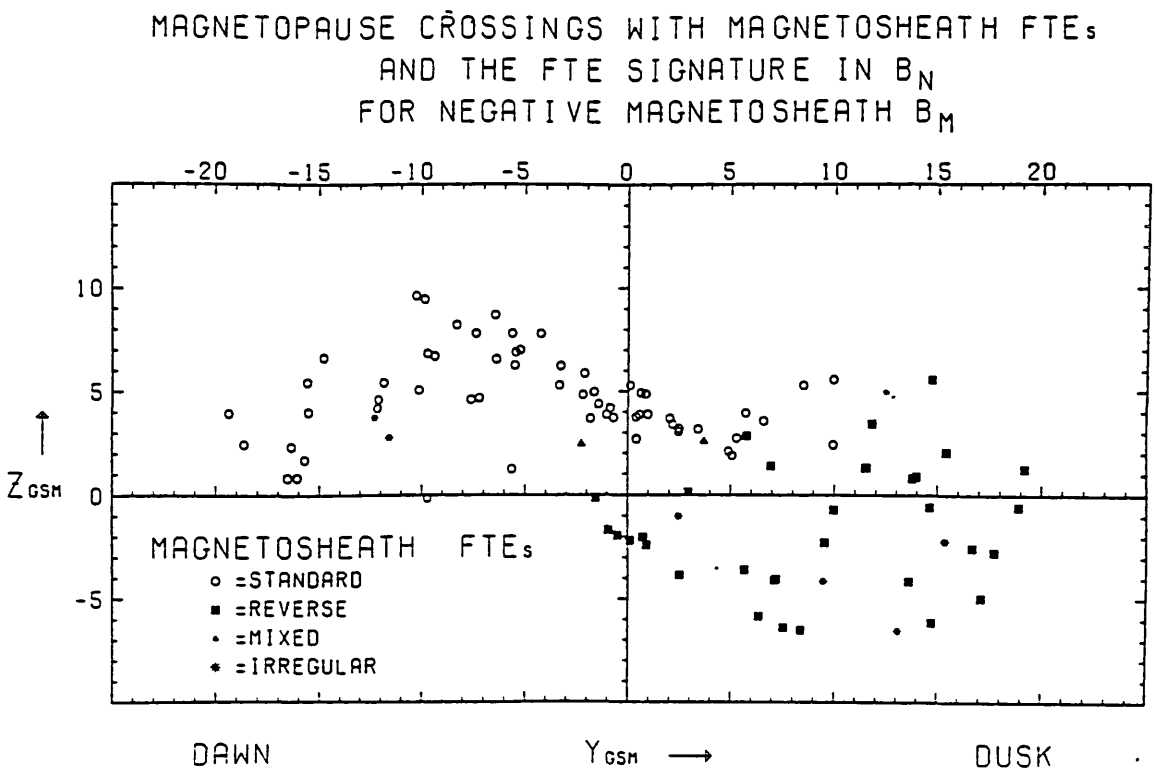


Fig. 4.8(a).

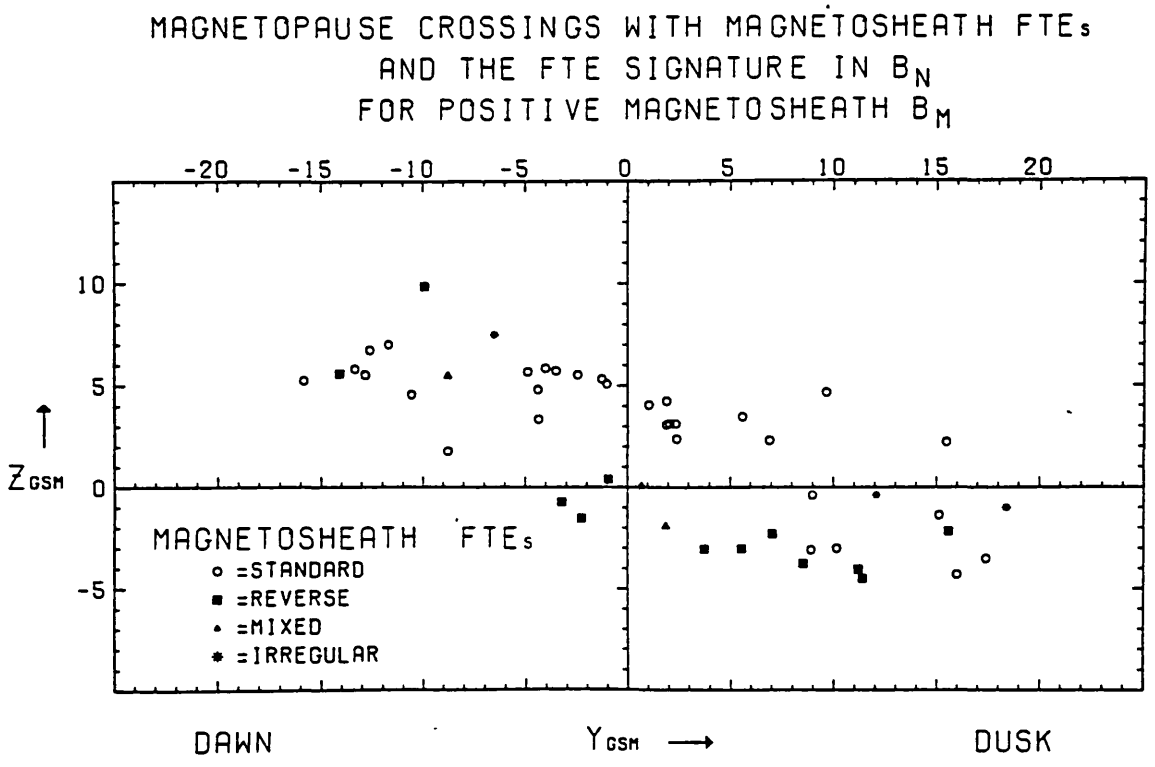


Fig. 4.8(b).

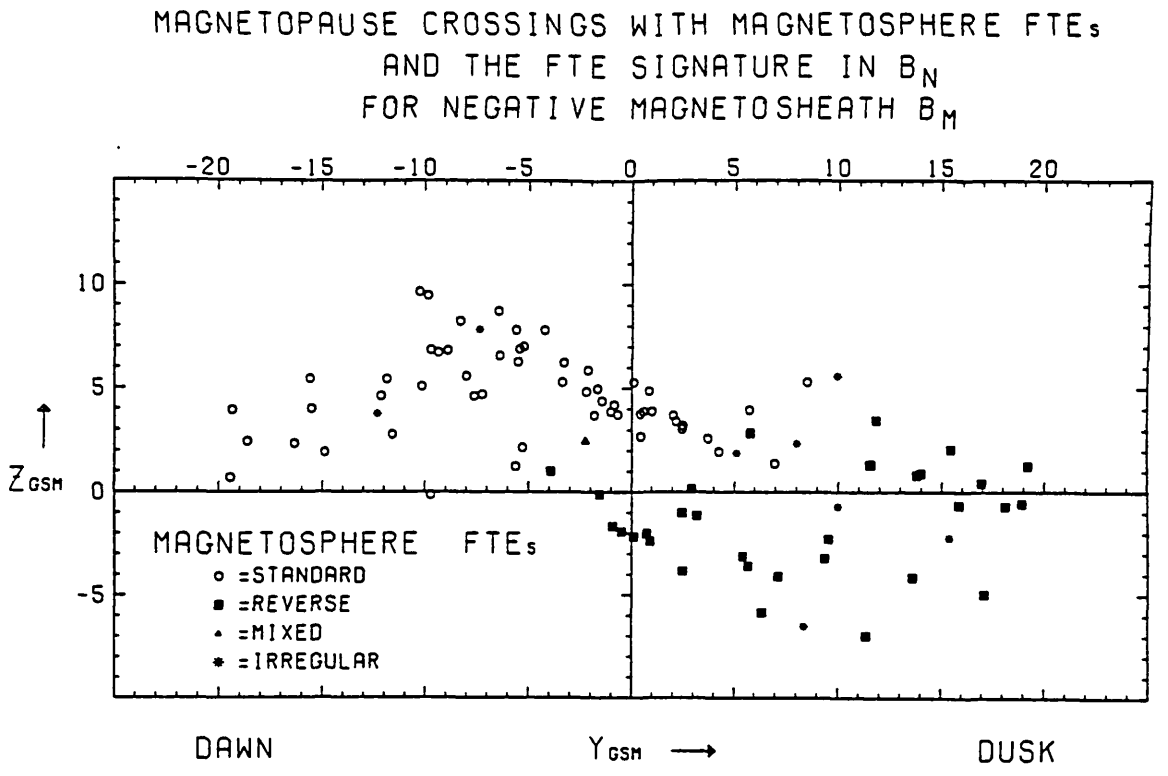


Fig. 4.9(a).

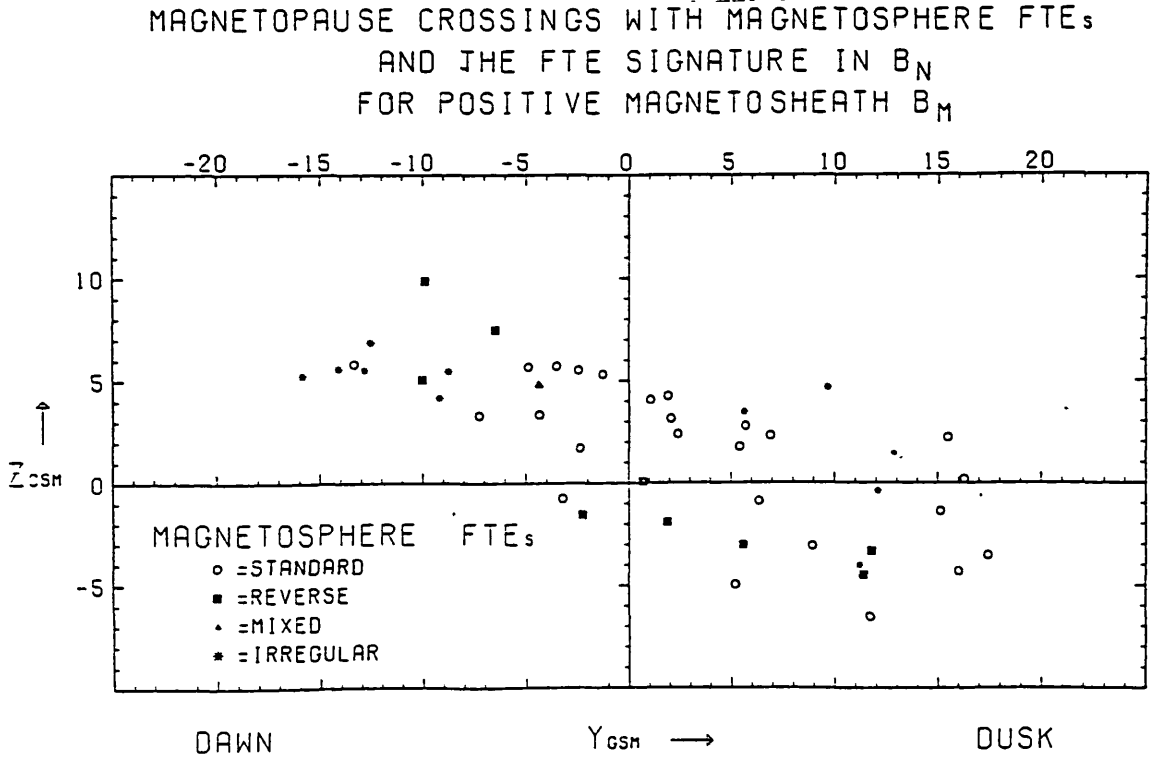


Fig. 4.9(b).

associated with a negative magnetosheath B_M polarity. However, we have previously noted in Table 4.1 that most of the crossings with negative B_L also have a negative B_M component. Therefore, we cannot conclude from Table 4.2 that the magnetosheath B_M component exerts any control on FTE occurrence. The ratio of the total number crossings with negative or positive B_M divided by the number of crossings with FTEs having negative or positive B_M is approximately the same, which suggests that FTE occurrence is not significantly affected by the polarity of magnetosheath B_M.

In 4.3.4 we noted that the FTE B_N signature is ordered to a large degree by magnetic latitude, with standard and reverse FTEs occurring predominantly at northern and southern latitudes, respectively. Figure 4.6 shows a number of exceptions to this simple rule, however. We will therefore make an attempt to see whether these exceptions can be related to the magnetosheath B_M polarity. Figures 4.8 and 4.9 show the crossing locations associated with magnetosheath and magnetosphere FTEs, respectively, plotted in the same format as Figure 4.6. In Figures 4.8(a) and 4.9(a) the crossings with negative magnetosheath B_M are plotted, while Figures 4.8(b) and 4.9(b) show crossings with positive B_M. Examination of these plots reveals that with a few exceptions the anomalous FTE B_N signatures can be related to the polarity of magnetosheath B_M: standard FTEs in the Southern Hemisphere occur only in the dusk sector when B_M is positive, and only in the dawn sector (one event) when B_M is negative. Similarly, reverse FTEs occur in the Northern Hemisphere only in the dawn sector when B_M is positive, and only in the dusk sector when B_M is negative. Figures 4.4 and 4.5 show two case examples of this feature and we shall return to it in the discussion section.

4.3.6 Coordinate system and FTEs

So far we have examined the distributions of magnetopause crossings solely in the GSM coordinate system. This system is frequently used to examine magnetopause crossing locations and magnetosheath parameters (Russell, 1971). Two other global magnetospheric coordinate systems which are in common use are the GSE and SM coordinate systems (Appendix B). To see whether a choice of these coordinate systems affects the conclusions reached in previous subsections, the data points in Figures 4.6(a) and 4.8 have been replotted in the GSE and SM

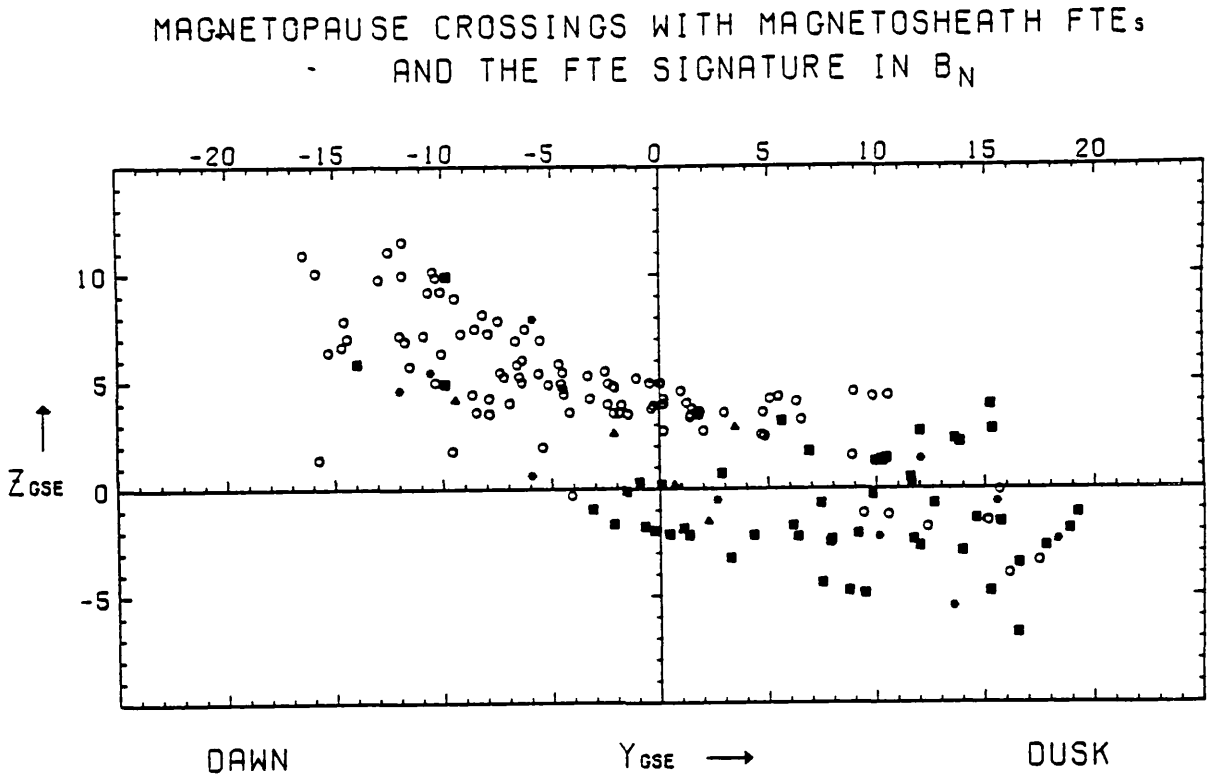


Fig. 4.10(a).

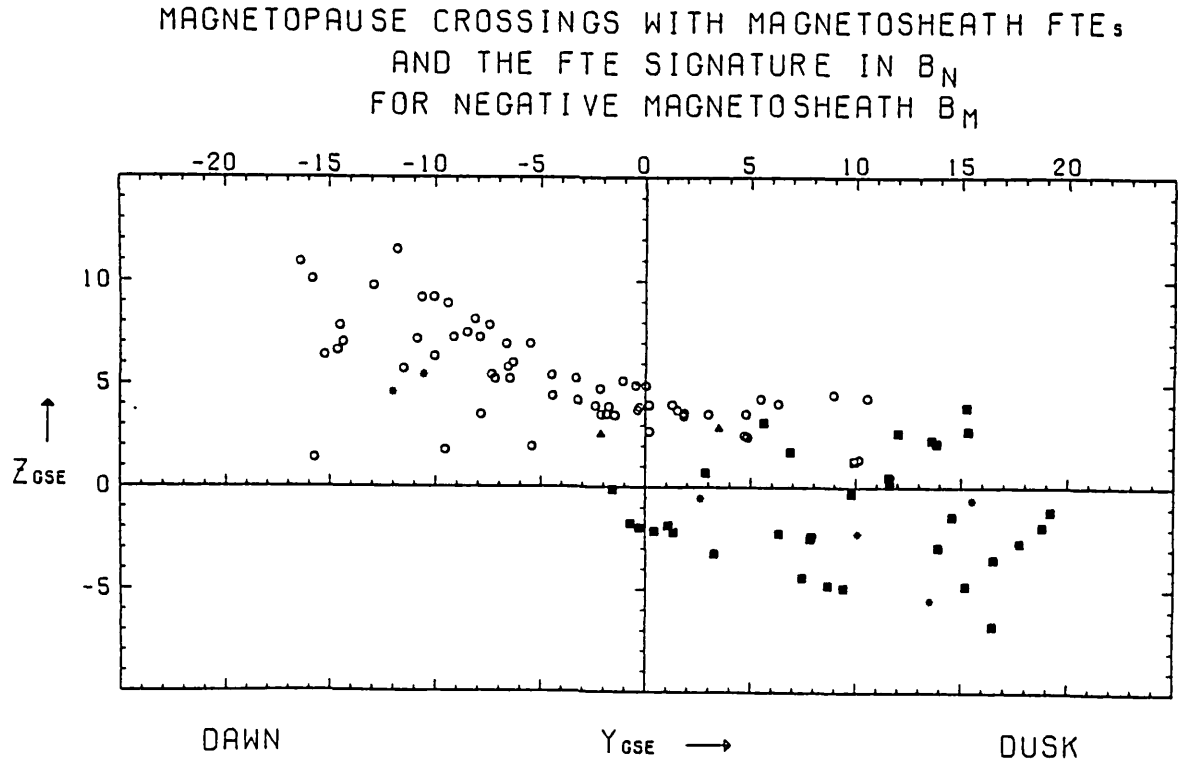


Fig. 4.10(b).

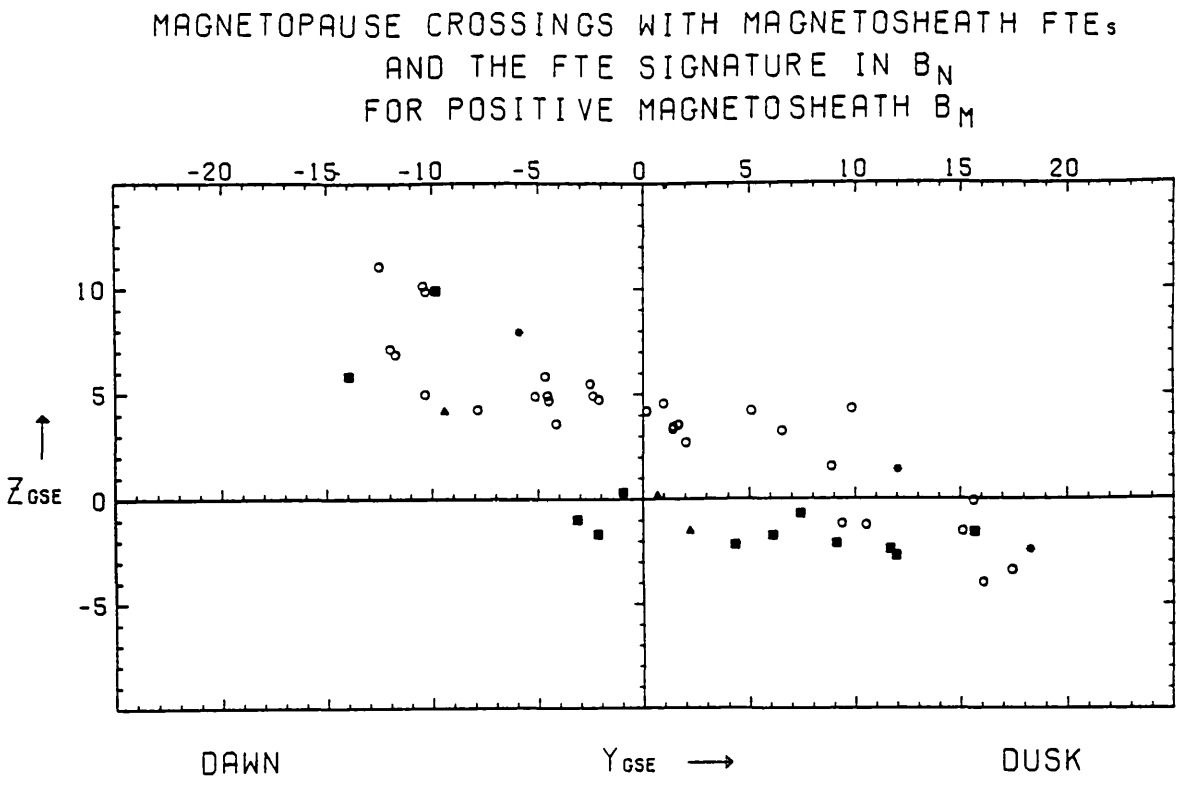


Fig. 4.10(c).

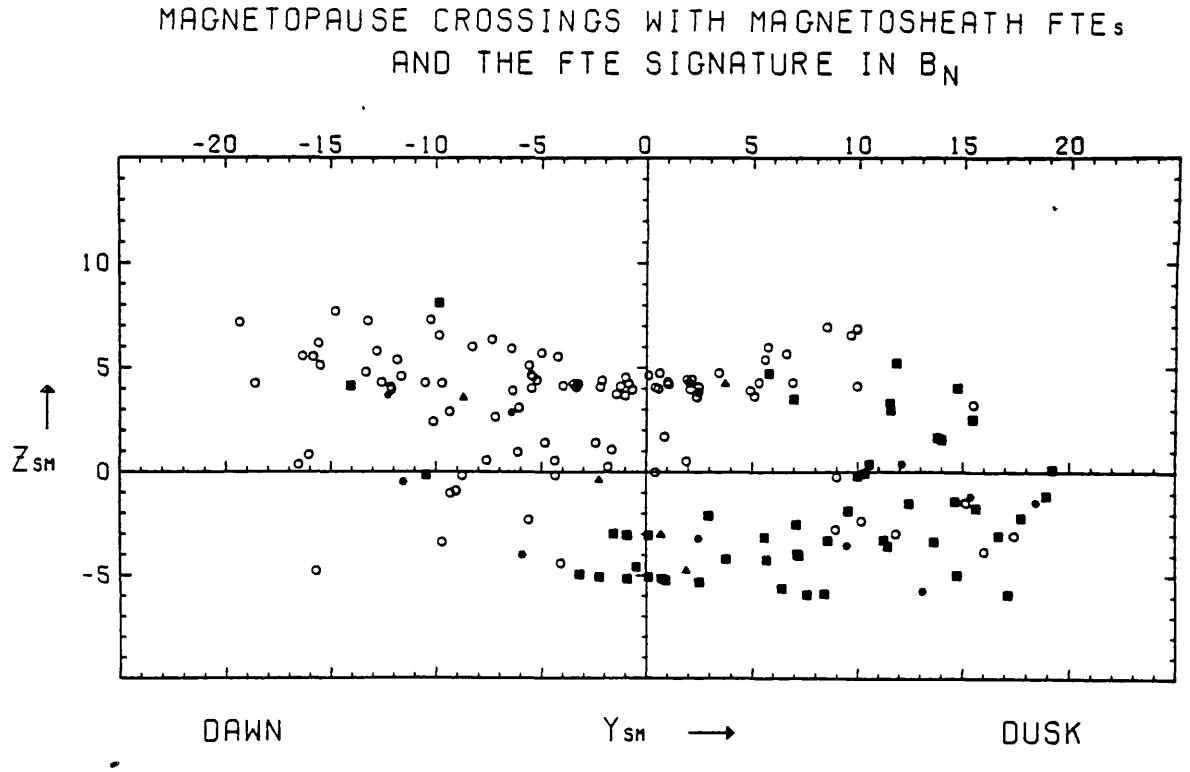


Fig. 4.11(a).

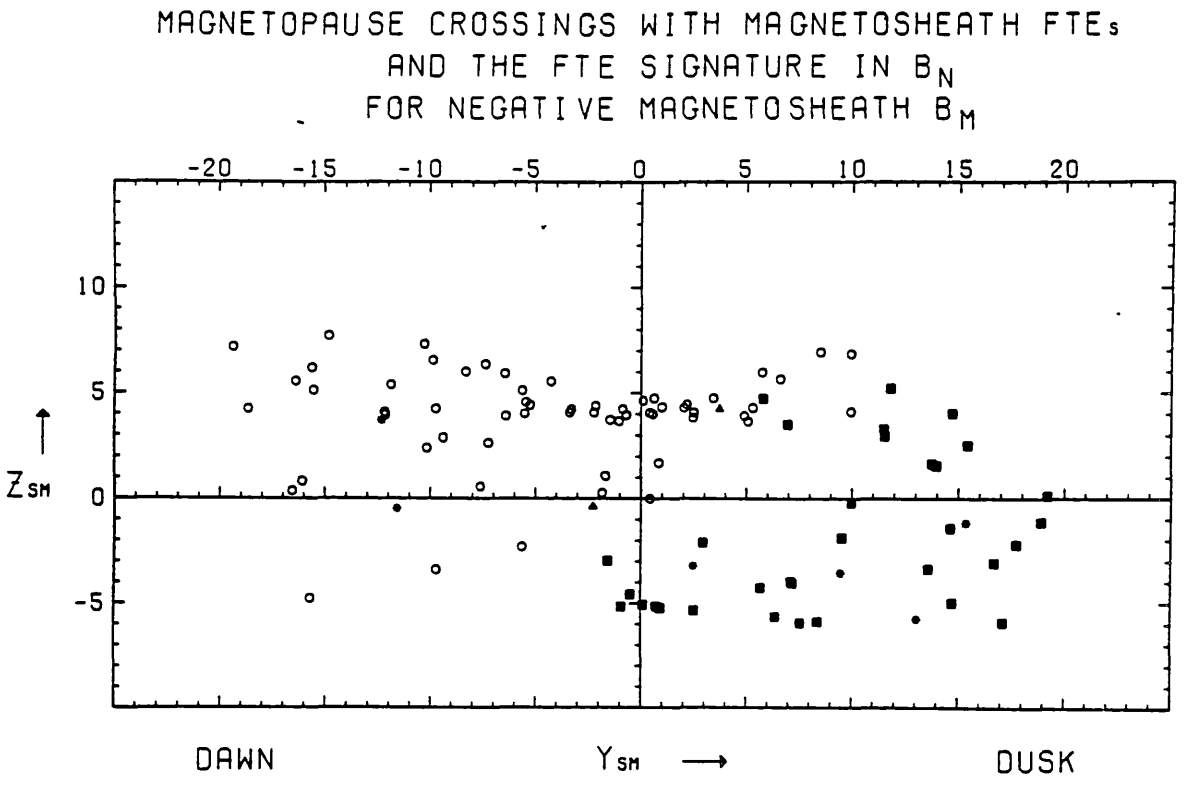


Fig. 4.11(b).

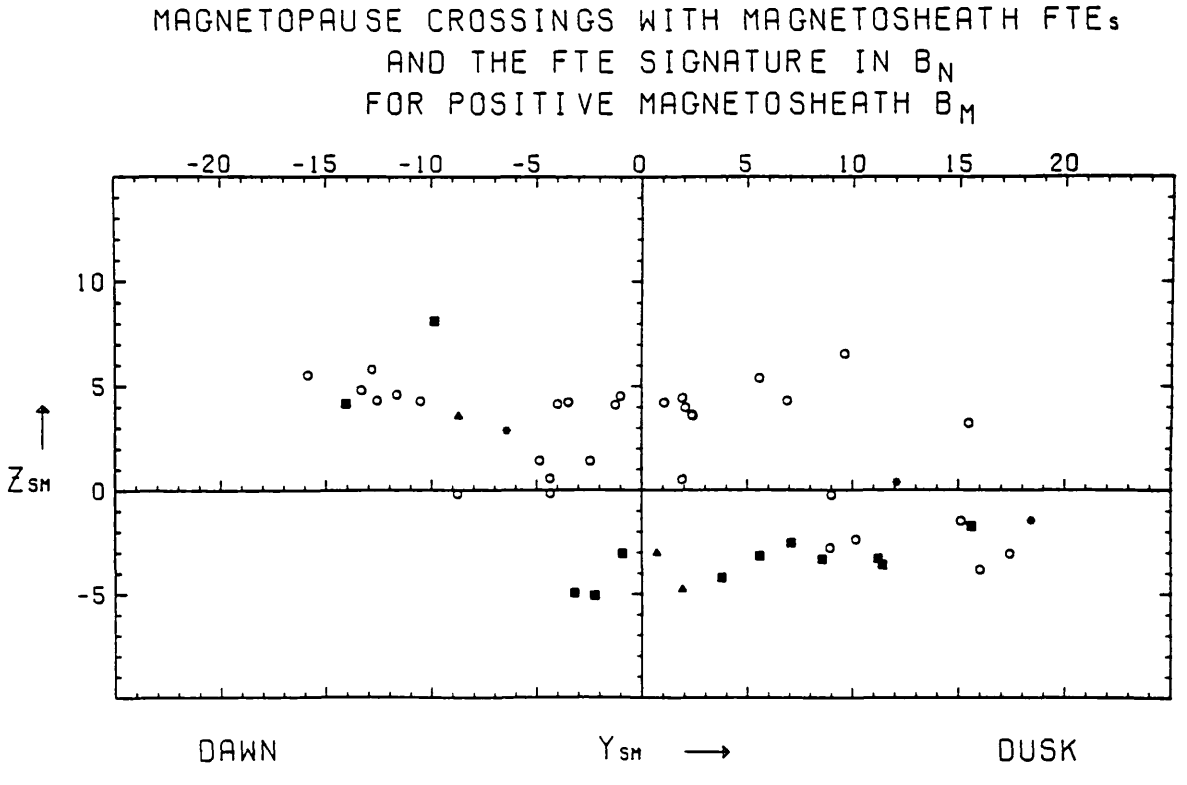


Fig. 4.11(c).

coordinate systems. Figure 4.10 shows the GSE plots and Figure 4.11 shows the SM plots corresponding to Figures 4.6(a) and 4.8. Examination of these plots reveals that although the general appearance of the magnetopause crossing distributions is altered, the conclusions reached previously concerning FTEs are not affected by the choice of a particular coordinate system. Although we have chosen not to display them, the same result also holds for the plots of crossings with magnetosphere FTEs.

4.3.7 When do FTEs occur?

In section 4.3.5 we noted that magnetosheath and magnetosphere FTEs occur predominantly when the magnetosheath field adjacent to the magnetopause has a southward component. In order to determine whether a southward field component is a sufficient condition for FTEs to occur, we need to compare the field orientation for crossings associated with FTEs to those without FTEs. However, since FTEs have a finite recurrence time and spatial extent they may be missed easily, because of data gaps. We shall therefore first apply some selection criteria to our data set.

From results presented in the previous chapter and from Figures 4.2-4.5 it is reasonable to estimate the FTE recurrence time to be of order 10 min. Also, FTE signatures are observed to last a few minutes. We therefore reject all magnetopause crossings with magnetosheath encounters less than 30 min and/or with data gaps larger than $\sim$ 5 min. We also eliminate crossings beyond the dawn and dusk (GSM) meridians, so that we are left only with crossings between 0600 and 1800 GSM local time. The reasons for the latter are that the ISEE orbit is more tangential to the magnetopause on the dawn and dusk flanks, so that often the magnetopause is encountered a large number of times on a single pass as the boundary flops back and forth. Although in many cases plasma plots are available, they are not always of sufficient resolution to make a reliable distinction between magnetosheath, magnetopause and boundary layer regions. Also, the ambient level of fluctuations in the B_N component is often high on the flanks even when the external field is strongly northward and this makes it difficult to identify the FTE signatures reliably.

The elimination procedure outlined above results in a data set of 217 magnetopause crossings spread over 102 in- and 100 outbound passes.

To determine the control exerted by the magnetosheath field on the occurrence of FTEs, the crossings are then classified in terms of this field as determined in the half-hour magnetosheath interval adjacent to each crossing. The B_L and B_M components are assigned a positive or negative label if they stay predominantly at that sign (not including FTE field deflections) during this half hour interval. If this condition is not satisfied, or if the magnitude of the B_L or B_M components is less than $\sim$ 5 nT, then they are labelled intermediate.

Table 4.3 and Figure 4.12 summarise the results obtained using the above classification scheme for magnetosheath FTEs. Clearly, the polarity of the magnetosheath B_L component can be used very effectively to predict whether FTEs will be seen in the dayside magnetosheath region. With few exceptions magnetosheath FTEs are seen whenever the magnetosheath field has a southward component and not when it has a northward component. Individual examples showing the close control exerted by the magnetosheath field orientation on FTE occurrence are given in Figures 4.13 and 4.14. Figure 4.13 shows ISEE 1 data from an inbound pass on 21 August 1978. As a result of boundary motion, the magnetopause is crossed three times during the interval shown: at 21:09, 21:27 and 21:41 UT. Initially, magnetosheath B_M is the strongest component and there is no sign of any FTE activity. In the second interval in the magnetosheath the B_L component has turned strongly southward and two reverse FTEs are seen at 21:31 and 21:35 UT. Figure 4.14 shows data from an outbound pass on 30 September 1979. The main magnetopause crossing occurs at 7:59 UT. Initially, the magnetosheath field is southward and dawnward. However, after 8:12 UT, the field turns northward (and duskward) such that the magnetosheath-magnetosphere field angle decreases, and straightaway the FTE activity subsides. Note that the 21:41 UT crossing in Figure 4.13 is not included in Figure 4.12 and Table 4.3 because of the short magnetosheath interval. Also, the crossing in Figure 4.14 is classed as having intermediate B_L in accordance with our criteria. In spite of this the conclusions reached from Figure 4.12 and Table 4.3 agree with those from the individual case examples.

Table 4.3 also shows the number of crossings with a particular magnetosheath B_M polarity. The most noteworthy feature is again that there are fewer crossings which have positive B_M polarity, a feature which is primarily evident for crossings associated with negative B_L.

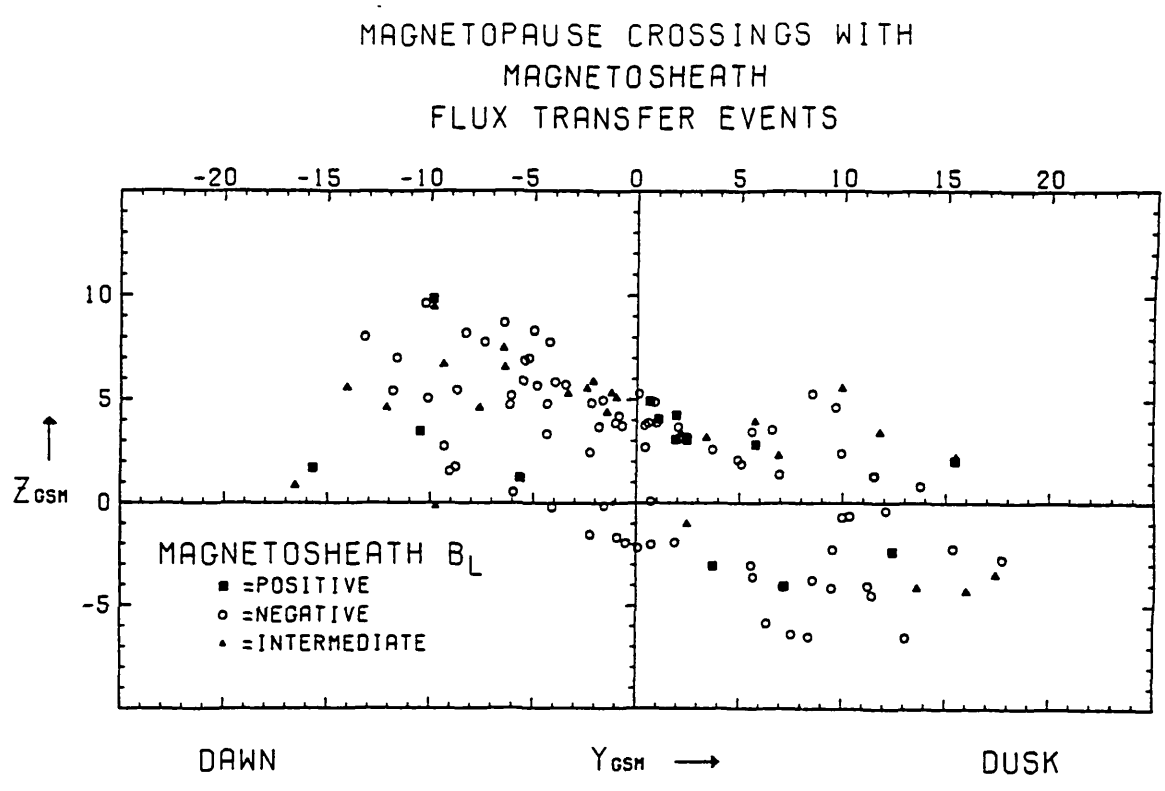


Fig. 4.12(a).

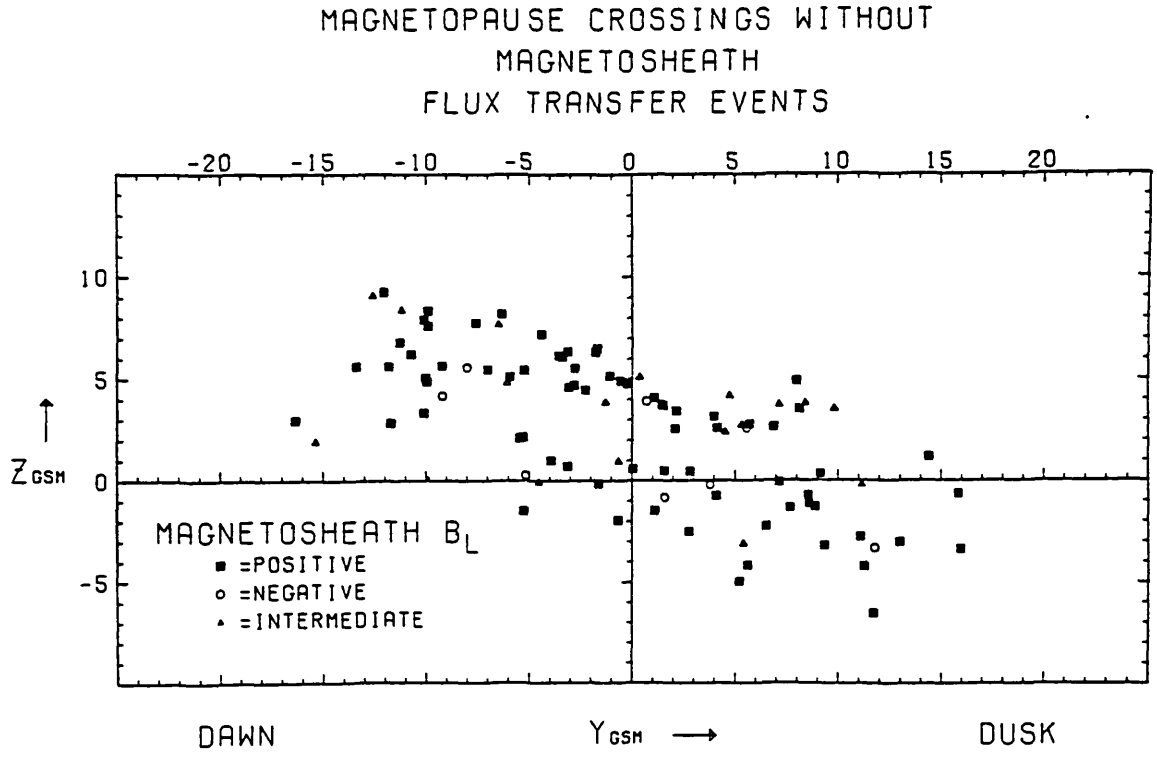


Fig. 4.12(b).

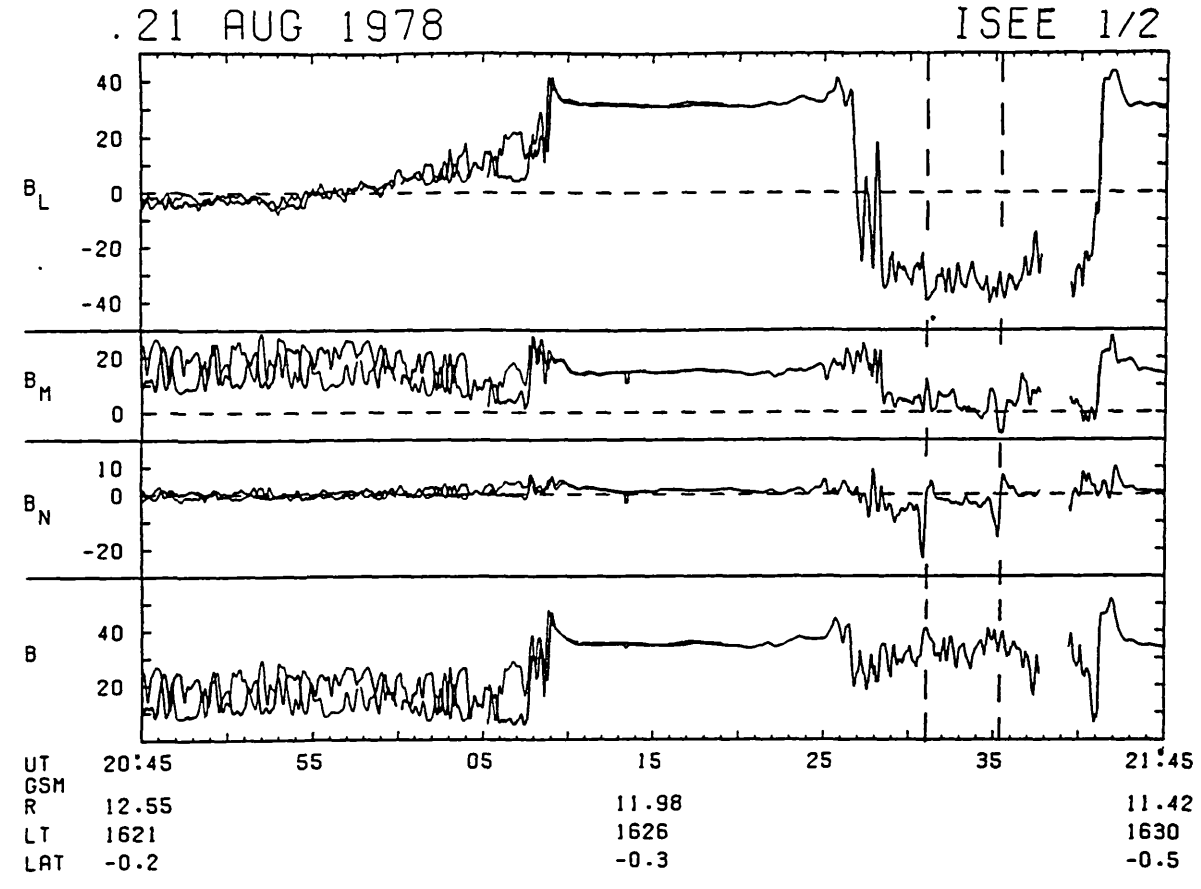


Fig. 4.13. FTEs on 21 August 1978.

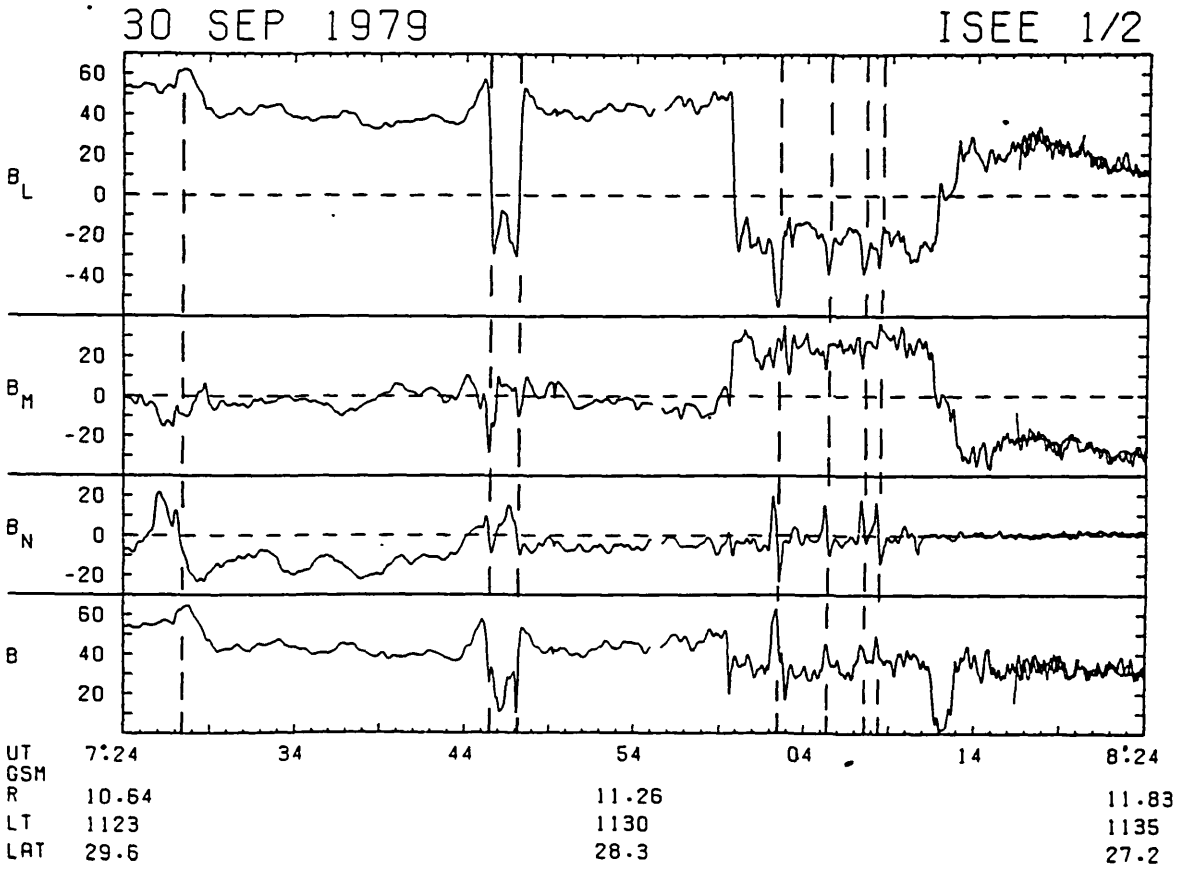


Fig. 4.14. FTEs on 30 September 1979.

From this table it appears that the polarity of magnetosheath B_M does not exert an appreciable influence on FTE occurrence, or at least the effect is second order compared to the polarity of the B_L component.

Table 4.3

Magnetosheath Field Orientation* for Magnetosheath FTEs

B_M \ B_L	Negative	Positive	Intermediate	Subtotal B_M
Negative	49(4)	8(35)	16(9)	73(48)
Positive	18(3)	4(29)	9(6)	31(38)
Intermediate	12(1)	2(9)	1(2)	15(12)
Subtotal B_L	79(8)	14(73)	26(17)	

* determined in half-hour interval adjacent to magnetopause

** figures refer to crossings with magnetosheath FTEs (no parentheses) and without magnetosheath FTEs (in parentheses)

We shall next investigate whether the conclusions reached above also hold for magnetosphere FTEs. In order to do this we need to allow for the finite recurrence time of magnetosphere FTEs, which as before we take to be of order 10 min. We shall therefore require all crossings to have at least half an hour of magnetic field measurements inside the magnetosphere, with no data gaps longer than $\sim$ 5 min. Also, if there are rapid multiple crossings which follow (precede) the initial (final) entry into the magnetosphere, then the starting time for the half-hour interval is reset to zero following (preceding) each magnetosphere entry. We also need to allow for changes in magnetosheath B_L or B_M while the satellite is inside the magnetosphere. We shall therefore reject a set of multiple crossings if B_L and/or B_M changes sign (disregarding FTE signatures) during the short magnetosheath encounters. This then minimizes the effect of a possible change in magnetosheath field orientation while ISEE 1 and 2 are inside the magnetosphere.

Applying the procedure above eliminates 30 of the crossings listed in Table 4.3, to leave us with a data set of 187 crossings. The results

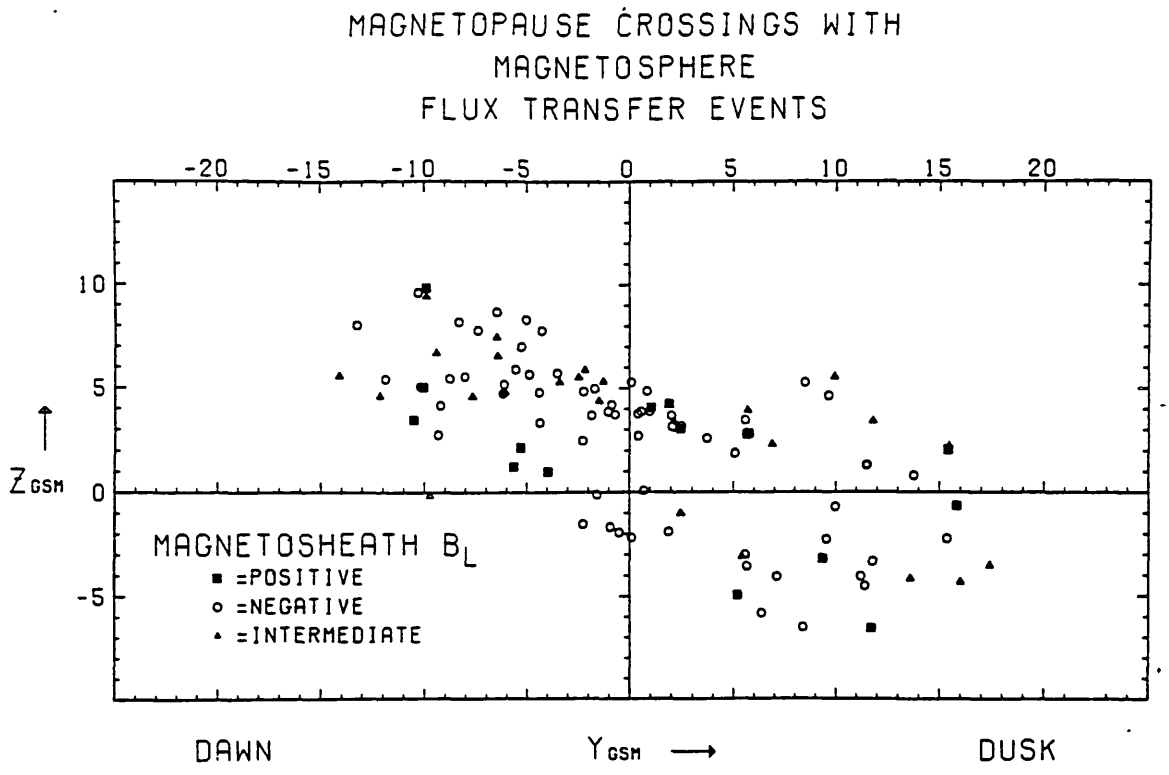


Fig. 4.15(a).

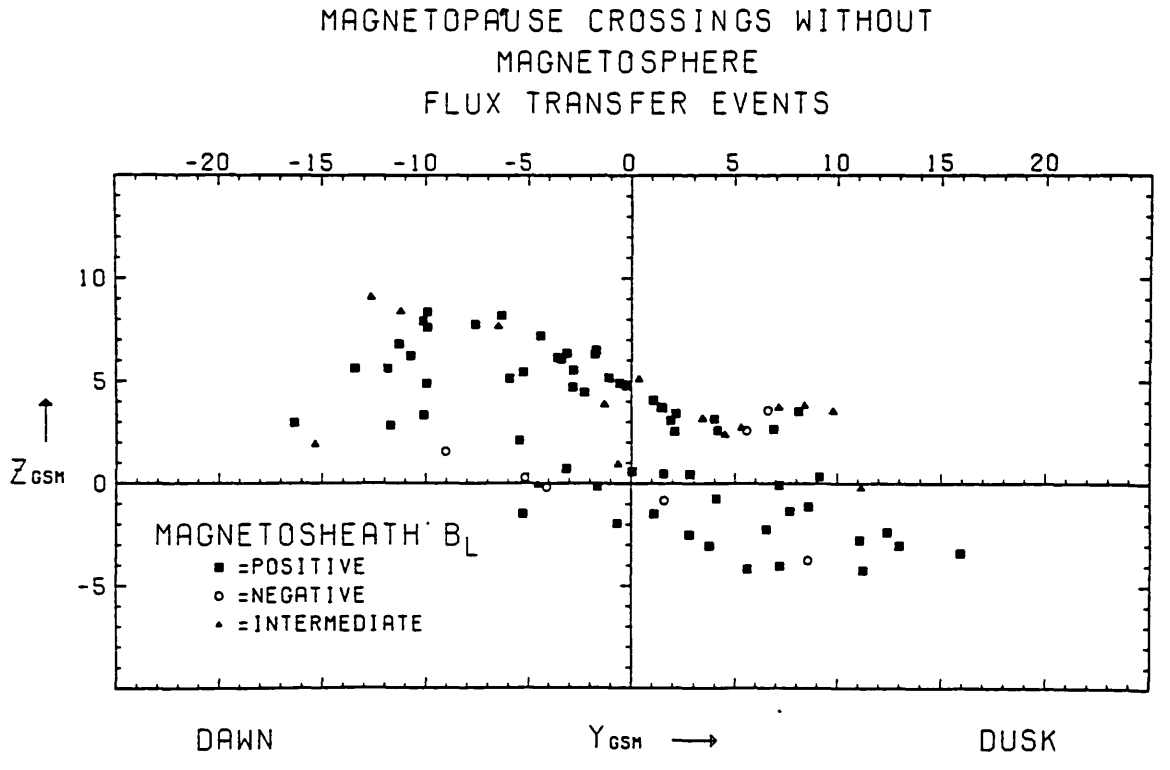


Fig. 4.15(b).

obtained for magnetosphere FTEs are shown in Table 4.4 and Figure 4.15, in the same format as Table 4.3 and Figure 4.12. The same conclusions can be drawn for the magnetosphere FTEs as has been done for the magnetosheath FTEs.

Table 4.4

Magnetosheath Field Orientation* for Magnetosphere FTEs

B_M \ B_L	Negative	Positive	Intermediate	Subtotal B_M
Negative	40(3)	8(29)	15(9)	63(41)
Positive	16(1)	7(25)	8(5)	31(31)
Intermediate	7(3)	1(7)	2(1)	10(11)
Subtotal B_L	63(7)	16(61)	25(15)	

* determined in half-hour interval adjacent to magnetopause

** figures refer to crossings with magnetosphere FTEs (no parentheses) and without magnetosphere FTEs (in parentheses)

4.3.8 Solar wind parameters and FTEs

On traversing the dayside bow shock region the IMF is compressed and it drapes over the magnetopause surface to form the magnetosheath field. The IMF and magnetosheath fields are thus intimately related and FTEs should show the same qualitative dependence on the IMF orientation as they do on the magnetosheath field orientation. In order to investigate the dependence of FTEs on the IMF orientation and on the solar wind velocity and number density, these solar wind parameter values were noted for each of the magnetopause crossings plotted in Figure 4.12. The interplanetary medium data book (King, 1979 and 1983) lists hourly averages of solar wind parameters determined upstream of the bow shock. The parameter values corresponding most closely to the time of each magnetopause crossing were used. No attempt was made to introduce a correction for the time lag involved in travelling from the IMF observation point to the dayside magnetopause. However, when

the magnetopause crossing occurred close to the half-hour point, either an average of the IMF parameters determined over the two adjacent hourly averages was used, or the set of parameters for which the IMF orientation most closely resembles that observed in the magnetosheath was used.

Figure 4.16 shows the FTE occurrence as a function of the IMF B_z and B_y components in GSM coordinates. The Y-Z plane is divided into eight bins, with an angular width of 45° each. The size of each sector is determined by the number of magnetopause crossings occurring in that sector. The shaded part of each sector shows the number of crossings with magnetosheath FTEs, while the red part shows the number without magnetosheath FTEs. Again, we can verify from this diagram the dependence of FTE occurrence on the orientation of the field external to the magnetopause. When the IMF is southward, very few crossings occur without associated FTEs, and the situation is reversed when the IMF is strongly northward. Another notable feature which we have come across before is the relatively small number of crossings in the quadrant with IMF B_y and B_z both negative.

Figure 4.17 shows the results obtained for the crossings with and without magnetosphere FTEs. Again, the conclusions which can be drawn are identical to those for the magnetosheath FTEs.

The interplanetary medium data book also lists the solar wind velocity and number density, so we can investigate the dependence of FTE occurrence on these parameters. Figures 4.18 and 4.19 show histograms for magnetosheath FTEs. In the first plot the solar wind velocity is plotted in 50 km s^{-1} intervals, along the horizontal axis, while in the second plot the number density is plotted in intervals of 5 cm^{-3}. The number of magnetopause crossings is plotted along the vertical axis. The shaded part of each bar shows the number of crossings with FTEs in each particular interval, while the red part shows the number of crossings without FTEs. It can be seen that the distribution of crossings with FTEs is not noticeably different from the total number of crossings or the crossings without FTEs. In other words, any dependence of FTE occurrence on either solar wind velocity or density must be at least second order in comparison with either the IMF/magnetosheath field orientation. These conclusions are also valid for magnetospheric FTEs.

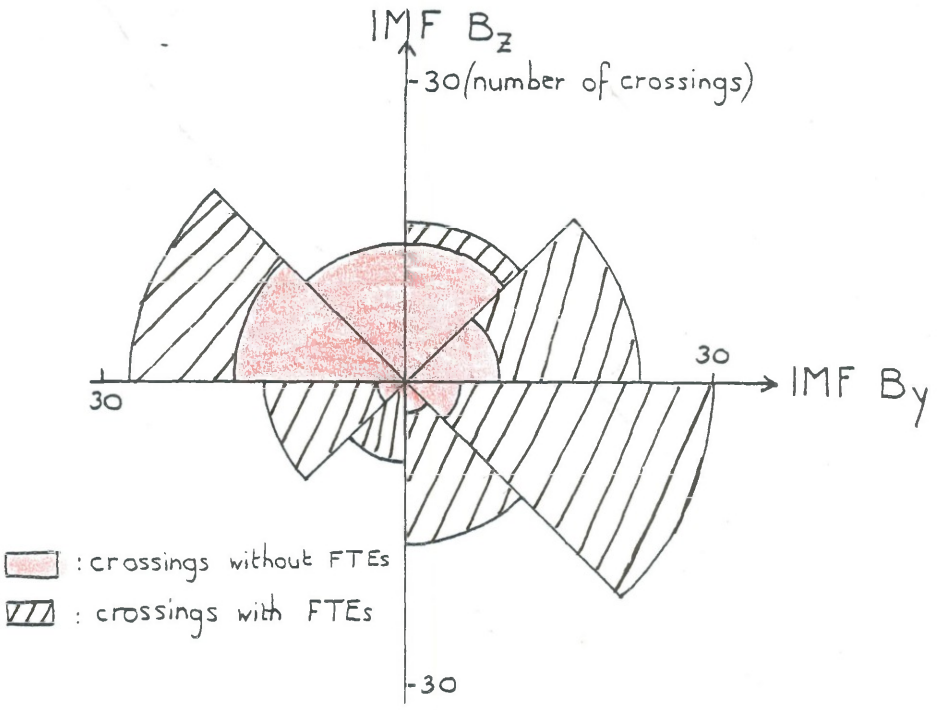


Fig. 16. Occurrence of magnetosheath FTEs vs. orientation of the IMF.

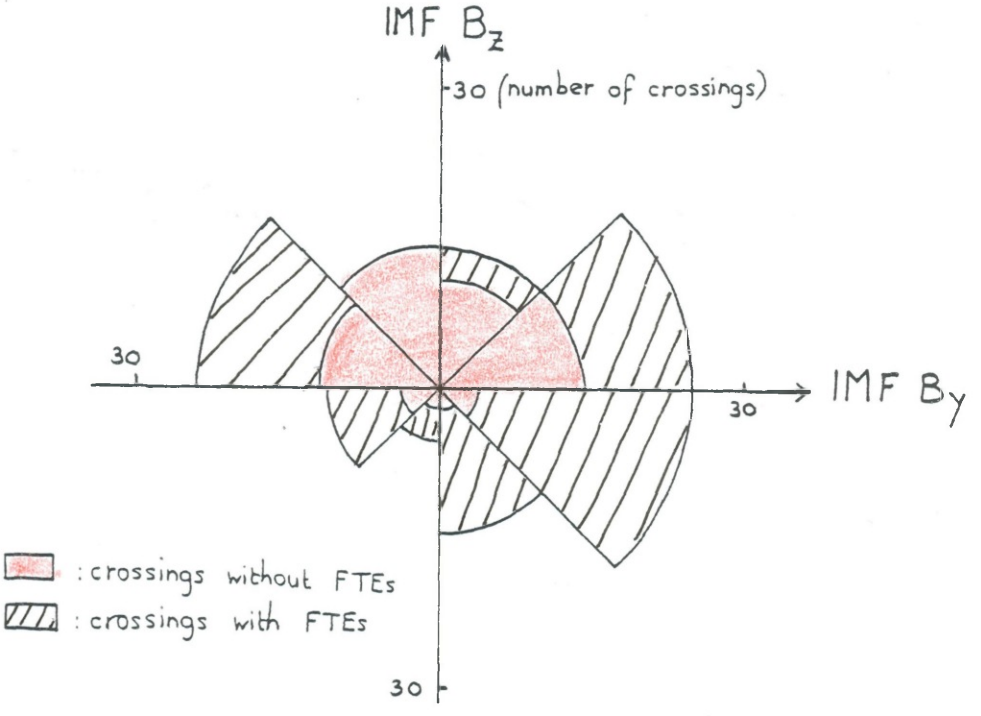


Fig. 17. Occurrence of magnetosphere FTEs vs. orientation of the IMF.

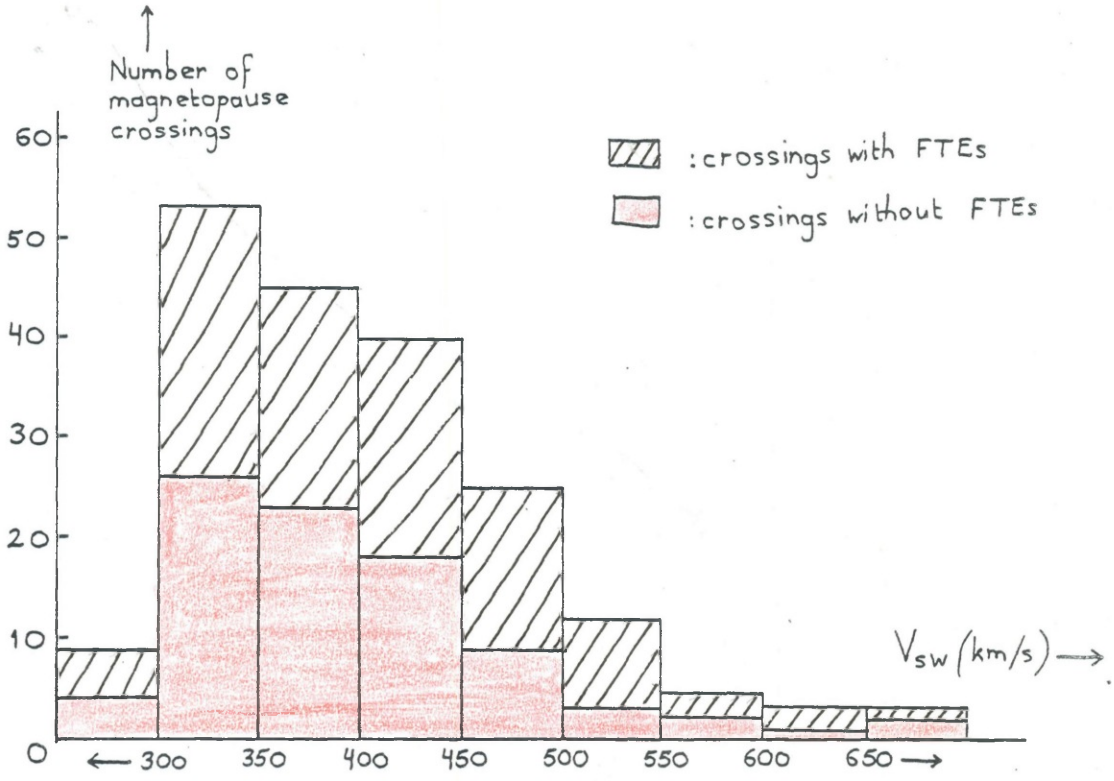


Fig. 18. Occurrence of magnetosheath FTEs vs. solar wind velocity.

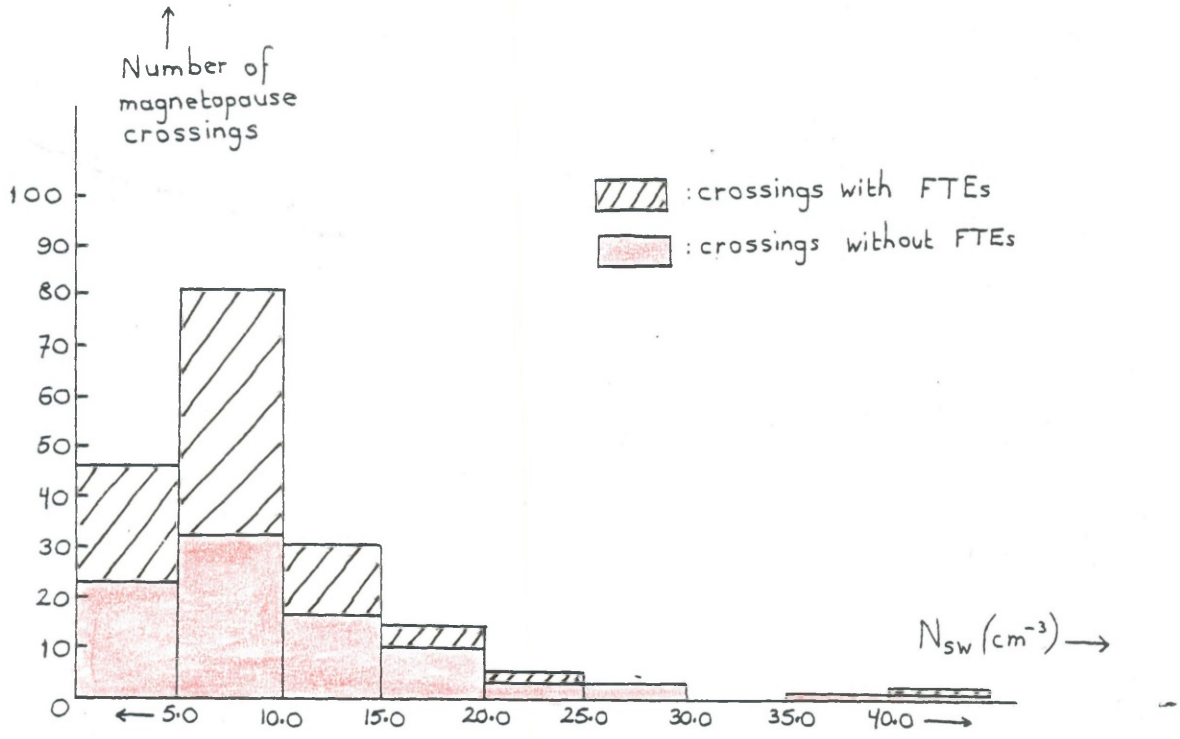


Fig. 19. Occurrence of magnetosheath FTEs vs. solar wind density.

4.3.9 Occurrence rate of FTEs

In this subsection we wish to determine the number of FTEs, N_{FTE} and the recurrence time, T_R, for a typical pass under conditions in which FTEs may be expected to occur. As shown in 4.3.7, a southward magnetosheath field component is almost a sufficient condition for ISEE 1 and 2 to observe FTEs in the dayside magnetopause region. We shall therefore base our estimates of N_{FTE} and T_R on those crossings which are listed as having negative magnetosheath B_L in Tables 4.3 and 4.4 for magnetosheath and magnetosphere FTEs, respectively.

We cannot expect N_{FTE} to be constant for all passes, since magnetopause motion may, for example, cause the ISEE 1 and 2 satellites to traverse rapidly the region in which FTEs are observed, in which case N_{FTE} will be lower than typical. Also, we cannot a priori expect T_R to be a constant. We shall therefore determine average values of N_{FTE} and T_R from the crossings with a southward magnetosheath B_L component. Since the magnetopause is stationary on average, we can make the assumption that for a large data set of crossings the magnetopause has no net motion and hence that our estimate for L_N is solely determined by the speed with which ISEE traverses the magnetopause region. However, it should be noted that L_N may also be affected by satellite location (as we shall see presently) and by variations in T_R on individual passes.

Table 4.5 shows the results obtained for magnetosheath and magnetosphere FTEs. For each of the crossings with negative B_L the number of FTEs observed by one of the ISEE satellites was counted, and from this the FTE recurrence time was calculated, by using the time difference between the magnetopause crossing and the FTE farthest away from it in time. The results in Table 4.5 show that the values of $\overline{N}_{FTE}$ of 4.5 and 3.4, and the values of $\overline{T}_R$ of 9.2 and 8.7 min for magnetosheath and magnetosphere FTEs are very similar.

Also shown in Table 4.5 is the distribution of $\overline{N}_{FTE}$ with latitude of the magnetopause crossing above or below the GSM equator (in 10° bins). Although there are individual fluctuations in the case of the magnetosphere FTEs, possibly caused by the inherent uncertainty in determining the magnetosheath field orientation while inside the magnetosphere, the results taken as a whole confirm the suggestion by Rijnbeek et al. (1984) that fewer FTE signatures are observed at low latitudes.

Table 4.5

Spatial Distribution of FTEs *

	Total	Latitude of Magnetopause Crossing, GSM				
		0 - 10°	10 - 20°	20 - 30°	30 - 40°	40 - 50°
No. of crossings with -ve B_L	87(70)	21(14)	18(14)	32(28)	9(7)	7(7)
Number of FTEs	392(235)	75(31)	68(53)	157(91)	46(18)	46(42)
Average number, $\bar{N}_{FTE}$	4.5(3.4)	3.6(2.2)	3.8(3.8)	4.9(3.3)	5.1(2.6)	6.6(6.0)
Average recurrence time $\bar{T}_R$	9.2(8.7)					

* Figures in parentheses refer to magnetosphere FTEs.

4.3.10 Scale size of FTEs

The values of N_{FTE} and T_R which we have determined allow us to make an order of magnitude estimate for the scale size of a typical FTE perpendicular to the magnetopause. Figure 4.20 shows a satellite trajectory intersecting the region in which an FTE may be observed, of width L_N, where L_N is the scale size of the FTE magnetic signature. Assuming a stationary magnetopause, a situation which we approximate by using average values of N_{FTE} and T_R, it can be seen that L_N is given by

$$L_N = N_{FTE}\ T_R\ V_{ISEE} \quad .$$

where V_{ISEE} is the satellite velocity. We assume here that the satellite trajectory is normal to the magnetopause (which is approximately true under normal circumstances) and that the time spent by the satellite in a region of size L_N is longer than T_R. The value of V_{ISEE} depends on the radial distance from Earth (it slows down approaching apogee or perigee) but it is reasonable to use a value of $\sim$ 2 km s^{-1}. We then obtain a scale size of $\sim$ 0.8 R_E and $\sim$ 0.6 R_E for magnetosheath and magnetosphere FTEs, respectively, normal to the magnetopause.

Note that an alternative method to that given above is to calculate the average time interval between the magnetopause crossing and the FTE observed furthest away from it in time. Multiplying this time interval by V_{ISEE} then also gives an estimate for L_N. However, this method is less effective in smoothing out magnetopause oscillations and in any case leads to the same results as above.

We can also make a rough estimate of the scale size of a typical FTE along the magnetopause. The typical duration of an FTE is $\sim$ 1-2 min. If we assume the average magnetosheath bulk velocity of $\sim$ 100-200 km s^{-1} to give us a reasonable estimate of the convection velocity of FTEs along the magnetopause, then we arrive at a value of $\sim$ 2 R_E.

Estimates similar to the ones above have also been given by others. Russell and Elphic (1978) found values of $\sim$ 4 R_E and $\sim$ 0.8 R_E for the FTE dimension along the magnetopause during two separate crossings. They infer a similar dimension normal to the magnetopause from the 45° rotation of the B_N component during the passage of the FTEs. From the time of passage and convection speed of the energetic particle boundaries of the FTEs observed during a single crossing, Daly and Keppler (1983a,b) calculate a normal dimension of $\sim$ 1 R_E. Finally Saunders et al.

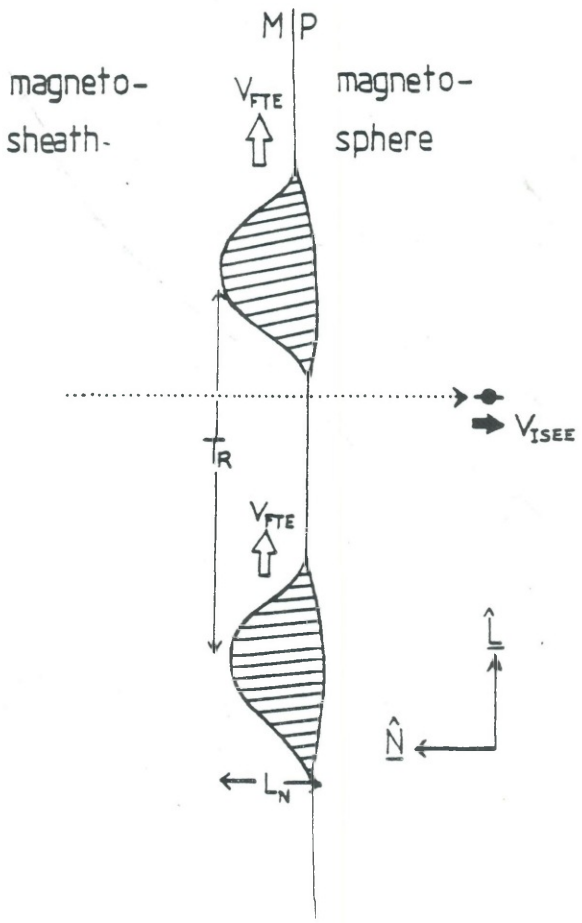


Fig. 4.20. Estimating the scale size of an FTE.

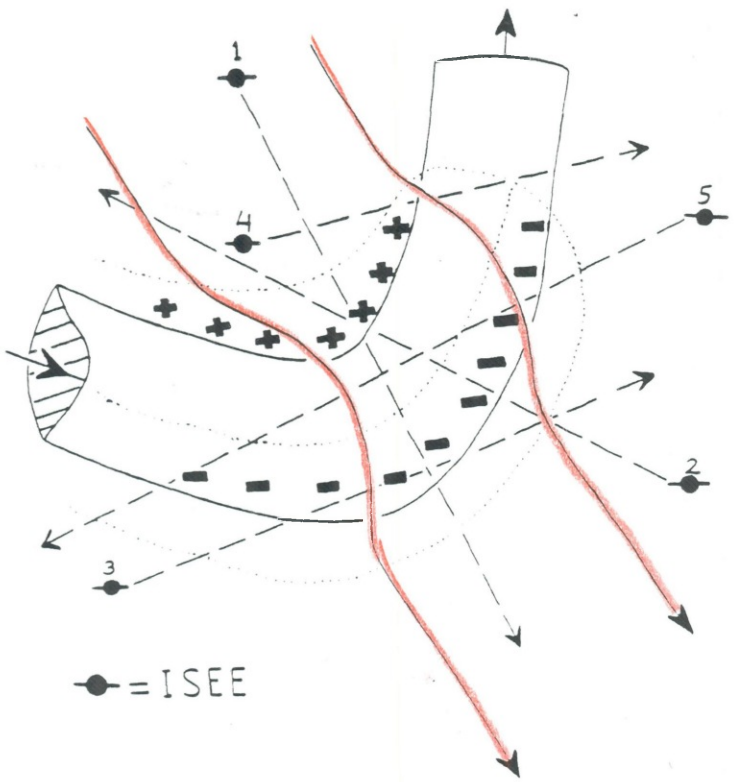


Fig. 4.21. Satellite trajectories relative to an FTE flux tube.

(1984a,b) have measured the scale size of FTE magnetic signatures directly, by taking advantage of the variable separation of the ISEE 1 and 2 satellites. They find that the FTE dimension perpendicular to the magnetopause is of order 1 R_E, which is in good agreement with our results obtained in a more indirect (and therefore less accurate) manner.

4.4 Discussion

4.4.1 FTE magnetic signatures

In our statistical survey of FTEs we have used an extended definition of the FTE magnetic signature compared to the ones adopted by Russell and Elphic (1978) and Berchem and Russell (1984). There are a number of reasons to justify the use of this more liberal definition of the FTE signature, as we shall now discuss.

In Chapter 3 it was shown that FTE flux tubes are associated with a field-aligned current (FAC) which is either suggested to flow along the central axis of the FTE tube (e.g., Saunders, 1983) or along its outer edges (Southwood, 1984). The FAC is associated with a twisting of field lines and explains the continuous nature of the FTE B_N signature as well as the anomalous field orientations, i.e., the tangential field component rotates away from the field direction on the opposite side of the magnetopause. The presence of the FAC may lead to strong spatial structure inside FTE flux tubes, thus giving rise to more complex magnetic field signatures than those originally envisaged.

The dynamical equilibrium of FTE magnetic field structures still needs investigating. Paschmann et al. (1982) showed that the increase in total pressure which they observe inside FTEs is due to the tension of ambient field lines as they drape over the FTE flux tubes and also the field twist associated with the FAC. As Southwood (reported in Cowley (1982)) has noted, however, the field tension forces must reverse at the edges of FTE flux tubes. As a result, a flux tube which initially has a circular cross-sectional shape will be squashed into a long thin slab downstream from the region in which it originates. The shape of an FTE tube, and hence its signature, may therefore evolve in time/latitude as it moves over the dayside magnetopause into the tail. This may therefore be another reason why FTE signatures can potentially be quite complex and variable in time, although the ISEE latitude coverage is probably too limited to investigate this question in detail.

During the course of this survey a number of FTEs have been found which do not show the field strength increases noted originally by Russell and Elphic (1978). For these events the field magnitude does not change appreciably, or it oscillates, or it may even decrease relative to the ambient value (e.g., Fig. 4.5). Such field strength decreases are not necessarily at variance with the Paschmann et al. (1982) observations since the field decreases may be accompanied by compensatory increases in the plasma pressure. We should like to argue, however, that a field strength increase is not a necessary feature of the FTE phenomenon.

Observations suggest that FTE flux tubes have spatial magnetic field structure. Rapid irregular motion of the magnetopause can carry an FTE tube back and forth across the observing satellite, which then sees a complex magnetic field signature. Also, FTEs are often observed rapidly one after another and with insufficient time resolution the individual events may not be resolved because of a partial merging of the magnetic signatures. Figure 4.21 (after Cowley, 1982) shows how the FTE B_N signature may be affected by the motion of a flux tube across a satellite. This figure shows a number of satellite trajectories, labelled 1 to 5, across a flux tube observed in the magnetosheath which is connected to the Northern Hemisphere, for a southward and duskward magnetosheath field orientation (similar arguments apply to other configurations). The path of an FTE flux tube across a satellite depends on the location of the observation site, the region where the FTE is initiated, the ambient magnetosheath plasma flow and finally the release of magnetic tension so that all 5 trajectories are possible in general. The plusses and minuses refer to the B_N perturbations which result from the exterior draped magnetosheath field lines. Along trajectory 1 a positive-negative B_N perturbation is observed, while a reverse negative-positive signature is seen along 2. If the flux tube motion is not mainly along a north-south line, then other signatures may also result, e.g., negative along 3, positive along 4 and negative-positive-negative along 5. Such signatures occur if the tube is carried mainly dawnward or duskward, such as may occur in the super-alfvénic region on the flanks of the magnetosphere. Figure 4.21 can also be used to illustrate that the different signs of B_N perturbation need not have the same amplitude. The amplitude depends on how far the flux tube juts into the magnetosheath and how far away from the magnetopause the tube is crossed.

In summary, therefore, we can conclude that the magnetic signature of a FTE does not necessarily have to take the form as originally reported by Russell and Elphic (1978). More work needs to be done to determine the magnetic field structure of FTEs, both theoretically and observationally. A promising start in this respect has already been made by Saunders et al. (1984a,b). Finally we should note that our results are fully compatible with those of Berchem and Russell (1984), which shows that in spite of our extended definition of the FTE magnetic signature we are still dealing with the same phenomenon, except that it is more frequent and thus more significant than the results of Berchem and Russell (1984) suggest.

4.4.2 FTEs: reconnection phenomena?

Dungey's (1961) model predicts that a southward IMF is the most favourable condition for the occurrence of dayside reconnection. The striking dependence of FTE occurrence on the southward magnetic field component external to the magnetopause therefore lends substantial support to the interpretation of FTEs in terms of localised, reconnected flux tubes, especially if we combine it with the observations reviewed in the previous chapter. Another important supporting factor is the close relationship between the FTE signatures observed in the magnetosheath and in the magnetosphere. In this survey, we have analysed magnetosheath and magnetosphere FTEs separately, and the similarity in results shows that they are part of the same physical phenomenon, i.e., they are reconnected open flux tubes passing through the magnetopause.

Although we have shown that a southward external field component is the primary controlling factor, we have not been able to give a hard and fast rule(s) specifying all the necessary conditions for FTE occurrence. Individual cases are found in which no FTEs are observed even when there is a southward magnetosheath or IMF component; conversely, some crossings with a northward exterior field component do show FTEs. This could be the result of additional factors, apart from the exterior field orientation, influencing FTE occurrence. Alternatively, FTEs may have been missed as a result of their limited spatial extent and recurrence time, so that the satellite was not in the right place and/or at the right time to observe them. Local and/or temporal fluctuations in the exterior field orientation may also play a part, especially if it is remembered that magnetosphere FTEs do not necessarily occur under the

same conditions to those previously (subsequently) seen in the magnetosheath encounters, and that the IMF components are hourly averages. FTEs do sometimes occur under northward field conditions, but in these cases the magnetosheath and magnetosphere B_M components are of opposite sign, i.e., there is still a substantial angle between the two field directions. Figure 4.22 shows an example. The data are taken from an inbound crossing on 28 July 1978 and the magnetopause is crossed at 19:56 UT. The B_L component is stronger in the magnetosheath, but reverse FTEs are observed at 19:11 and 19:22 UT in the magnetosheath, and at 20:03 and 20:04 UT in the magnetosphere. These observations suggest that it is the relative orientation of the magnetosheath and magnetosphere fields which determines FTE occurrence, rather than just the B_L component on its own. In practice, however, it is the B_L component which primarily determines the relative orientation; hence our results. There may be a cutoff angle below which FTEs do not occur but it would be difficult to determine this in practice because of the fluctuations in the magnetosheath (and to a lesser extent the magnetosphere) field and also because the observed fields are not necessarily representative of the conditions under which FTEs are created, especially if we are viewing the flux tubes some time after reconnection has taken place.

4.4.3 Where are FTEs initiated?

For due southward IMF most magnetospheric reconnection models place the reconnection line along the magnetic equator. However, the two most widely referenced models disagree in the location of the reconnection line when the IMF is not due south. Crooker's (1979) hypothesis that reconnection only occurs where the fields are antiparallel results in the main site of reconnection occurring in the dayside cusp regions. In this model the reconnection line in each hemisphere starts at the cusp and then curves out toward the flanks and down to the equator. When IMF B_y is positive, the reconnection line in the Northern (Southern) Hemisphere extends towards dusk (dawn). The situation is reversed for IMF B_y negative (see Figure 1.9; Crooker (1979); Luhmann et al. (1984)). In the other model (e.g., Gonzalez and Mozer (1974); Sonnerup (1974)), the reconnection line still passes through the subsolar point even when there is an IMF B_y component. However, in response to IMF B_y the reconnection line tilts away from the equator on either side. For IMF

B_y positive, the reconnection line tilts southward in the dawn sector and northward in the dusk sector. The situation is again reversed for IMF B_y negative (see Figure 1.7).

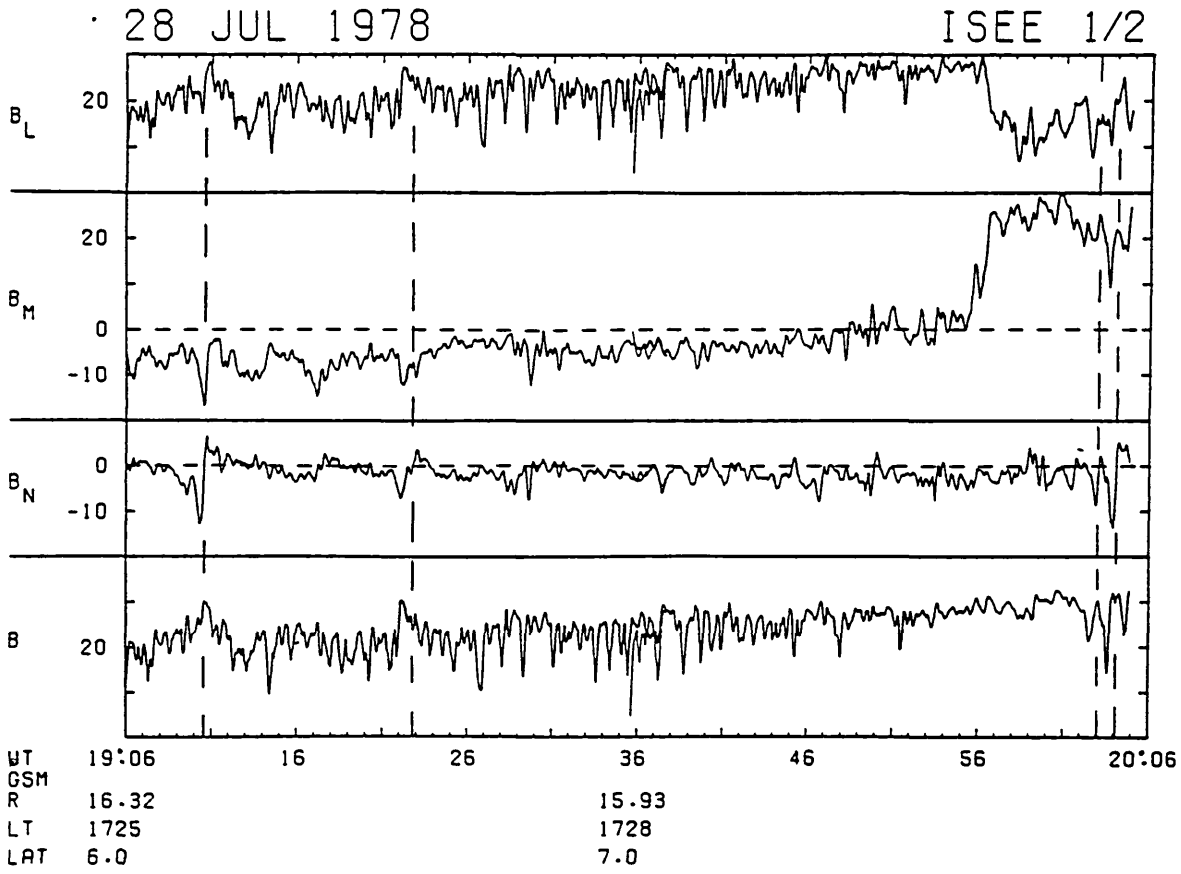


Fig. 4.22. FTEs on 28 July 1978.

Since it seems that the FTE is a reconnection phenomenon, albeit on a shorter temporal and spatial scale than originally envisaged, we may compare our observations with the above two models. If the reconnection line along which FTEs are created lies along the magnetic equator, then we should expect to observe flux tubes connected to the Northern Hemisphere and moving northward at northerly latitudes, while at southerly latitudes we should see flux tubes connected to the Southern Hemisphere moving southward. The northward and southward motion of, respectively, the northerly and southerly connected FTE tubes should give

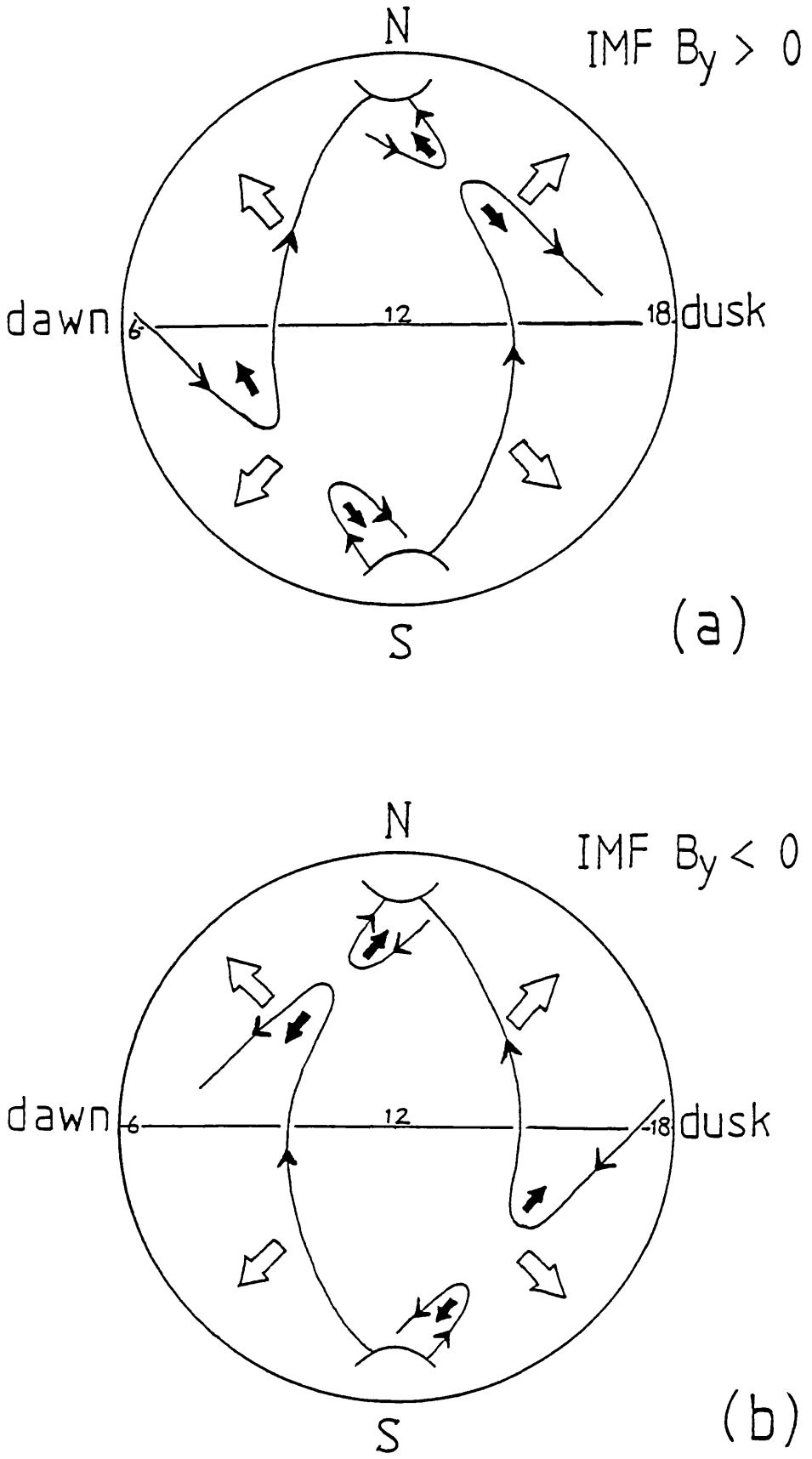


Fig. 4.23. Impulsive reconnection in the cusp regions.

rise to standard and reverse FTEs. Figure 4.6 shows broad agreement with this picture. However, there are a number of exceptions and these may perhaps be related to IMF B_y.

For the Crooker (1979) model the reader can compare the observed distributions of FTE signatures in Figure 4.6 with, e.g., Luhmann et al. (1984), which shows the locations of the reconnection line as a function of the IMF orientation. Note that negative B_M corresponds to positive IMF B_y and vice versa. For ease of visualization, Figure 4.23 shows two simplified reconnection configurations based on this model for IMF $B_y > 0$ and < 0. The path followed by an individual flux tube, whether connected to the Northern or to the Southern Hemisphere, results from a superposition of the ambient magnetosheath velocity and the magnetic tension release (at approximately the Alfvén speed). Comparing Figures 4.23 and 4.8, it can be seen that the two are not wholly compatible. It is difficult to observe either standard or reverse FTEs in the region centred on local noon. Neither the magnetosheath velocity nor the tension release has a component which might cause FTEs to be observed in this region.

The picture is much more promising if we compare the observations with the tilted reconnection line model of, e.g., Gonzalez and Mozer (1974). In this model, we should only expect to observe anomalous FTEs in the Northern Hemisphere (i.e., southerly connected or reverse FTEs) in the dawn sector when magnetosheath B_M is positive and in the dusk sector when B_M is negative. Conversely, anomalous (i.e., northerly connected or standard) FTEs in the Southern Hemisphere should only be observed in the dawn sector when B_M is negative and in the dusk sector when B_M is positive. With the odd exception this indeed holds true for the observed distributions of FTE signatures. However, we cannot yet tell which coordinate system orders the data best (compare Figures 4.8, 4.10 and 4.11).

The question as to which hemisphere the FTE flux tubes are connected to has been examined by Daly et al. (1984a,b), who used magnetic field data combined with high-resolution plasma and energetic particle data. The streaming direction of energetic ions inside an FTE flux tube can be used to identify unambiguously whether it is connected to the Northern or to the Southern Hemisphere (Figure 3.2). Figure 4.24 shows the results of this study. The symbols show the positions of magnetopause crossings with magnetosheath FTEs. Magneto-

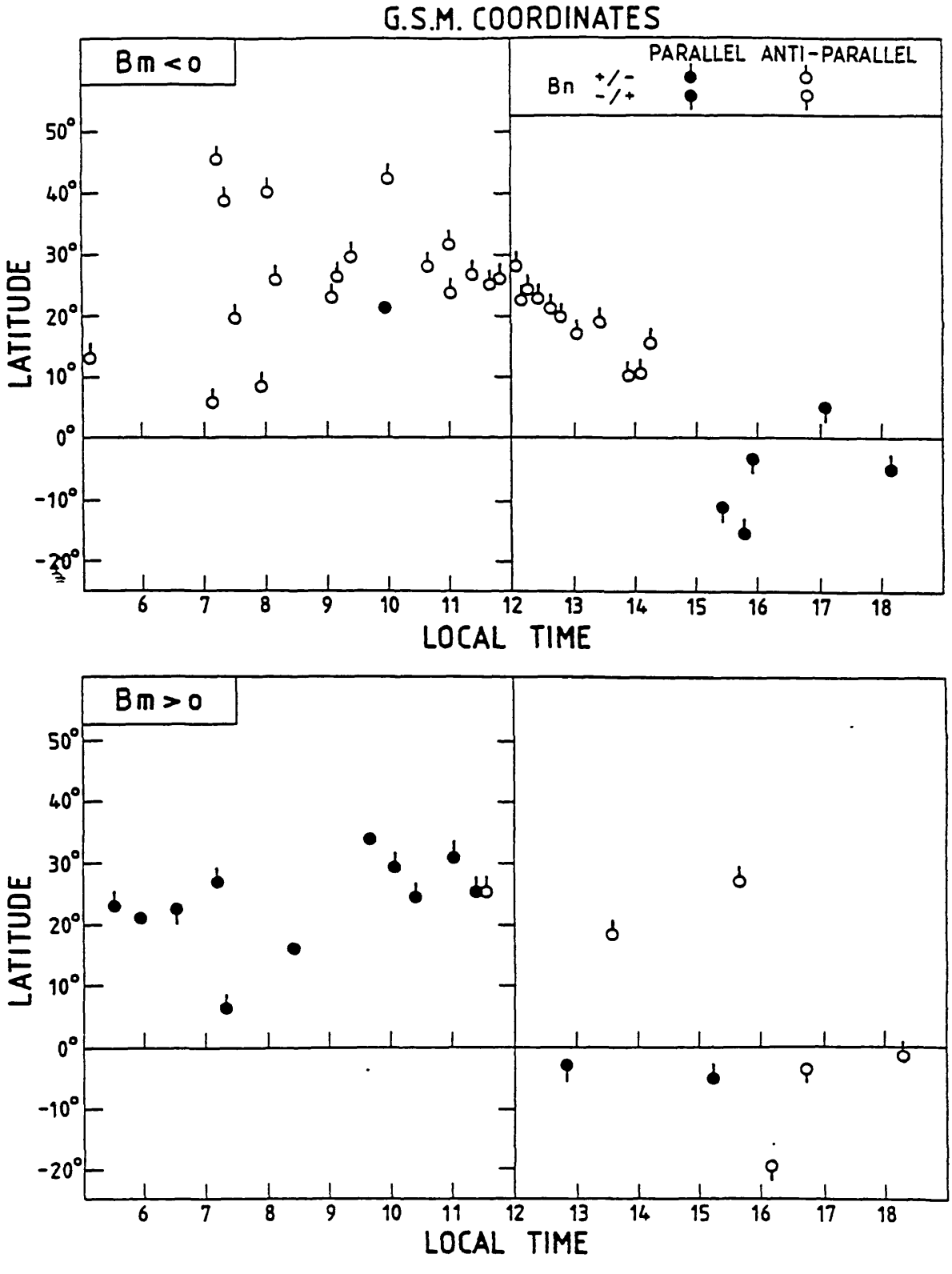


Fig. 4.24. Energetic ion streaming inside magnetosheath FTEs (Daly et al., 1984).

sphere FTEs are not included in this survey because of, e.g., the possibility of counter-streaming of the energetic magnetospheric particles resulting from reflection off the magnetopause (Daly et al., 1984a; Scholer and Ipavich, 1983). The caption in the right hand corner explains the symbols. In comparing this figure with Figure 4.8 one should bear in mind that only a subset of the crossings was used since the energetic particle instrument on board ISEE 2 suffered from increased noise levels as of May 1978. No crossings from 1979 are included. Figure 4.24 shows that the FTE B_N signature cannot always be used to infer the hemisphere connection. In many cases the ambient magnetosheath flow is super-alfvénic, so that it dominates the direction of motion of the flux tube. However, the conclusions do not disagree with and in fact fortify our conclusions reached above.

In future it may be useful to infer the FTE hemisphere connection for the events observed by ISEE in 1979 and later by making use of combined magnetic field and high resolution plasma data. The FTE B_N signature can be used to infer the flux tube motion relative to ISEE, while the plasma bulk velocity can be used to infer the direction of magnetic tension release. A further possibility is to make use of high resolution electron data (Ogilvie et al., 1978). Examples have been shown in which FTEs are accompanied by a heat flux layer (e.g., Scudder et al., 1984), emanating from the diffusion region. The direction of the heat flow relative to the local magnetic field may be used to determine the FTE hemisphere connection. At the time of writing such results have yet to be published.

4.4.4 Mixed FTE crossings

Although individual case examples have been cited as crossings of the reconnection line (e.g., Sonnerup, 1971), direct and unambiguous observation of the diffusion region in which the reconnection line is embedded has so far proved elusive. In part this may be because there is no general consensus as to what one should expect to observe in this region. Also, the physical dimension of the region is expected to be small, perhaps of order 1000 km. However, the identification of the diffusion region is clearly of importance in terms of our understanding of the reconnection process, since it is likely that in this region the most interesting physics occurs. For example, we should like to know the answers to such questions as what initiates reconnection, what

determines its rate and time development and into what forms of particle energies the electromagnetic energy is converted. Also, in a fortuitous set of circumstances a satellite may cross the reconnection line and be able to detect an electric field component along it, which would provide us with the ultimate piece of evidence for reconnection.

How can we detect the reconnection line? In the case of FTE-type of reconnection, we might expect a satellite travelling, say, from north to south across the reconnection line first of all to observe flux tubes connected to the Northern Hemisphere, and then flux tubes connected to the Southern Hemisphere. So far, there have been no reports of this happening. Also, the fact that the vast majority of crossings show FTE signatures of one type, i.e., either standard or reverse, argues that the location of the regions of intermittent reconnection is relatively stable, and does not move widely over the magnetopause surface at any one time. However, there are a few instances where both standard and reverse FTEs are observed on the same pass, as Figure 4.6 shows. Although, as we have noted, the FTE B_N signature is not an altogether reliable way of determining the FTE flux tube hemisphere connection, it is possible in these cases that the standard and reverse FTEs are observations of northerly and southerly connected tubes, respectively. This could result from the satellite crossing the reconnection line or vice versa (e.g., if the external field orientation changes). The likelihood of this is increased if the observations are made in the sub-alfvénic region close to the subsolar point, where magnetic tension release is expected to dominate the FTE motion.

Figures 4.25 and 4.26 show two examples of such an occurrence. We shall report an additional event in Chapter 5. Figure 4.25 shows ISEE 1 and 2 data taken from an inbound pass on 30 October 1978. Both satellites are close to the subsolar point and are travelling southward at the time, with ISEE 2 leading. At 6:00 UT, the satellite separation in LMN components is (5081, 3627, 5500) km. During the interval shown ISEE 2 is inside the magnetosphere and observes a reverse FTE at 6:02 UT. The magnetosheath field is southward and dawnward and ISEE 1 crosses the magnetopause at 6:34, 6:50 and 6:57 UT. ISEE 1 observes FTEs at 6:21, 6:26 and 6:53 UT in the magnetosheath and at 6:38 UT in the magnetosphere. Their B_N signatures are classed respectively as irregular, standard, reverse and reverse. The standard FTE is observed above the magnetic equator, while the reverse FTEs at 6:02 and 6:53 UT are observed below

it, and the one at 6:38 UT is observed very close to it. There is a distinct possibility therefore that in traversing the magnetic equator the ISEE satellites also cross the site of FTE-type reconnection.

Figure 4.26 shows another example, this time with data taken from an inbound pass on 18 October 1979. Figure 4.26(a) and (b) show successive hourly intervals of data taken from ISEE 2 and 1, respectively. Both satellites are close to local noon and $\sim 8°$ below the GSM equator. ISEE 2 is leading ISEE 1 by (2651, 3029, 4047) km in LMN components. The first data interval shows ISEE 2 to be almost exclusively inside the magnetosphere, except for a short magnetopause encounter at 21:04 UT. An irregular FTE occurs at 21:11 UT and a prominent reverse FTE at 21:20 UT, suggesting that ISEE 2 is located below the FTE reconnection line. ISEE 1 observes a standard magnetosheath FTE at 21:33 UT, a standard/irregular FTE at 21:38 UT, and then reverse magnetosheath FTEs at 21:51, 21:57, 21:59 and 2202 UT, and reverse magnetosphere FTEs at 22:14, 22:20 UT. This sequence of observations suggests that ISEE 1 is in the process of crossing the FTE reconnection site. This would require a slight southward tilt of the reconnection line, but this is consistent with the slightly duskward location and the dawnward magnetosheath field component.

It would be interesting to be able to verify whether the observations above do indeed represent FTEs connected to different hemispheres. If such were the case, a study using combined magnetic field, electric field, plasma and wave data of the FTEs and the magnetopause crossings might prove a worthwhile exercise.

4.4.5 FTE flux removal rate

Our final topic of discussion is the extent to which FTEs live up to their name, i.e., what is the rate at which they remove open magnetic flux from the dayside into the nightside magnetosphere. Knowing this we can assess their importance in driving magnetospheric convection flows.

We have already estimated the cross-sectional dimensions of an FTE signature. However, if, as Southwood (1984) suggests, the FAC associated with a flux tube flows along the outer edge of the tube, then it is clear that the FTE magnetic signature extends further away from the magnetopause than the open flux tube itself. We will therefore adopt a value of $\sim 0.5\ R_E$ (i.e., half the FTE signature scale size) for

the dimension perpendicular to the magnetopause. The total cross-sectional area of a typical open flux tube is therefore $\sim 2\ R_E \times 0.5\ R_E = 4 \times 10^{13}\ m^2$. Using an average field value of ~ 50 nT inside an FTE tube then gives a value of $\sim 2 \times 10^6$ Wb for the amount of open flux transported by a typical FTE. Dividing this number by the FTE recurrence time we then arrive at a voltage of ~ 4 kV. This, however, is a lower limit to the FTE voltage during periods of southward magnetosheath field.

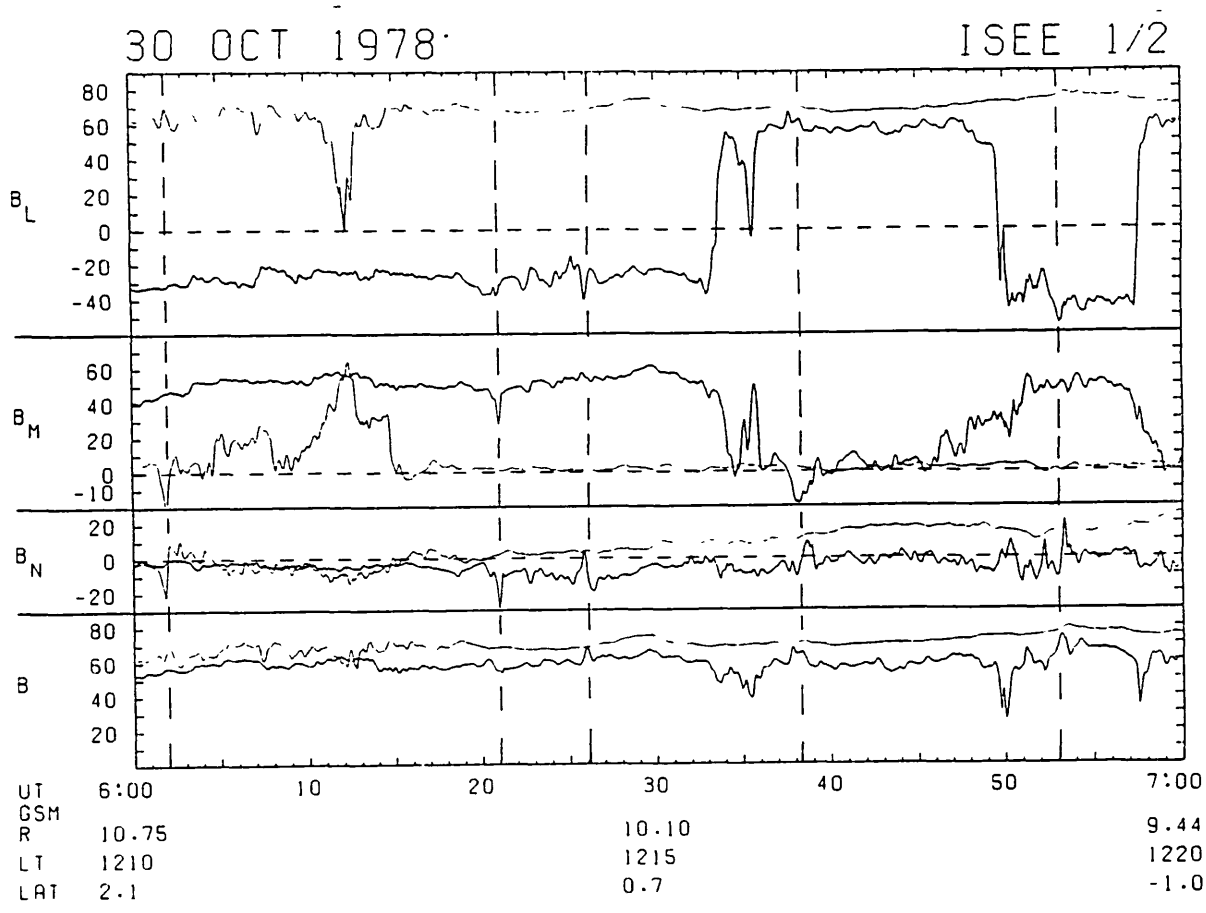


Fig. 4.25. FTEs on 30 October 1978.

In deriving the FTE voltage we have only used single satellite observations and we have not taken into account the limited local time extent of FTEs. Figure 4.27 illustrates that at a single observation point we cannot expect to see every single FTE moving along the dayside magnetopause at any particular time. Since FTEs are observed by ISEE at all local times across the dayside magnetopause virtually whenever

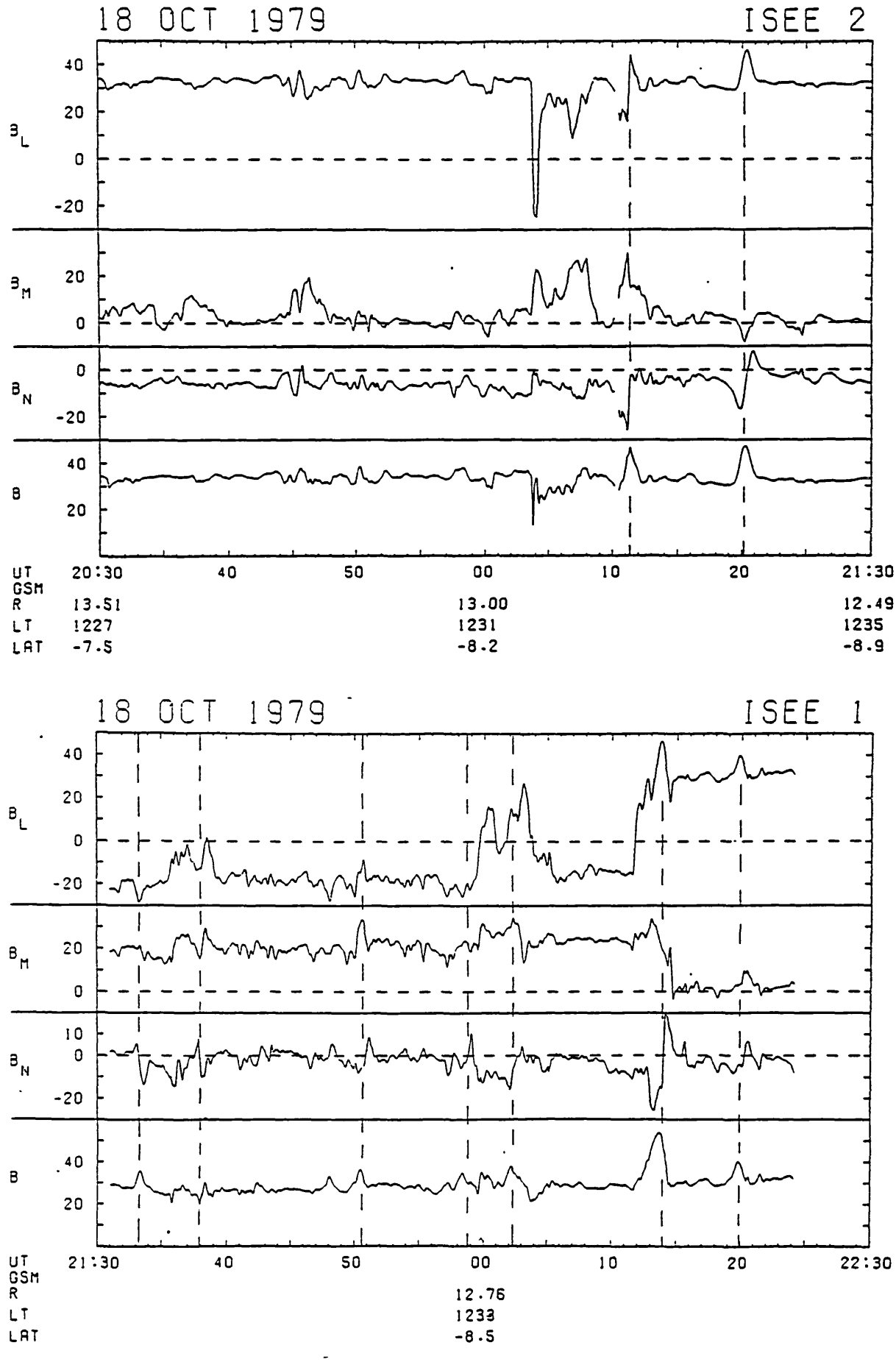


Fig. 4.26. FTEs on 18 October 1979.

the exterior field has a southward component, it seems likely that 4 kV represents only a small fraction of the FTE flux transport rate. The estimate of $\sim$ 2 R_E for the scale size of FTEs along the magnetopause corresponds to the closest local time spacing of FTEs that we can expect. Thus, the maximum number of FTEs that we can fit side by side across the equatorial dayside magnetopause of circumference π x 10 R_E is $\sim$ 16 FTEs. We should also remember that only prominent FTE signatures are considered in this survey. FTEs with shorter time and/or spatial scales may also provide a substantial contribution. It is not inconceivable, therefore, that the 4 kV value should be raised by an order of magnitude, in which case FTEs provide a substantial (perhaps at times dominant) fraction of the cross-magnetosphere voltages which are typically observed (of order 100 kV).

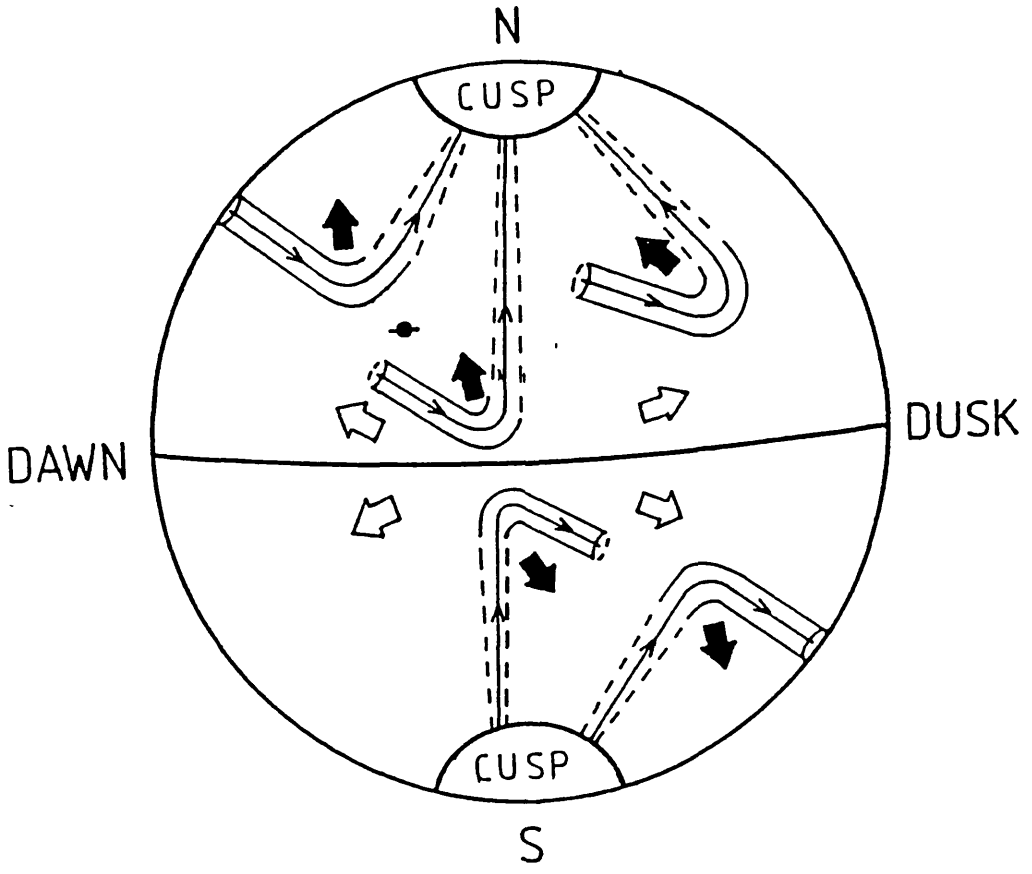


Fig. 4.27. FTE flux tubes propagating along the dayside magnetopause.

Finally, note that Figure 4.27 also suggests a possible explanation for the observation that, in general, more FTE signatures are observed at higher latitudes. FTEs which emanate from the equatorial region cover a larger area of the dayside magnetopause at higher latitudes, and thus there is an increased chance of observing any one of them.

CHAPTER 5

FLUX TRANSFER EVENTS AND QUASI-STEADY RECONNECTION

5.1 Introduction

In this chapter we examine in detail a set of passes identified as containing encounters with regions of steady reconnection. Figure 5.1 (after Paschmann, 1984) shows the locations (in GSM coordinates) of 17 ISEE magnetopause crossings identified as reconnection events on the basis that the plasma and magnetic field data satisfy tangential momentum balance. Twelve events have been published already (Paschmann et al., 1979; Sonnerup et al., 1981; Gosling et al., 1982) but five additional events have been provided to us by G. Paschmann (private communication, 1984). The circles and squares show events which occurred when the IMF B_y component was positive and negative, respectively (i.e., magnetosheath B_M negative and positive, respectively). The open and solid symbols refer respectively to events observed north and south of the reconnection line as inferred from the sign of B_N. The distribution of the crossings is consistent with the reconnection line passing through the subsolar point and tilting about the magnetic equator in response to IMF B_y (see Figure 1.7). More details about the 17 reconnection events are given in Table 5.1.

Of the 17 reconnection events, we have 16 passes with useable magnetic data. Examination of these passes shows that in all instances FTE signatures occur in close association with steady reconnection zones, within a time scale of order 10 mins or less. However, the connection runs even deeper in that in each instance the polarity of the FTE B_N signature, standard or reverse, correlates with steady reconnection events where the satellite is inferred to be respectively north or south of the reconnection line. The correlation of southward reconnection flow with reverse FTE occurrence noted for the 9 August 1978 event in Chapter 3 is thus borne out as a general feature.

We have studied in detail the magnetic field and (where available)

TABLE 5.1

Characteristics of Reconnection Passes

Date	[a]Magnetopause Location				[b]$\hat{N}$(GSM)	[c]Δ Sat	[d]Sat (RL)	[e]B_M	[f]FTEs
	R	LT	LAT	UT					
18 November 1977 (out)	14.6	0722	41.3	6:32	MV (0.602,-0.449,0.661)	205 (190)	N	-ve	S(S)
4 December 1977 (in)	13.2	0934	34.6	8:10	TD (0.830,-0.280,0.483)	564 (440)	S	+ve	I(R)
5 July 1978 (out)	11.7	1601	11.9	14:32	TD (0.713,0.574,0.404)	1759 (1070)	N	-ve	S(-)
3 August 1978 (out)	8.6	1347	17.5	4:21	MV (0.868,0.312,0.386)	753 (550)	N/S ?	-ve	M(S)
9 August 1978 (in)	14.4	1653	3.2	20:10	MV (0,652,0.735,0.187)	109 (60)	S	-ve	R(R)
29 August 1978 (out)	10.1	1300	18.4	12:16	MV (0.837,0.011,0.548)	1142 (880)	N	-ve	S(S)
3 September 1978 (out)	10.6	1247	20.3	7:20	MV (0.904,0.018,0.428)	1383 (1170)	N	-ve	S(S)
5 September 1978 (out)	9.8	1225	23.3	16:13	MV (0.721,0.062,0.691)	1628 (1300)	N	-ve	S(S)
8 September 1978 (out)	8.5	1139	26.0	0:44	MV (0.776,-0.216,0.593)	2024 (1630)	N	-ve	S(S)
12 September 1978 (out)	9.6	1137	25.9	19:54	TD (0.652,0.117,0.749)	2215 (1870)	N	-ve	S(S)
28 October 1978 (out)	12.3	0945	42.7	8:21	MV (0.689,-0.357,0.631)	--	N	∿ 0	S(S)
4 November 1978 (out)	12.8	0906	42.9	13:01	MV (0.649,-0.241,0.721)	--	N	-ve	S(S)
10 September 1979 (in)	10.2	1518	-23.6	18:02	TD (0.844,0.387,-0.371)	952 (910)	S	-ve	R(R)
11 September 1979 (out)	10.6	1213	21.4	4:11	MV (0.902,0.126,0.412)	828 (810)	N	-ve	S(S)
25 September 1979 (in)	10.5	1420	-20.0	2:03	TD (0.893,0.101,-0.439)	77 (10)	S	-ve	R(R)
16 October 1979 (in)	--	--	--	12:45*	--	--	S	+ve	?
22 November 1979 (in)	22.1	0858	4.4	23:47	TD (0.679,-0.449,0.661)	443 (80)	N	-ve	S(-)

a Location and time of main magnetopause crossing
(* Approximate time of reconnection event)

b Direction of boundary normal in GSM components:
MV = minimum variance, TD = tangential discontinuity

c Radial satellite separation (separation along $\hat{N}$) in km

d Inferred location of satellite relative to reconnection line:
N = north; S = south

e Sign of magnetosheath B_M component

f Type of magnetosheath (magnetosphere) FTE observed:
S = standard; R = reverse; I = irregular; M = mixed

the plasma data for each pass containing reconnection events. This study has led us to attempt a classification of FTE structure, which we shall report on in the second part of this chapter. We also note the regular occurrence of large spikes in B_L which, in general, are a common feature when the magnetosheath magnetic field has a southward component. B_L spikes refer to positive excursions of the B_L component just outside the magnetopause. They are observed over a time scale comparable to or shorter than the duration of FTE signatures but they are not, however, correlated with the unambiguous B_N signature used to define FTEs. We shall speculate that B_L spikes and FTEs are related phenomena.

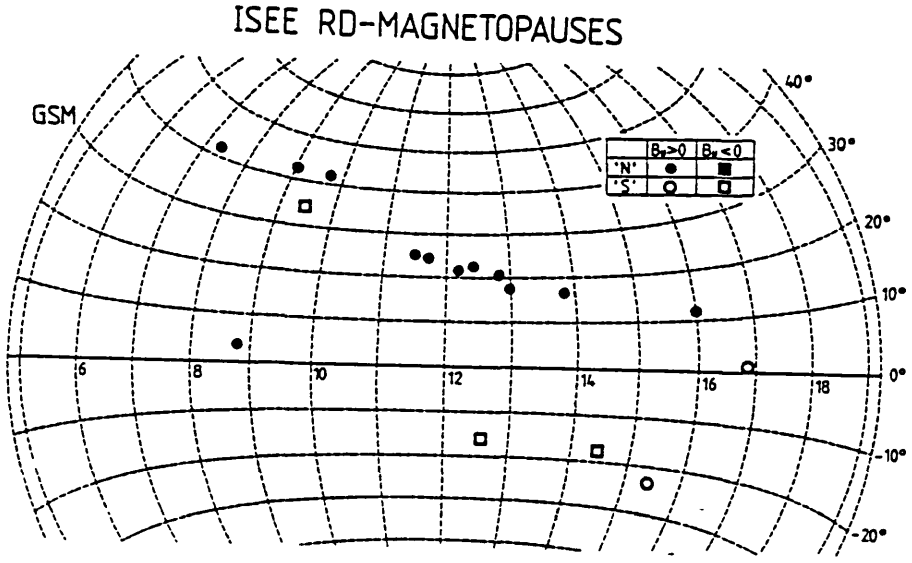


Fig. 5.1. Locations of 17 quasi-steady reconnection events (after Paschmann, 1984).

5.2 Reconnection Events and FTEs

In this section we describe in detail the plasma and magnetic field

data of three passes containing steady reconnection events in order to substantiate the correlation between FTE B_N signature and satellite location relative to the steady reconnection line.

5.2.1 3 September 1978, outbound pass

Figure 5.2 shows plasma and magnetic field data obtained from ISEE 1 (dark trace) and ISEE 2 (light trace) for a 1-hour interval during this pass. The top four panels show medium resolution magnetic field data plotted in boundary normal (LMN) coordinates. Dashed vertical lines refer to magnetic signatures in the ISEE 1 and/or 2 data which satisfy the identification criteria for FTEs (Chapter 4). The bottom four panels show 2-D plasma data obtained at a resolution of respectively 6 and 12 secs for ISEE 1 and 2. The solid traces in the N_p and N_E panels show respectively the total plasma and electron densities (cm^{-3}), while the dotted traces show the corresponding high-energy components ($\gtrsim$ 9 keV for protons, $\gtrsim$ 5 keV for electrons). The V_p panel shows the bulk plasma flow speed in km s^{-1}, while the ϕ_p panel shows the flow azimuth angle: 180° indicates tailward flow and 90° indicates duskward flow in satellite (approximately GSE) coordinates.

Both ISEE 1 and 2 are initially inside the magnetosphere. At 6:56 UT both satellites observe a field perturbation and the B_N amplitude is sufficiently large for this event to be identified as a standard FTE in the ISEE 2 data. ISEE 1 does not observe a plasma signature during this event but ISEE 2 observes a boundary layer pulse in the electron data as well as a slight flow perturbation. At 7:00 UT both ISEE 1 and 2 observe a standard FTE. ISEE 2 also observes a correlated boundary layer pulse and accelerated flow which reaches a magnitude and direction similar to that seen later at the magnetopause.

As ISEE 2 approaches the magnetopause it observes several small-amplitude short-lived B_N perturbations which look like small FTE signatures. One of these, at 7:06:30 UT, is accompanied by an electron boundary layer pulse and another, at 7:07 UT, occurs in association with a boundary layer pulse and accelerated flow. ISEE 2 crosses the magnetopause at 7:08 UT and within this layer observes enhanced flow speeds as noted by Sonnerup et al. (1981). Outside the magnetopause ISEE 2 observes large B_L spikes, i.e., short-lived positive excursions of B_L without the prominent B_N signature required for FTEs, at 7:09:30, 7:10 and 7:12 UT. ISEE 2 also observes three FTEs at 7:11, 7:15 and

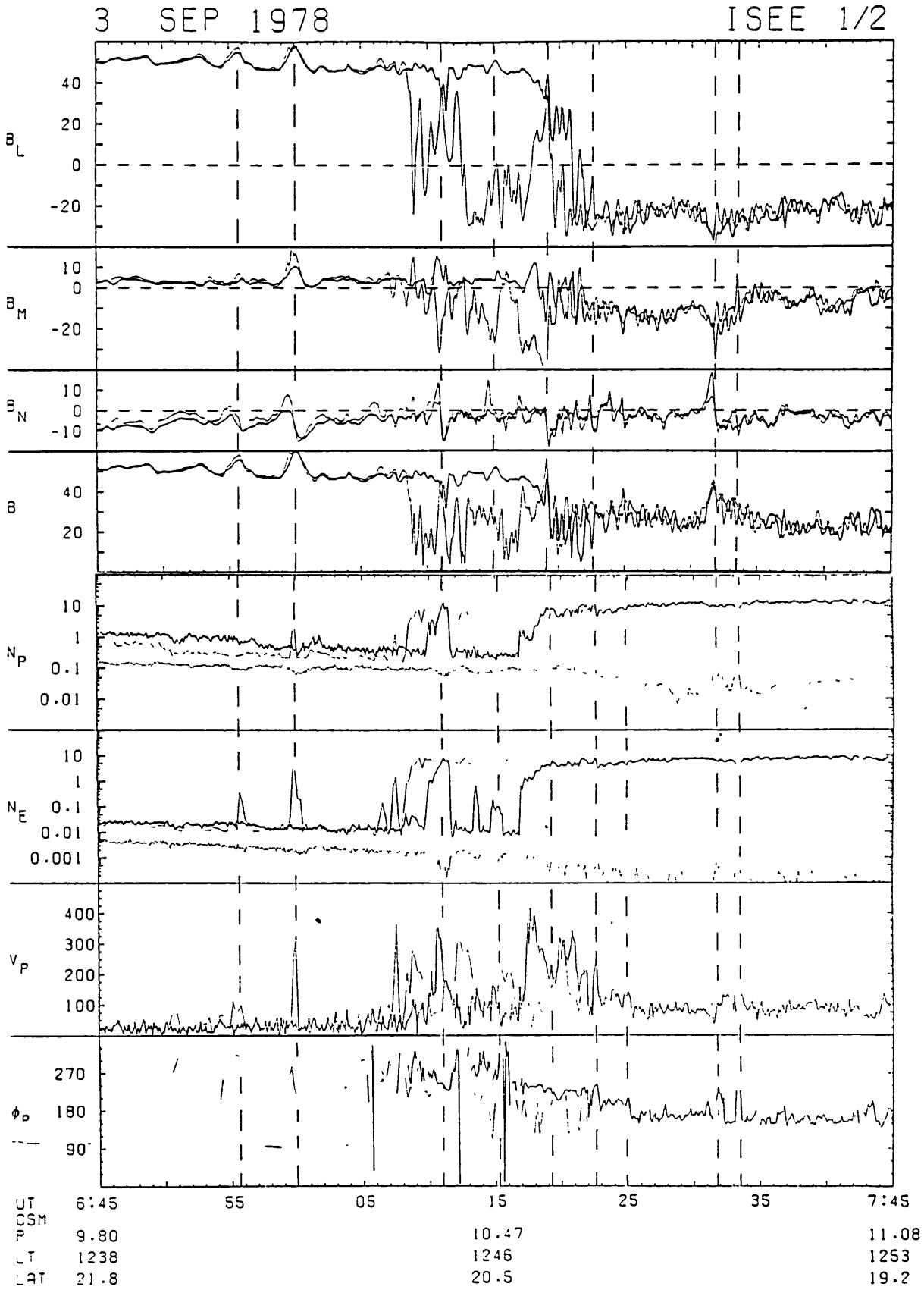


Fig. 5.2. Quasi-steady reconnection on 3 September 1978.

7:19 UT. The plasma signature and B_L behaviour of the FTEs and B_L spikes are very similar. However, the B_M component goes increasingly negative during the FTEs whilst it returns to the magnetospheric level during the B_L spikes. The FTE at 7:11 UT is also observed by ISEE 1, both in the field data and as a high-speed boundary layer pulse. During this event ISEE 2 sees the field strength increase while ISEE 1 observes a reduction in field magnitude, although there is a corresponding substantial increase in plasma pressure (not shown). This is a fine example for the argument that a field strength increase should not be regarded as an invariant feature of the FTE phenomenon (see previous chapter). During the ISEE 2 FTE at 7:15 UT ISEE 1 observes a small field perturbation and a boundary layer pulse in the electron data with perturbed plasma flow. The ISEE 2 FTE at 7:19 UT is also observed by ISEE 1. At this stage ISEE 1 has already entered the high-speed boundary layer region which starts at 7:17 UT and appears attached to the magnetopause.

ISEE 1 crosses the magnetopause at 7:20 UT and outside this layer observes several B_L spikes occurring close together. The B_L spike at 7:22 UT is observed by ISEE 2 (the leading satellite) as a magnetosheath FTE, but the plasma signature is similar. Moving further away from the magnetopause ISEE 1 observes standard magnetosheath FTEs at 7:23, 7:25, 7:32 (also observed by ISEE 2) and 7:33:30 UT. All events show flow perturbations and energetic particle density increases.

5.2.2 25 September 1979, inbound pass

Figure 5.3 shows two successive 1-hour invervals of magnetic field data from ISEE 2. The plasma and magnetic field data have properties consistent with the requirements for a rotational discontinuity during the approximate interval 1:50 - 2:20 UT. ISEE 2 is inferred to be located on open field lines south of the reconnection line during this interval.

ISEE 2 is initially inside the magnetosheath where it observes a southward and duskward field orientation. Five prominent reverse FTEs occur in the magnetosheath at 1:30, 1:33, 1:39, 1:42 and 1:49 UT. There is also evidence for FTE activity occurring on smaller scales in between. ISEE 2 encounters the magnetopause layer during the interval 1:50 - 1:58 UT. B_N fluctuates considerably during this interval and reverse FTEs are observed at 1:50:30, 1:57:30 and 1:58:30 UT, although

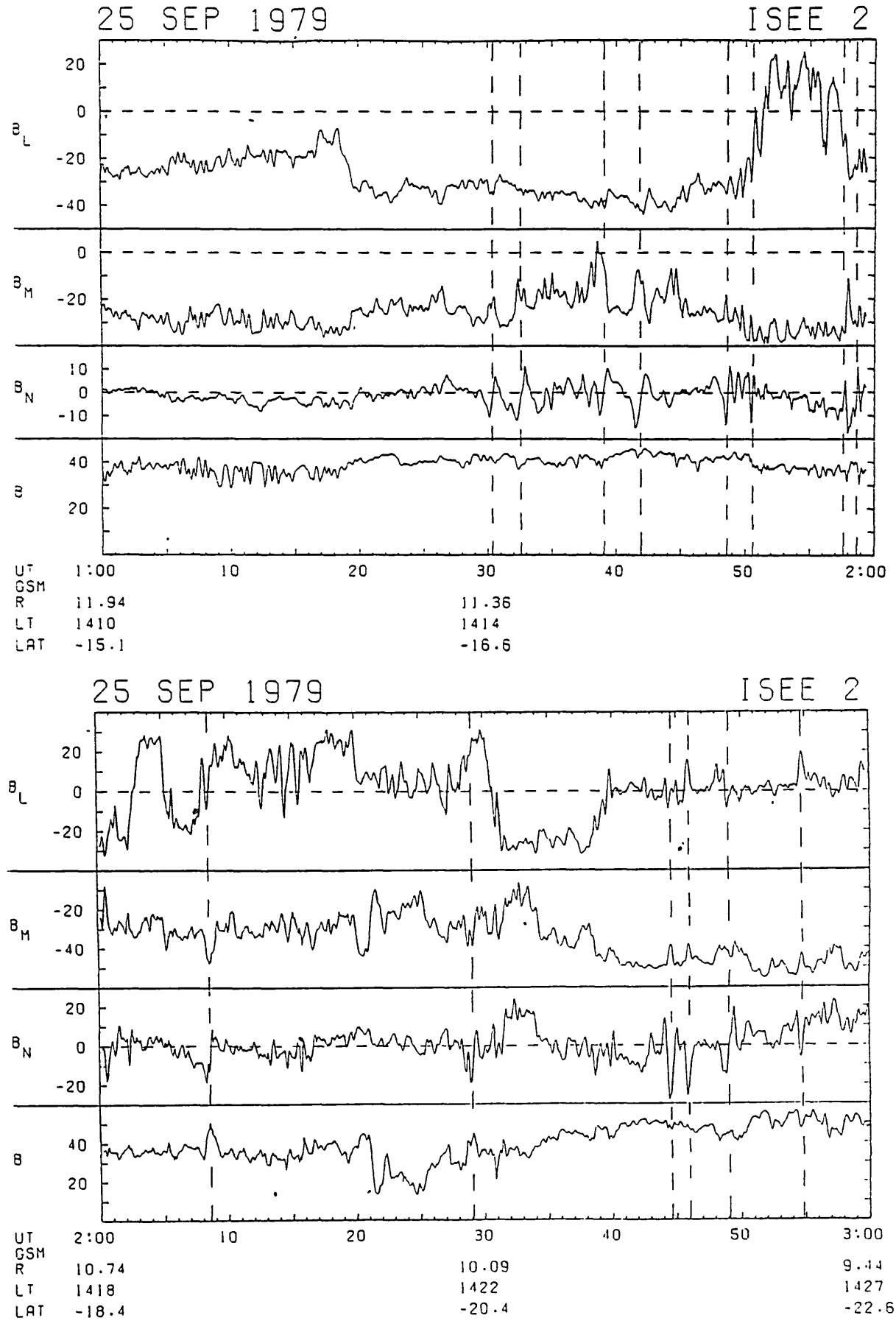


Fig. 5.3. Quasi-steady reconnection on 25 September 1979.

the determination of the B_N polarity is slightly complicated because the signatures follow so closely one after another.

During the second interval the magnetopause is again crossed several times as a result of boundary motions. The main crossings occur at 2:03, 2:05, 2:08, 2:31 and 2:39 UT. After the final crossing the magnetospheric field orientation is mainly duskward and tailward (B_M negative). In view of the satellite location (within 2½ hours of local noon) this may indicate a local or global distortion of the magnetosphere from its usual configuration. This could explain why B_N does not appear to be well-determined near 2:32 UT and towards the end of the interval displayed. The second interval shows additional FTE-like activity. Prominent reverse FTEs occur at 2:09, 2:29, 2:44 and 2:49 UT. Also, two irregular FTEs are observed at 2:46 and 2:55 UT.

5.2.3 3 August 1978, outbound pass

A 1-hour inverval of data for our final example is shown in Figure 5.4. The data format is the same as in Figure 5.2, except that there is an added V_z panel at the bottom which shows the z-component of the plasma flow obtained from 3-D data (12 sec resolution), in units of km s^{-1} and with positive values indicating northward flow. The 2-D plasma data have a resolution of respectively 6 secs and 3 secs for ISEE 1 and 2. This pass contains reconnected flows inferred to be north of the reconnection line (Sonnerup et al., 1981) as well as a possible crossing of the reconnection line (Cowley et al., 1983).

Both satellites are initially inside the magnetosphere with ISEE 1 leading. The magnetosheath is encountered for a short interval starting at 4:02 UT for ISEE 1. The ISEE 1 plasma data show a small boundary layer pulse immediately adjacent to the first crossing at 4:02 UT, which correlates with a small-amplitude B_N perturbation. Outside the magnetopause ISEE 1 observes two prominent B_L spikes at 4:02:30 and 4:04 UT and also an FTE at 4:06 UT, which is accompanied by a negative deflection in B_M. The B_L spikes correlate with small B_N perturbations and the second spike also has a negative deflection in B_M. These examples strongly resemble FTEs but with amplitude and time scale smaller than our acceptance criterion. Note that during all three events as well as at the magnetopause crossings ISEE 1 observes dawnward plasma flow, while the flow in the magnetosheath is slightly duskward (consistent with the duskward satellite location). This is

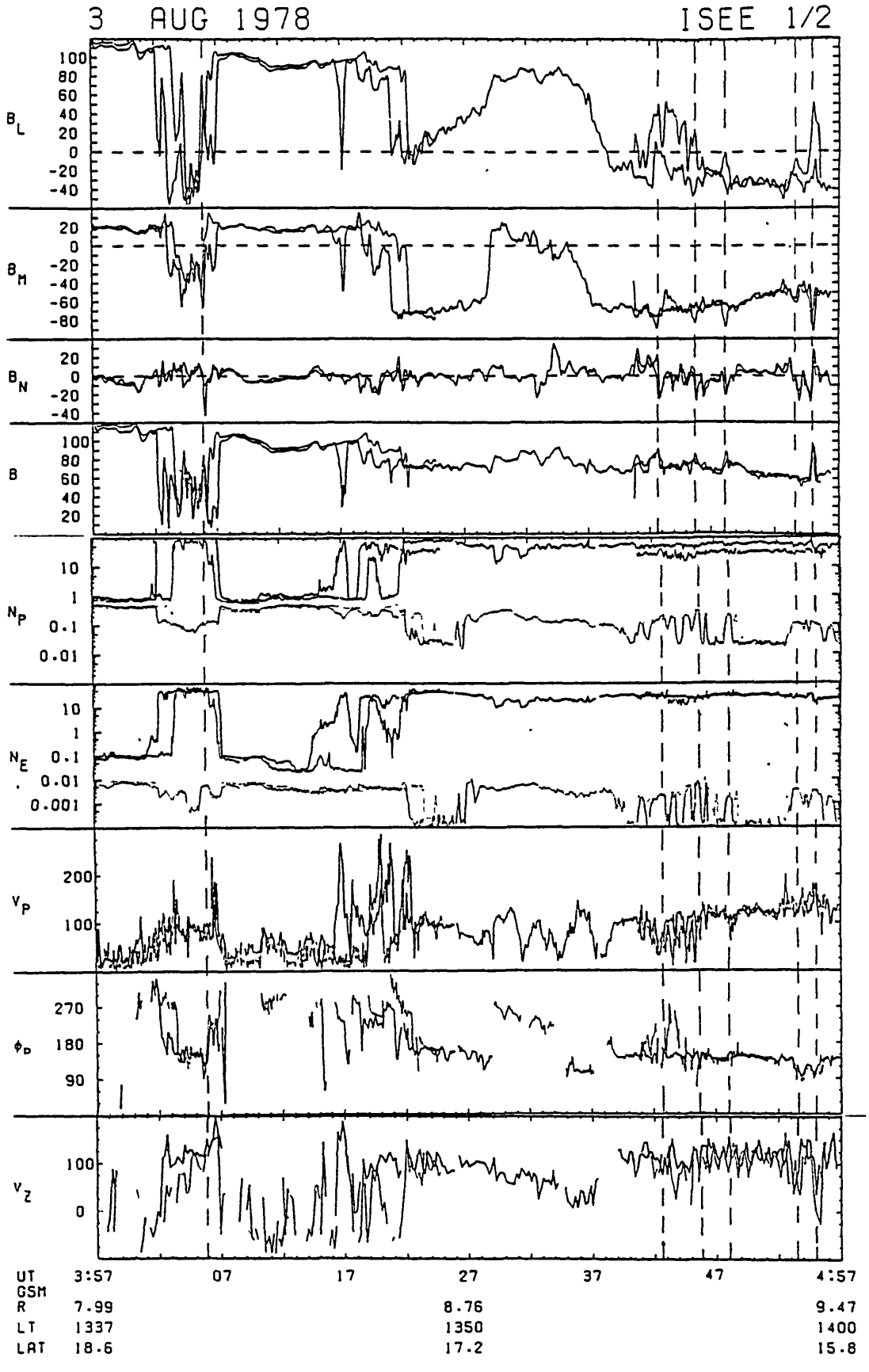


Fig. 5.4. Quasi-steady reconnection on 3 August 1978.

therefore an example of reconnection causing a flow reversal in the open field line region at the magnetopause (Cowley et al., 1983), and this signature is appropriate for a satellite location north of the reconnection line in the sub-alfvénic region (Figure 1.7). ISEE 2 also observes this feature but in addition it sees a substantially enhanced flow speed at the magnetopause, albeit at single data points. ISEE 1 may have missed the accelerated flow spikes because of the lower time-resolution of its plasma data. The short ISEE 2 encounters also suggest that the high-speed flow region is of small extent (i.e., we are close to the reconnection line) and/or that the magnetopause is moving rapidly at the time. Note that ISEE 2 also observes the ISEE 1 B_L spike at 4:04 UT and that it observes the ISEE 1 FTE at 4:06 UT as another B_L spike, even though it is closer to the magnetopause. In all observations of B_L spikes the satellite closest to the magnetopause sees the most positive B_L value.

ISEE 1 makes another brief excursion into the magnetosheath at 4:17 UT, while ISEE 2 remains in the magnetosphere. At this time the satellite separation is therefore larger than the extent of the boundary layer and magnetopause combined. There is boundary layer attached to the magnetopause which has a larger extent in the electron data (ISEE 2 also observes the latter briefly). At 4:18:30 UT ISEE 1 re-enters the boundary layer and again observes dawnward plasma flow which increases in magnitude as the magnetopause is approached. At 4:21 UT the plasma flow drops abruptly to the magnetosheath level. After an initial brief encounter (4:19 - 4:20 UT) ISEE 2 re-enters the high-speed boundary layer at 4:21:30 and also observes an abrupt drop in flow speed as it enters the magnetosheath at 4:22:30 UT. There is another short period at 4:21 UT when ISEE 2 is in the magnetosphere while ISEE 1 is in the magnetosheath. At 4:22 UT ISEE 1 observes a B_L spike, which has an FTE-like B_N signature in both ISEE 1 and 2 data. Both satellites observe dawnward flows during this event implying that the layer of dawnward flow is larger than the satellite separation at this time.

ISEE 1 encounters the magnetopause twice more at $\sim$ 4:29 and 4:37 UT. Approaching these crossings from the magnetosheath the magnetic field appears to rotate continuously northward. The northward magnetosheath field may result from a temporal variation in the IMF orientation. Such a northward rotation may cause the reconnection rate to decrease or to switch off completely and explain why the flow speed does not reach the

level observed at previous crossings. Another interpretation is that ISEE 1 makes a long-lived encounter with a magnetosheath boundary layer region (Cowley et al., 1983). Some support for the latter is given by the field behaviour around 4:44 UT, which shows ISEE 1 and 2 observing northward and southward field orientations, respectively, with B_M remaining duskward. However, if the energetic particle density enhancement at $\sim$ 4:26 UT represents a crossing of the outer separatrix then part of the northward field region must lie outside the open field line region.

In the boundary layer region centred $\sim$ 4:36 UT ISEE 1 observes several large B_N perturbations. Also, there is a brief period near 4:36 UT where the plasma flow is deflected southward and more strongly duskward relative to the magnetosheath flow. Such behaviour indicates that ISEE 1 is located on open field lines south of the reconnection line during this period (Figure 1.7).

After the final boundary crossing ISEE 1 and 2 observe much FTE-activity in the magnetosheath during the intervals 4:40 - 4:50 and 4:53 - 4:55 UT. Dashed vertical lines show the prominent signatures which are identified as FTEs. During the first interval standard FTEs are observed which are accompanied by flow speed decreases and energetic particle enhancements. During the second interval a standard and reverse FTE are observed in close proximity. The plasma flow increases slightly and goes more duskward during these events. During the reverse FTE the flow deflects to such an extent that ISEE 2 actually observes a southward V_Z component. Such signatures suggest that the FTEs represent observations of flux tubes connected to the Southern Hemisphere, in agreement with the plasma flow deflection in the boundary layer near $\sim$ 4:36 UT.

5.2.4 Conclusion

Our observations show that FTEs occur in close association with reconnection events. The polarity of the FTE B_N signatures, i.e., standard or reverse, as well as the plasma flow perturbations during the FTEs are consistent with the inferred location of the steady reconnection site relative to ISEE in all the cases we have examined. The agreement is so good that on one occasion both FTE and steady reconnection signatures seem to indicate an actual crossing of the reconnection line (Figure 5.4). This crossing may have resulted from

the duskward and southward ISEE motion and/or an increased tilting of the reconnection line in response to a more strongly negative magnetosheath B_M component (compare field values at 4:04, 4:17, 4:24 and 4:50 UT in Figure 5.4). It is very unlikely that the close correlation between FTE signatures and steady reconnection flows is the result of pure chance but rather it suggests that the two phenomena are closely related, as also noted by Rijnbeek et al. (1982).

5.3 Plasma Properties of FTEs

5.3.1 Classification of FTE plasma signatures

Detailed examination of all the passes containing quasi-steady reconnection events for which both plasma and magnetic field data are available (13 passes) shows that there is a lot of temporal/spatial structure associated with FTEs. The model described in section 3.2 can therefore only be regarded as a first order approximation. Roughly, the FTE plasma signatures fall into three different types, as follows (in order of decreasing occurrence frequency):

Type A: FTEs of this type show prominent magnetic signatures and corresponding plasma signatures. The plasma signature consists of a perturbation in the plasma flow in both magnitude and direction. Although the flow speed is often enhanced during the events, it does not reach the level of the steady reconnection flows observed at the magnetopause. The plasma densities (total and high-energy component) indicate a mixture of particles of magnetosheath and magnetospheric origin. An example of a type A FTE occurs at 4:48 UT in Figure 5.4.

A further subdivision in this category can be made into events which show plasma mixing in only the electron data (e.g., the ISEE 2 FTE at 6:56 UT in Figure 5.2), events which show mixing in only the proton data, and finally, events which show plasma mixing in both the proton and electron data.

Type B: Events of this type display prominent magnetic field and plasma signatures. The plasma signature consists of a pulse of boundary layer plasma (in both the proton and electron data) as well as accelerated plasma flow which reaches a magnitude and direction similar to the reconnection flows observed at the magnetopause. These events usually show pronounced tangential field tilts with an orientation intermediate to those observed inside and outside the magnetopause.

Type C: The final type of events show a magnetic signature, but there is no corresponding plasma signature. Events of this type which have a prominent tangential field tilt show a field tilt away from the orientation on the opposite side of the magnetopause. An example of a type C event occurs at 7:00 UT in Figure 5.2 (ISEE 1 data).

Tables 5.2 and 5.3 show respectively the numbers of magnetosheath and magnetosphere FTEs observed for each of the above types during 13 of the passes in Table 5.1. Data from both satellites were used in cases where the satellite separation was large enough to distinguish between the superposed data traces (5 July, 3 August, 3 September and 8 September 1978 events). Tables 5.2 and 5.3 show that about twice as many magnetosheath FTEs are listed as magnetosphere FTEs. However, it should be noted that a substantial number of boundary layer pulses occur in the magnetosphere which have B_N perturbations, but with amplitude and duration below our acceptance criterion (an example occurs at 7:07:30 UT in Figure 5.2). A number of these boundary layer pulses show accelerated flow similar to that observed at the magnetopause.

We can make a few speculations as to the physical distinction between the different FTE types. First of all, the two-satellite data sets (e.g., Figure 5.2) as well as the time of observation of the FTE types relative to the magnetopause crossings suggest that much of the variation in FTE signature can be attributed to spatial structure inside the flux tubes. Type C events are observed furthest away in time or by the satellite furthest away from the magnetopause and probably do not represent crossings through the open field line region. Rather, we are observing the effects of displaced magnetic field lines draping over the open flux tubes. Type A events may or may not represent actual crossings through the open field line region. In the former case we are probably observing open field lines which have reconnected sometime in the past, in which case we do not necessarily expect to observe the same flow magnitude as during the reconnection events. In the latter case the effects are due to displaced plasma and field lines overlying an open flux tube. The mixture of particle populations could in this case result from diffusion or leakage out of the open flux tube onto the surrounding unreconnected field lines. Type B events finally are observed closest to the magnetopause and almost certainly do represent actual entries into an open flux tube. The plasma flow signature is very similar to that observed during the reconnection events at the

Table 5.2

Magnetosheath FTE Plasma Signature

B	N_p	N_E	$\overline{N}_p$	$\overline{N}_E$	ΔV_p	$\Delta V_p\uparrow$	Number	Type
✓	✓	✓	✓	✓	✓	X	48	A
✓	✓	✓	✓	X	✓	X	7	A
✓	✓	✓	✓	✓	✓	✓	11	B
✓	X	X	X	X	X	X	2	C

Key: $\underline{B}$ = magnetic signature

N_p, N_E = magnetosheath particles

$\overline{N}_p$, $\overline{N}_E$ = magnetosphere particles

ΔV_p = flow perturbation

$\Delta V_p\uparrow$ = flow velocity similar to reconnection flow

Table 5.3

Magnetosphere FTE Plasma Signature

$\underline{B}$	N_p	N_E	$\overline{N}_p$	$\overline{N}_E$	ΔV_p	$\Delta V_p\uparrow$	Number	Type
✓	✓	✓	✓	✓	✓	X	10	A
✓	✓	✓	X	✓	✓	X	1	A
✓	✓	✓	✓	✓	✓	✓	20	B
✓	X	X	X	X	X	X	3	C

magnetopause which suggests that reconnection is still occurring while we are observing the FTE.

An interesting observation from the plasma data is that in the magnetosphere the electron boundary layer (whether or not associated with an FTE) often extends beyond the proton boundary layer. Figure 5.2 gives a good example of this feature, e.g., at 6:56 and 7:13 UT. This feature may result from the faster travelling speed of electrons along field lines. It could also result from strong electron scattering processes produced by the electrostatic turbulence found at the magnetopause, inside FTEs and in the boundary layer (e.g., Gurnett et al., 1979; Anderson et al., 1982). The finite energy detection range of the plasma detector may also play a part. Another interesting feature is that in the magnetosphere energetic electron density dropouts are often more noticeable than those of the protons (e.g., 7:00 UT in Figure 5.2), while in the magnetosheath the energetic proton enhancements show up more clearly than the energetic electron density enhancements (e.g., 7:32 UT in the magnetosheath). In Tables 5.2 and 5.3 this feature results in a subdivision of type A events which is different for magnetosheath and magnetosphere FTEs. Also, comparing Figures 5.2 and 5.4, it is apparent that sometimes only the energetic protons seem to define the outer separatrix (7:28 UT in Figure 5.2), while other times energetic electrons also extend to the outer separatrix (Figure 5.4). Of the other passes, 4 show clear behaviour similar to the former, and 5 show behaviour similar to the latter. This again may be the result of instrumental limitation or it could be that the energetic particle resupply process (e.g., electric field drift) is not always fast enough to maintain a supply of electrons on external open field lines. Finite gyroradius effects may also play a part (e.g., Daly, 1982). These features deserve further investigation with electron plasma instruments.

We should note that the above FTE type division is probably valid in general, and is not a feature peculiar to the passes containing the steady reconnection events. This conclusion has been reached from an examination of about a dozen other passes with FTEs for which high time-resolution plasma data were available (mostly 1977 data; see also Paschmann et al., 1982). Accelerated flows are often observed at the magnetopause so that in these cases one can retain the type B classification (e.g., Figure 3.11). In general, however, the relative numbers of FTEs of each type may differ from that in Tables 5.2 and 5.3. It should also be noted that temporal effects probably play a part as well.

We may anticipate, for example, that a switch-on or -off of reconnection during a flux tube crossing may lead to a time-dependent FTE signature. Magnetopause motion may also lead to different spatial regions being sampled during a single FTE observation. Such effects may account, for example, why accelerated flow is only observed during the latter part of the magnetosheath FTEs in Figure 3.11 (see also Paschmann et al., 1982). Finally, we should note that the overwhelming majority of FTEs for which we have plasma data available show a mixture of magnetosheath and magnetospheric plasma as well as flow perturbations. These signatures are similar to the plasma signatures of the original FTE observations (Russell and Elphic, 1978), and once more indicate that we are still dealing with the same phenomenon in spite of our broadening of the FTE identification criteria.

5.3.2 B_L spikes

B_L spikes, i.e., short-lived ($\lesssim$ 1 min) positive excursions in B_L not associated with an FTE B_N signature, are interesting features which need further investigation with high time-resolution plasma and field data. At first sight the observations seem to imply that we are observing partial re-entries into the magnetopause layer caused, for example, by solar wind-driven surface waves resulting from Kelvin-Helmholtz instability of the magnetopause (e.g., Southwood, 1979) propagating tailward. However, there are several arguments against such an interpretation. B_L spikes are a common feature only during periods of southward magnetosheath field (although for small rotation angles at the magnetopause they probably would not readily show up). They have a plasma signature which is very similar to that of the reconnected flow at the magnetopause; they probably represent a brief widening of the accelerated flow region at both its inner and outer edges, as the observation at 4:22 UT in Figure 5.4 seems to suggest. They are often accompanied by perturbations in B_N, although the amplitude does not reach the level required of FTEs. In fact, many of the B_L spikes resemble FTEs but with B_N signatures of a smaller time and/or amplitude scale. Finally, a number of B_L spikes are observed by one satellite while the other satellite observes a simultaneous FTE (e.g., 4:06 UT in Figure 5.4).

The B_L spike signatures suggest that they are closely related to FTEs and hence that they are part of the reconnection process. For

example, they may represent encounters with open flux tubes which are smaller than the average FTE scale size and thus have a shorter duration and smaller B_N amplitude. Some B_L spikes could result from crossings of the outer part of the magnetospheric arm of FTE flux tubes, close to where it grazes the magnetopause (Figure 5.5). Whatever their explanation, B_L spikes are often observed in rapid succession near the magnetopause, with a recurrence time of order a minute. If they are reconnection phenomena, then this suggests that there is a significant contribution to the total cross-magnetospheric voltage in addition to the FTE voltage we estimated in Chapter 4.

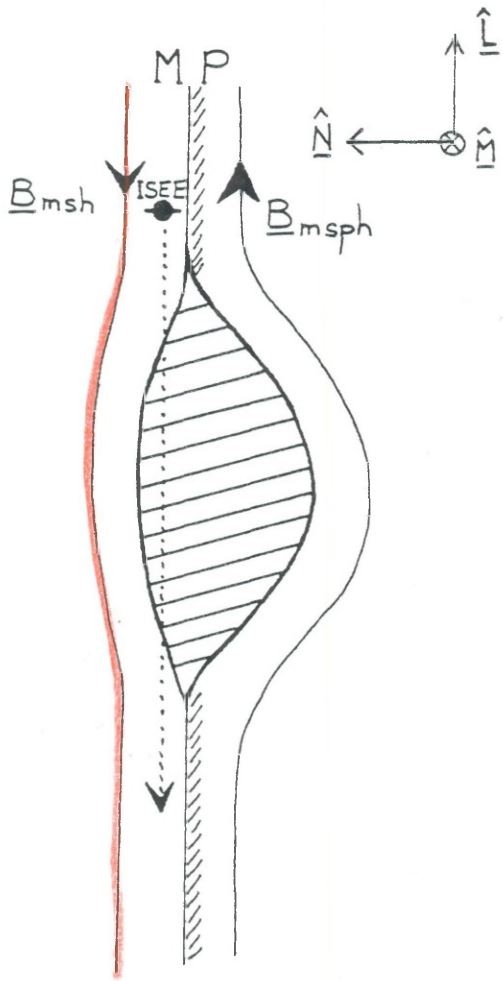


Fig. 5.5. Possible interpretation of a B_L spike.

5.3.3 Discussion

Examination of magnetic field and plasma data for the passes containing quasi-steady reconnection events has led us to suggest that the quasi-steady reconnection events, FTEs and B_L spikes are closely

related phenomena, as well as proposing a classification of FTE structure. We are now therefore presented with the question as to what form this relationship takes.

One possibility is that the reconnection rate at the dayside magnetopause is variable. For example, within a region of relatively steady reconnection occurrence, there may be sudden localised enhancements in the reconnection rate. The enhancements, although not leading to increased plasma flow speeds (e.g., Sonnerup et al., 1979), will lead to increases in the volume of reconnected plasma and magnetic field lines. If the resulting bulges of enhanced volumes of reconnected flux are sufficiently large, we may observe their effects in the form of FTE signatures as they propagate along the magnetopause away from the initial reconnection site. In between (in space and/or time) the localised bursts of rapid reconnection (FTEs), the reconnection rate may remain at a relatively steady value rather than switching off. In this scenario the B_L spikes could perhaps represent smaller bulges of reconnected flux resulting from smaller-scale variations in the reconnection rate (Figure 5.6).

Another possibility is that the region of patchy, FTE-type of reconnection is spatially separated from the steady reconnection region. For example, steady reconnection could occur quasi-continuously in a 2 to 4 hour wide local time band centred on local noon (e.g., Cowley, 1982), while FTEs result from the peeling away of flux filaments on the edges of this steady reconnection region. At the moment the data do not allow us to decide whether one, none or both of the above models is correct: this would probably require a network of simultaneous observation points on the magnetopause.

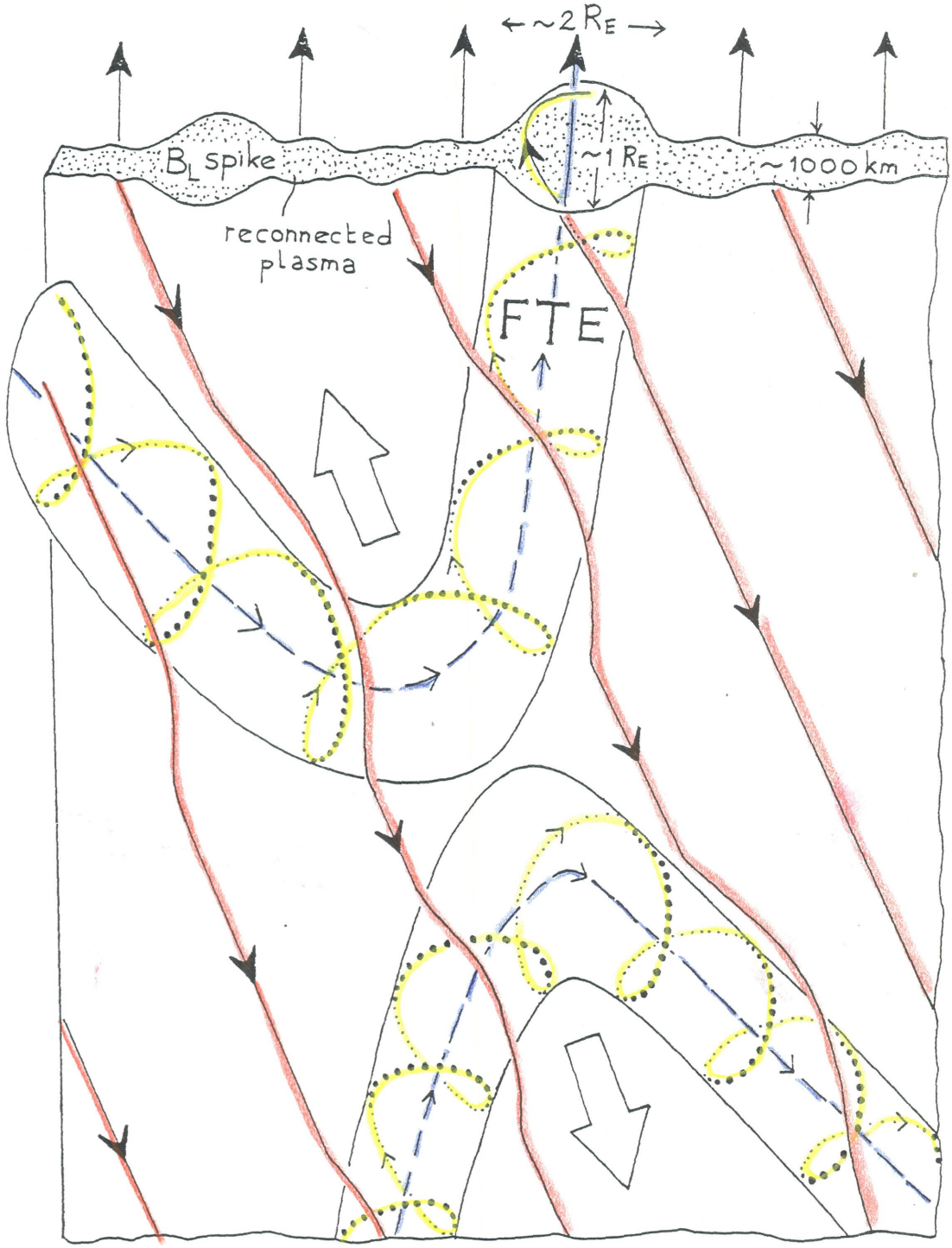


Fig. 5.6. Possible schematic for reconnection.

CHAPTER 6

FLUX EROSION EVENTS

6.1 Introduction

In this chapter we discuss HEOS 2 observations of impulsive reconnection signatures. Such signatures were first discovered by Haerendel et al. (1978) in the form of short time scale magnetic field perturbations inside the high-latitude magnetopause and termed flux erosion events (FEEs) by them. Here we show that FEEs represent the same phenomenon as FTEs.

6.2 Flux Erosion Events

6.2.1 Observations

Flux erosion event (FEE) is the name given by Haerendel et al. (1978) to short-lived ($\sim$ 1 min) large-amplitude magnetic field perturbations which were found in the HEOS 2 data in the dayside boundary layer (see Figure 2.5). Haerendel et al. (1978) interpreted FEEs as signatures resulting from transient, localised reconnection in the polar cusp regions. In the light of subsequent ISEE observations it has often been suggested that FTEs and FEEs are somehow related. Since HEOS 2 and the ISEE 1 and 2 satellite pair have instrumentation which differs in time resolution and since they also cover different areas of the magnetopause (Appendix A), it is not immediately obvious what the relation between FEEs and FTEs is. Most significantly, however, we need to establish common ground by applying to FEEs the same analysis techniques which led to the discovery and interpretation of FTEs (Russell and Elphic, 1978).

We need to re-examine the HEOS 2 magnetic field data by converting the field data into boundary normal coordinates (Appendix B). This has been done in Figures 6.1 and 6.2, which show two examples of HEOS 2 passes which contain FEEs (Haerendel et al., 1978). It should be noted

that the field data are plotted at what is normally the full time resolution of one data point every 32 secs. For each of the passes shown the direction of the normal to the local magnetopause, $\hat{N}$, was determined using the procedure outlined in section 4.2 for the 1979 ISEE data.

Figure 6.1 shows HEOS 2 data obtained during an inbound pass of the magnetopause region on 1 December 1973. This pass contains the clearest examples of FEEs found in the HEOS 2 data so far (see also Figure 2.5(a)). Except for the different time resolution and the 2-hour interval, the format of the plot is the same as in previous chapters (e.g., Figure 3.5). At the start of the interval HEOS 2 is located in the magnetosheath, where the magnetic field has a southward and duskward orientation. The magnetopause, which can be identified from the change in magnetic field orientation, is crossed at $\sim$ 0:58 UT at a location just duskward of noon and a GSM latitude of $\sim$ 64°. Subsequently, HEOS 2 enters the magnetosphere where the magnetic field has its expected northward and slightly dawnward orientation. The large field perturbations at, e.g., 1:07, 1:12 and 1:16 UT are the features described as FEEs by Haerendel et al. (1978). Note that FEEs only refer to field perturbations observed inside the magnetopause. Dashed vertical lines in Figure 6.1 refer to magnetic field signatures which satisfy the identification criteria for FTEs outlined in Chapter 4. By lining up the B_N perturbations with the field strength increases and tangential field perturbations, standard FTEs can be identified at 0:26, 0:42 and 0:56 UT in the magnetosheath, and at 1:00, 1:12 and 1:29 UT in the magnetopause and magnetosphere regions. Irregular FTEs occur at 0:54 UT in the magnetosheath and at 1:07 and 1:16 UT in the magnetosphere. FTE-like perturbations on a smaller scale occur at 0:46, 1:03, 1:22, 1:26 and 1:32 UT.. Presentation of the HEOS 2 magnetic field data in the boundary normal coordinate system shows clearly that FEEs and FTEs are the same physical phenomenon.

Figure 6.2 shows a 2-hour interval of data from an inbound pass on 10 October 1973. The magnetopause is crossed at 3:34 UT on the dusk flank of the magnetosphere at a northerly GSM latitude of 38°. The magnetosheath field is mainly dawnward and has a variable B_L component which is southward just prior to the magnetopause crossing. FEEs occur inside the magnetosphere in the interval between the dashed vertical lines centred at $\sim$ 3:50 UT. Again, these signatures can clearly be

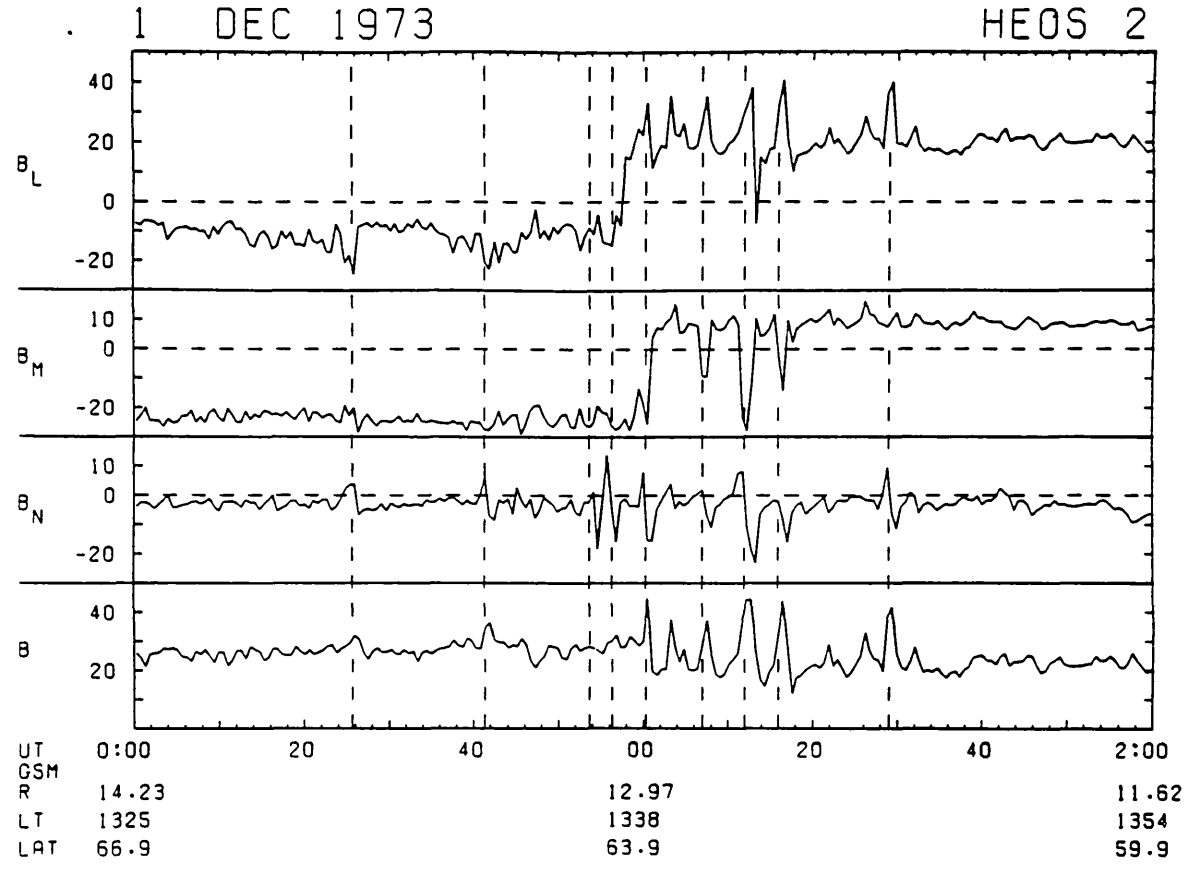


Fig. 6.1. Flux erosion events on 1 December 1973.

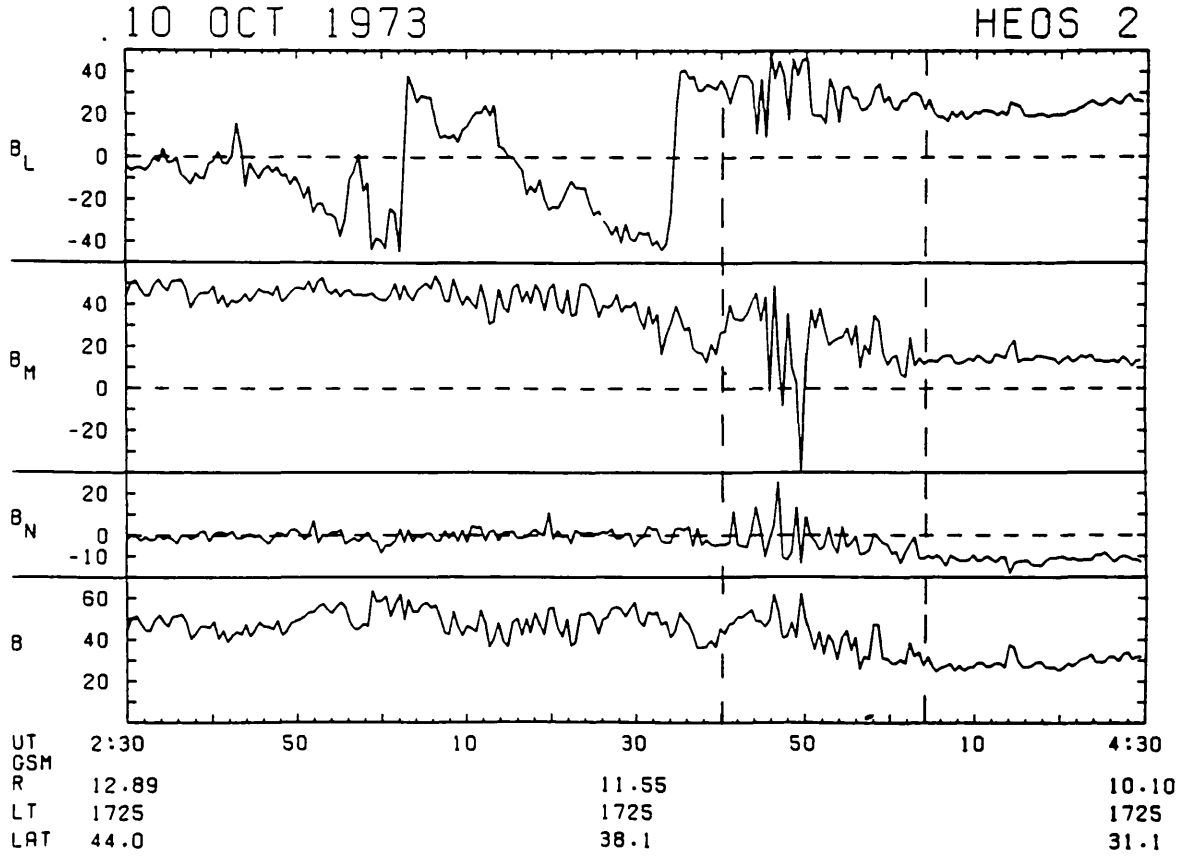
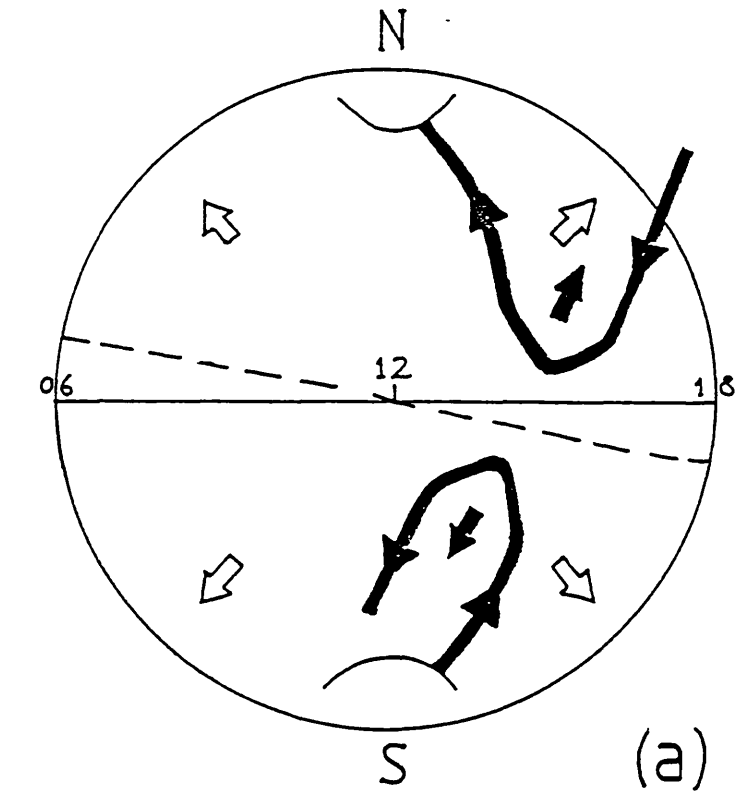


Fig. 6.2. Flux erosion events on 10 October 1973.

interpreted in terms of FTEs. However, the time resolution of the field data (32 secs) is too low to determine unambiguously the polarity of the B_N signatures. Note that during the event at 3:50 UT the tangential field component rotates away from the magnetosheath field orientation observed prior to the magnetopause crossing.

6.2.2 Interpretation

The observations in Figures 6.1 and 6.2 were interpreted in terms of localised, transient reconnection in the polar cusp regions by Haerendel et al. (1978) and Haerendel and Paschmann (1982). This interpretation was based mainly on the field strength increases during the FEEs, which can be explained in terms of a stretching of the open field lines as the open flux tube propagates downstream into the tail. However, the observations in Figure 6.1 are not inconsistent with an equatorial source region for the FEEs, as discussed by Rijnbeek and Cowley (1984). In fact, in view of the subsequent ISEE investigations on FTEs the latter alternative seems the more likely one. It is unfortunate that the low time resolution ($\sim$ 4 min) of the HEOS 2 plasma instrument meant that no plasma measurements were obtained during the FEEs/FTEs in Figure 6.1, so that this question cannot be fully resolved here (see Haerendel et al. (1978), Figure 10). The situation with the plasma data is more favourable for the observations in Figure 6.2 (Haerendel et al. (1978), Figure 8). Figure 8a in Haerendel et al. (1978) shows that the plasma flow is duskward during the interval in which FEEs are observed in Figure 6.2. Figure 6.3 shows two possible interpretations which may be applied to Figure 6.2. Figure 6.3(a) shows a pair of open flux tubes resulting from reconnection close to the equator. Note that the reconnection line is shown slightly tilted in response to the positive magnetosheath B_M component (compare with Figure 1.7(b)). Inspection of this Figure shows that the flux tube connected to the Northern Hemisphere readily explains the FEEs and the duskward flow during the 10 October 1973 pass. Figure 6.3(b) shows the situation corresponding to the models of Crooker (1979) and Luhmann et al. (1984), Figure 2, with reconnection occurring for anti-parallel orientations in the cusp region. Again, the FEEs in Figure 6.2 can be explained in terms of a flux tube connected to the Northern Hemisphere, but this time resulting from reconnection in the southern cusp region. In this latter situation the northward flux tube tension release is



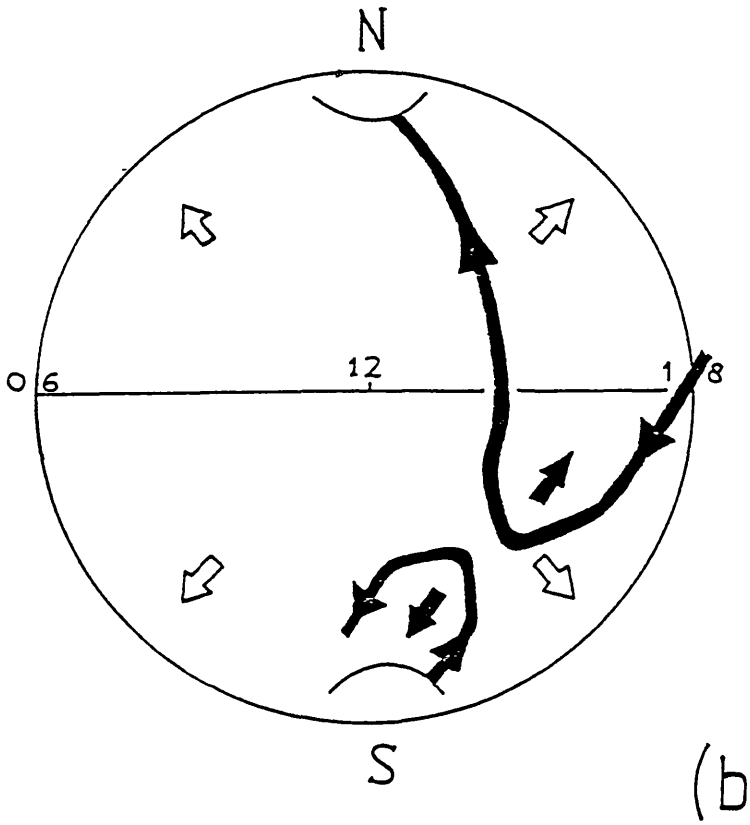


Fig. 6.3. Two possible interpretations for Figure 6.2.

opposed by the southward magnetosheath flow, so that we should expect to observe the flux tube (at the HEOS 2 location) well away from the point at which it crosses the magnetopause (i.e., the sharp bend).

In conclusion, we cannot yet tell conclusively from these HEOS 2 data what the source region for FEEs is, although the ISEE data suggest a near-equatorial source region as the most likely possibility. It may be worthwhile to examine more examples of FEEs to determine whether there are situations in which the HEOS 2 plasma data can give conclusive evidence concerning the source region.

6.3 FTEs: Other Satellites, Other Planets

Apart from ISEE 1 and 2 and HEOS 2, OGO 5 has also observed FTEs at the magnetopause (J. Slavin, private communication). FTEs have also been observed at synchronous orbit ($\sim$ 6 R_E) at times of disturbed magnetic activity with SCATHA (Croley et al., 1983) and GEOS 2 (G. Wrenn, private communication, 1984).

Other planets with intrinsic magnetic fields have also got their own magnetospheres. FTEs have now also been observed at the Jupiter and Mercury magnetopauses (Russell, 1983; Walker and Russell, 1983; Russell, 1984).

CHAPTER 7

QUESTIONS

7.1 Introduction

Although observations and theoretical advances have led to much progress in our understanding of the nature of the interaction processes at the boundary between the solar wind and the Earth's magnetosphere, much still remains to be explained and discovered. In this chapter we shall discuss a number of areas of research related to this topic, which are summarised in Table 7.1. The main areas of research comprise the boundary layer, FTEs and steady reconnection. We shall discuss a selection of questions (illustrated with observational data) and suggest how satellite data may be used to investigate them.

7.2 Solar wind-magnetosphere interaction: some remaining questions

7.2.1 The boundary layer revisited

The boundary layer is a direct manifestation of the solar wind-magnetosphere interaction. Examination of its properties should therefore enable us to study the nature of the coupling process(es) by which plasma momentum and energy are transferred across the magnetopause. From ion composition experiments we know that the boundary layer contains plasma of both solar wind and ionospheric origin. However, we still do not know in enough detail how the boundary layer is formed and where the entry locations of solar wind and ionospheric plasma are. Partly, our lack of knowledge stems from the highly variable nature of the boundary layer in both space and time. This problem may be overcome with the use of high-resolution instrumentation and such satellite data sets are in existence, notably from ISEE 1 and 2. In the following we shall discuss a selection of unsolved questions relating to various boundary layer regions and suggest which existing satellite data sets may be used to resolve these questions.

Table 7.1

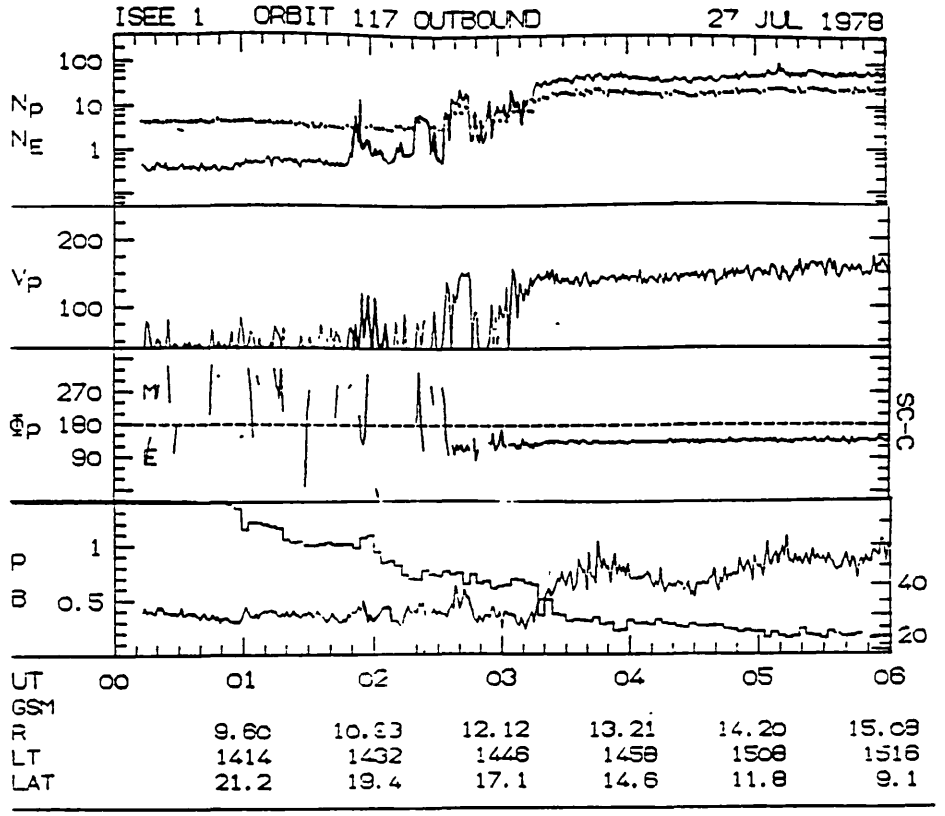
Solar wind-magnetosphere interaction: some questions

Research Topic	Region[(a)]	Signatures[(b)]
1. Entry, formation and properties of the boundary layer	Dayside; flanks; high-latitude cusp/ionosphere; tail	Reconnection; diffusion; plasma composition; FACs; waves; .....
2. Flux transfer events:		
Plasma signature	Dayside	Plasma density; flow
Source region	"	Particle streaming; plasma flow
3-D structure	"	Multi-satellite observations; modelling of FTEs
Evolution of signature	Dayside; high-latitude MP; tail	Plasma and field data
Spectrum of sizes	Dayside	B_L spikes; small B_N signatures
Pulsations and MP surface waves	Dayside	Correlation with southward IMF
Ionospheric signatures	Dayside, high-latitude ionosphere	Convection; FACs; $\underline{E}$; particle dispersions; .....
3. Steady reconnection:		
Importance	Dayside	Flow and field behaviour at the MP
Energy conversion modes	"	Plasma acceleration (deceleration); thermal heating; plasma waves
Diffusion region	Subsolar regions; cusps (?)	Mixed FTEs; large-amplitude plasma waves
Energetic particle behaviour	Dayside	Ion and electron streaming; trapped distributions
Northward IMF	High-latitude MP	Sunward flows; FTEs
Relationship with FTEs	Dayside	Simultaneous FTE and steady reconnection observations
Theory	Earth's magnetosphere	--

(a): principal region(s) of interest
(b): some signatures to look for and investigate

Low-latitude boundary layer (LLBL). ISEE data reveal that the LLBL often appears in the form of isolated, relatively sharp-edged pulses when the exterior magnetic field has a southward component (e.g., Paschmann et al., 1978, 1982; Sckopke et al., 1981). Such boundary layer pulses are often accompanied by magnetospheric FTE magnetic signatures (e.g., Figures 3.11 and 3.12) which suggests that they are in general associated with reconnection, albeit on short space and time scales. However, this conclusion is based on a limited number of case event studies. A more general survey of high resolution ISEE plasma and magnetic field data is required in order to substantiate this conclusion. The quasi-steady reconnection events and FTE observations imply that at least part of LLBL is located on open field lines, but not all observations are immediately amenable to an interpretation in terms of open field lines. In Chapter 5 we have seen examples which show that there is not an exact one-to-one correspondence between FTEs and boundary layer pulses. Figure 3.11 shows an example where a boundary layer pulse extends outside the region of the FTE magnetic signature (2:55 UT). Figure 2.7 shows the presence of a halo region on the edges of a series of boundary layer pulses, with properties different from the pulses (Sckopke et al., 1981). We need to know how typical such observations are, and whether they result, e.g., from plasma diffusing onto closed field lines from the edges of the open field line region as a result of scattering processes associated with plasma waves inside FTEs, or whether the open field line region is more prevalent/broader than the FTE magnetic signatures seem to imply.

A cursory examination of low time resolution plasma data plots and simultaneous magnetic field data gives the impression that the nature of the boundary layer changes when the IMF is northward. Figure 7.1 shows an example of a pass for which the magnetic field has a small rotation angle at the magnetopause. The top panels containing plasma data show the proton (N_p) and electron (N_E: dots) densities, the plasma bulk flow speed V_p, azimuthal angle of the plasma flow ϕ_p, and plasma (P) and magnetic field (B: step-like trace) pressures. A 1-hour plot of magnetic field data is shown below the plasma data. The magnetopause is crossed at $\sim$ 3:20 UT. Examination of Figure 7.1 shows that there are no obvious reconnection signatures: there are no accelerated flows and/or FTE signatures. However, the plasma data do show that there is boundary layer present inside the magnetopause. This observation is in agreement with, e.g., the HEOS 2 results (Haerendel et al., 1978),



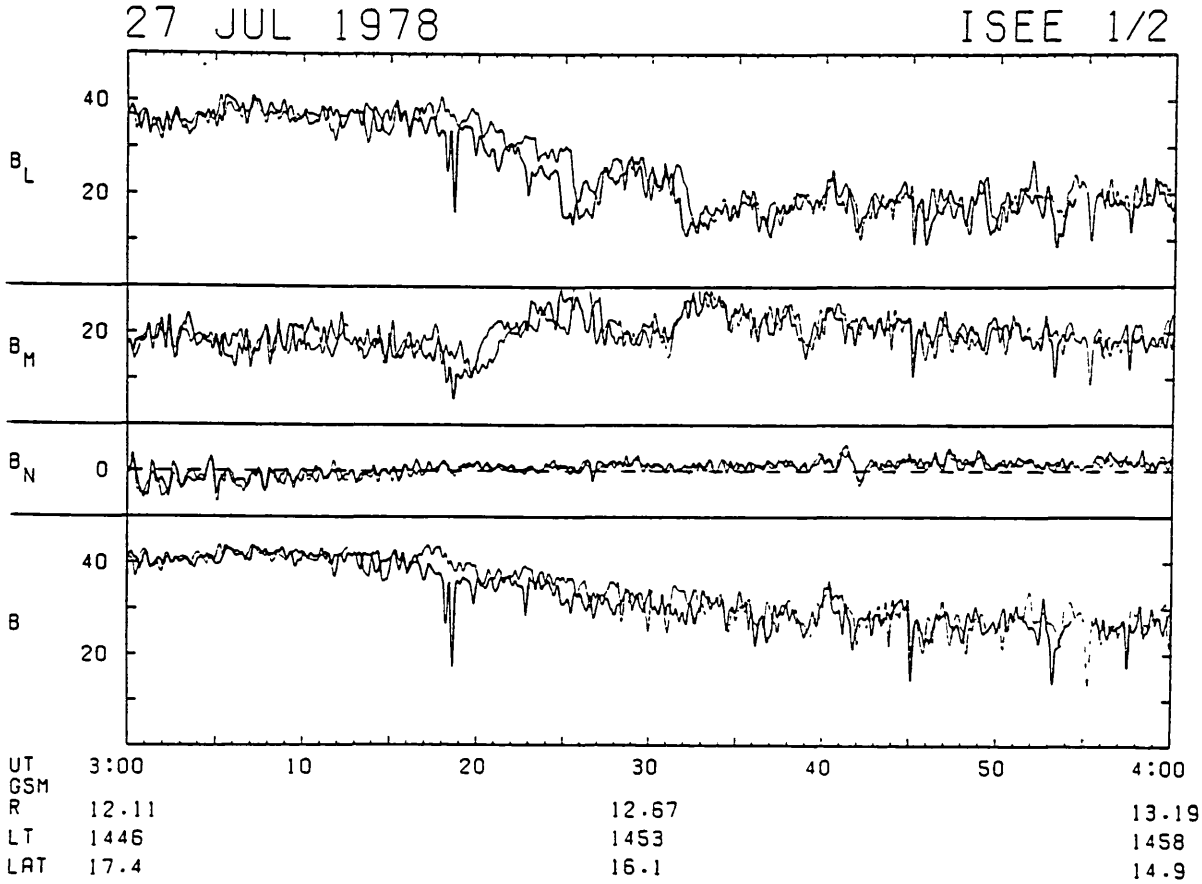


Fig. 7.1. Plasma and field data on 27 July 1978.

which also show that there is boundary layer present during periods of northward IMF. It seems likely that the process(es) giving rise to the boundary layer in Figure 7.1 are different from those which result in the boundary layer pulses of, e.g., Figure 3.11. High-resolution data sets from satellite missions such as ISEE and AMPTE need to be scrutinized in order to determine what these processes are. It has, for example, been suggested that the entry layer may provide a source region of plasma for the LLBL. Local diffusive transport may also play a major role in the formation of the LLBL, especially when conditions are not favourable for subsolar reconnection, i.e., strongly northward IMF (e.g., Eastman et al., 1976).

Recently, the ISEE and PROGNOZ 7 satellites have given us important information concerning the ion composition of the LLBL (e.g., Peterson et al., 1982; Hultqvist, 1982; Lundin et al., 1984). Such studies are important in that heavy ions can be used as tracers which enable us to determine the source regions for the boundary layer as well as the transport and energisation processes of plasma within the magnetosphere. The composition studies are still limited and need to be extended. The AMPTE mission should provide us with a good opportunity to do this. One specific question which needs to be addressed is whether the "magnetosheath injection regions" referred to by Lundin et al. (1984) and Lundin (1984) bear any relation to magnetospheric FTEs.

Electron distribution measurements provide another means of determining the processes giving rise to the LLBL. Such studies (e.g., Rodgers et al., 1984; Ogilvie et al., 1984) are still in their infancy and definitely need to be followed up. A final point worth mentioning is that the opportunity exists to combine satellite observations from the boundary layer with those from low altitudes (e.g., Dynamics Explorer) or from the magnetosheath. For example, GEOS 2 or SCATHA can be used to observe the boundary layer (at time of high magnetic activity) while ISEE 1 and 2 can be used to monitor conditions external to the magnetopause, and thus the response of the boundary layer to a change in external conditions can be determined. It may also be possible in future to combine simultaneous observations from the ISEE and AMPTE satellites to determine the structure of the LLBL on different portions of the magnetopause.

The flank boundary layer (flank BL). In the past most boundary layer

observations on the flanks of the magnetosphere have been interpreted in terms of closed flux tube transport (e.g., Eastman and Hones, 1979). Hones (1983) has made a preliminary investigation of the dawn and dusk flank BL regions using ISEE 1 and 2 data, but not at the full time resolution available. He reports an asymmetry in the properties of the dawn and dusk flank BL which he suggests may be a permanent feature, or result from seasonal effects and/or different latitudinal coverage of the regions. Reverse draping signatures in the magnetic field (Hones et al., 1982), suggestive of high-latitude plasma entry, seem confined to the dawn flank BL and are found here more often than enhanced draping signatures, which are appropriate for low-latitude entry processes (Cowley et al., 1983). The Hones (1983) study needs to be pursued with data at a higher time resolution in order to clarify these observations.

The Mozer (1984) results show that even if it is assumed that the entire flank BL is on closed field lines, closed flux tube transport process(es) contribute very little to the total cross-magnetosphere voltage. However, the flank BL need not be entirely on closed field lines. ISEE observations suggest that open flux tubes may also be transported along the near-Earth flanks. Figure 4.7 shows that FTEs occur during ISEE passes of the magnetospheric flanks. Figure 7.2 shows a plasma data plot and two successive hourly intervals of magnetic field data obtained during an outbound pass on the dawn flank on 10 January 1978. The magnetopause is crossed close to the GSM equator at $\sim$ 1:38 UT, and other partial crossings occur subsequently. Examination of this figure reveals the occurrence of FTEs as well as accelerated flows at the magnetopause crossings. These observations seem to imply that part of the flank BL is on open field lines, at least some of the time. It remains to be determined whether the observations in Figure 7.2 represent isolated examples or not and whether reconnection is a subsolar phenomenon or whether the reconnection site extends along the flanks as well. It would also be of interest to see if any FTEs occur during the passes reported by Mozer (1984).

Figures 7.3 and 7.4 show that the flank BL can also be observed if the field external to the magnetopause is strongly northward. Figure 7.3 shows a plasma data plot and a 1-hour plot of magnetic field data from an outbound pass on 17 January 1978. The magnetopause region is crossed on the dawn flank and at a northerly GSM latitude of $\sim$ 20°.

The plasma data show that there is boundary layer present, but it is difficult to tell from Figure 7.3 when precisely the ISEE satellites cross the magnetopause. The pulsed appearance of the boundary layer may result partly from the magnetopause flapping back and forth across the satellites. It is difficult to tell on the time-scale of the plasma data, but the boundary layer pulses probably correspond to the positive deflections in the B_M field component, i.e., these are more examples of reverse draping of field lines in the boundary layer (Hones, 1983). Note that many of the positive B_M pulses are associated with large-amplitude B_N perturbations, somewhat reminiscent of FTEs. However, it is unclear whether the pulses are related to FTEs.
Figure 7.4 shows data during an inbound pass on 26 July 1978. The magnetopause is crossed on the dusk flank and south of the GSM equator at $\sim$ 9:40 UT. Prior to 9:40 UT, presumably outside the magnetopause, the B_N component oscillates quasi-periodically with an amplitude of $\lesssim$ 5 nT, while after 9:40 UT the perturbations die away rather abruptly. The B_N oscillations start at 8:18 UT (not shown), coincident with the first observations of density and temperature levels intermediate to those observed in the magnetosheath and magnetosphere proper.

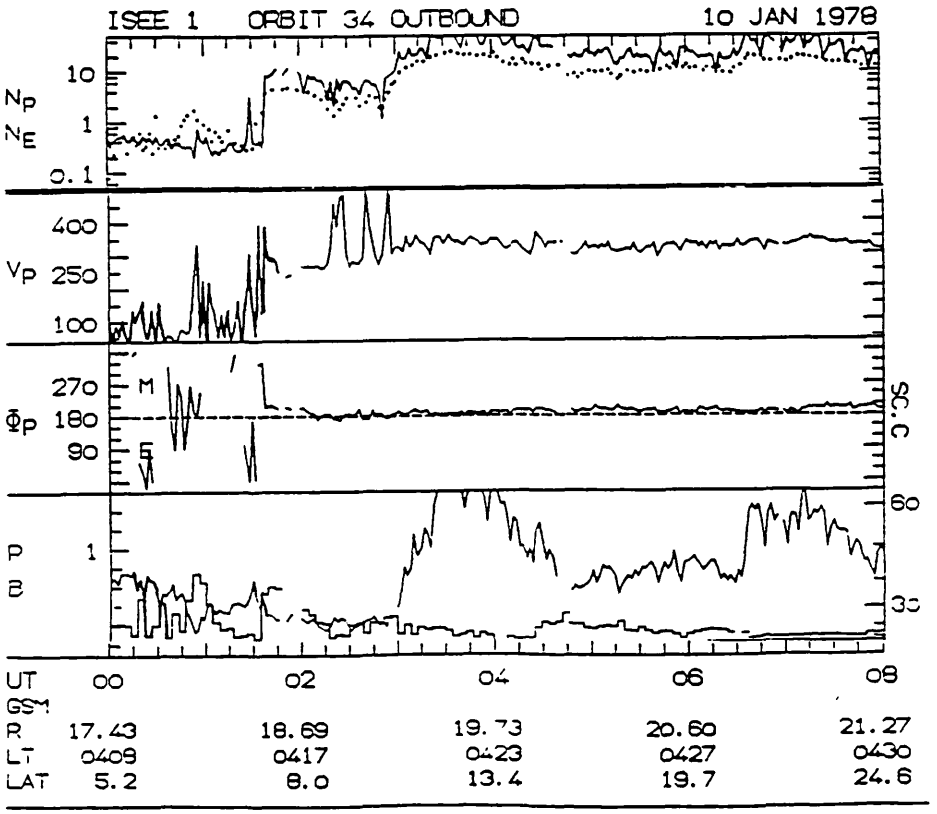


Fig. 7.2(a). Plasma data on 10 January 1978.

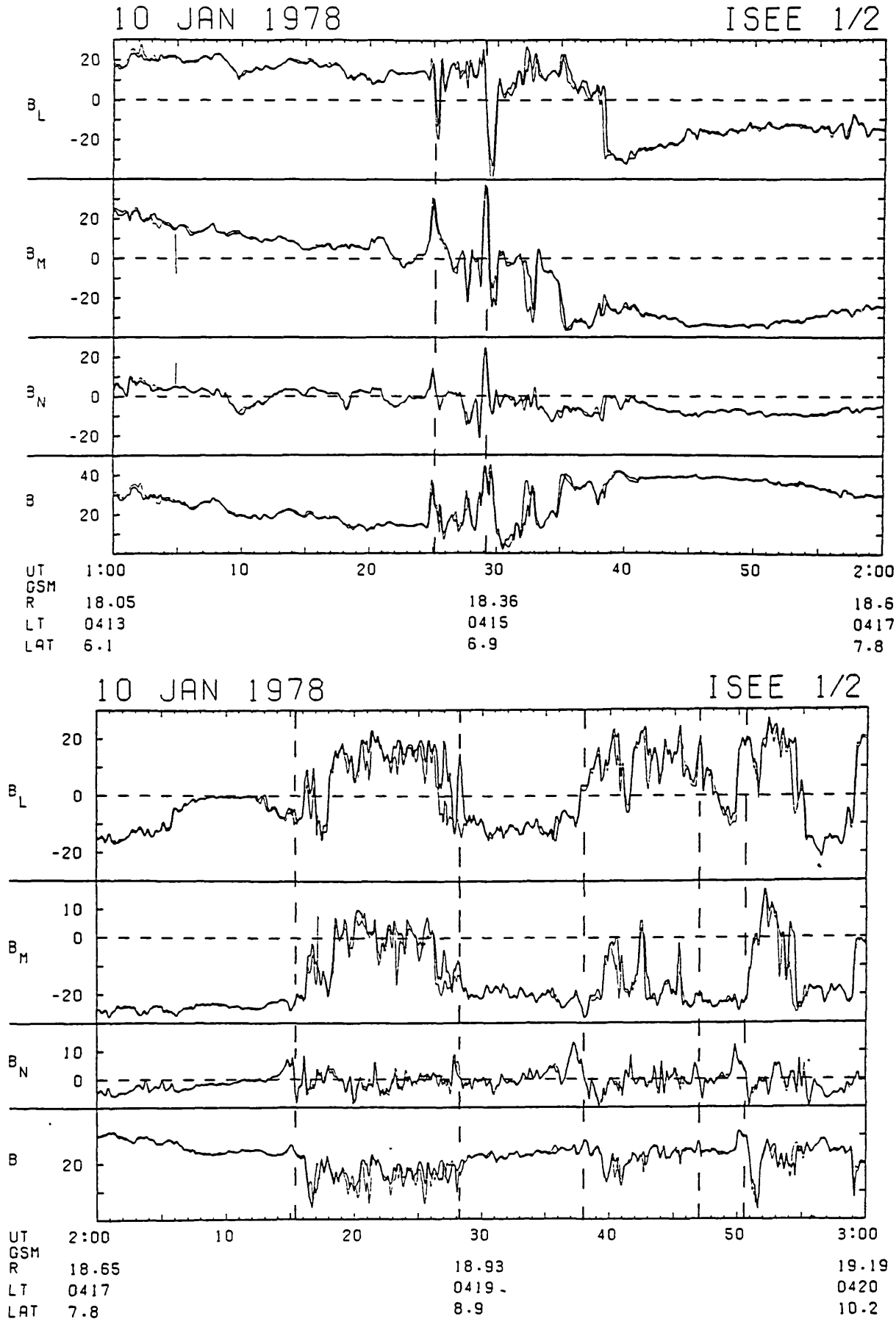
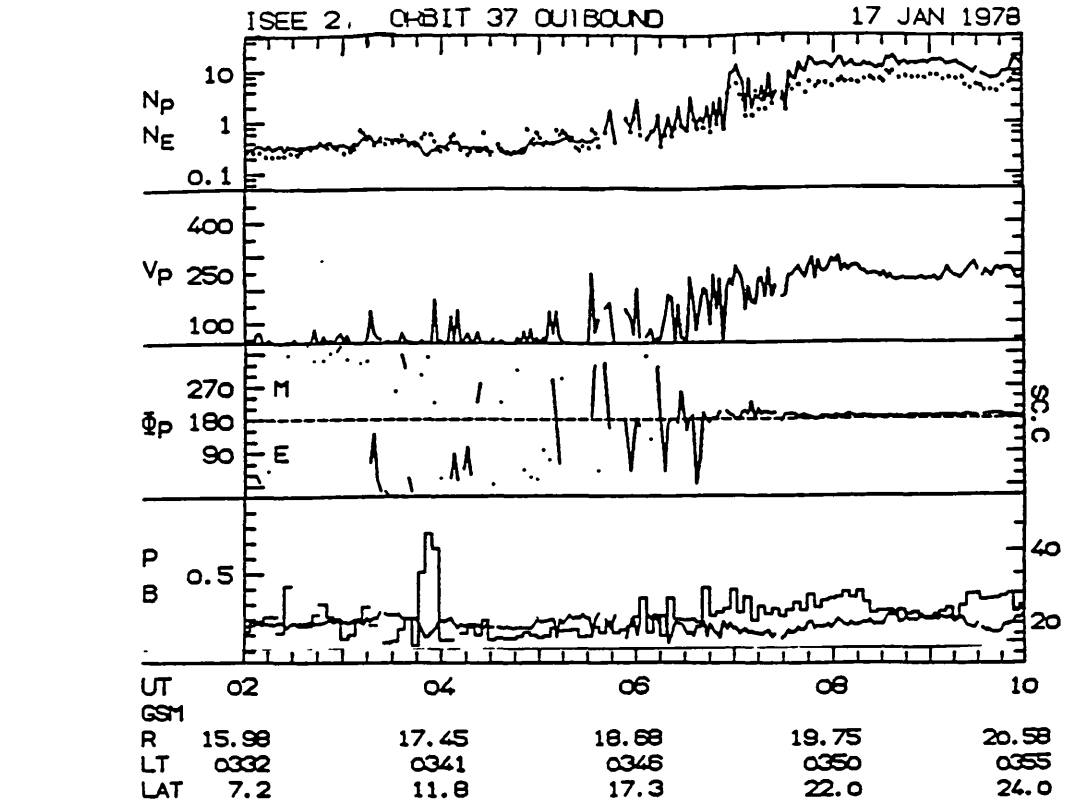


Fig. 7.2(b). Field data on 10 January 1978.



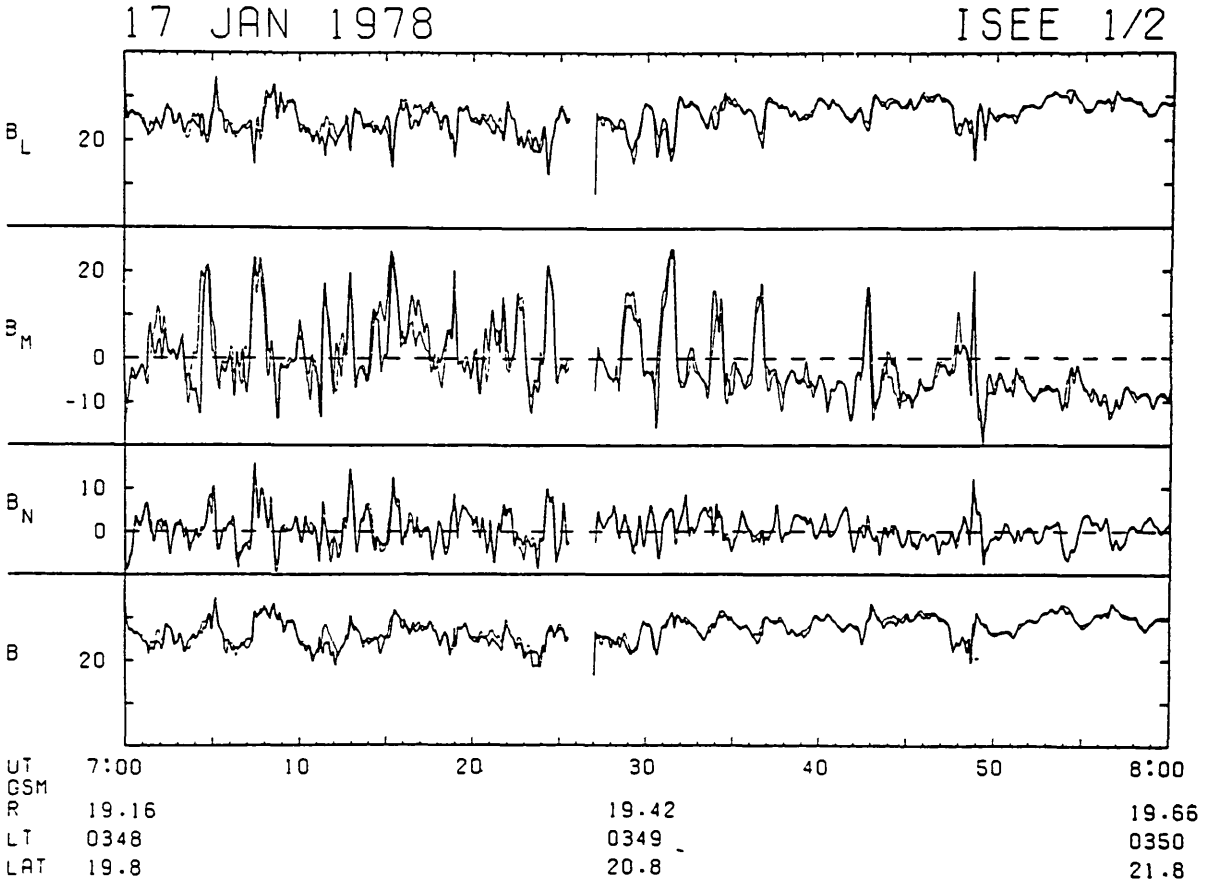


Fig. 7.3. Plasma and field data on 17 January 1978.

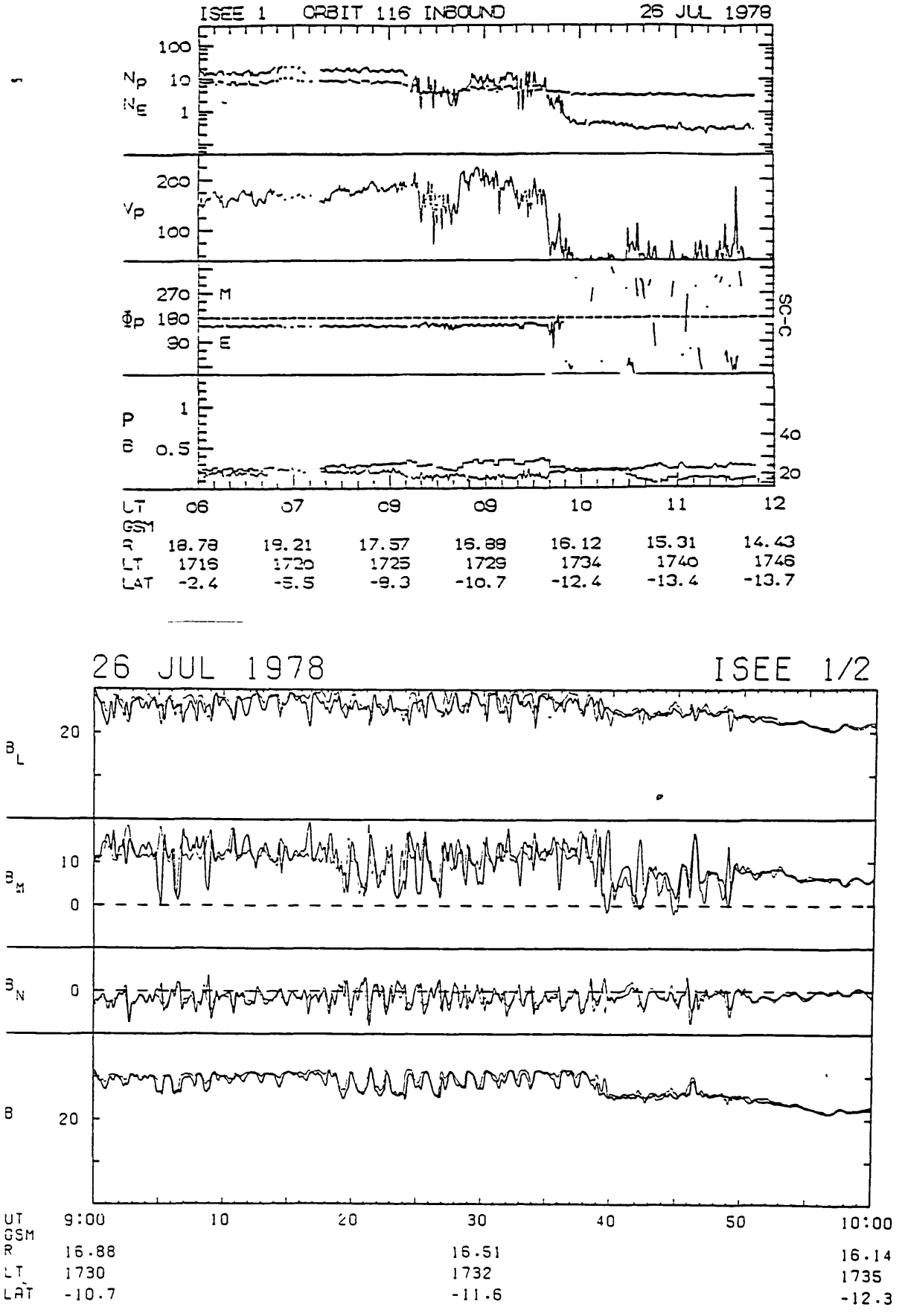


Fig. 7.4. Plasma and field data on 26 July 1978.

High-resolution ISEE data should provide the opportunity to gain some insight into the process(es) responsible for the observations in Figures 7.3 and 7.4, and it is clear from these figures that the flank regions are certainly not devoid of interest, even when the IMF is strongly northward.

The cusp and entry layer (EL). Past observations, notably from HEOS 2, suggest that the EL region is not simply an extension of the LLBL, and that high-latitude entry processes may play an important role in its formation and in generating ionospheric FACs (e.g., Paschmann et al., 1976; Haerendel et al., 1978). It is unfortunate that a detailed investigation of this region is hampered by the low temporal resolution of the HEOS 2 plasma data. However, the HEOS 2 magnetic field data have a much higher time resolution, but up to now these data have not been exploited as fully as they should have been. IMP 6 data (Fairfield and Hones, 1978) show that the scope of investigation can be increased with the aid of higher resolution plasma instrumentation. It is interesting to note, therefore, that the ISEE orbit does occasionally pass through the cusp region, both on the dayside and on the nightside (e.g., Formisano, 1982). Figure 4.1 shows that most ISEE magnetopause crossings occur at low latitudes. However, during the survey described in Chapter 4 a number of passes were found which contained field orientations inside the magnetopause indicative of (close) encounters with the dayside cusp region. Figure 7.5 shows one such example. This Figure shows two successive 1-hour intervals of magnetic field data obtained during an outward bound pass on 30 October 1978. The ISEE 1 and 2 separation at this time is approximately 7724 km along the boundary normal with ISEE 2 leading. Note that the magnetospheric B_L component is strongly negative, which, in combination with the relatively high latitude ($\sim 39°$), suggests that ISEE 1 and 2 are located within the northern cusp region. The large negative B_M component in the magnetosphere is consistent with the dawnward satellite location. The B_M component in the magnetosheath is positive, although the IMF data book (King, 1983) shows that IMF B_y changes sign and goes positive between 16:00 and 17:00 UT. Thus we may infer that the change in sign of B_M at 16:52 UT (ISEE 2 data) probably does not represent a magnetopause crossing. However, the B_M sign-changes near $\sim$ 15:50, 16:02 (ISEE 2) and 16:19 UT (ISEE 1) do represent magnetopause crossings. It is interesting to note, therefore, that large B_N perturbations occur,

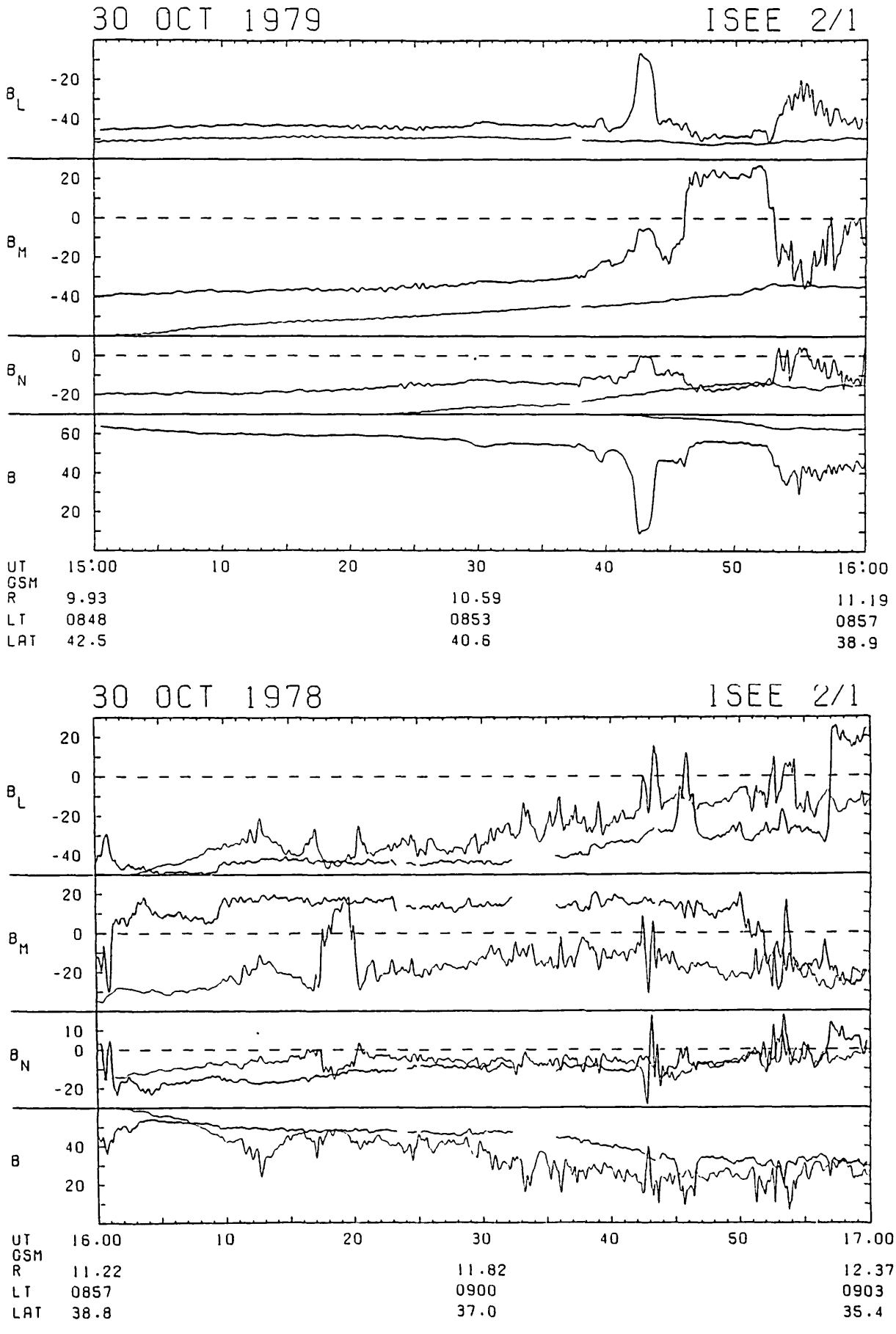


Fig. 7.5. Magnetic field data on 30 October 1979.

notably at 16:43 UT. Examining passes such as these in conjunction with the plasma data could lead to interesting results. Such passes can also provide useful comparisons with the HEOS 2 data, in order to gauge the adequacy of HEOS 2 data in investigating this region.

An important aspect of the dayside cusp regions is that field lines in these regions connect through the LLBL. These field lines form a path along which the outer magnetosphere and ionosphere can exchange ions and electrons directly. It is interesting to note then that recently evidence for such a process has been found in the electron data from the LLBL. Ogilvie et al. (1984) report observing beams of electrons (with E $\sim$ 100 eV) which sometimes form an important component in the LLBL and whose properties are similar to beams of electrons in the cusp region (e.g., Burch et al., 1983). Such observations are important in that it has been sgugested that these electron beams along cusp field lines give rise to the high-latitude FAC regions. Future ion composition data from PROGNOZ 7 in the cusp region should also help clarify the role of the ionosphere/outer magnetosphere exchange processes.

The plasma mantle (PM). The PM arouses least controversy regarding its source processes, the generally accepted view being that it is formed by the tailward convection of plasma on open field lines. The two satellites which have contributed most in elucidating the near-Earth PM properties are HEOS 2 (e.g., Rosenbauer et al., 1975) and PROGNOZ 7 (e.g., Lundin et al., 1982). Again, however, there still remain many unresolved questions. It is unfortunate that the plasma data obtained and presented from the PM so far do not have the high time resolution we are used to from ISEE. Even so, existing data sets have not been fully analysed yet: the HEOS 2 and PROGNOZ 7 data still have a lot to offer.

We do not know enough about the location(s) of entry of the PM plasma into the magnetosphere. Observations of density gaps at the magnetopause (Rosenbauer et al., 1975) seem to indicate that locally at least the magnetopause does not allow significant penetration of magnetosheath plasma into the PM. Also, composition experiments (e.g., Hultqvist, 1982) indicate that the magnetopause forms a solid boundary to the ionospheric component in the PM. It therefore appears that at times at least there is no transport of plasma across the tail magnetopause, and hence that the magnetosheath PM component enters the magnetosphere on the dayside. We also need to investigate when, where and how the ionospheric plasma component is injected into the PM and

what its relative contribution is to the total population there. The so-called magnetosheath-like intrusions reported by Lundin et al. (1982) provide another topic for future investigation. It may be that they are related to the FTE signatures observed by ISEE on the dayside. Finally, ISEE 3 and IMP 8 data could be used to explore the properties of the boundary layer region at distances further down-tail.

7.2.2 Flux transfer events (again)

Our understanding of FTEs has progressed significantly ever since their initial discovery by Russell and Elphic (1978). Many questions still remain, however.

Plasma signatures and source region. Published surveys of FTEs have been based mainly on their magnetic field characteristics (Chapter 4). There is a need for a similar large survey to be done using the high-resolution ISEE plasma data, perhaps along the lines described by Paschmann et al. (1982) and in section 5.2. One pay-off of such a study could be that it leads to a greater understanding of the origin of the boundary layer, as we discussed previously. It could also help clarify what the extent and orientation of the reconnection line is along which FTEs are created. Daly et al. (1984) have already used the ISEE 2 energetic particle instrument (Williams et al., 1978) to investigate this question. They used the direction of energetic ion streaming to infer the hemisphere connection of magnetosheath FTEs. Although partial failure of the particle instrument as of 1979 necessarily limited the magnetopause coverage of this survey, the results show general agreement with an equatorial source region for FTEs, with perhaps a tilt of the reconnection line in response to IMF B_y in a manner similar to that observed for the quasi-steady reconnection events (Figures 1.7 and 5.1). This is in agreement with results based on the polarity of FTE B_N signature (sections 4.3 and 4.4). However, individual cases of FTEs resulting from reconnection at high latitudes, as suggested, e.g., by Haerendel et al. (1978), cannot be completely ruled out. A different interpretation based on the Berchem and Russell (1984) observations has been given by Russell et al. (1984). They suggest that the FTE source region is located in a small region (of $\sim$ 4 R_E radial extent) which is centred on the subsolar point, and that the IMF orientation exerts a strong control on where the FTE signatures are subsequently observed. It is important to continue the

type of investigation initiated by Daly et al. (1984) in order to decide between the above alternatives. In future investigations it may be possible to determine the hemisphere connection of FTEs with means other than those used by Daly et al. (1984). The ISEE 1 energetic particle instrument (Williams et al., 1978) could be used to determine ion anisotropies in a similar way to the ISEE 2 instrument. Another alternative is to use the ISEE 1 electron plasma spectrometer (Ogilvie et al., 1978). Scudder et al. (1984) report that many FTEs are accompanied by a heat flux layer. The direction of the heat flow can be used to determine which hemisphere an FTE is connected to. Finally, the AMPTE mission promises to provide coverage of dayside magnetopause regions not readily accessible to ISEE, such as the southern dawn sector.

3-D structure. Simple modelling of data has given us some insight into the magnetic field structure of FTEs (Speiser et al., 1981; Paschmann et al., 1982). The existence of FACs, the presence of which are implied by the continuous nature of FTE B_N signatures, have now been confirmed directly using the dual-satellite capability of ISEE (Saunders et al., 1984a,b). Clearly, however, further work needs to be done to establish the full 3-D structure of FTEs. It would also be of interest to know whether the results of Paschmann et al. (1982, Figure 8) are generally valid, in particular for the FTEs which are accompanied by significant field strength decreases (e.g., Figure 4.5). Saunders et al. (1984a) have shown that the plasma and field data for a few FTEs can be described in terms of a propagating Alfvén wave (the Walén relation): does this result hold for other FTEs as well? Also, we need to know what the contributions of internal FACs and external draping effects are to the observed FTE B_N signatures. Such knowledge may affect the way in which we interpret FTE B_N signatures (e.g., Daly et al., 1984; Saunders et al., 1984a,b; Rijnbeek and Cowley, 1984). It is also important to know what determines the direction of FACs associated with FTEs, in order to investigate the relation between FTEs and the large-scale FAC regions observed in the dayside high-latitude ionosphere. Most importantly, however, it is not yet fully resolved how the FTE FACs originate in the first place. Such studies are best suited to times when the ISEE 1 and 2 satellites were far apart ($\lesssim$ 1000 km) in view of the large spatial scale of the prominent FTE signatures ($\sim$ 1 R_E). At large separations we may also perhaps be

fortunate enough to witness ISEE 1 and 2 cross different arms of the same FTE flux tube, one in the magnetosheath and one in the magnetosphere. Investigation of events such as those described in section 3.3.6 may lead ultimately to the identification of such an occurrence. The CLUSTER mission, which is part of the ISTP programme (due for implementation in the 1990s), could potentially provide a snapshot of an FTE flux tube in four different places and should therefore enable us to work out the geometry of the flux tube in much greater detail.

Evolution of FTE signature. The evolution of the FTE signature (in both space and time) as the open flux tube travels across the dayside magnetopause into the tail cannot be fully determined with the ISEE data because of limited magnetopause coverage. However, (re-)examination of data sets from other satellites can be used to extend the coverage to higher latitudes to include the cusp and mantle regions. Possible data sets include those from HEOS 2, IMP 6,8 and PROGNOZ 7. HEOS 2 magnetic field data are still easily accessible at Imperial College and merely require conversion into boundary normal coordinates. One problem which we have noted previously with the HEOS 2 data (Figure 6.2) is that the usual time resolution of data points every 32 secs is not always sufficient to fully resolve FTE signatures. However, this problem need not be insurmountable since field data are available at a higher rate ($\lesssim$ 6 secs resolution) during certain stages of the HEOS 2 mission. These data have not yet been exploited. As a foretaste, Figures 7.6 and 7.7 show two examples of high-latitude, outbound HEOS 2 passes, using 32 sec resolution data. Figure 7.6 shows a 1-hour plot of data obtained on 1 October 1972. There is an FTE-like signature which occurs at 21:56 UT inside the main magnetopause crossing at 22:05 UT. Note, however, that the main deflections in B_L and B_M line up with the positive peak in B_N, rather than halfway during the downstroke of the B_N signature. This may have something to do with the low time resolution of the data. Figure 7.7 shows HEOS 2 data from 1 and 2 November 1972. After an initial magnetopause encounter at 23:33 UT, HEOS 2 makes several other entries into the boundary layer. The interesting features to note are the brief ($\sim$ 1-2 min) but large-amplitude positive excursions in the B_L component at the magnetopause crossings, such that the field points mainly sunward. Also, some of these features are accompanied by large B_N perturbations (e.g., 1:00 UT). Perhaps these features can be explained in terms of open field lines

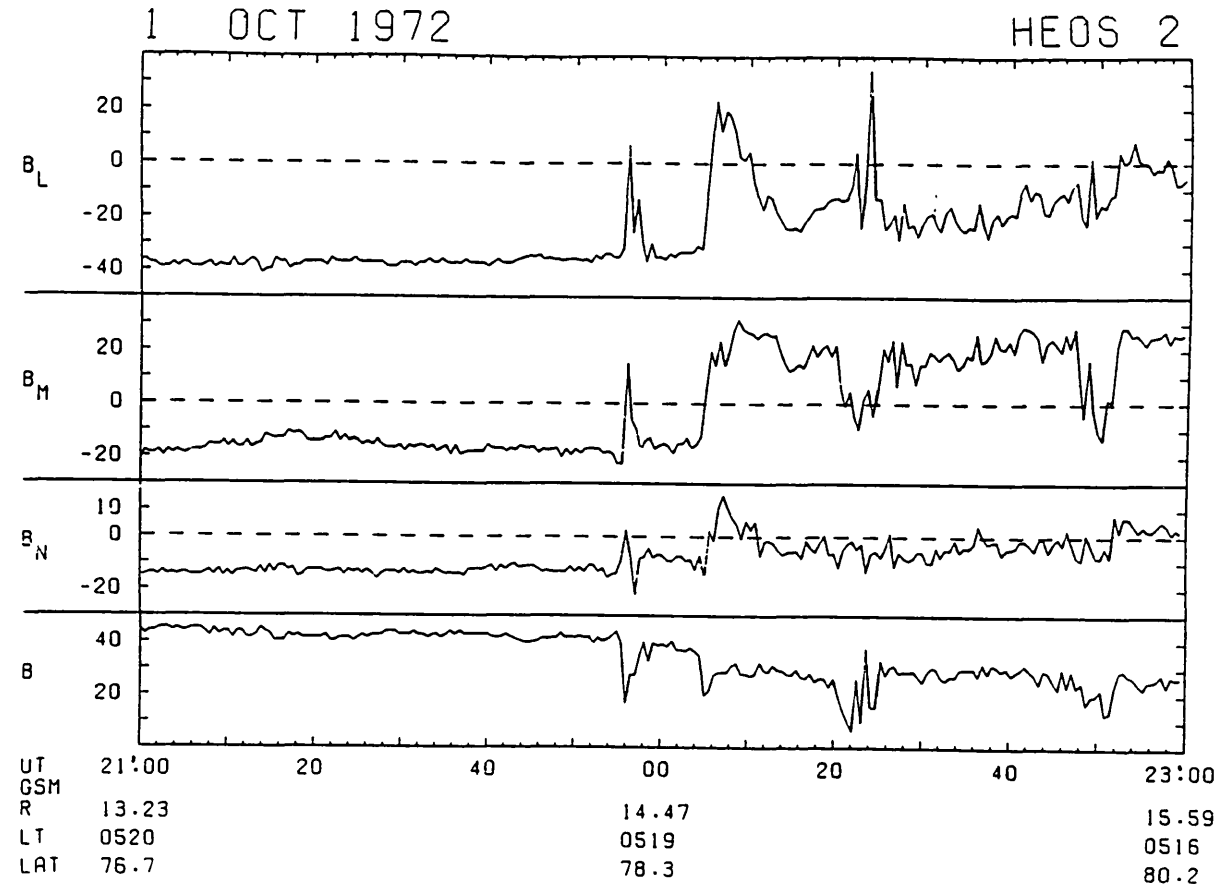


Fig. 7.6. HEOS 2 field data on 1 October 1972.

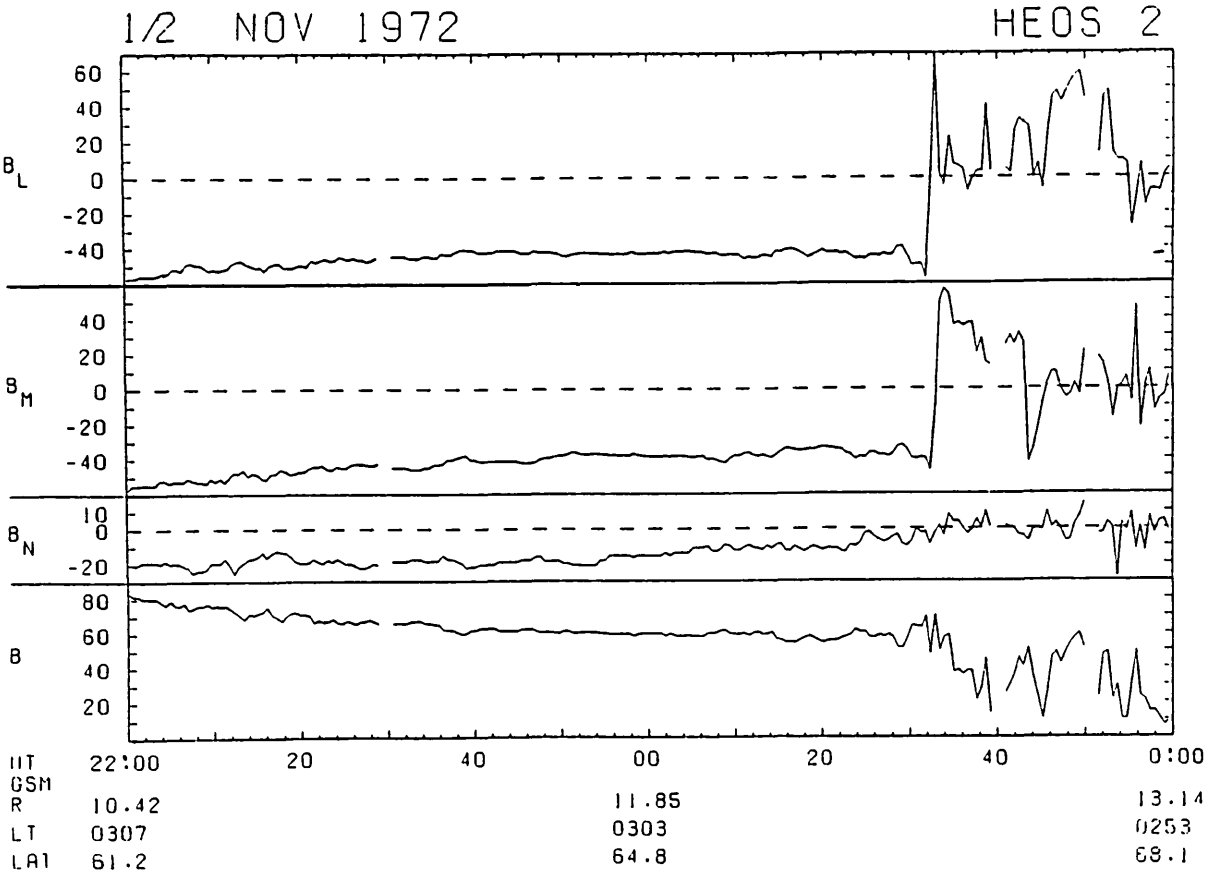


Fig. 7.7(a). HEOS 2 field data on 1 November 1972.

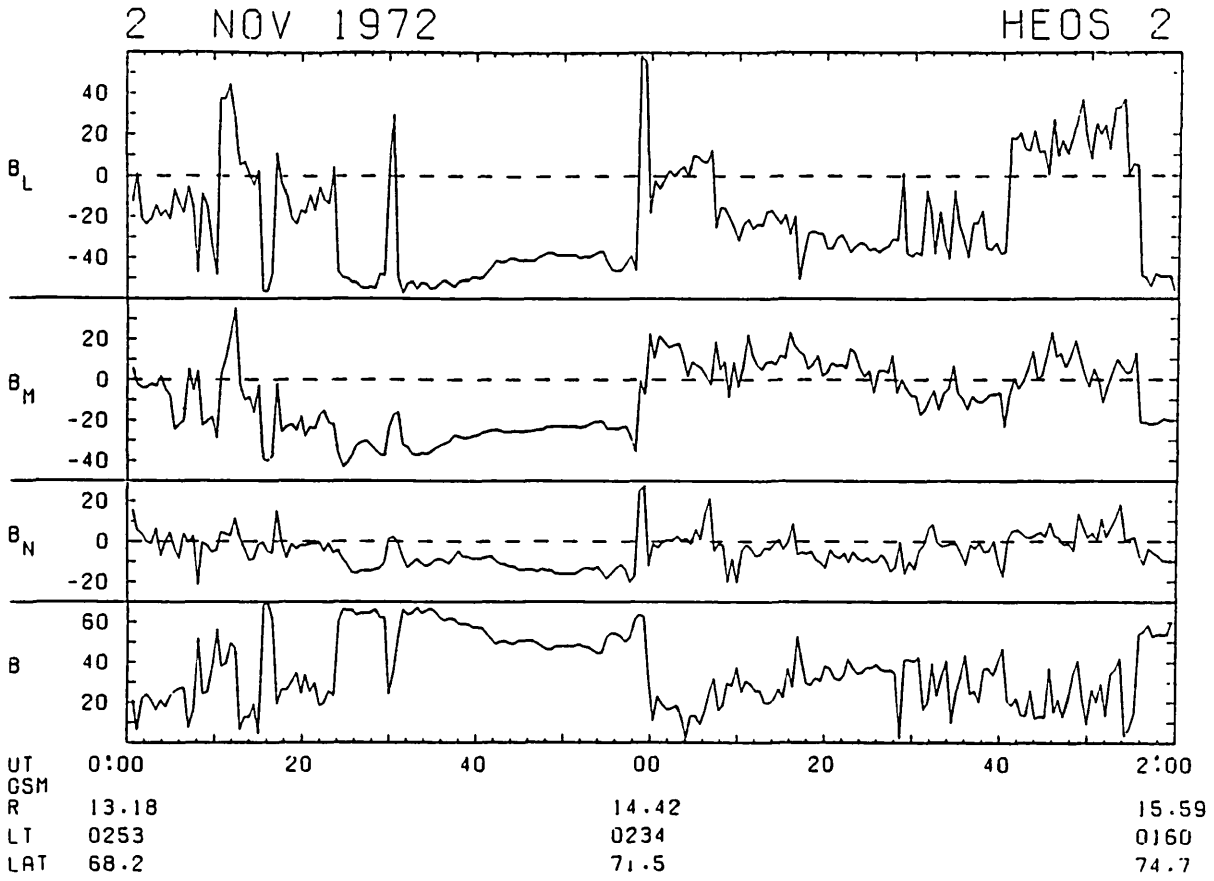


Fig. 7.7(b). HEOS 2 field data on 2 November 1972.

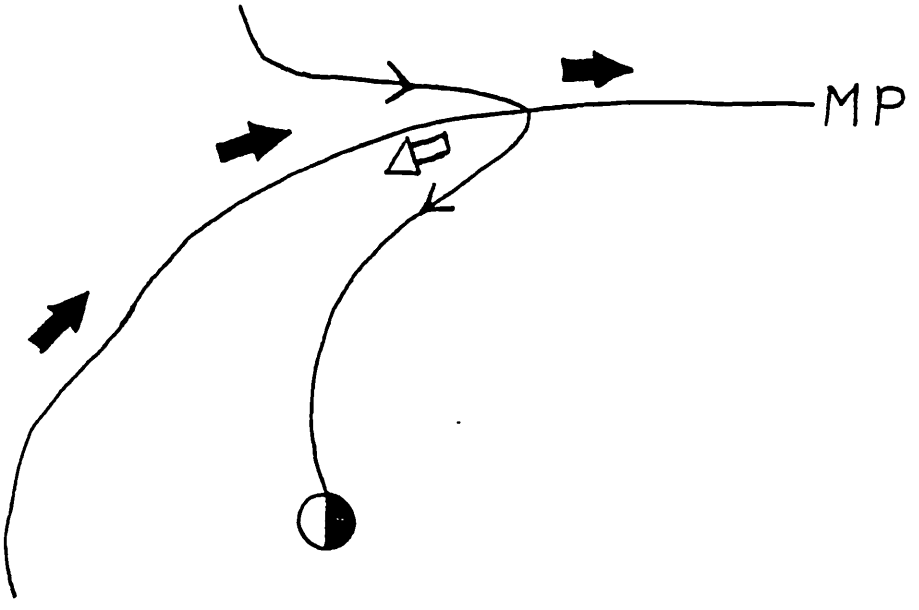


Fig. 7.8. Possible interpretation for Figs. 7.7 (a) and (b).

draping along the magnetopause and lying anti-parallel to the magnetospheric field lines as drawn in Figure 7.8. In this situation the magnetic tension acts against the ambient magnetosheath flow, so that we may expect to observe plasma flow speed decreases.

Spectrum of FTEs. The more prominent FTE signatures, which satisfy the identification criteria described in section 4.2, have a scale size of order 1 R_E, as shown by Saunders et al. (1984a,b). However, it seems likely that FTEs occur with signatures below the B_N amplitude and duration cut-offs we assigned somewhat arbitrarily. The full spectrum of FTE signatures is something that is yet to be established. If the FTE phenomenon occurs on spatial and temporal scales which are smaller than we have considered, then we should expect the signature for such a process to be observable closer to the magnetopause and with shorter ($\lesssim$ 1 min) duration. It is therefore interesting to note that short time-scale, small-amplitude B_N perturbations can often be observed close to the magnetopause when the external field has a southward component. Often such features occur in close association with B_L spikes (discussed in Chapter 5). To determine whether such observations represent small-scale FTEs requires the use of high time resolution data sets, and this topic is well suited for investigation as part of the AMPTE mission.

Pulsations. Another topic for future investigation is the possible relationship between FTEs and magnetic pulsations. The propagation of FTE open flux tubes along the magnetopause surface causes the boundary to oscillate. Thus FTEs provide a plausible alternative to the Kelvin-Helmholtz instability as a generator of magnetopause surface waves. The magnetopause oscillation in turn provides a mechanism for generating magnetic pulsations deeper in the magnetosphere. If FTEs rather than Kelvin-Helmholtz instability are more important in producing magnetopause surface waves and magnetic pulsations, then both boundary oscillations ($\lesssim$ few min) and pulsations should show a strong correlation with a southward IMF/magnetosheath field component. This correlation needs to be tested for. An example of observations of magnetic pulsations is shown in Figure 7.9. This figure shows two successive 1-hour plots of magnetic field data inside the magnetosphere taken from an inbound pass on 31 July 1978. These plots closely follow magnetospheric FTE observations (see Figure 3 in Rijnbeek et al., 1984; note the reverse FTE at 6:03 UT) and there is clear evidence that deeper in the magneto-

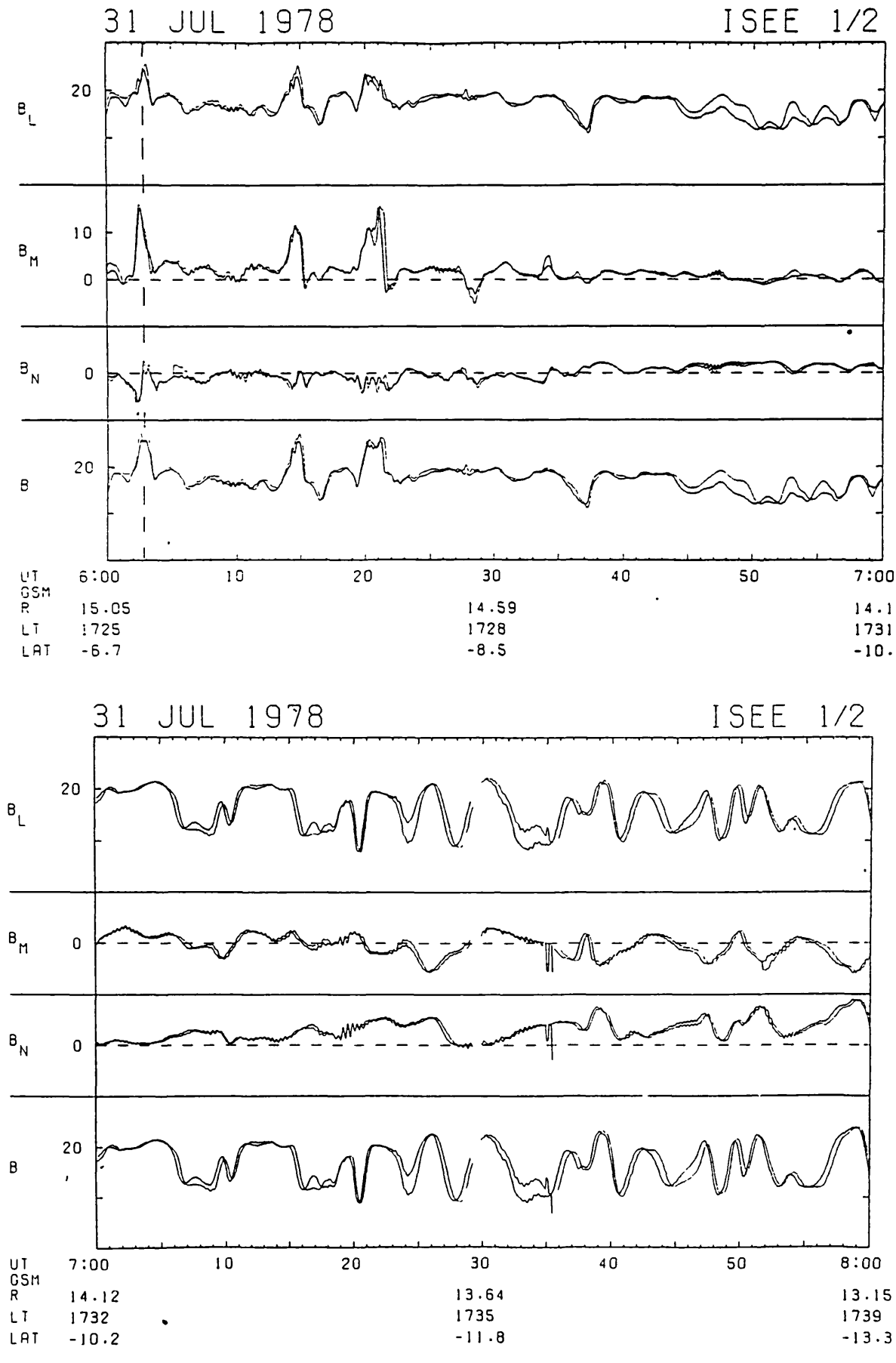
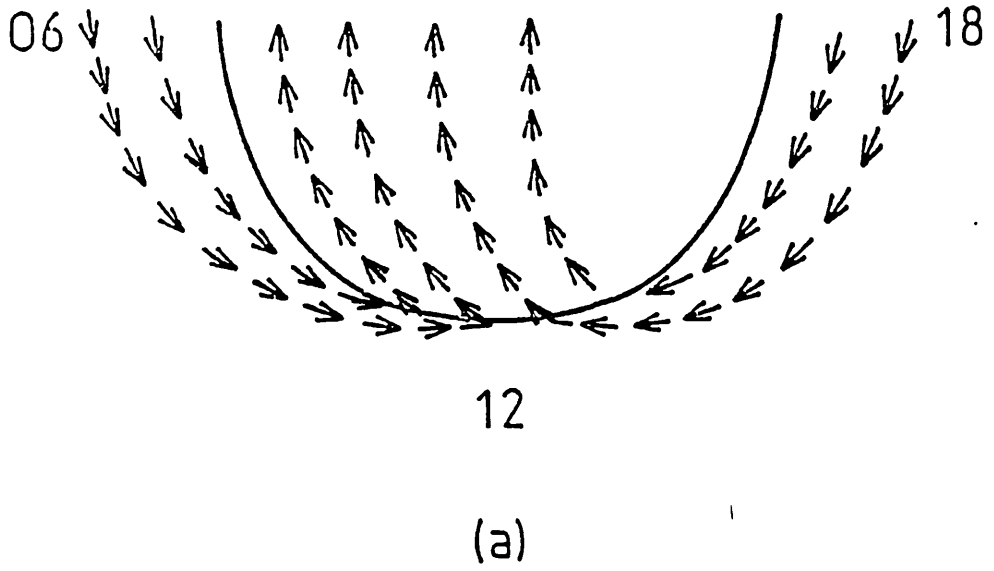


Fig. 7.9. FTE and pulsations on 31 July 1978.

sphere there occur quasi-periodic magnetic oscillations, with periods ranging from $\sim$ 5 min down to $\lesssim$ ½-min. There is a distinct possibility, which needs to be investigated, that at least some of these pulsations are related to and perhaps directly result from FTEs propagating along the magnetopause.

Ionospheric signatures. A topic which has received scant attention so far is the identification of FTE signatures at low altitudes. From the scale size and the estimated amount of magnetic flux which an FTE at the magnetopause contains (Chapter 4), we can use conservation of flux to derive a spatial scale of $\sim$ 200 km for an FTE signature in the ionosphere. The duration over which FTEs are observed gives a temporal scale of a few minutes for such signatures. Present day instrumentation is well capable of detecting ionospheric signatures on these scales. Cowley (1984) has given a description of the effects of FTEs expected in the ionosphere. Briefly, FTE signatures should be observable in the region which maps to the reconnection line, i.e., the polar cap boundary, which separates regions of open and closed field lines. Figure 7.10(a) shows the situation for steady reconnection, when there is a steady flow from the auroral zone into the polar cap across the dayside boundary. When reconnection is in the patchy, FTE-mode, restricted sections of the boundary will make equatorward jumps with the formation of each FTE. If reconnection switches off between successive FTEs, then the boundary will jump poleward again during these intervals. The net result is that the polar cap boundary will have a corrugated appearance as shown in Figure 7.10(b). The corrugations should propagate tailward and have a spatial scale of a few 100 km. Magnetopause observations show that FTEs have associated FACs and internal, vortical plasma motion (Saunders et al., 1984a,b). These features should also map to low altitudes and vortical flows may therefore be associated with the corrugations in Figure 8.10(b). (see also Southwood, 1984).

The effects of FTEs in the ionosphere can be studied in a number of possible ways. FTEs affect dayside high-latitude FACs and ionospheric currents. These in turn produce magnetic signatures which can be detected by ground magnetometer stations. FTEs also affect ionospheric electric fields and convection patterns. The STARE and EISCAT radar systems, for example, can be used to study plasma convection patterns in the high-latitude ionosphere. In fact, Van Eyken et al. (1984) have already described an ionospheric flow signature close to the



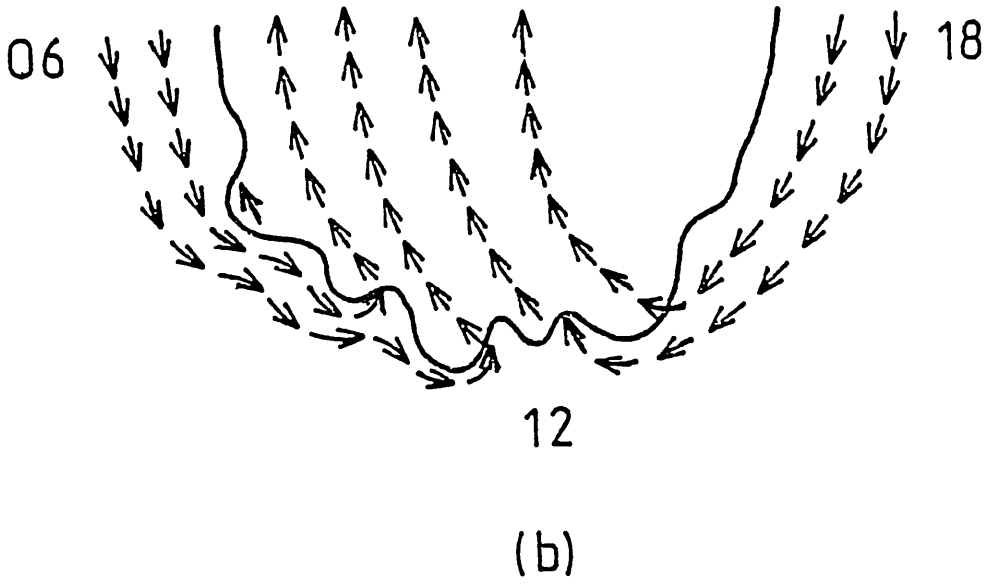


Fig. 7.10. Dayside Northern Hemisphere high-latitude flows for (a) steady reconnection, and (b) impulsive, FTE-like reconnection for positive IMF B_y (Cowley, 1984).

estimated location of the polar cap boundary which they suggest may be attributed to an FTE. Currently, solar wind data from the AMPTE mission are being combined with EISCAT data to study the response of the ionosphere to the IMF and also to identify possible FTE signatures in the polar cap region (P. R. Smith, personal communication, 1984). Low-altitude particle distributions can also be used to study FTEs. It has, for example, been suggested that dispersive ion injection events observed in the polar cusp region and reported by Torbert and Carlson (1976) are low-altitude manifestations of FTEs (Reiff, 1984). As a future project it may be possible to combine data sets from, say, ISEE 1 and 2 and Dynamics Explorer (DE; see September 1982 GRL issue) to observe FTE signatures simultaneously at the magnetopause and at low altitudes. It should be noted, however, that such comparative studies should take into account the limited local time extent of FTEs, which requires an accurate procedure to map magnetopause observations down to conjugate regions in the ionosphere.

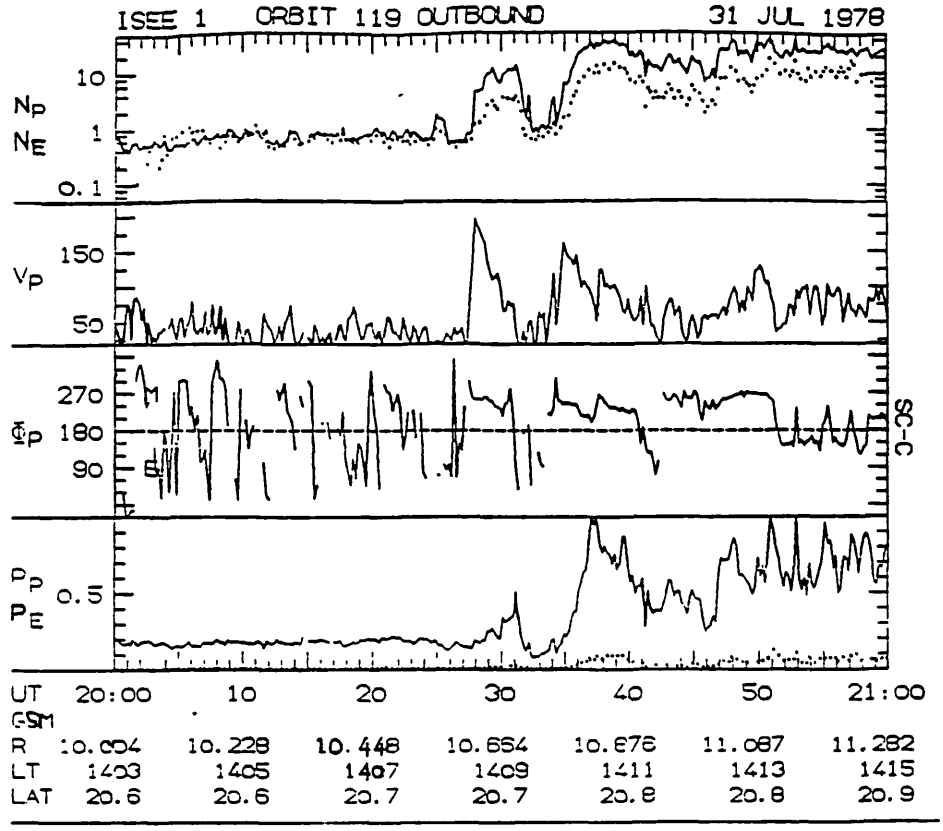
7.2.3 Quasi-steady reconnection

Importance. Thus far, 17 quasi-steady reconnection events have been identified on the basis of ISEE 1 and 2 magnetic field and 3-D Fast Plasma Analyser measurements made during 1977, 1978 and 1979 (Chapter 5). In view of the large number of ISEE magnetopause crossings during this period (e.g., Figure 4.1) this could lead to the impression that such events are a relatively rare occurrence, and hence that steady reconnection is of small significance in magnetospheric dynamics. However, there are several factors which make it more than likely that this impression is erroneous.

Steady reconnection probably occurs along a reconnection line of limited longitudinal extent. Cowley (1982), for example, suggests that steady reconnection probably occurs in a region centred on local noon which is only 2 to 4 hours wide in local time. If this is the case, then the chances of detecting steady reconnection signatures in the ISEE data are considerably reduced because of the limited number of crossings within this region. Also, Paschmann (1984) notes that most crossings occur too rapidly for them to be reliably identified as either tangential or rotational discontinuities. 3-D plasma data often have a time resolution as low as one data point every 48 sec, and the instrument is not truly 3-D since it has a limited acceptance angle

($\lesssim$ 55° out of the spin plane; see, e.g., Sonnerup et al. (1981)). A cursory scan of 2-D plasma data plots (such as Figure 7.2) often reveals brief occurrences of accelerated plasma flows at the magnetopause. These accelerated flows could well represent additional occurrence of reconnection events which cannot be identified as such because of instrumental limitations. It should also be taken into account that the selection procedure for the quasi-steady reconnection events is somewhat stringent. Observations are compared with a 2-D, time-independent model which also assumes that the plasma acceleration takes place locally (Chapter 2). In the real situation, 3-D and time-dependent effects are likely to play a significant role, as the observations of FTEs testify. In view of the limitations of the theoretical model it is therefore perhaps unrealistic to expect quantitative agreement with observational data all of the time, although qualitatively the reconnection signatures should still remain observable.

Identification of reconnection signatures at the magnetopause need not necessarily be based on the ISEE 3-D plasma data. Cowley et al. (1983) discuss the magnetic field and plasma behaviour at the magnetopause appropriate to various reconnection and diffusion models. They note that in the super-alfvénic magnetosheath regions on the flanks it is difficult to distinguish between reconnection and diffusion signatures for individual case events, although statistical studies may be able to separate them. However, in the sub-alfvénic region open field line tension effects dominate the plasma behaviour at the magnetopause in reconnection models. In certain situations (in response to IMF B_y) this can lead to reversals in the north-south and/or dawn-dusk plasma flow component at the magnetopause (e.g., Figures 3.14 and 5.4). The 2-D plasma data, which have a higher time resolution than the 3-D data (a factor of 4), are adequate to identify the latter type of signature as illustrated in Figure 7.11. This figure shows magnetic field and 2-D plasma data for a 1-hour interval during an outbound pass on 31 July 1978. The field in the magnetosheath is southward and duskward and ISEE 1 leads ISEE 2 by $\sim$ 550 km along the estimated boundary normal direction. The important point to note in this figure is that the plasma velocity is duskward in the magnetosheath (consistent with the duskward satellite location), while it is enhanced and flows dawnward at the magnetopause (e.g., at 20:30 UT). Interestingly, two standard FTEs also occur during the interval shown. The dawnward magnetopause flows



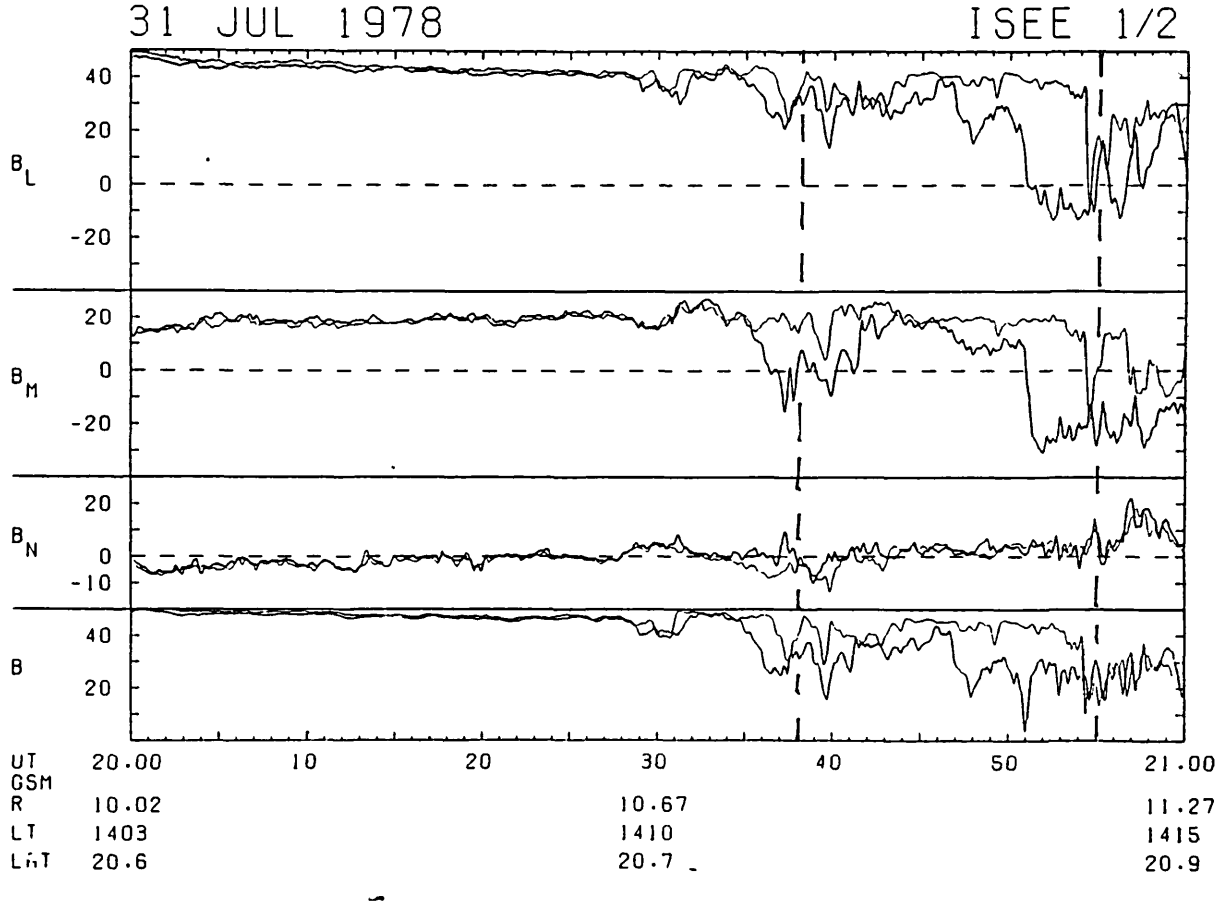


Fig. 7.11. Plasma and field data for 31 July 1978.

are consistent with ISEE 1 encountering open field lines north of the reconnection line (Figure 1.7). The field tilt in the boundary layer region is also consistent with this interpretation (Cowley et al., 1983). Yet, this pass has not been included in the list of quasi-steady reconnection events.

Figure 7.11 shows that it is possible to extend the list of reconnection events using 2-D plasma data, provided the identification procedure is relaxed somewhat. An altogether different procedure of identifying reconnection events has been developed by Aggson et al. (1983). They use ISEE 1 electric field data (Heppner et al., 1978) in conjunction with plasma flow measurements from the electron plasma instruments (Ogilvie et al., 1978) to identify quantitatively magnetopause rotational discontinuities. The electric field experiment provides data points every 3 sec, and this high resolution has led to the identification of 5 additional instances of reconnection events (Aggson et al., 1983, 1984). The list of reconnection events in Table 5.1 is therefore far from exhaustive. A final point worth noting is that the search for reconnection events should not just be confined to instances of accelerated plasma flow at the magnetopause. In certain situations open field line tension effects opposing the ambient magnetosheath plasma flow can lead to plasma flow deceleration at the magnetopause. Flow deceleration in fact occurs during the 4 December 1977 quasi-steady reconnection event (Table 5.1) and during the pass reported by Aggson et al. (1984). We should therefore consider changes in direction and magnitude of the plasma velocity when looking for reconnection signatures at the magnetopause.

Energy conversion. MHD models for steady reconnection consider bulk acceleration of magnetosheath plasma (i.e., kinetic energy) as the major sink for the energy released during the reconnection process (e.g., Levy et al., 1964). However, actual observations indicate that the electromagnetic energy released during reconnection can be dissipated in several other ways. Cowley (1980) suggests that magnetospheric ions can sometimes take up a large fraction of the energy (see also Cowley, 1982). Haerendel et al. (1978) suggest that for an intermittent reconnection process the energy may be quickly expended through local heating, mixing with unreconnected plasma, electronic heat conduction and excitation of plasma waves. The results from Rodgers et al. (1984), who report GEOS 2 electron data showing possible heating of magnetosheath

electrons in the boundary layer, might have a bearing on this question. Finally, the results from Paschmann et al. (1983) do in fact show that a significant fraction of plasma energy can appear as an increase in thermal energy, rather than just kinetic energy. It is important to increase our knowledge (experimental and theoretical) of the various modes of reconnection energy release, since if the energy is distributed among many sinks, this could lead to difficulties in detecting the coherent plasma bulk flows implicit in most attempts to identify reconnection events.

Diffusion region. As yet the diffusion region has not been positively identified in the ISEE data. The search for this region should be intensified since observations from this region can potentially lead to a significant enhancement in our knowledge of the reconnection process. As mentioned in Chapter 4, a good starting point is provided by the observations of mixed FTE signatures and the 3 August 1978 outbound pass (Figure 5.4) seems the ideal candidate since it also contains a reported quasi-steady reconnection event. As Paschmann (1982) states, another likely signature which can be used to identify the diffusion region is the presence of plasma waves with extremely large amplitudes.

Energetic particle behaviour. Several publications (reviewed in Chapters 2 and 3) have shown that energetic particles can be successfully used to trace the open field line topology during reconnection events. Such studies need to be extended to include all the quasi-steady reconnection events published so far, and ideally the general behaviour of magnetospheric energetic particles (ions and electrons) at the magnetopause needs to be looked at as well. Specific questions in this area which need to be looked at include the following:

- What are the conditions which lead to the reflection of magnetospheric energetic ions off the magnetopause (e.g., during quasi-steady reconnection events (Scholer and Ipavich, 1983) and during magnetospheric FTEs (Daly et al., 1984))?
- What are the resupply mechanism(s) which lead to observations of energetic ion (and occasionally electron (Korth et al., 1983)) streaming on open field lines?
- What determines the energetic electron behaviour inside FTE flux tubes (e.g., isotropic intensities)?
- To what extent are the energetic ions and electrons inside FTEs modified by plasma waves?

- Are pancake-like electron distributions generally indicative of closed field lines, or are the observations of trapped electrons on open field lines more prevalent than the one example published so far (Daly and Fritz, 1982)?
etc.....

Northward IMF. Low-altitude measurements show that when the IMF is strongly northward, various magnetospheric phenomena such as polar cap convective flows assume a qualitatively different aspect (see, e.g., review by Reiff, 1984). Many of these observations can be successfully interpreted in terms of reconnection in the high-latitude tail magnetopause region (Figure 1.9). However, in-situ signatures of such a reconnection process have not yet been identified. The nature of the orbit probably prohibits a search for these signatures with the ISEE data. Other satellite data sets which cover the high-latitude region should therefore be carefully examined. HEOS 2 data can be used for this purpose, although it should be remembered that the plasma experiment has only limited capabilities (e.g., Rosenbauer et al., 1975). However, magnetic field data at a high time resolution could be used to search for FTE-type signatures resulting from an impulsive northward IMF reconnection process in the high-latitude tail region. As yet we know relatively little of the dynamics in the magnetopause region for northward IMF. It would, for example, be important to know whether the boundary layer observations in Figures 7.1, 7.3 and 7.4 result from a diffusively-driven process or whether they result from reconnection tailward of the cusp region.

Relationship with FTEs. In Chapter 5 we discussed observations which suggest that quasi-steady reconnection events and FTEs are closely related. However, it is not fully clear what this relationship is. On occasion FTEs are observed to be embedded inside the steady reconnection flow region close to the magnetopause (Saunders, 1983; Figure 3.14), and also the satellite furthest away from the magnetopause sometimes sees the most prominent FTE B_N signature (Saunders, 1983; Figures 5.2, 5.4). These observations suggest that FTEs and steady reconnection signatures can occur simultaneously and that FTEs result from localised variations in the rate of reconnection. Full clarification of this question may be achieved through the implementation of the ISTP program (Appendix A), which includes a four-satellite mission (CLUSTER) able to explore the 3-D structure of the magnetopause region.

Theory. Finally, to round off this chapter, we should like to emphasize that a full understanding of the reconnection process, e.g., its precise onset conditions and subsequent time dependency, will not be achieved without developments on the theoretical front. Steady-state reconnection models provide a very useful description and explain much of the physics. Their prediction of reconnection as a large-scale, externally-driven process which is controlled by the southward IMF component has been borne out to some extent, but many puzzling observations remain. For example, during one particular inbound pass through the magnetopause region (Figure 3.14), ISEE observed FTEs (Rijnbeek et al., 1982), quasi-steady reconnection (Sonnerup et al., 1981) and a tangential magnetopause discontinuity (Papamastorakis et al., 1984). There were no obvious changes in the external plasma or field parameters to explain these different observations and the magnetosheath field was consistently southward. Such observations indicate that the reconnection rate at any given point on the magnetopause is variable and a theoretical understanding of the role which time-dependent and (3-D) spatial effects play in the reconnection process at the dayside magnetopause is required. A start in this direction has already been made by, e.g., Greenly and Sonnerup (1981) and Quest and Coroniti (1981), who emphasize the importance of the tearing mode instability in setting up the reconnection topology and suggest it as a possible explanation for the patchy nature of dayside reconnection.

The Earth's magnetopause region provides an ideal opportunity to study the reconnection process in-situ and observations in this region can act as input information and also a means of testing theoretical developments. Such developments may lead in turn to a better understanding of the reconnection process elsewhere, in laboratory fusion experiments and astrophysical plasmas which are less (or not) accessible to detailed in-situ investigations (Hones (1984) provides an up-to-date review on reconnection theory and observation in most of its aspects).

REFERENCES

Aggson, T. L., et al., Electric field measurements at the magnetopause. 1. Observation of large convective velocities at rotational magnetopause discontinuities, J. Geophys. Res. 88, 10000, 1983.

Aggson, T. L., et al., Observation of plasma deceleration at a rotational magnetopause discontinuity, Geophys. Res. Lett. 11, 8, 1984.

Akasofu, S.-I., et al., Magnetotail and boundary layer plasmas at a geocentric distance of 18 R_E: Vela 5 and 6 observations, J. Geophys. Res. 78, 7257, 1973.

Anderson, R. R., et al., Plasma waves near the magnetopause, J. Geophys. Res. 87, 2087, 1982.

Arnoldy, R. L., Signature in the interplanetary medium for substorms, J. Geophys. Res. 76, 5189, 1971.

Aubry, M. P., et al., Inward motion of the magnetopause before a substorm, J. Geophys. Res. 75, 7018, 1970.

Axford, W. I., The polar wind and the terrestrial helium budget, J. Geophys. Res. 73, 6855, 1968.

Axford, W. I., and C. O. Hines, A unifying theory of high-latitude geophysical phenomena and geomagnetic storms, Can. J. Phys. 39, 1433, 1961.

Bahnsen, A., Recent techniques of observations and results from the magnetopause regions, J. Atmos. Terr. Phys. 40, 235, 1978.

Baker, D. N., and E. C. Stone, The magnetopause electron layer along the distant magnetotail, Geophys. Res. Lett. 4, 133, 1977a.

Baker, D. N., and E. C. Stone, The relationship of energy flow at the magnetopause to geomagnetic activity, Geophys. Res. Lett. 4, 395, 1977b.

Baker, D. N., and E. C. Stone, The magnetopause energetic electron layer: 1. observations along the distant magnetotail, J. Geophys. Res. 83, 4327, 1978.

Bame, S. J., et al., ISEE-1 and ISEE-2 fast plasma experiment and the ISEE-1 solar wind experiment, IEEE Trans. Geosci. Electron. GE-16, 216, 1978.

Bavassano-Cattaneo, M.B., and V. Formisano, Low energy electrons and protons in the magnetosphere, Planet. Space Sci. 26, 51, 1978.

Berchem, J., and C. T. Russell, The thickness of the magnetopause current layer: ISEE 1 and 2 observations, J. Geophys. Res. 87, 2108, 1982a.

Berchem, J., and C. T. Russell, Magnetic field rotation through the magnetopause: ISEE 1 and 2 observations, J. Geophys. Res. 87, 8139, 1982b.

Berchem, J., and C. T. Russell, Flux transfer events on the dayside magnetopause: spatial distribution and controlling factors, J. Geophys. Res. 89, 6689, 1984.

Burch, J. L., Precipitation of low-energy electrons at high latitudes: effects of interplanetary magnetic field and dipole tilt angle, J. Geophys. Res. 77, 6696, 1972.

Burch, J. L., Rate of erosion of dayside magnetic flux based on a quantitative study of the dependence of polar cusp latitude on the interplanetary magnetic field, Radio Sci. 8, 955, 1973.

Burch, J. L., Observation of interactions between interplanetary and geomagnetic fields, Rev. Geophys. Space Phys. 12, 363, 1974.

Burch. J. L., et al., Cusp region particle precipitation and ion convection for northward interplanetary magnetic field, Geophys. Res. Lett. 7, 393, 1980.

Burch, J. L., et al., Plasma injection and transport in the mid-altitude polar cusp, Geophys. Res. Lett. 9, 921, 1982.

Burch, J. L., et al., Upward electron beams measured by DE-1: a primary source of dayside region 1 Birkeland currents, Geophys. Res. Lett. 10, 753, 1983.

Burke, W. J., et al., Polar cap electric field structures with a northward interplanetary magnetic field, Geophys. Res. Lett. 6, 21, 1979.

Burton, R. K., et al., An empirical relationship between interplanetary conditions and D_{st}, J. Geophys. Res. 80, 4204, 1975.

Caufmann, D. P., and D. A. Gurnett, Double-probe measurements of convection electric fields with the Injun-5 satellite, J. Geophys. Res. 76, 6014, 1971.

Cauffman, D. P., and D. A. Gurnett, Satellite measurements of high latitude convection electric fields, Space Sci. Rev. 13, 369, 1972.

Chappell, C. R., Detached plasma regions in the magnetosphere, J. Geophys. Res. 79, 1861, 1974.

Coroniti, F. V., and C. F. Kennel, Can the ionosphere regulate magnetospheric convection?, J. Geophys. Res. 78, 2837, 1973.

Cowley, S. W. H., A qualitative study of the reconnection between the Earth's magnetic field and an interplanetary magnetic field of arbitrary orientation, Radio Sci. 8, 903, 1973.

Cowley, S. W. H., Comments on the merging of nonantiparallel magnetic fields, J. Geophys. Res. 81, 3455, 1976.

Cowley, S. W. H., Plasma populations in a simple open model magnetosphere, Space Sci. Rev. 26, 217, 1980.

Cowley, S. W. H., The causes of convection in the Earth's magnetosphere - a review of developments during the IMS, Revs. Geophys. Space Phys. 20, 531, 1982.

Cowley, S. W. H., Evidence for the occurrence and importance of reconnection between the Earth's magnetic field and the interplanetary magnetic field, in Magnetic Reconnection in Space and Laboratory Plasmas, ed. E. W. Hones, Jr., p.375, AGU, Washington, 1984.

Cowley, S. W. H., et al., Interpretation of magnetic field perturbations in the Earth's magnetopause boundary layers, Planet. Space Sci. 31, 1237, 1983.

Cowling, T. G., Magnetohydrodynamics, Adam Hilger Ltd., Bristol, 1976.

Croley, D. R., et al., A search for reconnection phenomena at synchronous orbit (abstract), AGU Chapman Conference on Magnetic Reconnection, book of abstracts, 1983.

Crooker, N. U., Explorer 33 entry layer observations, J. Geophys. Res. 82, 515, 1977.

Crooker, N. U., Dayside merging and cusp geometry, J. Geophys. Res. 84, 951, 1979.

Daly, P. W., Remote sensing of energetic particle boundaries, Geophys. Res. Lett. 9, 1329, 1982.

Daly, P. W., and E. Keppler, Observation of a flux transfer event on the Earthward side of the magnetopause, Planet. Space Sci. 30, 331, 1982.

Daly, P. W., and T. A. Fritz, Trapped electron distributions on open magnetic field lines, J. Geophys. Res. 87, 6081, 1982.

Daly, P. W., and E. Keppler, Remote sensing of a flux transfer event with energetic particles, J. Geophys. Res. 88, 3971, 1983a.

Daly, P. W., and E. Keppler, Motion of flux transfer events on 10 November 1977 determined by energetic particles on ISEE 2, J. Geophys. 52, 199, 1983b.

Daly, P. W., et al., Particle signature of magnetic flux transfer events at the magnetopause, J. Geophys. Res. 86, 1628, 1981.

Daly, P. W., et al., The distribution of reconnection geometry in flux transfer events using energetic ion, plasma and magnetic field data, J. Geophys. Res. 89, 3843, 1984.

Domingo, V., et al., Where do charged particles enter in and exit from the magnetosphere? Some HEOS 2 measurements, J. Atmos. Terr. Phys. 40, 279, 1978.

Dungey, J. W., Interplanetary magnetic field and the auroral zones, Phys. Rev. Lett. 6, 47, 1961.

Dungey, J. W., The structure of the exosphere or adventures in velocity space, in Geophysics, the Earth's Environment, ed. C. DeWitt, J. Hieblot and A. Lebeau, p.503, Gordon and Breach, New York, 1963.

Dungey, J. W., The length of the magnetospheric tail, J. Geophys. Res. 70, 1753, 1965.

Dungey, J. W., The history of the magnetopause regions, J. Atmos. Terr. Phys. 40, 231, 1978.

Eastman, T. E., and E. W. Hones, Jr., Characteristics of the magnetospheric boundary layer and magnetopause layer as observed by IMP 6, J. Geophys. Res. 84, 2019, 1979.

Eastman, T. E., and L. A. Frank, Observations of high-speed plasma flow near the Earth's magnetopause: evidence for reconnection?, J. Geophys. Res. 87, 2187, 1982.

Eastman, T. E., et al., The magnetospheric boundary layer: site of plasma momentum and energy transfer from the magnetosheath into the magnetosphere, Geophys. Res. Lett. 3, 685, 1976.

Eastman, T. E., et al., Three-dimensional plasma observations near the outer magnetospheric boundary, preprint, 1982.

van Eyken, A. P., et al., Initial EISCAT observations of plasma convection at invariant latitudes 70°-77°, preprint, 1984.

Fahleson, U. V., et al., Quasistatic electric fields observed during a number of magnetopause crossings by ISEE-1, in Magnetospheric Boundary Layers, Rep. ESA SP-148, ed. B. Battrick, p.51, Noordwijk, Netherlands, 1979.

Fairfield, D. H., Simultaneous measurements on three satellites and the observation of the geomagnetic tail at 1000 R_E, J. Geophys. Res. 73, 6179, 1968.

Fairfield, D. H., Average and unusual locations of the Earth's magnetopause and bow shock, J. Geophys. Res. 76, 6700, 1971.

Fairfield, D. H., and L. J. Cahill, Jr., Transition region magnetic field and polar magnetic disturbances, J. Geophys. Res. 71, 155, 1966.

Fairfield, D. H., and E. W. Hones, Jr., IMP 6 measurements in the distant polar cusp during substorms, J. Geophys. Res. 83, 4273, 1978.

Formisano, V., HEOS-2 observations of the boundary layer from the magnetopause to the ionosphere, Planet. Space Sci. 28, 245, 1980.

Formisano, V., The International Sun Earth Explorer Mission - ISEE 2, in The IMS Source Book, ed. C. T. Russell and D. J. Southwood, p.27, AGU, Washington, 1982.

Formisano, V., and M. B. Bavassano-Cattaneo, Plasma properties in the dayside cusp region, Planet. Space Sci. 26, 993, 1978.

Formisano, V., et al., The three-dimensional shape of the magnetopause, Planet. Space Sci. 27, 1137, 1979.

Frank, L. A., Plasma in the Earth's polar magnetosphere, J. Geophys. Res. 76, 5202, 1971.

Frank, L. A., and K. L. Ackerson, Observations of charged particle precipitation in the auroral zone, J. Geophys. Res. 76, 3612, 1971.

Frank, L. A., and D. A. Gurnett, Distributions of plasmas and electric fields over the auroral zones and polar caps, J. Geophys. Res. 76, 6829, 1971.

Frank, L. A., et al., Three-dimensional plasma measurements within the Earth's magnetosphere, Space Sci. Rev. 22, 739, 1978.

Freeman, J. W., et al., Heavy ion circulation in the Earth's magnetosphere, Geophys. Res. Lett. 4, 195, 1977.

Friis-Christensen, E., and J. Wilhjelm, Polar cap currents for different directions of the interplanetary magnetic field in the Y-Z plane, J. Geophys. Res. 80, 1248, 1975.

Fukushima, N., Equivalence in ground geomagnetic effect of Chapman-Vestine's and Birkeland-Alfvén's electric current-systems for polar magnetic storms, Rep. Ionos. Res. Space Res. Jap. 23, 219, 1969.

Fukushima, N., Generalized theorem for no ground magnetic effect of vertical currents connected with Pedersen currents in the uniform-conductivity ionosphere, Rep. Ionos. Space Res. Jap. 30, 35, 1976.

Gonzalez, W. D., and F. S. Mozer, A quantitative model for the potential resulting from reconnection with an arbitrary interplanetary magnetic field, J. Geophys. Res. 79, 4186, 1974.

Gosling, J. T., et al., Evidence for quasi-stationary reconnection at the dayside magnetopause, J. Geophys. Res. 87, 2147, 1982.

Grard, R., et al., Magnetopause electric and magnetic field signatures at times of magnetospheric compressions, in Magnetospheric Boundary Layers, Rep. ESA SP-148, ed. B. Battrick, p.67, Noordwijk, Netherlands, 1979.

Greenly, J. B., and B. U. Ö. Sonnerup, Tearing modes at the magnetopause, J. Geophys. Res. 86, 1305, 1981.

Gurnett, D. A., et al., Plasma wave turbulence at the magnetopause: observations from ISEE 1 and 2, J. Geophys. Res. 84, 7043, 1979.

Haerendel, G., Microscopic plasma processes related to reconnection, J. Atmos. Terr. Phys. 40, 343, 1978.

Haerendel, G., and G. Paschmann, Entry of solar wind plasma into the magnetosphere, in Physics of the Hot Plasma in the Magnetosphere, ed. B. Hultqvist and L. Stenflo, p.23, Plenum, New York, 1975.

Haerendel, G., and G. Paschmann, Interaction of the solar wind with the dayside magnetosphere, in Magnetospheric Plasma Physics, ed. A. Nishida, p.49, D. Reidel, Dordrecht, Holland, 1982.

Haerendel, G., et al., The frontside boundary layer of the magnetosphere and the problem of reconnection, J. Geophys. Res. 83, 3195, 1978.

Hansen, A. M., et al., The cusp-magnetosheath interface, J. Geophys. Res. 81, 556, 1976.

Hardy, D. A., et al., A new plasma regime in the distant geomagnetic tail, Geophys. Res. Lett. 2, 169, 1975.

Hardy, D. A., et al., Plasma observations in the magnetotail, in Magnetospheric Particles and Fields, ed. B. M. McCormac, p.89, D. Reidel, Dordrecht, Holland, 1976.

Hardy, D. A., et al., Double-peaked ion spectra in the lobe plasma: evidence for massive ions?, J. Geophys. Res. 82, 5529, 1977.

Hardy, D. A., et al., Response of magnetotail plasma at lunar distance to changes in the interplanetary magnetic field, the solar wind and substorm activity, J. Geophys. Res. 84, 1382, 1979.

Hedgecock, P. C., Magnetometer experiments in the European Space Research Organisation's HEOS satellites, Space Sci. Instrum. 1, 61, 1975.

Heelis, R. A., et al., Ion convection velocity reversals in the dayside cleft, J. Geophys. Res. 81, 3803, 1976.

Heikkila, W. J., Criticism of reconnection models of the magnetosphere, Planet. Space Sci. 26, 121, 1978.

Heikkila, W. J., and J. D. Winningham, Penetration of magnetosheath plasma to low altitudes through the dayside magnetospheric cusps, J. Geophys. Res. 76, 883, 1971.

Heppner, J. P., Polar-cap electric field distributions related to the interplanetary magnetic field direction, J. Geophys. Res. 77, 4877, 1972.

Heppner, J. P., High latitude electric fields and the modulations related to interplanetary magnetic field parameters, Radio Sci. 8, 933, 1973.

Heppner, J. P., et al., Instrumentation for DC and low frequency electric field measurements on ISEE-A, IEEE Trans. Geosci. Electron. GE-16, 253, 1978.

Hill, T. W., Magnetic merging in a collisionless plasma, J. Geophys. Res. 80, 4689, 1975.

Hill, T. W., and P. H. Reiff, Evidence of magnetospheric cusp proton acceleration by magnetic merging at the dayside magnetopause, J. Geophys. Res. 82, 3623, 1977.

Hirshberg, J., and D. S. Colburn, Interplanetary field and geomagnetic variations - a unified view, Planet. Space Sci. 17, 1183, 1969.

Holzer, T. E., and G. C. Reid, The response of the dayside magnetosphere-ionosphere system to time-varying field line reconnection at the magnetopause. 1. Theoretical model, J. Geophys. Res. 80, 2041, 1975.

Holzer, R. E., and J. A. Slavin, Magnetic flux transfer associated with expansions and contractions of the dayside magnetosphere, J. Geophys. Res. 83, 3831, 1978.

Holzer, R. E., and J. A. Slavin, A correlative study of magnetic flux transfer in the magnetosphere, J. Geophys. Res. 84, 2573, 1979.

Hones, E. W., Jr., Magnetic structure of the boundary layer, Space Sci. Rev. 34, 201, 1983.

Hones, E. W., Jr., (editor), Magnetic Reconnection in Space and Laboratory Plasmas, AGU, Washington, 1984.

Hones, E. W., Jr., et al., Measurements of magnetotail plasma flow made with Vela 4B, J. Geophys. Res. 77, 5503, 1972.

Hones, E. W., Jr., et al., "Reverse draping" of magnetic field lines in the boundary layer, Geophys. Res. Lett. 9, 523, 1982.

Hudson, P. D., Discontinuities in an anisotropic plasma and their identification in the solar wind, Planet. Space Sci. 18, 1611, 1970.

Hultqvist, B., Recent progress in the understanding of the ion composition in the magnetosphere and some major question marks, Rev. Geophys. Space Phys. 20, 589, 1982.

Iijima, T., and T. A. Potemra, The amplitude distribution of field-aligned currents at northern high latitudes observed by TRIAD, J. Geophys. Res. 81, 2165, 1976a.

Iijima, T., and T. A. Potemra, Field-aligned currents in the dayside cusp observed by TRIAD, J. Geophys. Res. 81, 5971, 1976b.

Iijima, T., et al., Field-aligned currents in the south polar cusp and their relationship to the interplanetary magnetic field, J. Geophys. Res. 83, 5595, 1978.

Intriligator, D. S., and J. H. Wolfe, Evidence of a diffuse magnetopause boundary, J. Geophys. Res. 77, 5480, 1972.

King, J. H., Interplanetary Medium Data Book, NASA National Space Science Data Center/World Data Center A, Goddard Space Flight Center, Greenbelt, MD, 1979 and 1983.

Korth, A., et al., Observations of field-aligned energetic electron and ion distributions near the magnetopause at geosynchronous orbit, preprint, 1983.

Landau, L. D., and E. M. Lifshitz, Electrodynamics of Continuous Media, Pergamon, New York, 1960.

Lepping, R. P., and K. W. Behannon, Magnetic field directional discontinuities. 1. Minimum variance errors, J. Geophys. Res. 85, 4695, 1980.

Levy, R. H., et al., Aerodynamic aspects of the magnetospheric flow, AIAA J. 2, 2065, 1964.

Luhmann, J. G., et al., Patterns of potential magnetic field merging sites on the dayside magnetopause, J. Geophys. Res. 89, 1739, 1984.

Lundin, R., Solar wind energy transfer regions inside the dayside magnetopause. II. Evidence for an MHD generator process, Planet. Space Sci. 32, 757, 1984.

Lundin, R., and E. Dubinin, Solar wind energy transfer regions inside the dayside magnetopause. I. Evidence for magnetosheath plasma penetration, Planet. Space Sci. 32, 745, 1984.

Lundin, R., et al., The plasma mantle: composition and other characteristics observed by means of the PROGNOZ-7 satellite, Space Sci. Rev. 31, 247, 1982.

Maezewa, K., Dependence of the magnetopause position on the southward interplanetary magnetic field, Planet. Space Sci. 22, 1443, 1974.

Maezewa, K., Magnetospheric convection induced by the positive and negative Z components of the interplanetary magnetic field: quantitative analysis using polar cap magnetic records, J. Geophys. Res. 81, 2289, 1976.

McDiarmid, I. B., et al., Comparison of magnetic field perturbations at high latitudes with charged particle and IMF measurements, J. Geophys. Res. 83, 681, 1978a.

McDiarmid, I. B., et al., Magnetic field perturbations in the dayside cleft and their relationship to the IMF, J. Geophys. Res. 83, 5753, 1978b.

McDiarmid, I. B., et al., Large-scale magnetic field perturbations and particle measurements at 1400 km on the dayside, J. Geophys. Res. 84, 1431, 1979.

McDiarmid, I. B., et al., Comparison of magnetic field perturbations and solar electron profiles in the polar cap, J. Geophys. Res. 85, 1163, 1980.

Meng, C. I., and K. A. Anderson, A layer of energetic electrons (> 40 keV) near the magnetopause, J. Geophys. Res. 75, 1827, 1970.

Meng, C. I., and K. A. Anderson, Characteristics of the magnetopause energetic electron layer, J. Geophys. Res. 80, 4237, 1975.

Mozer, F. S., Analyses of techniques for measuring dc and ac electric fields in the magnetosphere, Space Sci. Rev. 14, 272, 1973.

Mozer, F. S., Electric field evidence on the viscous interaction at the magnetopause, Geophys. Res. Lett. 11, 135, 1984.

Mozer, F. S., et al., High-latitude electric fields and the three-dimensional interaction between the interplanetary and terrestrial magnetic fields, J. Geophys. Res. 79, 56, 1974.

Mozer, F. S., et al., Electric field measurements in the solar wind, bow shock, magnetosheath, magnetopause and magnetosphere, Space Sci. Rev. 22, 791, 1978.

Mozer, F. S., et al., Direct observation of a tangential electric field component at the magnetopause, Geophys. Res. Lett. 6, 305, 1979.

Nishida, A., Coherence of geomagnetic DP-2 fluctuations with interplanetary magnetic variations, J. Geophys. Res. 73, 5549, 1968.

Nishida, A., Interplanetary origin of electric fields in the magnetosphere, Cosmic Electrodyn. 2, 350, 1971.

Ogilvie, K. W., and J. D. Scudder, Stochastic energy flux emanating from the vicinity of a suggested merging site (abstract), EOS Trans. AGU 60, 362, 1979.

Ogilvie, K. W., et al., Descriptions of experiments and instruments for the ISEE spacecraft, IEEE Trans. Geosci. Electron. GE-16, 151, 1978a.

Ogilvie, K. W., et al., Electron spectrometer experiment on ISEE-1, IEEE Trans. Geosci. Electron. GE-16, 261, 1978b.

Ogilvie, K. W., et al., Observations of electron beams in the low latitude boundary layer, preprint, 1984.

Palmer, I. D., and E. W. Hones, Jr., Characteristics of energetic electrons in the vicinity of the magnetospheric boundary layer at Vela orbit, J. Geophys. Res. 83, 2584, 1978.

Papamastorakis, I., et al., The magnetopause as a tangential discontinuity for large field rotation angles, J. Geophys. Res. 89, 127, 1984.

Paschmann, G., ISEE magnetopause observations: workshop results, in IMS Sourcebook, ed. C. T. Russell and D. J. Southwood, p.272, AGU, Washington, 1982.

Paschmann, G., Plasma and particle observations at the magnetopause: implications for reconnection, in Magnetic Reconnection in Space and Laboratory Plasmas, ed. E. W. Hones, Jr., p.114, AGU, Washington, 1984.

Paschmann, G., et al., Plasma and magnetic field characteristics of the distant polar cusp near local noon: the entry layer, J. Geophys. Res. 81, 2883, 1976.

Paschmann, G., et al., ISEE plasma observations near the subsolar magnetopause, Space Sci. Rev. 22, 717, 1978.

Paschmann, G., et al., Plasma acceleration at the Earth's magnetopause: evidence for reconnection, Nature, 282, 243, 1979.

Paschmann, G., et al., Plasma and magnetic field characteristics of magnetic flux transfer events, J. Geophys. Res. 87, 2159, 1982.

Paschmann, G., et al., ISEE observations of magnetopause reconnection: the energy balance (abstract), EOS Trans. AGU, 64, 799, 1983.

Perreault, P., and S.-I. Akasofu, A study of geomagnetic storms, Geophys. J. R. Astron. Soc. 54, 547, 1978.

Peterson, W. K., et al., Energetic ion composition in the subsolar magnetopause and boundary layer, J. Geophys. Res. 87, 2139, 1982.

Petschek, H. E., Magnetic field annihilation, AAS-NASA Symposium on the Physics of Solar Flares, NASA Spec. Publ. SP-50, 425, 1964.

Potemra, T. A., Observation of Birkeland currents with the TRIAD satellite, Astrophys. Space Sci. 58, 207, 1978.

Potemra, T. A., et al., Large-scale characteristics of Birkeland currents, in Dynamics of the Magnetosphere, ed. S.-I. Akasofu, p.165, D. Reidel, Dordrecht, Holland, 1980.

Quest, K. B., and F. V. Coroniti, Tearing at the dayside magnetopause, J. Geophys. Res. 86, 3289, 1981.

Reiff, P. H., Low-altitude signatures of the boundary layers, in Magnetospheric Boundary Layers, Rep. ESA SP-148, ed. B. Battrick, p.167, Noordwijk, Netherlands, 1979.

Reiff, P. H., Evidence of magnetic merging from low-altitude spacecraft and ground-based experiments, in Magnetic Reconnection in Space and Laboratory Plasmas, ed. E. W. Hones, Jr., p.104, AGU, Washington, 1984.

Reiff, P. H., et al., Solar wind plasma injection at the dayside magnetospheric cusp, J. Geophys. Res. 82, 479, 1977.

Reiff, P. H., et al., Dependence of polar cap potential drop on interplanetary parameters, J. Geophys. Res. 86, 7639, 1981.

Rijnbeek, R. P., and S. W. H. Cowley, Magnetospheric flux erosion events are flux transfer events, Nature 309, 135, 1984.

Rijnbeek, R. P., et al., Observations of reverse polarity flux transfer events at the Earth's dayside magnetopause, Nature 300, 23, 1982.

Rijnbeek, R. P., et al., A survey of dayside flux transfer events observed by ISEE 1 and 2 magnetometers, J. Geophys. Res. 89, 786, 1984.

Rodgers, D. J., et al., Evidence for the heating of thermal electrons at the magnetopause boundary layer, Planet. Space Sci. 32, 657, 1984.

Rosenbauer, H., et al., HEOS 2 plasma observations in the distant polar magnetosphere: the plasma mantle, J. Geophys. Res. 80, 2723, 1975.

Rostoker, G., Geomagnetic indices, Rev. Geophys. Space Phys. 10, 935, 1972.

Rostoker, G., and C.-G. Fälthammar, Relationship between changes in the interplanetary magnetic field and variations in the magnetic field at the Earth's surface, J. Geophys. Res. 72, 5853, 1967.

Russell, C. T., Geophysical coordinate transformations, Cosmic Electrodyn. 2, 184, 1971.

Russell, C. T., The configuration of the magnetosphere, in Critical Problems of Magnetospheric Physics, ed. E. R. Dyer, p.6, National Academy of Sciences, Washington, 1972.

Russell, C. T., The ISEE-1 and -2 fluxgate magnetometers, IEEE Trans. Geosci. Electron. GE16, 239, 1978.

Russell, C. T., Patchy reconnection and magnetic ropes in astrophysical plasmas, IAU Proc., Smposium 107, in press, 1983.

Russell, C. T., Reconnection at the Earth's magnetopause: magnetic field observations and flux transfer events, in Magnetic Reconnection in Space and Laboratory Plasmas, ed. E. W. Hones, Jr., p.124, AGU, Washington, 1984.

Russell, C. T., and R. C. Elphic, Initial ISEE magnetometer results: magnetopause observations, Space Sci. Rev. 22, 681, 1978.

Russell, C. T., and D. J. Southwood (Editors), the IMS Source Book: Guide to the International Magnetospheric Study Data Analysis, AGU, Washington, 1982.

Russell, C. T., et al., OGO 5 observations of the polar cusp on November 1, 1968, J. Geophys. Res. 76, 6743, 1971.

Russell, C. T., et al., On the source region of flux transfer events, in Physics of Ionosphere-Magnetosphere Connection, ed. E. R. Schmerling, Space Research Series, Pergamon, 1984.

Saflekos, N. A., et al., Field-aligned currents, convection electric fields, and ULF-ELF waves in the cusp, J. Geophys. Res. 84, 1391, 1979.

Saunders, M. A., Analysis of ISEE 1 and 2 spacecraft magnetometer data, Ph.D. thesis, University of London, Imperial College, 1982.

Saunders, M. A., Recent ISEE observations of the magnetopause and low latitude boundary layer: a review, J. Geophys. 52, 190, 1983.

Saunders, M. A., et al., Flux transfer events: scale size and interior structure, Geophys. Res. Lett. 11, 131, 1984a.

Saunders, M. A., et al., A dual-satellite study of the spatial properties of FTEs, in Magnetic Reconnection in Space and Laboratory Plasmas, ed. E. W. Hones, Jr., p.145, AGU, Washington, 1984b.

Scholer, M., Energetic particle signatures near magnetospheric boundaries, J. Geophys. 52, 176, 1983.

Scholer, M., and F. M. Ipavich, Interaction of ring current ions with the magnetopause, J. Geophys. Res. 88, 6937, 1983.

Scholer, M., et al., Leakage of magnetospheric ions into the magnetosheath along reconnected field lines at the dayside magnetopause, J. Geophys. Res. 86, 1299, 1981.

Scholer, M., et al., Energetic protons, alpha particles, and electrons in magnetic flux transfer events, J. Geophys. Res. 87, 2169, 1982a.

Scholer, M., et al., Field line topology determined by energetic particles during a possible magnetopause reconnection event, J. Geophys. Res. 87, 6073, 1982b.

Sckopke, N., and G. Paschmann, The plasma mantle. A survey of magnetotail boundary layer observations, J. Atmos. Terr. Phys. 40, 261, 1978.

Sckopke, N., External plasma flow, in Magnetospheric Boundary Layers, Rep. ESA SP-148, ed. B. Battrick, p.37, Noordwijk, Netherlands, 1979.

Sckopke, N., et al., Influence of the interplanetary magnetic field on the occurrence and thickness of the plasma mantle, J. Geophys. Res. 81, 2687, 1976.

Sckopke, N., et al., Structure of the low-latitude boundary layer, J. Geophys. Res. 86, 2099, 1981.

Scudder, J. D., et al., The relation of flux transfer events to magnetic reconnection, in Magnetic Reconnection in Space and Laboratory Plasmas, ed. E. W. Hones, Jr., p.153, AGU, Washington, 1984.

Shelley, E. G., et al., He^{++} and H^{+} flux measurements in the dayside cusp: estimates of convection electric field, J. Geophys. Res. 81, 2363, 1976.

Shelley, E. G., et al., On the origin of the magnetospheric boundary layer plasma, EOS Trans. AGU 59, 1163, 1978.

Sonnerup, B. U. Ö., Magnetopause structure during the magnetic storm of September 24, 1961, J. Geophys. Res. 76, 6717, 1971.

Sonnerup, B. U. Ö., Magnetopause reconnection rate, J. Geophys. Res. 79, 1546, 1974.

Sonnerup, B. U. Ö., Magnetopause and boundary layer, in Physics of Solar Planetary Environments, ed. D. J. Williams, p.541, AGU, Washington, 1976.

Sonnerup, B. U. Ö., Magnetic field reconnection, in Solar System Plasma Physics, ed. L. J. Lanzerotti, C. F. Kennel and E. N. Parker, p.45, (Vol.3), North Holland, Amsterdam, 1979.

Sonnerup, B. U. Ö., Transport mechanisms at the magnetopause, in Dynamics of the Magnetosphere, ed. S.-I. Akasofu, p.77, D. Reidel, Dordrecht, Holland, 1980.

Sonnerup, B. U. Ö., Theory of the low-latitude boundary layer, J. Geophys. Res. 85, 2017, 1980.

Sonnerup, B. U. Ö., and L. J. Cahill, Jr., Magnetopause structure and attitude from Explorer 12 observations, J. Geophys. Res. 72, 171, 1967.

Sonnerup, B. U. Ö., and L. J. Cahill, Jr., Explorer 12 observations of the magnetopause current layer, J. Geophys. Res. 73, 1757, 1968.

Sonnerup, B. U. Ö., and B. G. Ledley, OGO 5 magnetopause structure and classical reconnection, J. Geophys. Res. 84, 399, 1979a.

Sonnerup, B. U. Ö., and B. G. Ledley, Electromagnetic structure of the magnetopause and boundary layer, in Magnetospheric Boundary Layers, Rep. ESA SP-148, ed. B. Battrick, p.401, Noordwijk, Netherlands, 1979b.

Sonnerup, B. U. Ö., et al., Evidence for magnetic field reconnection at the Earth's magnetopause, J. Geophys. Res. 86, 10049, 1981.

Southwood, D. J., Magnetopause Kelvin-Helmholtz instability, in Magnetospheric Boundary Layers, Rep. ESA SP-148, ed. B. Battrick, p.357, Noordwijk, Netherlands, 1979.

Southwood, D. J., Theoretical aspects of ionosphere-magnetosphere-solar wind coupling, in Physics of Ionosphere-Magnetosphere Connection, ed. E. R. Schmerling, Space Research Series, Pergamon, 1984.

Southwood, D. J., and C. T. Russell, Special Collection in International Magnetospheric Study Assessment Symposium, Rev. Geophys. Space Phys. 20, 529, 1982.

Speiser, T. W., et al., Magnetospherically trapped ions as a source of magnetosheath energetic ions, J. Geophys. Res. 86, 723, 1981.

Speiser, T. W., and D. J. Williams, Magnetopause modelling: flux transfer events and magnetosheath quasi-trapped distributions, J. Geophys. Res. 87, 2177, 1982.

Spreiter, J. R., and A. Y. Alksne, Plasma flow around the magnetosphere, Rev. Geophys. Space Phys. 7, 11, 1969.

Stern, D. P., A study of the electric field in an open magnetospheric model, J. Geophys. Res. 78, 7292, 1973.

Stern, D. P., Large-scale electric fields in the Earth's magnetosphere, Rev. Geophys. Space Phys. 15, 156, 1977.

Swift, D. W., and L. C. Lee, Rotational discontinuities and the structure of the magnetopause, J. Geophys. Res. 88, 111, 1983.

Torbert, R. B., and C. W. Carlson, Impulsive ion injection into the polar cusp, in Magnetospheric Particles and Fields, ed. B. M. McCormac, p.47, D. Reidel, Dordrecht, Holland, 1976.

Vasyliunas, V. M., Theoretical models of magnetic field-line merging, Rev. Geophys. Space Phys. 13, 303, 1975.

Walker, R. J., and C. T. Russell, Dayside reconnection at Jupiter and the Earth, Paper PA.20 (abstract), XVIII IAGA General Assembly, Hamburg, August, 1983.

Wilcox, J. M., et al., Influence of interplanetary magnetic field and plasma on geomagnetic activity during quiet sun conditions, J. Geophys. Res. 72, 19, 1967.

Wilhjelm, J., et al., The relationship between ionospheric and field-aligned currents in the dayside cusp, J. Geophys. Res. 83, 5586, 1978.

Williams, D. J., and L. A. Frank, ISEE 1 charged particle observations indicative of open magnetospheric field lines near the subsolar region, J. Geophys. Res. 85, 2037, 1980.

Williams, D. J., et al., The ISEE 1 and 2 medium energy particles experiment, IEEE Trans. Geosci. Electron., GE-16, 270, 1978.

Wygant, J. R., et al., Comparison of S3-3 polar cap potential drops with the interplanetary magnetic field and models of magnetopause reconnection, J. Geophys. Res. 88, 5727, 1983.

Yang, C. K., and B. U. Ö. Sonnerup, Compressible magnetopause reconnection, J. Geophys. Res. 82, 699, 1977.

Zanetti, L. J., et al., Interplanetary magnetic field control of high-latitude activity on July 29, 1977, J. Geophys. Res. 87, 5963, 1982.

Zmuda, A. J., and J. C. Armstrong, The diurnal pattern of field-aligned currents, J. Geophys. Res. 79, 4611, 1974.

APPENDIX A

SATELLITE MISSIONS

Here we briefly describe a selection of outer magnetosphere satellite missions which have played, are playing or are likely to play a major role in elucidating the subject contained in this thesis, specifically the nature of the solar wind-magnetosphere interaction at the Earth's magnetopause.

A.1 The HEOS 2 satellite (31 January 1972-2 August 1974)

HEOS (Highly Eccentric Orbiting Satellite) 2 was launched into a highly eccentric polar orbit, with an orbital period of $\sim$ 5.2 days and an apogee situated almost directly above the North Pole in the solar wind, $\sim$ 40 R_E away from the Earth (Figure A.1). The unique nature of its orbit allowed HEOS 2 to explore the previously unknown distant polar magnetosphere region and its boundaries. Major successes of the mission include the discovery of the plasma mantle and entry layer regions (see Chapter 2), and the first observational identification of impulsive reconnection signatures (Chapter 6). The HEOS 2 satellite was equipped with an array of 7 experiments. A brief description of the instrumentation is given by Bahnsen (1978). For our purposes the most important instruments are the magnetometer (Hedgecock, 1975) and the plasma instrument (e.g., Rosenbauer et al., 1975). Further details and references on HEOS 2 can be found in the yearly reports by ESRO (now ESA) to COSPAR (particularly 1973 and 1974).

A.2 The ISEE mission (22 October 1977 - ?)

The ISEE (International Sun-Earth Explorer) mission is a joint project between NASA and ESA and consists of three satellites: ISEE 1, 2 and 3. The data received from the three ISEE satellites form a major part of the IMS (see Southwood and Russell (1982) and Russell and Southwood (1982) for details about the aims and achievements of the IMS).

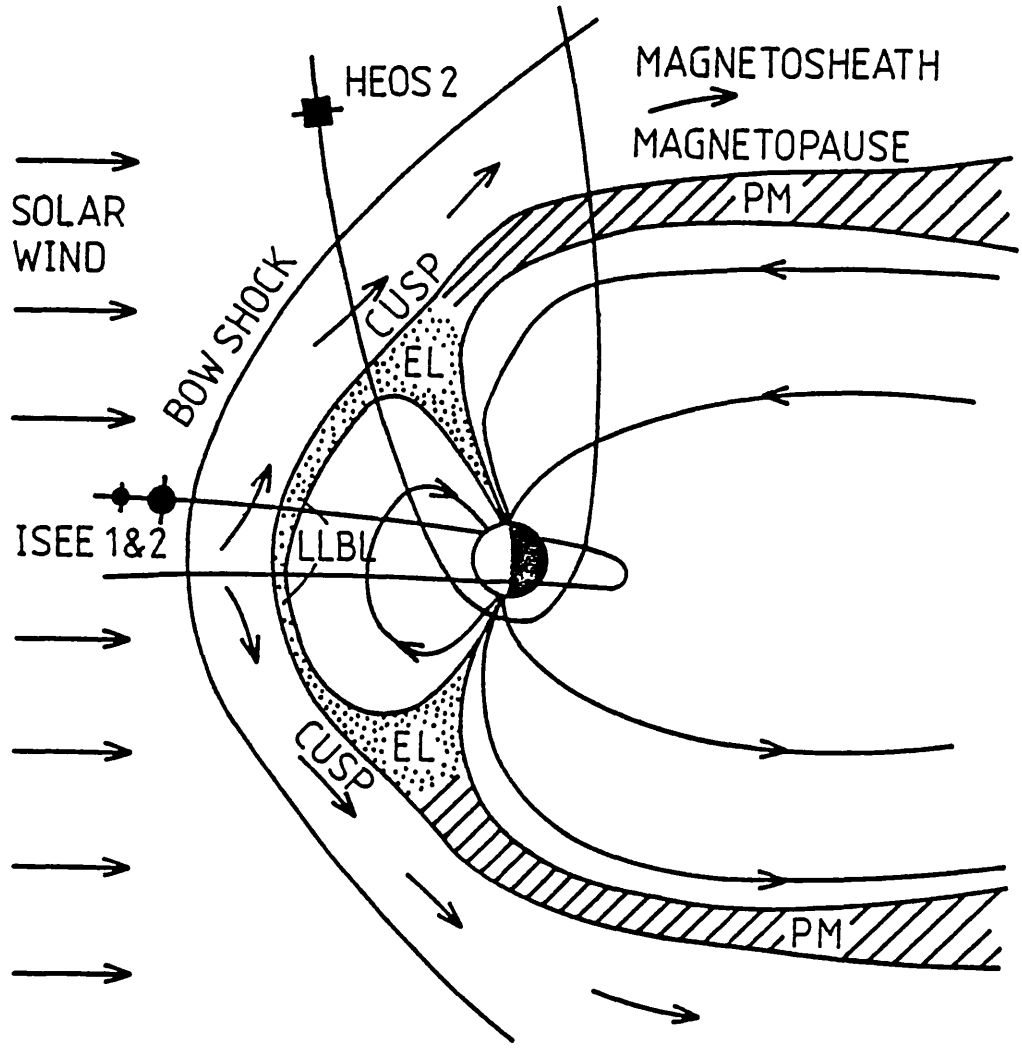


Fig. A.1. The HEOS 2 and ISEE 1 and 2 orbits in relation to the magnetosphere.

ISEE 1 and 2 were launched into an identical orbit with an inclination of 30°, an orbital period of 57 hours and an apogee 22.6 R_E away from the Earth (Figure A.1). Both satellites have carefully matched payloads and circulate through the magnetosphere a controllable distance apart. The satellite separation is varied throughout the mission and at times has reached a value in excess of 1 R_E. The nature of the orbit, the unique (at the time of launch) dual-satellite capability and the high resolution of the instrumentation make ISEE 1 and 2 ideally suited to study and analyse dynamic magnetospheric processes. The success story of the mission includes the first convincing in-situ observations of steady reconnection at the Earth's dayside magnetopause (e.g., Sonnerup et al., 1981). Another major discovery is the identification and successful interpretation of signatures relating to a more impulsive, hitherto unpredicted form of reconnection: flux transfer events (Russell and Elphic, 1978). Details about the ISEE instrumentation can be found in Ogilvie et al. (1978) and further references and progress reports on the mission itself may be found in the yearly ESA reports to COSPAR.

A.3 The GEOS 2 satellite (14 July 1978 - ?)

The GEOS 2 satellite was launched by ESA into a geostationary orbit. The nature of its orbit (Figure A.2) allows GEOS 2 to monitor conditions in the magnetospheric equatorial plane at a geocentric distance of $\sim$ 6.6 R_E. It is well-suited to study the magnetopause region at time of strong solar wind compression and flux erosion. Details about the GEOS mission can be found in the ESA reports to COSPAR.

A.4 The AMPTE mission (22 August 1984 - ?)

AMPTE (Active Magnetospheric Particle Tracer Explorer) is a joint project between West Germany, the United States and the United Kingdom and consists of three satellites, one of which is located permanently inside the magnetosphere (Figure A.3). One of the aims of the mission is to continue the type of investigation initiated by ISEE, with the IRM (Ion Release Module) and the UKS (United Kingdom Subsatellite) playing roles similar to those of ISEE 1 and 2. The inclination of the IRM and UKS orbit is similar to that of ISEE 1 and 2, but it seems likely that the AMPTE mission will help to extend the coverage of the

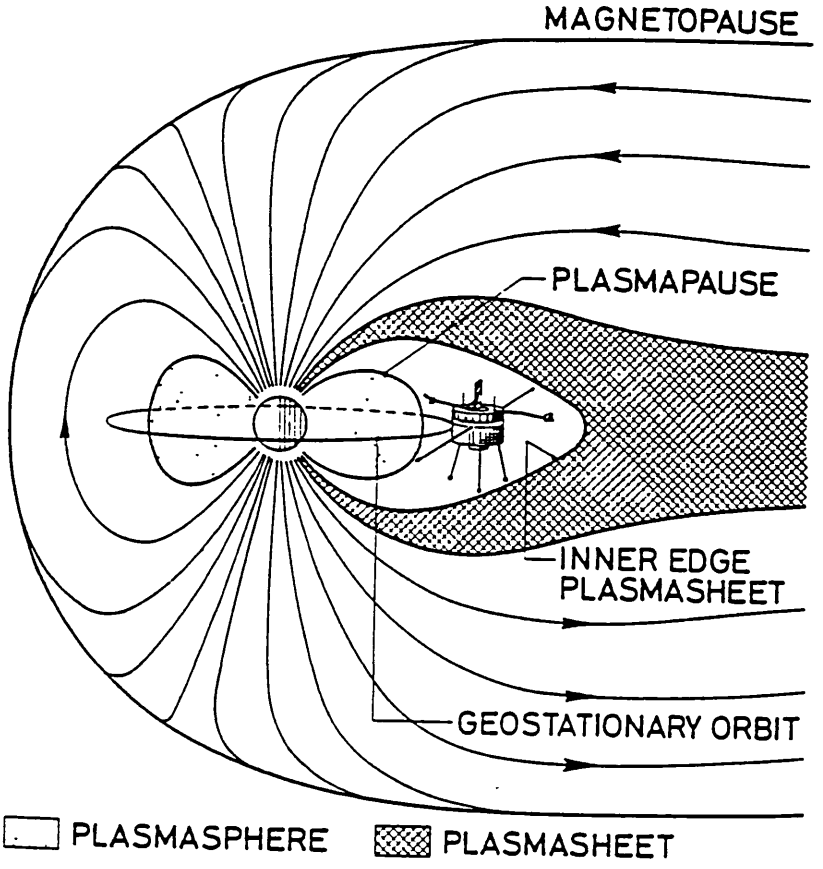


Fig. A.2. The orbit of GEOS.

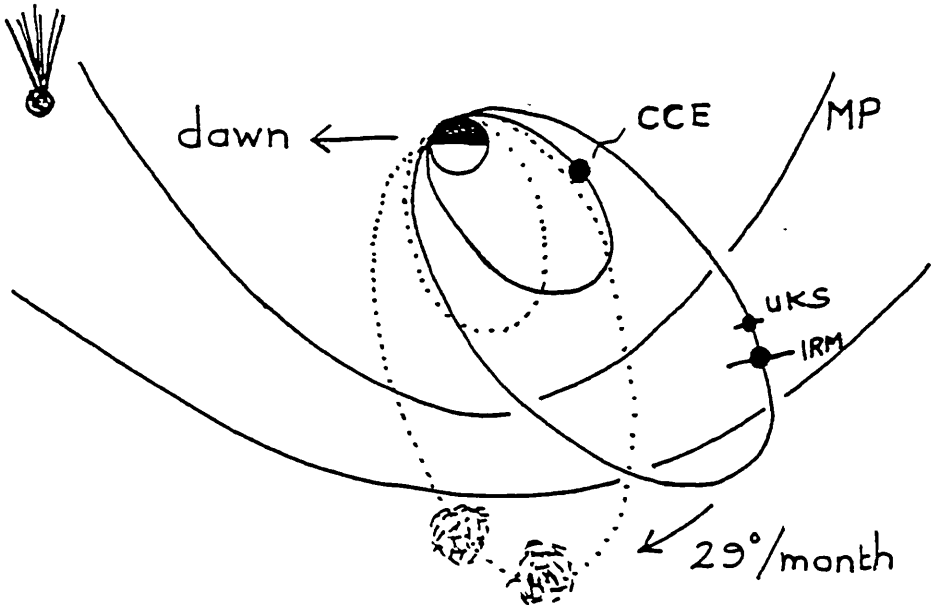


Fig. A.3. The AMPTE satellites in orbit.

dayside magnetopause by providing data from regions unexplored by ISEE. The combination of high time resolution magnetic field ($\lesssim$ 1/8 sec), ion, electron and waves instrumentation on board the UKS shows much promise of giving us further insight into phenomena such as FTEs. Further details about the AMPTE mission may be obtained by writing to the project coordinators G. Haerendel (Max Planck, West Germany), S. M. Krimigis (Johns Hopkins University, U.S.A.) or D. A. Bryant (Rutherford Appleton Laboratory, Oxfordshire, England).

A.5 The ISTP programme (1990s)

The ISTP (International Solar-Terrestrial Physics) programme currently consists of 6 spacecraft missions to be launched in the period 1989-93. The overall strategy of the ISTP programme is to study the interaction of the Sun with the Earth's plasma environment by monitoring conditions on the Sun, the solar wind, the outer magnetosphere, the inner magnetosphere and the geotail (Figure A.4). Two satellite missions which are of particular interest are POLAR and CLUSTER, which aim to provide the first high resolution data from the outer polar magnetosphere region. CLUSTER, which consists of a cluster of 4 satellites with controllable separations (from $\lesssim$ 100 km to several R_E), provides the opportunity to study magnetospheric features in 3-D and will be particularly useful in the study of magnetic reconnection at the dayside magnetopause (for further details write to NASA).

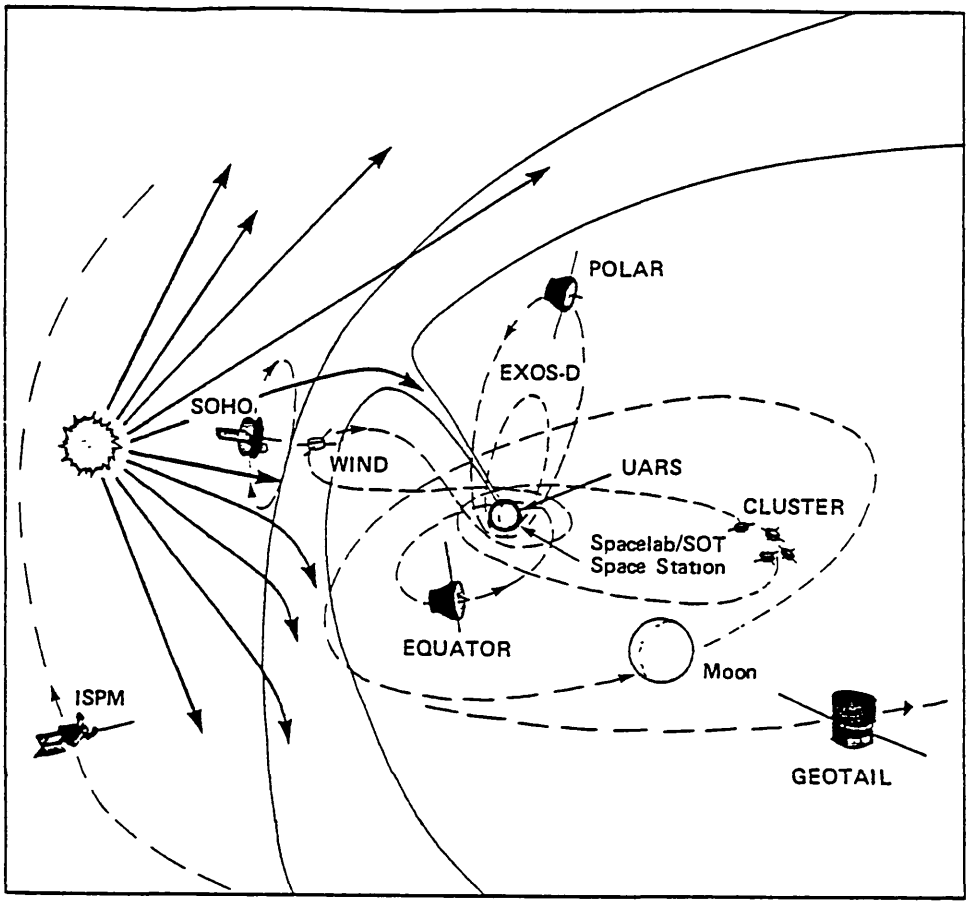


Fig. A.4. The ISTP programme in action.

APPENDIX B

COORDINATE SYSTEMS

Here we briefly describe some of the coordinate systems which are commonly used in studies of the magnetopause and adjacent regions (see also Russell, 1971; Russell and Elphic, 1978).

B.1 Geocentric Solar Magnetospheric (GSM) coordinates

The GSM system has its X-axis pointing along the line drawn from the centre of the Earth to the Sun, and is positive in the sunward sense. The Z-axis is perpendicular to $\hat{X}$, such that the X-Z plane contains the Earth's magnetic dipole axis, and is positive in the northward sense. The Y-axis, which is perpendicular to both $\hat{X}$ and $\hat{Z}$, lies in the magnetic equatorial plane and is positive towards dusk (East).

The GSM system confines the Earth's dipole axis motion to a plane (the X-Z plane) and it is one of the most commonly used coordinate systems to display magnetopause and bow shock crossing locations, and magnetic field and plasma flow observations at and near the magnetopause.

B.2 Geocentric Solar Ecliptic (GSE) coordinates

The GSE and GSM systems have the X-axis in common, but differ by a rotation angle about this axis which varies in time. The GSE X-axis is defined to be parallel to the ecliptic pole. The Y-axis, which is perpendicular to both $\hat{X}$ and $\hat{Z}$, lies in the ecliptic plane and is positive towards dusk.

The GSE system is frequently used to display satellite trajectories and locations.

B.3 Solar Magnetic (SM) coordinates

The SM system has its Y-axis in common with the GSM system, but differs by a rotation angle about this axis. The Z-axis is defined to

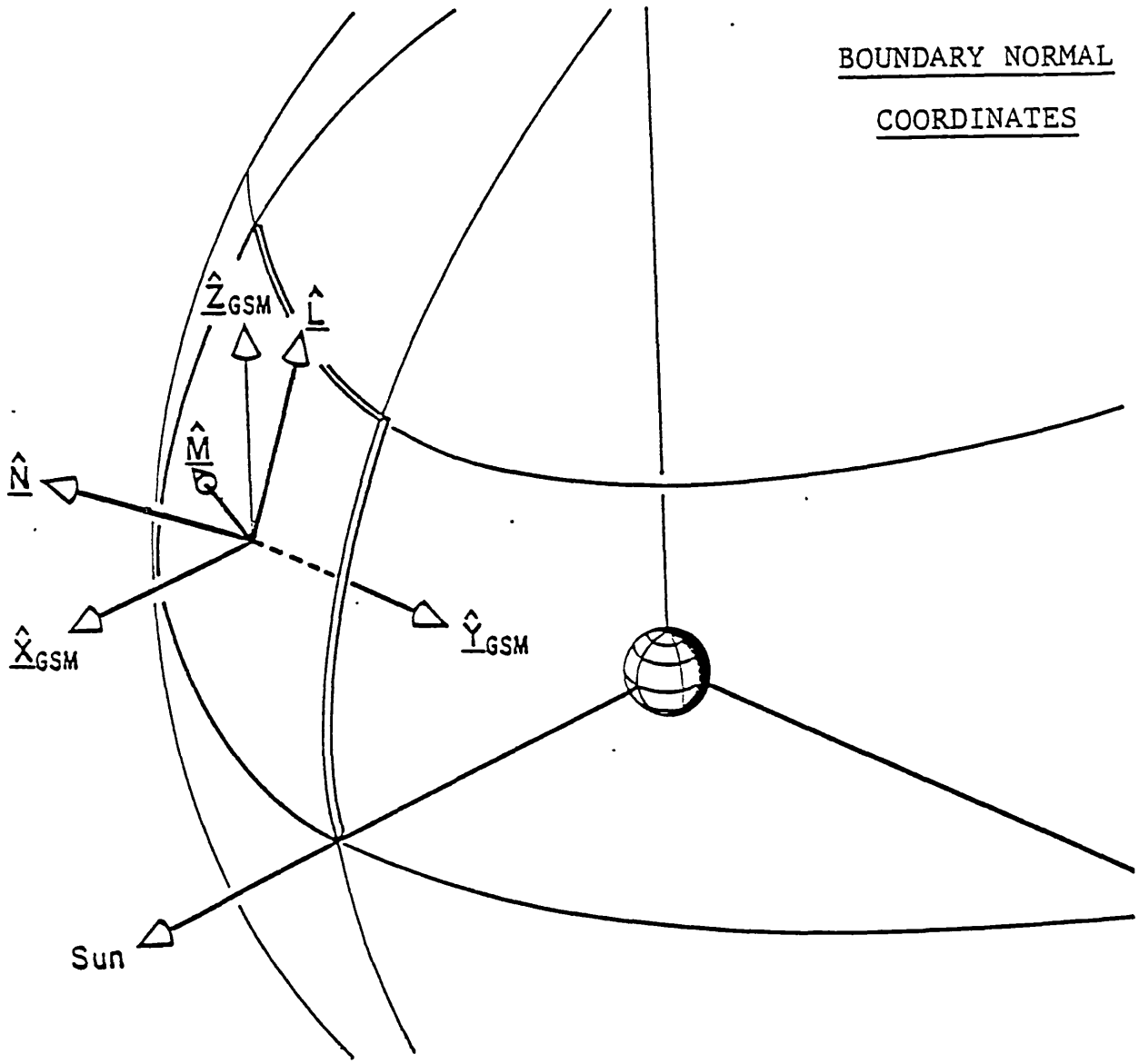


Fig. B.1. Magnetospheric Coordinate systems.

be parallel to the Earth's magnetic dipole axis, and is positive northwards. The X-axis is perpendicular to both $\hat{Y}$ and $\hat{Z}$ and is positive in the sunward sense, although in general it does not point directly at the Sun.

In the SM system the subsolar (stagnation) point is not generally on the equator, but moves along the noon meridian in time. However, it is better than the GSM or GSE systems in ordering data which are strongly controlled by the Earth's magnetic dipole field (rather than the solar wind flow). For example, it gives a better ordering of the location of the cusp region than does the GSM system (e.g., Haerendel et al., 1978).

B.4 Boundary Normal (LMN) coordinates

The GSM, GSE and SM systems are all global coordinate systems, i.e., they have their origin centred on the Earth. To provide a better ordering of magnetic field data at the Earth's magnetopause, Russell and Elphic (1978) introduced the boundary normal coordinate system. This system is referenced to the local magnetopause surface and has three mutually orthogonal components. $\hat{N}$ is perpendicular to the boundary and is positive along the outward normal (directed away from the Earth). $\hat{L}$ points approximately northwards such that the L-N plane contains the GSM Z-axis. Finally, $\underline{M}$ completes the right-handed triad and is positive in the dawnward (westward) sense. For a model magnetopause surface (which is symmetrical about the equatorial plane), $\hat{L}$, $\hat{M}$ and $\hat{N}$ correspond to GSM $\hat{Z}$, $-\hat{Y}$ and $\hat{X}$, respectively, at the subsolar point.

B.5 Determination of the boundary normal, $\hat{N}$

The boundary normal coordinate system depends critically on the correct determination of $\hat{N}$. We shall therefore describe three different methods which can be used to estimate its direction.

Model normal. From large data sets of satellite magnetopause crossing locations a model magnetopause surface can be constructed which describes the average shape and location of the magnetopause (e.g., Fairfield, 1971; Formisano et al., 1979). The model magnetopause surface can in turn be used to estimate $\hat{N}$ for individual magnetopause crossings. The model normal is easy to calculate in that it merely requires a knowledge

of the satellite location at the magnetopause. Disadvantages of using this method are that it takes no account of the variability of the magnetopause, resulting, e.g., from surface waves. Thus on individual passes the magnetopause often does not correspond to its average location or shape.

Tangential discontinuity (TD) normal. In this method the direction of $\hat{N}$ is estimated by taking the cross-product of two suitably chosen (individual or averaged) magnetic field vectors on opposite sides of the magnetopause. The method relies on the assumption that the normal field component through the magnetopause is zero ($B_N = 0$), or at least very small compared to the tangential field components on opposite sides of the magnetopause. Disadvantages of the method are that the magnetic field at the magnetopause is often variable, so that it may not be straightforward to choose the appropriate field vectors. Also, the magnetopause may at times have a substantial normal field component through it. Finally, the determination of $\hat{N}$ using this method becomes increasingly prone to error as the magnetic field vectors on opposite sides of the magnetopause become more nearly aligned (either parallel or antiparallel).

Minimum Variance (MV) normal. For a steady-state, 1-D magnetopause (no variations along it) the condition $\nabla.\underline{B} = 0$ requires that B_N remains constant across the magnetopause. In practice B_N does not remain constant, but instead the direction of the boundary normal may be estimated by finding the direction in which the magnetic field across the magnetopause varies least. This is done through a technique known as minimum variance analysis, which was first applied to magnetopause studies by Sonnerup and Cahill (1967). Minimum variance analysis leads to the determination of three eigenvalues λ_1, λ_2, λ_3 and corresponding (unit) eigenvectors $\hat{N}_1$, $\hat{N}_2$, $\hat{N}_3$, which lie, respectively, along the directions of maximum, intermediate and minimum variance of the magnetic field. The minimum variance vector, $\hat{N}_3$, can usually be interpreted as the direction of the boundary normal vector, $\hat{N}$. As for the tangential discontinuity method, minimum variance analysis relies on the measured magnetic field vectors at the magnetopause, but it has the advantage of making no assumptions about the presence or absence of a normal field component, B_N. Minimum variance analysis (and the other two methods as well) does not take into account any systematic changes such as time variations or variations in the magnetopause attitude which may

take place during the time interval of the magnetopause crossing. Also, if the ratio of the two smallest eigenvalues is small ($\lambda_2/\lambda_3 \lesssim 3$), i.e., if the magnetopause current is unidirectional ($\underline{J}_{MP}$ always perpendicular to the difference vector $\underline{B}_{msph} - \underline{B}_{msh}$), then $\hat{\underline{N}}_3$ becomes unreliable as an estimate of $\underline{N}$ (e.g., Sonnerup, 1976; Sonnerup and Ledley, 1979).

Example. To illustrate the above discussion, Figure B.2(a) shows a 1-hour plot of magnetic field data and Figure B.2(b) shows the behaviour of the magnetopause magnetic field in hodogram format. To determine the direction of the normal to the magnetopause an interval for analysis is chosen in the magnetic field data which is approximately centred on the magnetopause layer. The interval is chosen such that it includes the magnetopause layer, i.e., the region in which the field magnitude and/or direction changes, as well as a short interval (a few minutes or less) of magnetosheath and magnetospheric field data on either side of the magnetopause layer. A general rule for choosing the interval is that it should include all the information about the rotation of the field at the magnetopause in the shortest possible time, in order to minimise the risk of any attitude changes of the magnetopause. In the present instance this interval is chosen to be from 3:10 to 3:18 UT. Details concerning this crossing can be found in Table B.1. The model magnetopause normals are determined using the satellite (ISEE 1) location at the centre of the analysis interval. The tangential discontinuity normals are obtained from the cross-product of the magnetic field data points at the start and end of the interval, or by using an average of the field determined over the first and last ½-min of the interval. Data points from the whole of the interval are used in the minimum variance analysis to determine the eigenvalues and corresponding eigenvectors. In Figure B.2(b), B_1, B_2 and B_3 correspond to the magnetic field components along the direction of maximum, intermediate and minimum variance ($\hat{\underline{N}}_1$, $\hat{\underline{N}}_2$, $\hat{\underline{N}}_3$). The hodograms in Figure B.2(b) trace out the tip of the field vectors (anchored at the origin) in the B_2B_1 and B_3B_1 planes.

Table B.1 shows that in the present example there is fairly good agreement between the different methods of estimating $\hat{\underline{N}}$. The data in Figure B.2(a) have been plotted using the normal determined by minimum variance analysis, since this direction was found to order the data best over the 1-hour interval. Table B.1 also gives some additional information about the magnetic field behaviour in the magnetopause layer.

The sense of rotation refers to the sense of rotation of the tangential field components (B_1 and B_2) from the magnetospheric to the magnetosheath field orientation, as viewed from the Earth. It is determined by using equation (16) in Sonnerup and Cahill (1968). Equation (22) in the same paper has been used to determine that the rotation angle is less than 2π. Analysis of ISEE magnetopause crossings during 1979 shows that a rotation angle smaller than 2π is a general feature of the magnetopause, in agreement with the results obtained by Berchem and Russell (1982b; see also Swift and Lee, 1983). The quantity s gives a measure of the variation of the field magnitude across the magnetopause and is zero if the field strength stays constant. It is given by the ratio of the standard deviation of individual measurements of the field magnitude divided by the field magnitude averaged over the crossing and was used by Sonnerup and Cahill (1968) to separate crossings into those of the rotational discontinuity type and those of the tangential discontinuity type. The error estimates of $\underline{\hat{N}}_3$ in the N_1N_3 and N_2N_3 planes and the error ΔB_3 in the magnitude of B_3 are obtained using the error analysis discussed in Sonnerup (1971; 1976; note that Lepping and Behannon (1980) give an alternative, empirically determined formula for ΔB_3). The error estimates are lower limits, since they only account for random errors. Note in the present example that the presence of a prominent magnetopause FTE at 3:12 UT leads to a substantial variation in B_3 and a correspondingly large error estimate ΔB_3.

TABLE B.1

Analysis of 11 August 1979 Magnetopause Crossing

Date	11 August 179 (ISEE 1)
Time	3:10 - 3:18 UT
MP Location	11.53 R_E, 1401 LT, 13.8 LAT
$\hat{\underline{N}}^{Fa}$	(0.904, 0.383, 0.188)
$\hat{\underline{N}}^{Fo}$	(0.890, 0.395, 0.228)
$\hat{\underline{N}}^{TD_1}$	(0.853, 0.378, 0.359)
$\hat{\underline{N}}^{TD_2}$	(0.861, 0.339, 0.379)

Minimum Variance Analysis

No. of data points	120
λ_1, $\hat{\underline{N}}_1$	733.0 (-0.430, 0.216, 0.876)
λ_2, $\hat{\underline{N}}_2$	50.5 (0.250, -0.904, 0.346)
λ_3, $\hat{\underline{N}}_3$	5.7 (0.867, 0.368, 0.335)
Sense of rotation	right-hand
Rotation angle	$< 2\pi$
S (= $\overline{\sigma}/B$)	0.08 (= 3.5/46.3)
$\overline{B}_3 \pm \Delta B_3$	- 1.1 ± 6.6
$\Delta\hat{\underline{N}}_3 . \hat{\underline{N}}_1$	0.1°
$\Delta\hat{\underline{N}}_3 . \hat{\underline{N}}_2$	2.0°

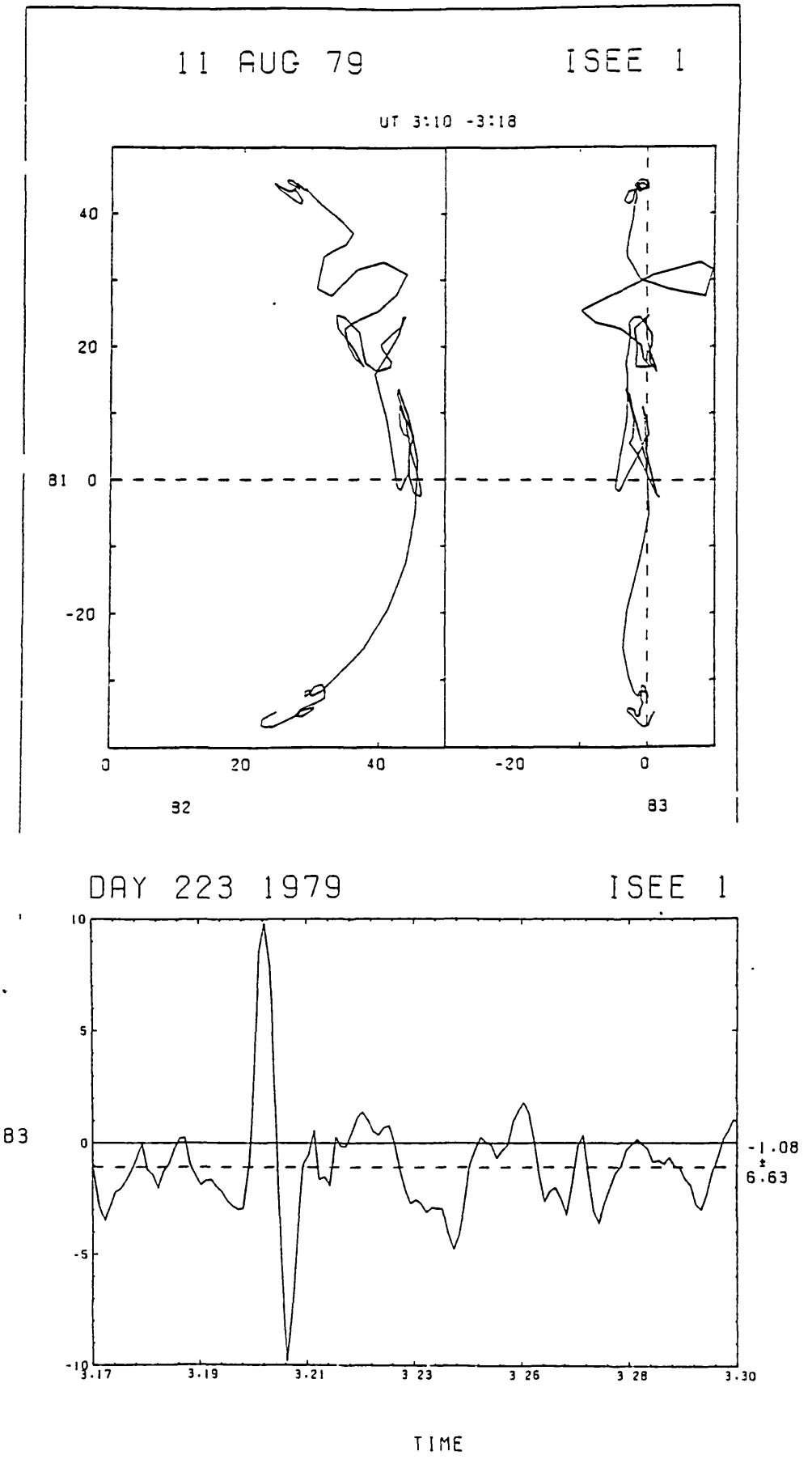


Fig. B.2. Determination of the magnetopause normal.

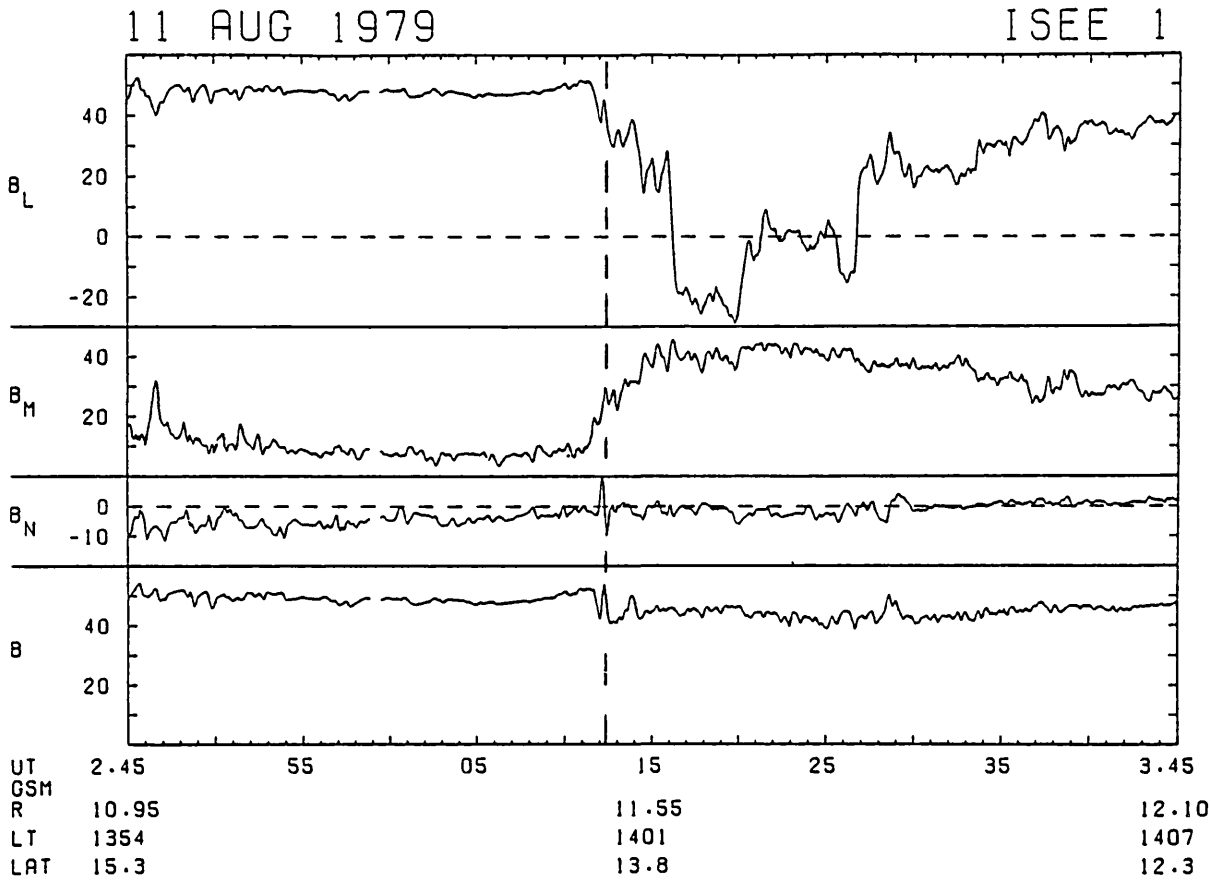


Fig. B.2. Determination of the magnetopause normal.

APPENDIX C

LISTING OF MAGNETOPAUSE CROSSINGS

The computer print-out gives a listing of the dates, locations, times and various other characteristics of ISEE 1 and 2 magnetopause crossings which were used as part of the survey described in Chapter 4. This information may be of use to any scientific researcher wishing to study the properties of flux transfer events.

Key:

Magnetosheath FTEs:
Magnetosphere FTEs

0= no FTEs
1= standard FTEs
2= reverse FTEs
3= irregular FTEs
4= mixed FTEs

Magnetosheath B_L
Magnetosheath B_M

1= negative
2= positive
3= intermediate

Sign of B_L and B_M determined immediately adjacent to the crossing or in the half hour interval adjacent to the crossing (the latter is indicated in parentheses).

```
MP LOCATION IS: YEAR=1977; MONTH=10; DAY=24; TIME=14.15 UT; INBOUND; R=11.8; LT=1218; LAT= 24.3
MAGNETOSHEATH FTES:  1;  MAGNETOSPHERE FTES:  1
SIGN OF MAGNETOSHEATH BL IS:  1( 1);  SIGN OF MAGNETOSHEATH BM IS:  1( 1)
DIRECTION OF NORMAL USED FOR PLOTTING DATA IN GSM: ( .798; .109; .593)
*****
MP LOCATION IS: YEAR=1977; MONTH=10; DAY=25; TIME= 6.14 UT; OUTBOUND; R=11.9; LT= 858; LAT= 40.2
MAGNETOSHEATH FTES:  0;  MAGNETOSPHERE FTES:  0
SIGN OF MAGNETOSHEATH BL IS:  3( 3);  SIGN OF MAGNETOSHEATH BM IS:  2( 2)
DIRECTION OF NORMAL USED FOR PLOTTING DATA IN GSM: ( .760;-.327; .561)
*****
MP LOCATION IS: YEAR=1977; MONTH=10; DAY=27; TIME= 5.46 UT; INBOUND; R= 9.0; LT=1252; LAT= 20.0
MAGNETOSHEATH FTES:  1;  MAGNETOSPHERE FTES:  0
SIGN OF MAGNETOSHEATH BL IS:  2( 2);  SIGN OF MAGNETOSHEATH BM IS:  2( 2)
DIRECTION OF NORMAL USED FOR PLOTTING DATA IN GSM: ( .964; .159; .214)
*****
MP LOCATION IS: YEAR=1977; MONTH=10; DAY=27; TIME=13.20 UT; OUTBOUND; R= 8.8; LT= 807; LAT= 42.3
MAGNETOSHEATH FTES:  1;  MAGNETOSPHERE FTES:  1
SIGN OF MAGNETOSHEATH BL IS:  1( 1);  SIGN OF MAGNETOSHEATH BM IS:  3( 3)
DIRECTION OF NORMAL USED FOR PLOTTING DATA IN GSM: ( .785;-.530; .322)
*****
MP LOCATION IS: YEAR=1977; MONTH=10; DAY=29; TIME=14.28 UT; INBOUND; R= 9.9; LT=1236; LAT= 22.1
MAGNETOSHEATH FTES:  0;  MAGNETOSPHERE FTES:  0
SIGN OF MAGNETOSHEATH BL IS:  3( 2);  SIGN OF MAGNETOSHEATH BM IS:  1( 1)
DIRECTION OF NORMAL USED FOR PLOTTING DATA IN GSM: ( .955; .105; .279)
*****
MP LOCATION IS: YEAR=1977; MONTH=10; DAY=30; TIME=  .47 UT; OUTBOUND; R=11.6; LT= 805; LAT= 28.2
MAGNETOSHEATH FTES:  4;  MAGNETOSPHERE FTES:  3
SIGN OF MAGNETOSHEATH BL IS:  1( 1);  SIGN OF MAGNETOSHEATH BM IS:  2( 2)
DIRECTION OF NORMAL USED FOR PLOTTING DATA IN GSM: ( .588;-.578; .438)
*****
MP LOCATION IS: YEAR=1977; MONTH=10; DAY=31; TIME=22.17 UT; INBOUND; R=11.9; LT=1136; LAT= 25.2
MAGNETOSHEATH FTES:  0;  MAGNETOSPHERE FTES:  0
SIGN OF MAGNETOSHEATH BL IS:  2;  SIGN OF MAGNETOSHEATH BM IS:  3
DIRECTION OF NORMAL USED FOR PLOTTING DATA IN GSM: ( .921;-.143; .362)
*****
MP LOCATION IS: YEAR=1977; MONTH=10; DAY=31; TIME=23.25 UT; INBOUND; R=10.4; LT=1151; LAT= 24.3
MAGNETOSHEATH FTES:  0;  MAGNETOSPHERE FTES:  0
SIGN OF MAGNETOSHEATH BL IS:  2;  SIGN OF MAGNETOSHEATH BM IS:  1
DIRECTION OF NORMAL USED FOR PLOTTING DATA IN GSM: ( .921;-.143; .362)
*****
MP LOCATION IS: YEAR=1977; MONTH=11; DAY= 1; TIME=10.00 UT; OUTBOUND; R=11.4; LT= 828; LAT= 46.0
MAGNETOSHEATH FTES:  0;  MAGNETOSPHERE FTES:  0
SIGN OF MAGNETOSHEATH BL IS:  2( 2);  SIGN OF MAGNETOSHEATH BM IS:  2( 2)
DIRECTION OF NORMAL USED FOR PLOTTING DATA IN GSM: ( .669;-.332; .720)
*****
MP LOCATION IS: YEAR=1977; MONTH=11; DAY= 3; TIME= 7.52 UT; INBOUND; R=11.6; LT=1208; LAT= 26.0
MAGNETOSHEATH FTES:  0;  MAGNETOSPHERE FTES:  0
SIGN OF MAGNETOSHEATH BL IS:  3( 3);  SIGN OF MAGNETOSHEATH BM IS:  1( 1)
DIRECTION OF NORMAL USED FOR PLOTTING DATA IN GSM: ( .917;-.234; .323)
*****
MP LOCATION IS: YEAR=1977; MONTH=11; DAY= 3; TIME=21.36 UT; OUTBOUND; R=14.0; LT= 804; LAT= 26.4
MAGNETOSHEATH FTES:  0;  MAGNETOSPHERE FTES:  0
SIGN OF MAGNETOSHEATH BL IS:  2( 2);  SIGN OF MAGNETOSHEATH BM IS:  1( 1)
DIRECTION OF NORMAL USED FOR PLOTTING DATA IN GSM: ( .659;-.573; .487)
*****
MP LOCATION IS: YEAR=1977; MONTH=11; DAY= 5; TIME=17.14 UT; INBOUND; R=11.6; LT=1136; LAT= 26.4
MAGNETOSHEATH FTES:  0;  MAGNETOSPHERE FTES:  0
SIGN OF MAGNETOSHEATH BL IS:  2( 2);  SIGN OF MAGNETOSHEATH BM IS:  1( 1)
DIRECTION OF NORMAL USED FOR PLOTTING DATA IN GSM: ( .879;-.008; .469)
*****
MP LOCATION IS: YEAR=1977; MONTH=11; DAY= 6; TIME= 5.50 UT; OUTBOUND; R=12.7; LT= 803; LAT= 40.4
MAGNETOSHEATH FTES:  1;  MAGNETOSPHERE FTES:  1
SIGN OF MAGNETOSHEATH BL IS:  1( 1);  SIGN OF MAGNETOSHEATH BM IS:  1( 1)
DIRECTION OF NORMAL USED FOR PLOTTING DATA IN GSM: ( .707;-.170; .687)
*****
MP LOCATION IS: YEAR=1977; MONTH=11; DAY= 8; TIME= 2.50 UT; INBOUND; R=11.3; LT=1122; LAT= 26.1
MAGNETOSHEATH FTES:  1;  MAGNETOSPHERE FTES:  1
SIGN OF MAGNETOSHEATH BL IS:  1( 1);  SIGN OF MAGNETOSHEATH BM IS:  1( 1)
DIRECTION OF NORMAL USED FOR PLOTTING DATA IN GSM: ( .950;-.204; .234)
*****
MP LOCATION IS: YEAR=1977; MONTH=11; DAY= 8; TIME=14.39 UT; OUTBOUND; R=12.1; LT= 745; LAT= 40.4
MAGNETOSHEATH FTES:  0;  MAGNETOSPHERE FTES:  0
SIGN OF MAGNETOSHEATH BL IS:  2;  SIGN OF MAGNETOSHEATH BM IS:  3
DIRECTION OF NORMAL USED FOR PLOTTING DATA IN GSM: ( .771;-.217; .599)
*****
MP LOCATION IS: YEAR=1977; MONTH=11; DAY=10; TIME=14.59 UT; INBOUND; R= 7.4; LT=1214; LAT= 21.3
MAGNETOSHEATH FTES:  1;  MAGNETOSPHERE FTES:  1
SIGN OF MAGNETOSHEATH BL IS:  1( 1);  SIGN OF MAGNETOSHEATH BM IS:  1( 1)
DIRECTION OF NORMAL USED FOR PLOTTING DATA IN GSM: ( .930; .066; .361)
*****
MP LOCATION IS: YEAR=1977; MONTH=11; DAY=10; TIME=22.40 UT; OUTBOUND; R=10.4; LT= 700; LAT= 23.7
MAGNETOSHEATH FTES:  0;  MAGNETOSPHERE FTES:  3
SIGN OF MAGNETOSHEATH BL IS:  1( 1);  SIGN OF MAGNETOSHEATH BM IS:  2( 2)
DIRECTION OF NORMAL USED FOR PLOTTING DATA IN GSM: ( .603;-.668; .295)
*****
MP LOCATION IS: YEAR=1977; MONTH=11; DAY=12; TIME=21.38 UT; INBOUND; R=11.2; LT=1050; LAT= 24.2
MAGNETOSHEATH FTES:  0;  MAGNETOSPHERE FTES:  0
SIGN OF MAGNETOSHEATH BL IS:  2( 2);  SIGN OF MAGNETOSHEATH BM IS:  1( 1)
DIRECTION OF NORMAL USED FOR PLOTTING DATA IN GSM: ( .948;-.143; .284)
*****
MP LOCATION IS: YEAR=1977; MONTH=11; DAY=12; TIME=22.57 UT; INBOUND; R= 9.4; LT=1111; LAT= 23.1
MAGNETOSHEATH FTES:  1;  MAGNETOSPHERE FTES:  1
SIGN OF MAGNETOSHEATH BL IS:  1( 1);  SIGN OF MAGNETOSHEATH BM IS:  1( 1)
DIRECTION OF NORMAL USED FOR PLOTTING DATA IN GSM: ( .948;-.143; .284)
*****
MP LOCATION IS: YEAR=1977; MONTH=11; DAY=13; TIME= 8.32 UT; OUTBOUND; R=11.0; LT= 710; LAT= 45.3
MAGNETOSHEATH FTES:  1;  MAGNETOSPHERE FTES:  3
SIGN OF MAGNETOSHEATH BL IS:  1( 1);  SIGN OF MAGNETOSHEATH BM IS:  1( 1)
DIRECTION OF NORMAL USED FOR PLOTTING DATA IN GSM: ( .661;-.534; .522)
*****
MP LOCATION IS: YEAR=1977; MONTH=11; DAY=15; TIME= 6.27 UT; INBOUND; R=11.8; LT=1106; LAT= 29.2
MAGNETOSHEATH FTES:  0;  MAGNETOSPHERE FTES:  0
SIGN OF MAGNETOSHEATH BL IS:  2;  SIGN OF MAGNETOSHEATH BM IS:  3
DIRECTION OF NORMAL USED FOR PLOTTING DATA IN GSM: ( .945;-.034; .326)
*****
MP LOCATION IS: YEAR=1977; MONTH=11; DAY=17; TIME=15.25 UT; INBOUND; R=12.3; LT=1046; LAT= 29.6
MAGNETOSHEATH FTES:  0;  MAGNETOSPHERE FTES:  0
SIGN OF MAGNETOSHEATH BL IS:  2( 2);  SIGN OF MAGNETOSHEATH BM IS:  3( 3)
DIRECTION OF NORMAL USED FOR PLOTTING DATA IN GSM: ( .483;-.228; .411)
*****
MP LOCATION IS: YEAR=1977; MONTH=11; DAY=18; TIME= 6.32 UT; OUTBOUND; R=14.6; LT= 722; LAT= 41.3
MAGNETOSHEATH FTES:  1;  MAGNETOSPHERE FTES:  1
SIGN OF MAGNETOSHEATH BL IS:  1( 1);  SIGN OF MAGNETOSHEATH BM IS:  1( 1)
DIRECTION OF NORMAL USED FOR PLOTTING DATA IN GSM: ( .602;-.449; .661)
```

```
*****
MP LOCATION IS: YEAR=1977; MONTH=11; DAY=20; TIME= 1.27 UT; INBOUND; R=11.5; LT=1021; LAT= 24
MAGNETOSHEATH FTLS:  2;  MAGNETOSPHERE FTES:  4
SIGN OF MAGNETOSHEATH BL IS:  1( 1);  SIGN OF MAGNETOSHEATH BM IS:  2( 2)
DIRECTION OF NORMAL USED FOR PLOTTING DATA IN GSM: ( .920;-.311; .239)

*****
MP LOCATION IS: YEAR=1977; MONTH=11; DAY=20; TIME=14.30 UT; OUTBOUND; R=13.2; LT= 655; LAT= 3
MAGNETOSHEATH FTLS:  0;  MAGNETOSPHERE FTES:  0
SIGN OF MAGNETOSHEATH BL IS:  2( 2);  SIGN OF MAGNETOSHEATH BM IS:  3( 1)
DIRECTION OF NORMAL USED FOR PLOTTING DATA IN GSM: ( .937;-.120; .329)

*****
MP LOCATION IS: YEAR=1977; MONTH=11; DAY=22; TIME=11.31 UT; INBOUND; R=10.7; LT=1058; LAT= 31.
MAGNETOSHEATH FTLS:  2;  MAGNETOSPHERE FTES:  1
SIGN OF MAGNETOSHEATH BL IS:  3( 3);  SIGN OF MAGNETOSHEATH BM IS:  2( 2)
DIRECTION OF NORMAL USED FOR PLOTTING DATA IN GSM: ( .839;-.241; .487)

*****
MP LOCATION IS: YEAR=1977; MONTH=11; DAY=24; TIME=19.26 UT; INBOUND; R=12.3; LT= 952; LAT= 24.
MAGNETOSHEATH FTLS:  0;  MAGNETOSPHERE FTES:  0
SIGN OF MAGNETOSHEATH BL IS:  2( 2);  SIGN OF MAGNETOSHEATH BM IS:  3( 3)
DIRECTION OF NORMAL USED FOR PLOTTING DATA IN GSM: ( .839;-.428; .335)

*****
MP LOCATION IS: YEAR=1977; MONTH=11; DAY=25; TIME=10.13 UT; OUTBOUND; R=14.1; LT= 643; LAT= 44
MAGNETOSHEATH FTLS:  2;  MAGNETOSPHERE FTES:  2
SIGN OF MAGNETOSHEATH BL IS:  2( 2);  SIGN OF MAGNETOSHEATH BM IS:  2( 2)
DIRECTION OF NORMAL USED FOR PLOTTING DATA IN GSM: ( .557;-.600; .574)

*****
MP LOCATION IS: YEAR=1977; MONTH=11; DAY=27; TIME= 7.05 UT; INBOUND; R= 9.6; LT=1041; LAT= 29.
MAGNETOSHEATH FTLS:  0;  MAGNETOSPHERE FTES:  0
SIGN OF MAGNETOSHEATH BL IS:  2( 2);  SIGN OF MAGNETOSHEATH BM IS:  2( 2)
DIRECTION OF NORMAL USED FOR PLOTTING DATA IN GSM: ( .929;-.352; .435)

*****
MP LOCATION IS: YEAR=1977; MONTH=11; DAY=27; TIME=20.44 UT; OUTBOUND; R=15.3; LT= 634; LAT= 21
MAGNETOSHEATH FTLS:  2;  MAGNETOSPHERE FTES:  3
SIGN OF MAGNETOSHEATH BL IS:  3( 3);  SIGN OF MAGNETOSHEATH BM IS:  2( 2)
DIRECTION OF NORMAL USED FOR PLOTTING DATA IN GSM: ( .735;-.603; .309)

*****
MP LOCATION IS: YEAR=1977; MONTH=11; DAY=29; TIME=14.56 UT; INBOUND; R=11.4; LT=1002; LAT= 29.
MAGNETOSHEATH FTLS:  1;  MAGNETOSPHERE FTES:  1
SIGN OF MAGNETOSHEATH BL IS:  2( 1);  SIGN OF MAGNETOSHEATH BM IS:  2( 2)
DIRECTION OF NORMAL USED FOR PLOTTING DATA IN GSM: ( .765;-.415; .439)

*****
MP LOCATION IS: YEAR=1977; MONTH=11; DAY=30; TIME= 2.30 UT; OUTBOUND; R=11.5; LT= 552; LAT= 23
MAGNETOSHEATH FTLS:  1;  MAGNETOSPHERE FTES:  0
SIGN OF MAGNETOSHEATH BL IS:  1;  SIGN OF MAGNETOSHEATH BM IS:  2
DIRECTION OF NORMAL USED FOR PLOTTING DATA IN GSM: ( .334;-.792; .526)

*****
MP LOCATION IS: YEAR=1977; MONTH=12; DAY= 2; TIME= 2.09 UT; INBOUND; R= 9.1; LT= 956; LAT= 21.
MAGNETOSHEATH FTLS:  1;  MAGNETOSPHERE FTES:  1
SIGN OF MAGNETOSHEATH BL IS:  1( 1);  SIGN OF MAGNETOSHEATH BM IS:  2( 2)
DIRECTION OF NORMAL USED FOR PLOTTING DATA IN GSM: ( .965; .133; .226)

*****
MP LOCATION IS: YEAR=1977; MONTH=12; DAY= 2; TIME= 3.26 UT; INBOUND; R= 6.8; LT=1036; LAT= 21.
MAGNETOSHEATH FTLS:  4;  MAGNETOSPHERE FTES:  4
SIGN OF MAGNETOSHEATH BL IS:  2( 1);  SIGN OF MAGNETOSHEATH BM IS:  1( 1)
DIRECTION OF NORMAL USED FOR PLOTTING DATA IN GSM: ( .965; .133; .226)

*****
MP LOCATION IS: YEAR=1977; MONTH=12; DAY= 2; TIME=14.07 UT; OUTBOUND; R=14.0; LT= 606; LAT= 36
MAGNETOSHEATH FTLS:  0;  MAGNETOSPHERE FTES:  0
SIGN OF MAGNETOSHEATH BL IS:  2( 3);  SIGN OF MAGNETOSHEATH BM IS:  1( 3)
DIRECTION OF NORMAL USED FOR PLOTTING DATA IN GSM: ( .475;-.616; .629)

*****
MP LOCATION IS: YEAR=1977; MONTH=12; DAY= 4; TIME= 8.10 UT; INBOUND; R=13.2; LT= 934; LAT= 34.
MAGNETOSHEATH FTLS:  3;  MAGNETOSPHERE FTES:  2
SIGN OF MAGNETOSHEATH BL IS:  1( 3);  SIGN OF MAGNETOSHEATH BM IS:  2( 2)
DIRECTION OF NORMAL USED FOR PLOTTING DATA IN GSM: ( .830;-.280; .483)

*****
MP LOCATION IS: YEAR=1977; MONTH=12; DAY= 4; TIME=22.21 UT; OUTBOUND; R=12.9; LT= 545; LAT= 16
MAGNETOSHEATH FTLS:  3;  MAGNETOSPHERE FTES:  3
SIGN OF MAGNETOSHEATH BL IS:  3;  SIGN OF MAGNETOSHEATH BM IS:  1
DIRECTION OF NORMAL USED FOR PLOTTING DATA IN GSM: ( .644;-.515; .566)

*****
MP LOCATION IS: YEAR=1977; MONTH=12; DAY= 4; TIME=20.34 UT; OUTBOUND; R=10.8; LT= 529; LAT= 15
MAGNETOSHEATH FTLS:  0;  MAGNETOSPHERE FTES:  0
SIGN OF MAGNETOSHEATH BL IS:  1;  SIGN OF MAGNETOSHEATH BM IS:  1
DIRECTION OF NORMAL USED FOR PLOTTING DATA IN GSM: ( .644;-.515; .566)

*****
MP LOCATION IS: YEAR=1977; MONTH=12; DAY= 6; TIME=18.37 UT; INBOUND; R=12.0; LT= 906; LAT= 22.
MAGNETOSHEATH FTLS:  1;  MAGNETOSPHERE FTES:  1
SIGN OF MAGNETOSHEATH BL IS:  2( 3);  SIGN OF MAGNETOSHEATH BM IS:  1( 1)
DIRECTION OF NORMAL USED FOR PLOTTING DATA IN GSM: ( .784;-.503; .363)

*****
MP LOCATION IS: YEAR=1977; MONTH=12; DAY= 7; TIME= 9.29 UT; OUTBOUND; R=14.6; LT= 549; LAT= 39
MAGNETOSHEATH FTLS:  0;  MAGNETOSPHERE FTES:  0
SIGN OF MAGNETOSHEATH BL IS:  2;  SIGN OF MAGNETOSHEATH BM IS:  3
DIRECTION OF NORMAL USED FOR PLOTTING DATA IN GSM: ( .712;-.335; .617)

*****
MP LOCATION IS: YEAR=1977; MONTH=12; DAY= 9; TIME= 5.04 UT; INBOUND; R=10.7; LT= 920; LAT= 26.
MAGNETOSHEATH FTLS:  2;  MAGNETOSPHERE FTES:  1
SIGN OF MAGNETOSHEATH BL IS:  2( 1);  SIGN OF MAGNETOSHEATH BM IS:  3( 3)
DIRECTION OF NORMAL USED FOR PLOTTING DATA IN GSM: ( .903;-.102; .414)

*****
MP LOCATION IS: YEAR=1977; MONTH=12; DAY=11; TIME=14.35 UT; INBOUND; R=10.4; LT= 916; LAT= 27.
MAGNETOSHEATH FTLS:  0;  MAGNETOSPHERE FTES:  1
SIGN OF MAGNETOSHEATH BL IS:  3( 3);  SIGN OF MAGNETOSHEATH BM IS:  3( 3)
DIRECTION OF NORMAL USED FOR PLOTTING DATA IN GSM: ( .870; .135; .474)

*****
MP LOCATION IS: YEAR=1977; MONTH=12; DAY=12; TIME= 3.43 UT; OUTBOUND; R=14.1; LT= 526; LAT= 23
MAGNETOSHEATH FTLS:  1;  MAGNETOSPHERE FTES:  3
SIGN OF MAGNETOSHEATH BL IS:  1;  SIGN OF MAGNETOSHEATH BM IS:  2
DIRECTION OF NORMAL USED FOR PLOTTING DATA IN GSM: ( .470;-.813; .343)

*****
MP LOCATION IS: YEAR=1977; MONTH=12; DAY=13; TIME=21.34 UT; INBOUND; R=13.2; LT= 818; LAT= 15.3
MAGNETOSHEATH FTLS:  2;  MAGNETOSPHERE FTES:  2
SIGN OF MAGNETOSHEATH BL IS:  2( 2);  SIGN OF MAGNETOSHEATH BM IS:  3( 3)
DIRECTION OF NORMAL USED FOR PLOTTING DATA IN GSM: ( .873;-.435; .220)

*****
MP LOCATION IS: YEAR=1977; MONTH=12; DAY=14; TIME=17.50 UT; OUTBOUND; R=17.9; LT= 547; LAT= 21.
MAGNETOSHEATH FTLS:  0;  MAGNETOSPHERE FTES:  3
SIGN OF MAGNETOSHEATH BL IS:  3;  SIGN OF MAGNETOSHEATH BM IS:  3
DIRECTION OF NORMAL USED FOR PLOTTING DATA IN GSM: ( .426;-.843; .329)

*****
MP LOCATION IS: YEAR=1977; MONTH=12; DAY=16; TIME= 6.39 UT; INBOUND; R=13.4; LT= 824; LAT= 30.1
MAGNETOSHEATH FTLS:  1;  MAGNETOSPHERE FTES:  1
SIGN OF MAGNETOSHEATH BL IS:  3( 3);  SIGN OF MAGNETOSHEATH BM IS:  1( 1)
DIRECTION OF NORMAL USED FOR PLOTTING DATA IN GSM: ( .670;-.589; .453)

*****
MP LOCATION IS: YEAR=1977; MONTH=12; DAY=16; TIME=23.29 UT; OUTBOUND; R=15.1; LT= 519; LAT= 12.
MAGNETOSHEATH FTLS:  0;  MAGNETOSPHERE FTES:  3
SIGN OF MAGNETOSHEATH BL IS:  1;  SIGN OF MAGNETOSHEATH BM IS:  3
DIRECTION OF NORMAL USED FOR PLOTTING DATA IN GSM: ( .491;-.880; .197)
```

```
*****  MP LOCATION IS: YEAR=1977; MONTH=12; DAY=10; TIME=16.29 UT; INBOUND; R=12.8; LT= 811; LAT= 22.4
       MAGNETOSHEATH FTES:  0;  MAGNETOSPHERE FTES:  0
       SIGN OF MAGNETOSHEATH BL IS:  2( 2);  SIGN OF MAGNETOSHEATH BM IS:  2( 2)
       DIRECTION OF NORMAL USED FOR PLOTTING DATA IN GSM: ( .750;-.563; .348)

*****  MP LOCATION IS: YEAR=1977; MONTH=12; DAY=10; TIME=13.26 UT; OUTBOUND; R=18.5; LT= 530; LAT= 32.5
       MAGNETOSHEATH FTES:  0;  MAGNETOSPHERE FTES:  0
       SIGN OF MAGNETOSHEATH BL IS:  2;  SIGN OF MAGNETOSHEATH BM IS:  3
       DIRECTION OF NORMAL USED FOR PLOTTING DATA IN GSM: ( .413;-.757; .507)

*****  MP LOCATION IS: YEAR=1977; MONTH=12; DAY=21; TIME= 1.08 UT; INBOUND; R=13.7; LT= 747; LAT= 13.2
       MAGNETOSHEATH FTES:  0;  MAGNETOSPHERE FTES:  0
       SIGN OF MAGNETOSHEATH BL IS:  2;  SIGN OF MAGNETOSHEATH BM IS:  3
       DIRECTION OF NORMAL USED FOR PLOTTING DATA IN GSM: ( .758;-.617; .212)

*****  MP LOCATION IS: YEAR=1977; MONTH=12; DAY=21; TIME= 2.34 UT; INBOUND; R=12.2; LT= 802; LAT= 15.9
       MAGNETOSHEATH FTES:  0;  MAGNETOSPHERE FTES:  0
       SIGN OF MAGNETOSHEATH BL IS:  2( 2);  SIGN OF MAGNETOSHEATH BM IS:  2( 2)
       DIRECTION OF NORMAL USED FOR PLOTTING DATA IN GSM: ( .758;-.617; .212)

*****  MP LOCATION IS: YEAR=1977; MONTH=12; DAY=21; TIME=19.46 UT; OUTBOUND; R=16.4; LT= 510; LAT= 14.1
       MAGNETOSHEATH FTES:  1;  MAGNETOSPHERE FTES:  1
       SIGN OF MAGNETOSHEATH BL IS:  1;  SIGN OF MAGNETOSHEATH BM IS:  1
       DIRECTION OF NORMAL USED FOR PLOTTING DATA IN GSM: ( .543;-.765; .346)

*****  MP LOCATION IS: YEAR=1977; MONTH=12; DAY=23; TIME=12.23 UT; INBOUND; R=11.5; LT= 812; LAT= 28.6
       MAGNETOSHEATH FTES:  0;  MAGNETOSPHERE FTES:  0
       SIGN OF MAGNETOSHEATH BL IS:  2;  SIGN OF MAGNETOSHEATH BM IS:  1
       DIRECTION OF NORMAL USED FOR PLOTTING DATA IN GSM: ( .737;-.569; .366)

*****  MP LOCATION IS: YEAR=1977; MONTH=12; DAY=24; TIME= 5.31 UT; OUTBOUND; R=16.7; LT= 500; LAT= 23.4
       MAGNETOSHEATH FTES:  1;  MAGNETOSPHERE FTES:  0
       SIGN OF MAGNETOSHEATH BL IS:  1;  SIGN OF MAGNETOSHEATH BM IS:  1
       DIRECTION OF NORMAL USED FOR PLOTTING DATA IN GSM: ( .376;-.846; .379)

*****  MP LOCATION IS: YEAR=1977; MONTH=12; DAY=25; TIME=22.33 UT; INBOUND; R=10.5; LT= 757; LAT=  8.5
       MAGNETOSHEATH FTES:  1;  MAGNETOSPHERE FTES:  0
       SIGN OF MAGNETOSHEATH BL IS:  2( 1);  SIGN OF MAGNETOSHEATH BM IS:  3( 3)
       DIRECTION OF NORMAL USED FOR PLOTTING DATA IN GSM: ( .750;-.651; .112)

*****  MP LOCATION IS: YEAR=1977; MONTH=12; DAY=26; TIME=12.51 UT; OUTBOUND; R=15.1; LT= 432; LAT= 29.2
       MAGNETOSHEATH FTES:  0;  MAGNETOSPHERE FTES:  0
       SIGN OF MAGNETOSHEATH BL IS:  2;  SIGN OF MAGNETOSHEATH BM IS:  2
       DIRECTION OF NORMAL USED FOR PLOTTING DATA IN GSM: ( .490;-.763; .423)

*****  MP LOCATION IS: YEAR=1977; MONTH=12; DAY=28; TIME= 6.24 UT; INBOUND; R=12.3; LT= 740; LAT= 24.4
       MAGNETOSHEATH FTES:  1;  MAGNETOSPHERE FTES:  1
       SIGN OF MAGNETOSHEATH BL IS:  1( 1);  SIGN OF MAGNETOSHEATH BM IS:  1( 1)
       DIRECTION OF NORMAL USED FOR PLOTTING DATA IN GSM: ( .650;-.688; .315)

*****  MP LOCATION IS: YEAR=1977; MONTH=12; DAY=30; TIME=13.23 UT; INBOUND; R=14.8; LT= 708; LAT= 27.1
       MAGNETOSHEATH FTES:  1;  MAGNETOSPHERE FTES:  0
       SIGN OF MAGNETOSHEATH BL IS:  2;  SIGN OF MAGNETOSHEATH BM IS:  2
       DIRECTION OF NORMAL USED FOR PLOTTING DATA IN GSM: ( .698;-.630; .341)

*****  MP LOCATION IS: YEAR=1977; MONTH=12; DAY=31; TIME=11.42 UT; OUTBOUND; R=16.2; LT= 437; LAT= 30.0
       MAGNETOSHEATH FTES:  0;  MAGNETOSPHERE FTES:  0
       SIGN OF MAGNETOSHEATH BL IS:  1;  SIGN OF MAGNETOSHEATH BM IS:  2
       DIRECTION OF NORMAL USED FOR PLOTTING DATA IN GSM: ( .327;-.817; .475)

*****  MP LOCATION IS: YEAR=1978; MONTH= 1; DAY= 2; TIME= 3.10 UT; INBOUND; R= 9.8; LT= 738; LAT= 10.4
       MAGNETOSHEATH FTES:  1;  MAGNETOSPHERE FTES:  0
       SIGN OF MAGNETOSHEATH BL IS:  1( 1);  SIGN OF MAGNETOSHEATH BM IS:  2( 2)
       DIRECTION OF NORMAL USED FOR PLOTTING DATA IN GSM: ( .464;-.402; .200)

*****  MP LOCATION IS: YEAR=1978; MONTH= 1; DAY= 2; TIME=21.15 UT; OUTBOUND; R=18.4; LT= 441; LAT=  7.6
       MAGNETOSHEATH FTES:  0;  MAGNETOSPHERE FTES:  0
       SIGN OF MAGNETOSHEATH BL IS:  2;  SIGN OF MAGNETOSHEATH BM IS:  2
       DIRECTION OF NORMAL USED FOR PLOTTING DATA IN GSM: ( .494;-.869; .024)

*****  MP LOCATION IS: YEAR=1978; MONTH= 1; DAY= 4; TIME=13.11 UT; INBOUND; R= 9.8; LT= 748; LAT= 22.1
       MAGNETOSHEATH FTES:  0;  MAGNETOSPHERE FTES:  1
       SIGN OF MAGNETOSHEATH BL IS:  1;  SIGN OF MAGNETOSHEATH BM IS:  2
       DIRECTION OF NORMAL USED FOR PLOTTING DATA IN GSM: ( .704;-.640; .307)

*****  MP LOCATION IS: YEAR=1978; MONTH= 1; DAY= 7; TIME=16.12 UT; OUTBOUND; R=18.4; LT= 419; LAT= 17.9
       MAGNETOSHEATH FTES:  0;  MAGNETOSPHERE FTES:  0
       SIGN OF MAGNETOSHEATH BL IS:  2;  SIGN OF MAGNETOSHEATH BM IS:  3
       DIRECTION OF NORMAL USED FOR PLOTTING DATA IN GSM: ( .478;-.859; .186)

*****  MP LOCATION IS: YEAR=1978; MONTH= 1; DAY= 7; TIME=19.10 UT; OUTBOUND; R=19.9; LT= 435; LAT= 10.0
       MAGNETOSHEATH FTES:  0;  MAGNETOSPHERE FTES:  0
       SIGN OF MAGNETOSHEATH BL IS:  2;  SIGN OF MAGNETOSHEATH BM IS:  3
       DIRECTION OF NORMAL USED FOR PLOTTING DATA IN GSM: ( .315;-.933; .176)

*****  MP LOCATION IS: YEAR=1978; MONTH= 1; DAY= 9; TIME=  .40 UT; INBOUND; R=16.6; LT= 613; LAT=  2.9
       MAGNETOSHEATH FTES:  1;  MAGNETOSPHERE FTES:  0
       SIGN OF MAGNETOSHEATH BL IS:  2( 2);  SIGN OF MAGNETOSHEATH BM IS:  1( 1)
       DIRECTION OF NORMAL USED FOR PLOTTING DATA IN GSM: ( .588;-.809;-.013)

*****  MP LOCATION IS: YEAR=1978; MONTH= 1; DAY= 9; TIME= 2.30 UT; INBOUND; R=15.1; LT= 624; LAT=  7.3
       MAGNETOSHEATH FTES:  0;  MAGNETOSPHERE FTES:  1
       SIGN OF MAGNETOSHEATH BL IS:  1;  SIGN OF MAGNETOSHEATH BM IS:  1
       DIRECTION OF NORMAL USED FOR PLOTTING DATA IN GSM: ( .493;-.867; .071)

*****  MP LOCATION IS: YEAR=1978; MONTH= 1; DAY=10; TIME= 1.35 UT; OUTBOUND; R=18.4; LT= 415; LAT=  7.3
       MAGNETOSHEATH FTES:  1;  MAGNETOSPHERE FTES:  1
       SIGN OF MAGNETOSHEATH BL IS:  1;  SIGN OF MAGNETOSHEATH BM IS:  1
       DIRECTION OF NORMAL USED FOR PLOTTING DATA IN GSM: ( .290;-.947; .140)

*****  MP LOCATION IS: YEAR=1978; MONTH= 1; DAY=11; TIME=12.33 UT; INBOUND; R=14.6; LT= 619; LAT= 23.5
       MAGNETOSHEATH FTES:  1;  MAGNETOSPHERE FTES:  1
       SIGN OF MAGNETOSHEATH BL IS:  1;  SIGN OF MAGNETOSHEATH BM IS:  2
       DIRECTION OF NORMAL USED FOR PLOTTING DATA IN GSM: ( .314;-.878; .361)

*****  MP LOCATION IS: YEAR=1978; MONTH= 1; DAY=12; TIME=19.15 UT; OUTBOUND; R=21.8; LT= 436; LAT=  7.8
       MAGNETOSHEATH FTES:  0;  MAGNETOSPHERE FTES:  0
       SIGN OF MAGNETOSHEATH BL IS:  2;  SIGN OF MAGNETOSHEATH BM IS:  1
       DIRECTION OF NORMAL USED FOR PLOTTING DATA IN GSM: ( .279;-.949; .149)

*****  MP LOCATION IS: YEAR=1978; MONTH= 1; DAY=13; TIME=10.51 UT; INBOUND; R=17.0; LT= 552; LAT=  5.0
       MAGNETOSHEATH FTES:  0;  MAGNETOSPHERE FTES:  0
       SIGN OF MAGNETOSHEATH BL IS:  1;  SIGN OF MAGNETOSHEATH BM IS:  1
       DIRECTION OF NORMAL USED FOR PLOTTING DATA IN GSM: ( .475;-.877; .072)

*****  MP LOCATION IS: YEAR=1978; MONTH= 1; DAY=13; TIME=20.00 UT; INBOUND; R=16.1; LT= 558; LAT=  3.0
       MAGNETOSHEATH FTES:  1;  MAGNETOSPHERE FTES:  0
       SIGN OF MAGNETOSHEATH BL IS:  1;  SIGN OF MAGNETOSHEATH BM IS:  1
       DIRECTION OF NORMAL USED FOR PLOTTING DATA IN GSM: ( .457;-.885; .087)
```

```
MP LOCATION IS: YEAR=1970; MONTH= 1; DAY=12; TIME=22.25 UT; INBOUND; R=14.0; LT= 613; LAT=  -.5
MAGNETOSHEATH FTES:  0;  MAGNETOSPHERE FTES:  0
SIGN OF MAGNETOSHEATH BL IS:  1;  SIGN OF MAGNETOSHEATH BM IS:  1
DIRECTION OF NORMAL USED FOR PLOTTING DATA IN GSM: ( .451;-.857;-.213)

*****

MP LOCATION IS: YEAR=1970; MONTH= 1; DAY=15; TIME= 3.39 UT; OUTBOUND; R=21.6; LT= 423; LAT= 10.5
MAGNETOSHEATH FTES:  1;  MAGNETOSPHERE FTES:  1
SIGN OF MAGNETOSHEATH BL IS:  1;  SIGN OF MAGNETOSHEATH BM IS:  1
DIRECTION OF NORMAL USED FOR PLOTTING DATA IN GSM: ( .316;-.949;0.000)

*****

MP LOCATION IS: YEAR=1970; MONTH= 1; DAY=16; TIME= 8.40 UT; INBOUND; R=13.0; LT= 612; LAT= 20.8
MAGNETOSHEATH FTES:  1;  MAGNETOSPHERE FTES:  1
SIGN OF MAGNETOSHEATH BL IS:  -1( 3);  SIGN OF MAGNETOSHEATH BM IS:  1( 3)
DIRECTION OF NORMAL USED FOR PLOTTING DATA IN GSM: ( .445;-.815; .371)

*****

MP LOCATION IS: YEAR=1970; MONTH= 1; DAY=17; TIME= 7.00 UT; OUTBOUND; R=19.2; LT= 349; LAT= 19.7
MAGNETOSHEATH FTES:  0;  MAGNETOSPHERE FTES:  0
SIGN OF MAGNETOSHEATH BL IS:  -1;  SIGN OF MAGNETOSHEATH BM IS:  1
DIRECTION OF NORMAL USED FOR PLOTTING DATA IN GSM: ( .269;-.846; .461)

*****

MP LOCATION IS: YEAR=1970; MONTH= 1; DAY=18; TIME=13.46 UT; INBOUND; R=16.8; LT= 534; LAT= 19.2
MAGNETOSHEATH FTES:  1;  MAGNETOSPHERE FTES:  3
SIGN OF MAGNETOSHEATH BL IS:  1;  SIGN OF MAGNETOSHEATH BM IS:  2
DIRECTION OF NORMAL USED FOR PLOTTING DATA IN GSM: ( .444;-.855; .268)

*****

MP LOCATION IS: YEAR=1970; MONTH= 1; DAY=19; TIME=23.36 UT; OUTBOUND; R=21.9; LT= 411; LAT=  1.8
MAGNETOSHEATH FTES:  0;  MAGNETOSPHERE FTES:  1
SIGN OF MAGNETOSHEATH BL IS:  1;  SIGN OF MAGNETOSHEATH BM IS:  1
DIRECTION OF NORMAL USED FOR PLOTTING DATA IN GSM: ( .340;-.939;-.021)


*****

MP LOCATION IS: YEAR=1970; MONTH= 1; DAY=20; TIME=19.23 UT; INBOUND; R=19.2; LT= 510; LAT=  2.5
MAGNETOSHEATH FTES:  0;  MAGNETOSPHERE FTES:  0
SIGN OF MAGNETOSHEATH BL IS:  -1;  SIGN OF MAGNETOSHEATH BM IS:  1
DIRECTION OF NORMAL USED FOR PLOTTING DATA IN GSM: ( .388;-.917;-.096)

*****

MP LOCATION IS: YEAR=1970; MONTH= 1; DAY=22; TIME= 5.00 UT; OUTBOUND; R=20.7; LT= 347; LAT= 12.7
MAGNETOSHEATH FTES:  0;  MAGNETOSPHERE FTES:  0
SIGN OF MAGNETOSHEATH BL IS:  -1;  SIGN OF MAGNETOSHEATH BM IS:  1
DIRECTION OF NORMAL USED FOR PLOTTING DATA IN GSM: ( .206;-.931; .303)

*****

MP LOCATION IS: YEAR=1970; MONTH= 1; DAY=23; TIME= 4.09 UT; INBOUND; R=19.5; LT= 458; LAT=  7.2
MAGNETOSHEATH FTES:  1;  MAGNETOSPHERE FTES:  1
SIGN OF MAGNETOSHEATH BL IS:  -1;  SIGN OF MAGNETOSHEATH BM IS:  1
DIRECTION OF NORMAL USED FOR PLOTTING DATA IN GSM: ( .457;-.885; .086)

*****

MP LOCATION IS: YEAR=1970; MONTH= 1; DAY=23; TIME= 8.29 UT; INBOUND; R=16.8; LT= 516; LAT= 18.9
MAGNETOSHEATH FTES:  1;  MAGNETOSPHERE FTES:  1
SIGN OF MAGNETOSHEATH BL IS:  1;  SIGN OF MAGNETOSHEATH BM IS:  1
DIRECTION OF NORMAL USED FOR PLOTTING DATA IN GSM: ( .474;-.838; .269)

*****

MP LOCATION IS: YEAR=1970; MONTH= 7; DAY= 2; TIME= 7.20 UT; OUTBOUND; R=19.5; LT=1839; LAT=  3.7
MAGNETOSHEATH FTES:  2;  MAGNETOSPHERE FTES:  2
SIGN OF MAGNETOSHEATH BL IS:  1;  SIGN OF MAGNETOSHEATH BM IS:  1
DIRECTION OF NORMAL USED FOR PLOTTING DATA IN GSM: ( .351; .936;-.023)

*****

MP LOCATION IS: YEAR=1970; MONTH= 7; DAY= 4; TIME=21.52 UT; INBOUND; R=16.2; LT=1859; LAT= 20.1
MAGNETOSHEATH FTES:  2;  MAGNETOSPHERE FTES:  0
SIGN OF MAGNETOSHEATH BL IS:  1;  SIGN OF MAGNETOSHEATH BM IS:  1
DIRECTION OF NORMAL USED FOR PLOTTING DATA IN GSM: ( .390; .871; .298)

*****

MP LOCATION IS: YEAR=1970; MONTH= 7; DAY= 5; TIME=14.32 UT; OUTBOUND; R=11.7; LT=1601; LAT= 11.9
MAGNETOSHEATH FTES:  1;  MAGNETOSPHERE FTES:  0
SIGN OF MAGNETOSHEATH BL IS:  1( 1);  SIGN OF MAGNETOSHEATH BM IS:  1( 1)
DIRECTION OF NORMAL USED FOR PLOTTING DATA IN GSM: ( .713; .574; .404)

*****

MP LOCATION IS: YEAR=1970; MONTH= 7; DAY= 7; TIME= 7.02 UT; INBOUND; R=16.3; LT=1845; LAT=  .8
MAGNETOSHEATH FTES:  0;  MAGNETOSPHERE FTES:  0
SIGN OF MAGNETOSHEATH BL IS:  -1;  SIGN OF MAGNETOSHEATH BM IS:  3
DIRECTION OF NORMAL USED FOR PLOTTING DATA IN GSM: ( .477; .876; .077)

*****

MP LOCATION IS: YEAR=1970; MONTH= 7; DAY= 7; TIME=23.51 UT; OUTBOUND; R=11.7; LT=1538; LAT= 26.9
MAGNETOSHEATH FTES:  1;  MAGNETOSPHERE FTES:  1
SIGN OF MAGNETOSHEATH BL IS:  1( 1);  SIGN OF MAGNETOSHEATH BM IS:  1( 1)
DIRECTION OF NORMAL USED FOR PLOTTING DATA IN GSM: ( .939; .280;-.199)

*****

MP LOCATION IS: YEAR=1970; MONTH= 7; DAY= 9; TIME=12.59 UT; INBOUND; R=18.5; LT=1820; LAT= -3.1
MAGNETOSHEATH FTES:  3;  MAGNETOSPHERE FTES:  0
SIGN OF MAGNETOSHEATH BL IS:  -1;  SIGN OF MAGNETOSHEATH BM IS:  2
DIRECTION OF NORMAL USED FOR PLOTTING DATA IN GSM: ( .405; .914;-.037)

*****

MP LOCATION IS: YEAR=1970; MONTH= 7; DAY= 9; TIME=13.38 UT; INBOUND; R=18.2; LT=1823; LAT= -2.2
MAGNETOSHEATH FTES:  0;  MAGNETOSPHERE FTES:  2
SIGN OF MAGNETOSHEATH BL IS:  1;  SIGN OF MAGNETOSHEATH BM IS:  1
DIRECTION OF NORMAL USED FOR PLOTTING DATA IN GSM: ( .405; .914;-.037)

*****

MP LOCATION IS: YEAR=1970; MONTH= 7; DAY= 9; TIME=15.20 UT; INBOUND; R=17.1; LT=1831; LAT=  1.4
MAGNETOSHEATH FTES:  0;  MAGNETOSPHERE FTES:  2
SIGN OF MAGNETOSHEATH BL IS:  1;  SIGN OF MAGNETOSHEATH BM IS:  1
DIRECTION OF NORMAL USED FOR PLOTTING DATA IN GSM: ( .403; .915; .014)

*****

MP LOCATION IS: YEAR=1970; MONTH= 7; DAY=10; TIME= 8.25 UT; OUTBOUND; R=10.9; LT=1539; LAT=  9.0
MAGNETOSHEATH FTES:  0;  MAGNETOSPHERE FTES:  0
SIGN OF MAGNETOSHEATH BL IS:  1;  SIGN OF MAGNETOSHEATH BM IS:  1
DIRECTION OF NORMAL USED FOR PLOTTING DATA IN GSM: ( .698; .543; .467)

*****

MP LOCATION IS: YEAR=1970; MONTH= 7; DAY=10; TIME=10.49 UT; OUTBOUND; R=13.3; LT=1601; LAT=  5.5
MAGNETOSHEATH FTES:  2;  MAGNETOSPHERE FTES:  2
SIGN OF MAGNETOSHEATH BL IS:  1( 1);  SIGN OF MAGNETOSHEATH BM IS:  1( 1)
DIRECTION OF NORMAL USED FOR PLOTTING DATA IN GSM: ( .772; .593; .202)

*****

MP LOCATION IS: YEAR=1970; MONTH= 7; DAY=12; TIME=17.40 UT; OUTBOUND; R=10.6; LT=1521; LAT= 18.5
MAGNETOSHEATH FTES:  0;  MAGNETOSPHERE FTES:  0
SIGN OF MAGNETOSHEATH BL IS:  -1;  SIGN OF MAGNETOSHEATH BM IS:  1
DIRECTION OF NORMAL USED FOR PLOTTING DATA IN GSM: ( .704; .558; .252)

*****

MP LOCATION IS: YEAR=1970; MONTH= 7; DAY=12; TIME=18.15 UT; OUTBOUND; R=11.3; LT=1528; LAT= 19.6
MAGNETOSHEATH FTES:  0;  MAGNETOSPHERE FTES:  0
SIGN OF MAGNETOSHEATH BL IS:  1( 3);  SIGN OF MAGNETOSHEATH BM IS:  1( 1)
DIRECTION OF NORMAL USED FOR PLOTTING DATA IN GSM: ( .704; .568; .252)

*****

MP LOCATION IS: YEAR=1970; MONTH= 7; DAY=13; TIME= 2.52 UT; OUTBOUND; R=10.5; LT=1509; LAT= 20.2
MAGNETOSHEATH FTES:  0;  MAGNETOSPHERE FTES:  0
SIGN OF MAGNETOSHEATH BL IS:  -1;  SIGN OF MAGNETOSHEATH BM IS:  2
DIRECTION OF NORMAL USED FOR PLOTTING DATA IN GSM: ( .811; .523; .262)
```

```
*****
MP LOCATION IS: YEAR=1978; MONTH= 7; DAY=19; TIME= 6.55 UT; INBOUND; R=15.2; LT=1809; LAT= -5.2
MAGNETOSHEATH FTES:  1;  MAGNETOSPHERE FTES:  1
SIGN OF MAGNETOSHEATH BL IS:  1;  SIGN OF MAGNETOSHEATH BM IS:  2
DIRECTION OF NORMAL USED FOR PLOTTING DATA IN GSM: ( .516; .856; .014)

*****
MP LOCATION IS: YEAR=1978; MONTH= 7; DAY=19; TIME=23.00 UT; OUTBOUND; R=12.2; LT=1502; LAT= 23.6
MAGNETOSHEATH FTES:  0;  MAGNETOSPHERE FTES:  0
SIGN OF MAGNETOSHEATH BL IS:  2( 2);  SIGN OF MAGNETOSHEATH BM IS:  2( 2)
DIRECTION OF NORMAL USED FOR PLOTTING DATA IN GSM: ( .792; .520; .319)

*****
MP LOCATION IS: YEAR=1978; MONTH= 7; DAY=21; TIME=12.37 UT; INBOUND; R=18.0; LT=1740; LAT= -8.8
MAGNETOSHEATH FTES:  2;  MAGNETOSPHERE FTES:  0
SIGN OF MAGNETOSHEATH BL IS:  1( 1);  SIGN OF MAGNETOSHEATH BM IS:  1( 1)
DIRECTION OF NORMAL USED FOR PLOTTING DATA IN GSM: ( .725; .588;-.358)

*****
MP LOCATION IS: YEAR=1978; MONTH= 7; DAY=24; TIME=  .30 UT; INBOUND; R=16.2; LT=1743; LAT= 10.8
MAGNETOSHEATH FTES:  0;  MAGNETOSPHERE FTES:  0
SIGN OF MAGNETOSHEATH BL IS:  2;  SIGN OF MAGNETOSHEATH BM IS:  2
DIRECTION OF NORMAL USED FOR PLOTTING DATA IN GSM: ( .445; .712; .544)

*****
MP LOCATION IS: YEAR=1978; MONTH= 7; DAY=24; TIME=16.30 UT; OUTBOUND; R=10.7; LT=1446; LAT= 14.3
MAGNETOSHEATH FTES:  0;  MAGNETOSPHERE FTES:  0
SIGN OF MAGNETOSHEATH BL IS:  2( 2);  SIGN OF MAGNETOSHEATH BM IS:  2( 2)
DIRECTION OF NORMAL USED FOR PLOTTING DATA IN GSM: ( .703; .142; .696)

*****
MP LOCATION IS: YEAR=1978; MONTH= 7; DAY=26; TIME= 9.40 UT; INBOUND; R=16.4; LT=1733; LAT=-11.9
MAGNETOSHEATH FTES:  0;  MAGNETOSPHERE FTES:  0
SIGN OF MAGNETOSHEATH BL IS:  2( 2);  SIGN OF MAGNETOSHEATH BM IS:  2( 2)
DIRECTION OF NORMAL USED FOR PLOTTING DATA IN GSM: ( .398; .906;-.145)

*****
MP LOCATION IS: YEAR=1978; MONTH= 7; DAY=27; TIME= 3.20 UT; OUTBOUND; R=12.5; LT=1450; LAT= 16.3
MAGNETOSHEATH FTES:  0;  MAGNETOSPHERE FTES:  0
SIGN OF MAGNETOSHEATH BL IS:  2( 2);  SIGN OF MAGNETOSHEATH BM IS:  2( 2)
DIRECTION OF NORMAL USED FOR PLOTTING DATA IN GSM: ( .932; .342; .347)

*****
MP LOCATION IS: YEAR=1978; MONTH= 7; DAY=28; TIME=19.56 UT; INBOUND; R=15.7; LT=1729; LAT=  7.5
MAGNETOSHEATH FTES:  2;  MAGNETOSPHERE FTES:  2
SIGN OF MAGNETOSHEATH BL IS:  1( 2);  SIGN OF MAGNETOSHEATH BM IS:  1( 1)
DIRECTION OF NORMAL USED FOR PLOTTING DATA IN GSM: ( .620; .784; .038)

*****
MP LOCATION IS: YEAR=1978; MONTH= 7; DAY=29; TIME=11.22 UT; OUTBOUND; R=11.0; LT=1438; LAT=  7.2
MAGNETOSHEATH FTES:  2;  MAGNETOSPHERE FTES:  1
SIGN OF MAGNETOSHEATH BL IS:  2( 1);  SIGN OF MAGNETOSHEATH BM IS:  1( 1)
DIRECTION OF NORMAL USED FOR PLOTTING DATA IN GSM: ( .840; .326; .434)

*****
MP LOCATION IS: YEAR=1978; MONTH= 7; DAY=31; TIME= 4.45 UT; INBOUND; R=16.1; LT=1718; LAT= -2.3
MAGNETOSHEATH FTES:  0;  MAGNETOSPHERE FTES:  2
SIGN OF MAGNETOSHEATH BL IS:  2( 2);  SIGN OF MAGNETOSHEATH BM IS:  1( 1)
DIRECTION OF NORMAL USED FOR PLOTTING DATA IN GSM: ( .535; .827;-.175)

*****
MP LOCATION IS: YEAR=1978; MONTH= 7; DAY=31; TIME=20.51 UT; OUTBOUND; R=11.1; LT=1414; LAT= 20.8
MAGNETOSHEATH FTES:  1;  MAGNETOSPHERE FTES:  1
SIGN OF MAGNETOSHEATH BL IS:  2( 3);  SIGN OF MAGNETOSHEATH BM IS:  1( 1)
DIRECTION OF NORMAL USED FOR PLOTTING DATA IN GSM: ( .486; .402; .776)

*****
MP LOCATION IS: YEAR=1978; MONTH= 8; DAY= 2; TIME= 4.21 UT; OUTBOUND; R= 8.6; LT=1347; LAT= 17.5
MAGNETOSHEATH FTES:  4;  MAGNETOSPHERE FTES:  1
SIGN OF MAGNETOSHEATH BL IS:  2( 1);  SIGN OF MAGNETOSHEATH BM IS:  1( 1)
DIRECTION OF NORMAL USED FOR PLOTTING DATA IN GSM: ( .868; .312; .386)

*****
MP LOCATION IS: YEAR=1978; MONTH= 8; DAY= 5; TIME=  .59 UT; INBOUND; R=14.8; LT=1709; LAT=  4.5
MAGNETOSHEATH FTES:  0;  MAGNETOSPHERE FTES:  0
SIGN OF MAGNETOSHEATH BL IS:  2( 2);  SIGN OF MAGNETOSHEATH BM IS:  1( 1)
DIRECTION OF NORMAL USED FOR PLOTTING DATA IN GSM: ( .531; .840;-.110)

*****
MP LOCATION IS: YEAR=1978; MONTH= 8; DAY= 5; TIME= 1.25 UT; INBOUND; R=14.3; LT=1712; LAT=  3.6
MAGNETOSHEATH FTES:  2;  MAGNETOSPHERE FTES:  2
SIGN OF MAGNETOSHEATH BL IS:  2;  SIGN OF MAGNETOSHEATH BM IS:  1
DIRECTION OF NORMAL USED FOR PLOTTING DATA IN GSM: ( .531; .840;-.110)

*****
MP LOCATION IS: YEAR=1978; MONTH= 8; DAY= 5; TIME=13.54 UT; OUTBOUND; R= 9.0; LT=1355; LAT= 12.5
MAGNETOSHEATH FTES:  0;  MAGNETOSPHERE FTES:  1
SIGN OF MAGNETOSHEATH BL IS:  2;  SIGN OF MAGNETOSHEATH BM IS:  1
DIRECTION OF NORMAL USED FOR PLOTTING DATA IN GSM: ( .885; .269; .379)

*****
MP LOCATION IS: YEAR=1978; MONTH= 8; DAY= 5; TIME=14.30 UT; OUTBOUND; R= 9.8; LT=1403; LAT= 12.3
MAGNETOSHEATH FTES:  1;  MAGNETOSPHERE FTES:  0
SIGN OF MAGNETOSHEATH BL IS:  2( 1);  SIGN OF MAGNETOSHEATH BM IS:  1( 1)
DIRECTION OF NORMAL USED FOR PLOTTING DATA IN GSM: ( .885; .269; .379)

*****
MP LOCATION IS: YEAR=1978; MONTH= 8; DAY= 7; TIME= 9.04 UT; INBOUND; R=15.9; LT=1649; LAT=-14.9
MAGNETOSHEATH FTES:  0;  MAGNETOSPHERE FTES:  0
SIGN OF MAGNETOSHEATH BL IS:  2;  SIGN OF MAGNETOSHEATH BM IS:  1
DIRECTION OF NORMAL USED FOR PLOTTING DATA IN GSM: ( .777; .537;-.328)

*****
MP LOCATION IS: YEAR=1978; MONTH= 8; DAY= 8; TIME= 2.43 UT; OUTBOUND; R=13.2; LT=1417; LAT= 16.3
MAGNETOSHEATH FTES:  0;  MAGNETOSPHERE FTES:  0
SIGN OF MAGNETOSHEATH BL IS:  1( 4);  SIGN OF MAGNETOSHEATH BM IS:  1( 1)
DIRECTION OF NORMAL USED FOR PLOTTING DATA IN GSM: ( .830; .207; .518)

*****
MP LOCATION IS: YEAR=1978; MONTH= 8; DAY= 9; TIME=20.10 UT; INBOUND; R=14.4; LT=1653; LAT=  3.2
MAGNETOSHEATH FTES:  2;  MAGNETOSPHERE FTES:  2
SIGN OF MAGNETOSHEATH BL IS:  1( 1);  SIGN OF MAGNETOSHEATH BM IS:  1( 1)
DIRECTION OF NORMAL USED FOR PLOTTING DATA IN GSM: ( .652; .735; .187)

*****
MP LOCATION IS: YEAR=1978; MONTH= 8; DAY=10; TIME= 9.38 UT; OUTBOUND; R=10.4; LT=1359; LAT= 10.4
MAGNETOSHEATH FTES:  1;  MAGNETOSPHERE FTES:  1
SIGN OF MAGNETOSHEATH BL IS:  2( 1);  SIGN OF MAGNETOSHEATH BM IS:  1( 1)
DIRECTION OF NORMAL USED FOR PLOTTING DATA IN GSM: ( .764; .504; .402)

*****
MP LOCATION IS: YEAR=1978; MONTH= 8; DAY=12; TIME= 7.11 UT; INBOUND; R=12.7; LT=1655; LAT=-15.2
MAGNETOSHEATH FTES:  0;  MAGNETOSPHERE FTES:  2
SIGN OF MAGNETOSHEATH BL IS:  2( 1);  SIGN OF MAGNETOSHEATH BM IS:  2( 2)
DIRECTION OF NORMAL USED FOR PLOTTING DATA IN GSM: ( .463; .694;-.552)

*****
MP LOCATION IS: YEAR=1978; MONTH= 8; DAY=12; TIME=18.37 UT; OUTBOUND; R= 9.7; LT=1327; LAT= 19.0
MAGNETOSHEATH FTES:  1;  MAGNETOSPHERE FTES:  0
SIGN OF MAGNETOSHEATH BL IS:  2( 3);  SIGN OF MAGNETOSHEATH BM IS:  1( 1)
DIRECTION OF NORMAL USED FOR PLOTTING DATA IN GSM: ( .703; .087; .701)

*****
MP LOCATION IS: YEAR=1978; MONTH= 8; DAY=14; TIME=14.55 UT; INBOUND; R=14.3; LT=1633; LAT=-12.2
MAGNETOSHEATH FTES:  0;  MAGNETOSPHERE FTES:  0
SIGN OF MAGNETOSHEATH BL IS:  2( 2);  SIGN OF MAGNETOSHEATH BM IS:  2( 2)
DIRECTION OF NORMAL USED FOR PLOTTING DATA IN GSM: ( .527; .850; .003)

*****
MP LOCATION IS: YEAR=1978; MONTH= 8; DAY=14; TIME=15.51 UT; INBOUND; R=13.4; LT=1641; LAT=-10.2
MAGNETOSHEATH FTES:  2;  MAGNETOSPHERE FTES:  0
SIGN OF MAGNETOSHEATH BL IS:  2( 2);  SIGN OF MAGNETOSHEATH BM IS:  3( 3)
DIRECTION OF NORMAL USED FOR PLOTTING DATA IN GSM: ( .527; .850; .003)
```

```
*****
MP LOCATION IS: YEAR=1978; MONTH= 8; DAY=15; TIME= 7.08 UT; OUTBOUND; R=13.5; LT=1405; LAT=  9.8
MAGNETOSHEATH FTES:  1;  MAGNETOSPHERE FTES:  1
SIGN OF MAGNETOSHEATH BL IS:  2( 2);  SIGN OF MAGNETOSHEATH BM IS:  2( 2)
DIRECTION OF NORMAL USED FOR PLOTTING DATA IN GSM: ( .879; .437; .193)

*****
MP LOCATION IS: YEAR=1978; MONTH= 8; DAY=17; TIME= 1.43 UT; INBOUND; R=12.9; LT=1638; LAT= -1.7
MAGNETOSHEATH FTES:  3;  MAGNETOSPHERE FTES:  3
SIGN OF MAGNETOSHEATH BL IS:  1( 1);  SIGN OF MAGNETOSHEATH BM IS:  2( 2)
DIRECTION OF NORMAL USED FOR PLOTTING DATA IN GSM: ( .617; .787; .011)

*****
MP LOCATION IS: YEAR=1978; MONTH= 8; DAY=17; TIME=12.08 UT; OUTBOUND; R= 8.1; LT=1312; LAT= 17.1
MAGNETOSHEATH FTES:  1;  MAGNETOSPHERE FTES:  1
SIGN OF MAGNETOSHEATH BL IS:  1;  SIGN OF MAGNETOSHEATH BM IS:  2
DIRECTION OF NORMAL USED FOR PLOTTING DATA IN GSM: ( .753; .280; .595)

*****
MP LOCATION IS: YEAR=1978; MONTH= 8; DAY=19; TIME=10.39 UT; INBOUND; R=13.4; LT=1618; LAT=-19.6
MAGNETOSHEATH FTES:  2;  MAGNETOSPHERE FTES:  2
SIGN OF MAGNETOSHEATH BL IS:  2( 1);  SIGN OF MAGNETOSHEATH BM IS:  2( 2)
DIRECTION OF NORMAL USED FOR PLOTTING DATA IN GSM: ( .596; .724;-.347)

*****
MP LOCATION IS: YEAR=1978; MONTH= 8; DAY=20; TIME= 1.12 UT; OUTBOUND; R=12.9; LT=1331; LAT= 18.8
MAGNETOSHEATH FTES:  0;  MAGNETOSPHERE FTES:  0
SIGN OF MAGNETOSHEATH BL IS:  3( 3);  SIGN OF MAGNETOSHEATH BM IS:  2( 2)
DIRECTION OF NORMAL USED FOR PLOTTING DATA IN GSM: ( .619; .464; .633)

*****
MP LOCATION IS: YEAR=1978; MONTH= 8; DAY=21; TIME=21.09 UT; INBOUND; R=12.2; LT=1624; LAT= -1.0
MAGNETOSHEATH FTES:  0;  MAGNETOSPHERE FTES:  0
SIGN OF MAGNETOSHEATH BL IS:  3( 3);  SIGN OF MAGNETOSHEATH BM IS:  2( 2)
DIRECTION OF NORMAL USED FOR PLOTTING DATA IN GSM: ( .735; .669; .110)

*****
MP LOCATION IS: YEAR=1978; MONTH= 8; DAY=21; TIME=21.41 UT; INBOUND; R=11.4; LT=1630; LAT= -1.4
MAGNETOSHEATH FTES:  2;  MAGNETOSPHERE FTES:  0
SIGN OF MAGNETOSHEATH BL IS:  1;  SIGN OF MAGNETOSHEATH BM IS:  3
DIRECTION OF NORMAL USED FOR PLOTTING DATA IN GSM: ( .735; .669; .110)

*****
MP LOCATION IS: YEAR=1978; MONTH= 8; DAY=22; TIME= 9.01 UT; OUTBOUND; R=11.1; LT=1330; LAT= 13.5
MAGNETOSHEATH FTES:  0;  MAGNETOSPHERE FTES:  0
SIGN OF MAGNETOSHEATH BL IS:  2( 2);  SIGN OF MAGNETOSHEATH BM IS:  2( 2)
DIRECTION OF NORMAL USED FOR PLOTTING DATA IN GSM: ( .892; .319; .320)

*****
MP LOCATION IS: YEAR=1978; MONTH= 8; DAY=24; TIME= 6.34 UT; INBOUND; R=12.1; LT=1611; LAT=-15.4
MAGNETOSHEATH FTES:  0;  MAGNETOSPHERE FTES:  0
SIGN OF MAGNETOSHEATH BL IS:  3;  SIGN OF MAGNETOSHEATH BM IS:  1
DIRECTION OF NORMAL USED FOR PLOTTING DATA IN GSM: ( .794; .565;-.222)

*****
MP LOCATION IS: YEAR=1978; MONTH= 8; DAY=24; TIME=17.18 UT; OUTBOUND; R= 9.8; LT=1254; LAT= 20.4
MAGNETOSHEATH FTES:  0;  MAGNETOSPHERE FTES:  0
SIGN OF MAGNETOSHEATH BL IS:  2( 2);  SIGN OF MAGNETOSHEATH BM IS:  2( 2)
DIRECTION OF NORMAL USED FOR PLOTTING DATA IN GSM: ( .957; .143; .251)

*****
MP LOCATION IS: YEAR=1978; MONTH= 8; DAY=26; TIME=12.50 UT; INBOUND; R=14.9; LT=1541; LAT=-15.4
MAGNETOSHEATH FTES:  1;  MAGNETOSPHERE FTES:  0
SIGN OF MAGNETOSHEATH BL IS:  1;  SIGN OF MAGNETOSHEATH BM IS:  3
DIRECTION OF NORMAL USED FOR PLOTTING DATA IN GSM: ( .664; .738;-.118)

*****
MP LOCATION IS: YEAR=1978; MONTH= 8; DAY=26; TIME=14.15 UT; INBOUND; R=13.8; LT=1549; LAT=-14.6
MAGNETOSHEATH FTES:  0;  MAGNETOSPHERE FTES:  0
SIGN OF MAGNETOSHEATH BL IS:  1;  SIGN OF MAGNETOSHEATH BM IS:  1
DIRECTION OF NORMAL USED FOR PLOTTING DATA IN GSM: ( .664; .738;-.118)

*****
MP LOCATION IS: YEAR=1978; MONTH= 8; DAY=27; TIME= 2.46 UT; OUTBOUND; R= 9.9; LT=1242; LAT= 21.5
MAGNETOSHEATH FTES:  0;  MAGNETOSPHERE FTES:  0
SIGN OF MAGNETOSHEATH BL IS:  1;  SIGN OF MAGNETOSHEATH BM IS:  1
DIRECTION OF NORMAL USED FOR PLOTTING DATA IN GSM: ( .746; .332; .577)

*****
MP LOCATION IS: YEAR=1978; MONTH= 8; DAY=29; TIME= 1.14 UT; INBOUND; R=12.0; LT=1558; LAT= -3.1
MAGNETOSHEATH FTES:  2;  MAGNETOSPHERE FTES:  3
SIGN OF MAGNETOSHEATH BL IS:  1( 1);  SIGN OF MAGNETOSHEATH BM IS:  3( 3)
DIRECTION OF NORMAL USED FOR PLOTTING DATA IN GSM: ( .933; .358;-.039)

*****
MP LOCATION IS: YEAR=1978; MONTH= 8; DAY=29; TIME=12.16 UT; OUTBOUND; R=10.1; LT=1300; LAT= 18.4
MAGNETOSHEATH FTES:  1;  MAGNETOSPHERE FTES:  1
SIGN OF MAGNETOSHEATH BL IS:  1( 1);  SIGN OF MAGNETOSHEATH BM IS:  1( 1)
DIRECTION OF NORMAL USED FOR PLOTTING DATA IN GSM: ( .837; .011; .548)

*****
MP LOCATION IS: YEAR=1978; MONTH= 8; DAY=31; TIME=10.18 UT; INBOUND; R=12.4; LT=1536; LAT=-19.5
MAGNETOSHEATH FTES:  3;  MAGNETOSPHERE FTES:  0
SIGN OF MAGNETOSHEATH BL IS:  1( 1);  SIGN OF MAGNETOSHEATH BM IS:  1( 1)
DIRECTION OF NORMAL USED FOR PLOTTING DATA IN GSM: ( .831; .396;-.390)

*****
MP LOCATION IS: YEAR=1978; MONTH= 8; DAY=31; TIME=21.55 UT; OUTBOUND; R=10.6; LT=1225; LAT= 22.6
MAGNETOSHEATH FTES:  0;  MAGNETOSPHERE FTES:  0
SIGN OF MAGNETOSHEATH BL IS:  2( 2);  SIGN OF MAGNETOSHEATH BM IS:  1( 1)
DIRECTION OF NORMAL USED FOR PLOTTING DATA IN GSM: ( .793;-.256; .553)

*****
MP LOCATION IS: YEAR=1978; MONTH= 9; DAY= 2; TIME=19.35 UT; INBOUND; R=12.3; LT=1537; LAT= -3.3
MAGNETOSHEATH FTES:  2;  MAGNETOSPHERE FTES:  3
SIGN OF MAGNETOSHEATH BL IS:  1( 1);  SIGN OF MAGNETOSHEATH BM IS:  1( 1)
DIRECTION OF NORMAL USED FOR PLOTTING DATA IN GSM: ( .809; .581; .086)

*****
MP LOCATION IS: YEAR=1978; MONTH= 9; DAY= 3; TIME= 7.20 UT; OUTBOUND; R=10.6; LT=1247; LAT= 20.3
MAGNETOSHEATH FTES:  1;  MAGNETOSPHERE FTES:  1
SIGN OF MAGNETOSHEATH BL IS:  1( 1);  SIGN OF MAGNETOSHEATH BM IS:  1( 1)
DIRECTION OF NORMAL USED FOR PLOTTING DATA IN GSM: ( .904; .018; .428)

*****
MP LOCATION IS: YEAR=1978; MONTH= 9; DAY= 3; TIME= 5.04 UT; INBOUND; R=12.5; LT=1523; LAT=-10.5
MAGNETOSHEATH FTES:  2;  MAGNETOSPHERE FTES:  2
SIGN OF MAGNETOSHEATH BL IS:  1( 1);  SIGN OF MAGNETOSHEATH BM IS:  1( 1)
DIRECTION OF NORMAL USED FOR PLOTTING DATA IN GSM: ( .848; .391;-.358)

*****
MP LOCATION IS: YEAR=1978; MONTH= 9; DAY= 5; TIME=16.13 UT; OUTBOUND; R= 9.8; LT=1225; LAT= 23.3
MAGNETOSHEATH FTES:  1;  MAGNETOSPHERE FTES:  1
SIGN OF MAGNETOSHEATH BL IS:  1( 1);  SIGN OF MAGNETOSHEATH BM IS:  1( 1)
DIRECTION OF NORMAL USED FOR PLOTTING DATA IN GSM: ( .721; .062; .691)

*****
MP LOCATION IS: YEAR=1978; MONTH= 9; DAY= 7; TIME=14.35 UT; INBOUND; R=12.4; LT=1512; LAT=-14.4
MAGNETOSHEATH FTES:  1;  MAGNETOSPHERE FTES:  1
SIGN OF MAGNETOSHEATH BL IS:  3;  SIGN OF MAGNETOSHEATH BM IS:  2
DIRECTION OF NORMAL USED FOR PLOTTING DATA IN GSM: ( .404; .911;-.088)

*****
MP LOCATION IS: YEAR=1978; MONTH= 9; DAY= 8; TIME=  .44 UT; OUTBOUND; R= 8.5; LT=1139; LAT= 26.0
MAGNETOSHEATH FTES:  1;  MAGNETOSPHERE FTES:  1
SIGN OF MAGNETOSHEATH BL IS:  1( 1);  SIGN OF MAGNETOSHEATH BM IS:  1( 1)
DIRECTION OF NORMAL USED FOR PLOTTING DATA IN GSM: ( .776;-.216; .593)

*****
MP LOCATION IS: YEAR=1978; MONTH= 9; DAY=10; TIME= 0.00 UT; INBOUND; R=12.2; LT=1510; LAT= -1.8
MAGNETOSHEATH FTES:  1;  MAGNETOSPHERE FTES:  0
SIGN OF MAGNETOSHEATH BL IS:  1;  SIGN OF MAGNETOSHEATH BM IS:  2
DIRECTION OF NORMAL USED FOR PLOTTING DATA IN GSM: ( .996; .017;-.083)

*****
MP LOCATION IS: YEAR=1978; MONTH= 9; DAY=10; TIME=  .45 UT; INBOUND; R=11.3; LT=1517; LAT= -3.7
MAGNETOSHEATH FTES:  0;  MAGNETOSPHERE FTES:  0
SIGN OF MAGNETOSHEATH BL IS:  3( 3);  SIGN OF MAGNETOSHEATH BM IS:  3( 3)
DIRECTION OF NORMAL USED FOR PLOTTING DATA IN GSM: ( .996; .017;-.083)
*****
```

```
*****  MP LOCATION IS: YEAR=1978; MONTH= 9; DAY=10; TIME= 2.04 UT; INBOUND; R= 9.7; LT=1532; LAT= -8.0
       MAGNETOSHEATH FLGS:  0;  MAGNETOSPHERE FLGS:  0
       SIGN OF MAGNETOSHEATH BL IS:  2( 2);  SIGN OF MAGNETOSHEATH BM IS:  2( 2)
       DIRECTION OF NORMAL USED FOR PLOTTING DATA IN GSM: ( .809; .583;-.079)

*****  MP LOCATION IS: YEAR=1978; MONTH= 9; DAY=10; TIME=10.55 UT; OUTBOUND; R= 9.8; LT=1227; LAT= 24.5
       MAGNETOSHEATH FLGS:  1;  MAGNETOSPHERE FLGS:  1
       SIGN OF MAGNETOSHEATH BL IS:  2( 2);  SIGN OF MAGNETOSHEATH BM IS:  2( 2)
       DIRECTION OF NORMAL USED FOR PLOTTING DATA IN GSM: ( .802; .267; .535)

*****  MP LOCATION IS: YEAR=1978; MONTH= 9; DAY=10; TIME=12.28 UT; OUTBOUND; R=11.8; LT=1240; LAT= 21.1
       MAGNETOSHEATH FLGS:  1;  MAGNETOSPHERE FLGS:  1
       SIGN OF MAGNETOSHEATH BL IS:  2( 2);  SIGN OF MAGNETOSHEATH BM IS:  2( 2)
       DIRECTION OF NORMAL USED FOR PLOTTING DATA IN GSM: ( .802; .267; .535)

*****  MP LOCATION IS: YEAR=1978; MONTH= 9; DAY=12; TIME=19.54 UT; OUTBOUND; R= 9.6; LT=1137; LAT= 25.9
       MAGNETOSHEATH FLGS:  1;  MAGNETOSPHERE FLGS:  1
       SIGN OF MAGNETOSHEATH BL IS:  2( 1);  SIGN OF MAGNETOSHEATH BM IS:  1( 1)
       DIRECTION OF NORMAL USED FOR PLOTTING DATA IN GSM: ( .652; .117; .749)

*****  MP LOCATION IS: YEAR=1978; MONTH= 9; DAY=14; TIME=16.55 UT; INBOUND; R=14.0; LT=1438; LAT= -5.3
       MAGNETOSHEATH FLGS:  0;  MAGNETOSPHERE FLGS:  0
       SIGN OF MAGNETOSHEATH BL IS:  2( 2);  SIGN OF MAGNETOSHEATH BM IS:  1( 1)
       DIRECTION OF NORMAL USED FOR PLOTTING DATA IN GSM: ( .940; .327;-.099)

*****  MP LOCATION IS: YEAR=1978; MONTH= 9; DAY=14; TIME=17.43 UT; INBOUND; R=13.2; LT=1443; LAT= -4.9
       MAGNETOSHEATH FLGS:  0;  MAGNETOSPHERE FLGS:  0
       SIGN OF MAGNETOSHEATH BL IS:  2( 2);  SIGN OF MAGNETOSHEATH BM IS:  1( 1)
       DIRECTION OF NORMAL USED FOR PLOTTING DATA IN GSM: ( .940; .327;-.099)

*****  MP LOCATION IS: YEAR=1978; MONTH= 9; DAY=15; TIME= 6.47 UT; OUTBOUND; R=11.3; LT=1214; LAT= 25.8
       MAGNETOSHEATH FLGS:  1;  MAGNETOSPHERE FLGS:  0
       SIGN OF MAGNETOSHEATH BL IS:  2( 2);  SIGN OF MAGNETOSHEATH BM IS:  1( 1)
       DIRECTION OF NORMAL USED FOR PLOTTING DATA IN GSM: ( .846;-.099; .524)

*****  MP LOCATION IS: YEAR=1978; MONTH= 9; DAY=17; TIME= 5.20 UT; INBOUND; R=10.7; LT=1450; LAT=-12.4
       MAGNETOSHEATH FLGS:  2;  MAGNETOSPHERE FLGS:  0
       SIGN OF MAGNETOSHEATH BL IS:  1;  SIGN OF MAGNETOSHEATH BM IS:  2
       DIRECTION OF NORMAL USED FOR PLOTTING DATA IN GSM: ( .349; .505;-.156)

*****  MP LOCATION IS: YEAR=1978; MONTH= 9; DAY=17; TIME=15.25 UT; OUTBOUND; R=10.4; LT=1154; LAT= 27.3
       MAGNETOSHEATH FLGS:  0;  MAGNETOSPHERE FLGS:  0
       SIGN OF MAGNETOSHEATH BL IS:  2( 2);  SIGN OF MAGNETOSHEATH BM IS:  2( 2)
       DIRECTION OF NORMAL USED FOR PLOTTING DATA IN GSM: ( .938;-.018; .347)

*****  MP LOCATION IS: YEAR=1978; MONTH= 9; DAY=20; TIME= 1.53 UT; OUTBOUND; R=11.8; LT=1138; LAT= 25.5
       MAGNETOSHEATH FLGS:  1;  MAGNETOSPHERE FLGS:  0
       SIGN OF MAGNETOSHEATH BL IS:  2( 3);  SIGN OF MAGNETOSHEATH BM IS:  2( 2)
       DIRECTION OF NORMAL USED FOR PLOTTING DATA IN GSM: ( .838; .210; .503)

*****  MP LOCATION IS: YEAR=1978; MONTH= 9; DAY=21; TIME=22.51 UT; INBOUND; R=12.1; LT=1425; LAT=  -.4
       MAGNETOSHEATH FLGS:  0;  MAGNETOSPHERE FLGS:  0
       SIGN OF MAGNETOSHEATH BL IS:  2( 2);  SIGN OF MAGNETOSHEATH BM IS:  1( 1)
       DIRECTION OF NORMAL USED FOR PLOTTING DATA IN GSM: ( .999;-.011;-.039)

*****  MP LOCATION IS: YEAR=1978; MONTH= 9; DAY=22; TIME=10.44 UT; OUTBOUND; R=11.1; LT=1202; LAT= 28.4
       MAGNETOSHEATH FLGS:  1;  MAGNETOSPHERE FLGS:  1
       SIGN OF MAGNETOSHEATH BL IS:  1( 1);  SIGN OF MAGNETOSHEATH BM IS:  1( 1)
       DIRECTION OF NORMAL USED FOR PLOTTING DATA IN GSM: ( .766; .184; .621)

*****  MP LOCATION IS: YEAR=1978; MONTH= 9; DAY=24; TIME= 7.48 UT; INBOUND; R=12.7; LT=1406; LAT=-10.2
       MAGNETOSHEATH FLGS:  0;  MAGNETOSPHERE FLGS:  0
       SIGN OF MAGNETOSHEATH BL IS:  2( 2);  SIGN OF MAGNETOSHEATH BM IS:  2( 2)
       DIRECTION OF NORMAL USED FOR PLOTTING DATA IN GSM: ( .891; .433;-.134)

*****  MP LOCATION IS: YEAR=1978; MONTH= 9; DAY=24; TIME=18.15 UT; OUTBOUND; R= 9.5; LT=1047; LAT= 31.6
       MAGNETOSHEATH FLGS:  0;  MAGNETOSPHERE FLGS:  0
       SIGN OF MAGNETOSHEATH BL IS:  2( 2);  SIGN OF MAGNETOSHEATH BM IS:  2( 2)
       DIRECTION OF NORMAL USED FOR PLOTTING DATA IN GSM: ( .919;-.184; .356)

*****  MP LOCATION IS: YEAR=1978; MONTH= 9; DAY=26; TIME=17.11 UT; INBOUND; R=12.6; LT=1402; LAT= -4.1
       MAGNETOSHEATH FLGS:  0;  MAGNETOSPHERE FLGS:  0
       SIGN OF MAGNETOSHEATH BL IS:  2;  SIGN OF MAGNETOSHEATH BM IS:  2
       DIRECTION OF NORMAL USED FOR PLOTTING DATA IN GSM: ( .917; .385; .108)

*****  MP LOCATION IS: YEAR=1978; MONTH= 9; DAY=26; TIME=17.29 UT; INBOUND; R=12.2; LT=1406; LAT= -4.2
       MAGNETOSHEATH FLGS:  0;  MAGNETOSPHERE FLGS:  1
       SIGN OF MAGNETOSHEATH BL IS:  2;  SIGN OF MAGNETOSHEATH BM IS:  2
       DIRECTION OF NORMAL USED FOR PLOTTING DATA IN GSM: ( .917; .385; .108)

*****  MP LOCATION IS: YEAR=1978; MONTH= 9; DAY=27; TIME= 4.01 UT; OUTBOUND; R= 9.1; LT=1053; LAT= 32.1
       MAGNETOSHEATH FLGS:  1;  MAGNETOSPHERE FLGS:  1
       SIGN OF MAGNETOSHEATH BL IS:  1( 1);  SIGN OF MAGNETOSHEATH BM IS:  1( 1)
       DIRECTION OF NORMAL USED FOR PLOTTING DATA IN GSM: ( .724;-.405; .558)

*****  MP LOCATION IS: YEAR=1978; MONTH= 9; DAY=29; TIME=18.30 UT; OUTBOUND; R=15.0; LT=1130; LAT= 24.9
       MAGNETOSHEATH FLGS:  0;  MAGNETOSPHERE FLGS:  0
       SIGN OF MAGNETOSHEATH BL IS:  2( 2);  SIGN OF MAGNETOSHEATH BM IS:  1( 1)
       DIRECTION OF NORMAL USED FOR PLOTTING DATA IN GSM: ( .845;-.243; .724)

*****  MP LOCATION IS: YEAR=1978; MONTH= 9; DAY=29; TIME=21.00 UT; OUTBOUND; R=17.0; LT=1135; LAT= 22.5
       MAGNETOSHEATH FLGS:  0;  MAGNETOSPHERE FLGS:  0
       SIGN OF MAGNETOSHEATH BL IS:  2( 2);  SIGN OF MAGNETOSHEATH BM IS:  1( 1)
       DIRECTION OF NORMAL USED FOR PLOTTING DATA IN GSM: ( .913;-.109; .392)

*****  MP LOCATION IS: YEAR=1978; MONTH=10; DAY= 1; TIME=23.52 UT; OUTBOUND; R=11.2; LT=1040; LAT= 28.2
       MAGNETOSHEATH FLGS:  1;  MAGNETOSPHERE FLGS:  1
       SIGN OF MAGNETOSHEATH BL IS:  3( 3);  SIGN OF MAGNETOSHEATH BM IS:  1( 1)
       DIRECTION OF NORMAL USED FOR PLOTTING DATA IN GSM: ( .859;-.043; .511)

*****  MP LOCATION IS: YEAR=1978; MONTH=10; DAY= 3; TIME=21.47 UT; INBOUND; R=12.2; LT=1338; LAT=  1.0
       MAGNETOSHEATH FLGS:  0;  MAGNETOSPHERE FLGS:  0
       SIGN OF MAGNETOSHEATH BL IS:  2;  SIGN OF MAGNETOSHEATH BM IS:  2
       DIRECTION OF NORMAL USED FOR PLOTTING DATA IN GSM: ( .962; .266;-.064)

*****  MP LOCATION IS: YEAR=1978; MONTH=10; DAY= 6; TIME= 6.42 UT; INBOUND; R=12.2; LT=1328; LAT= -5.3
       MAGNETOSHEATH FLGS:  0;  MAGNETOSPHERE FLGS:  0
       SIGN OF MAGNETOSHEATH BL IS:  3;  SIGN OF MAGNETOSHEATH BM IS:  3
       DIRECTION OF NORMAL USED FOR PLOTTING DATA IN GSM: ( .922; .225;-.316)

*****  MP LOCATION IS: YEAR=1978; MONTH=10; DAY= 6; TIME= 7.45 UT; INBOUND; R=10.8; LT=1334; LAT= -9.1
       MAGNETOSHEATH FLGS:  0;  MAGNETOSPHERE FLGS:  0
       SIGN OF MAGNETOSHEATH BL IS:  2;  SIGN OF MAGNETOSHEATH BM IS:  2
       DIRECTION OF NORMAL USED FOR PLOTTING DATA IN GSM: ( .922; .225;-.316)

*****  MP LOCATION IS: YEAR=1978; MONTH=10; DAY= 6; TIME=20.11 UT; OUTBOUND; R=12.4; LT=1034; LAT= 28.2
       MAGNETOSHEATH FLGS:  1;  MAGNETOSPHERE FLGS:  0
       SIGN OF MAGNETOSHEATH BL IS:  1( 1);  SIGN OF MAGNETOSHEATH BM IS:  2( 1)
       DIRECTION OF NORMAL USED FOR PLOTTING DATA IN GSM: ( .813;-.032; .581)
```

```
*****  MP LOCATION IS: YEAR=1978; MONTH=10; DAY= 8; TIME=18.35 UT; INBOUND; R= 9.5; LT=1342; LAT= -4.5
       MAGNETOSHEATH FTES:  0;  MAGNETOSPHERE FTES:  0
       SIGN OF MAGNETOSHEATH BL IS:  2( 2);  SIGN OF MAGNETOSHEATH BM IS:  1( 1)
       DIRECTION OF NORMAL USED FOR PLOTTING DATA IN GSM: ( .950; .307;-.057)

*****  MP LOCATION IS: YEAR=1978; MONTH=10; DAY= 9; TIME= 4.20 UT; OUTBOUND; R=11.2; LT=1030; LAT= 33.3
       MAGNETOSHEATH FTES:  0;  MAGNETOSPHERE FTES:  0
       SIGN OF MAGNETOSHEATH BL IS:  2( 2);  SIGN OF MAGNETOSHEATH BM IS:  1( 1)
       DIRECTION OF NORMAL USED FOR PLOTTING DATA IN GSM: ( .544;-.132; .815)

*****  MP LOCATION IS: YEAR=1978; MONTH=10; DAY=11; TIME= 2.44 UT; INBOUND; R=11.1; LT=1320; LAT= -1.1
       MAGNETOSHEATH FTES:  0;  MAGNETOSPHERE FTES:  0
       SIGN OF MAGNETOSHEATH BL IS:  2( 1);  SIGN OF MAGNETOSHEATH BM IS:  2( 2)
       DIRECTION OF NORMAL USED FOR PLOTTING DATA IN GSM: ( .905; .355;-.236)

*****  MP LOCATION IS: YEAR=1978; MONTH=10; DAY=11; TIME=13.50 UT; OUTBOUND; R=11.3; LT=1043; LAT= 36.8
       MAGNETOSHEATH FTES:  0;  MAGNETOSPHERE FTES:  0
       SIGN OF MAGNETOSHEATH BL IS:  2;  SIGN OF MAGNETOSHEATH BM IS:  1
       DIRECTION OF NORMAL USED FOR PLOTTING DATA IN GSM: ( .858;-.219; .464)

*****  MP LOCATION IS: YEAR=1978; MONTH=10; DAY=13; TIME=12.30 UT; INBOUND; R=10.6; LT=1310; LAT= -6.2
       MAGNETOSHEATH FTES:  0;  MAGNETOSPHERE FTES:  2
       SIGN OF MAGNETOSHEATH BL IS:  2;  SIGN OF MAGNETOSHEATH BM IS:  1
       DIRECTION OF NORMAL USED FOR PLOTTING DATA IN GSM: ( .949; .263;-.172)

*****  MP LOCATION IS: YEAR=1978; MONTH=10; DAY=13; TIME=23.05 UT; OUTBOUND; R=11.0; LT= 947; LAT= 29.6
       MAGNETOSHEATH FTES:  0;  MAGNETOSPHERE FTES:  0
       SIGN OF MAGNETOSHEATH BL IS:  2( 2);  SIGN OF MAGNETOSHEATH BM IS:  2( 3)
       DIRECTION OF NORMAL USED FOR PLOTTING DATA IN GSM: ( .845;-.374; .382)

*****  MP LOCATION IS: YEAR=1978; MONTH=10; DAY=15; TIME=21.02 UT; INBOUND; R=11.7; LT=1256; LAT=  2.2
       MAGNETOSHEATH FTES:  0;  MAGNETOSPHERE FTES:  0
       SIGN OF MAGNETOSHEATH BL IS:  2( 2);  SIGN OF MAGNETOSHEATH BM IS:  1( 1)
       DIRECTION OF NORMAL USED FOR PLOTTING DATA IN GSM: (-.984; .176; .029)

*****  MP LOCATION IS: YEAR=1978; MONTH=10; DAY=15; TIME=21.55 UT; INBOUND; R=10.6; LT=1304; LAT=   .8
       MAGNETOSHEATH FTES:  2;  MAGNETOSPHERE FTES:  2
       SIGN OF MAGNETOSHEATH BL IS:  1;  SIGN OF MAGNETOSHEATH BM IS:  1
       DIRECTION OF NORMAL USED FOR PLOTTING DATA IN GSM: ( .984; .176; .029)

*****  MP LOCATION IS: YEAR=1978; MONTH=10; DAY=16; TIME= 8.48 UT; OUTBOUND; R=11.5; LT=1040; LAT= 40.2
       MAGNETOSHEATH FTES:  0;  MAGNETOSPHERE FTES:  0
       SIGN OF MAGNETOSHEATH BL IS:  2;  SIGN OF MAGNETOSHEATH BM IS:  2
       DIRECTION OF NORMAL USED FOR PLOTTING DATA IN GSM: ( .745;-.044; .666)

*****  MP LOCATION IS: YEAR=1978; MONTH=10; DAY=18; TIME= 7.53 UT; INBOUND; R= 9.7; LT=1259; LAT= -6.0
       MAGNETOSHEATH FTES:  3;  MAGNETOSPHERE FTES:  2
       SIGN OF MAGNETOSHEATH BL IS:  2( 3);  SIGN OF MAGNETOSHEATH BM IS:  1( 1)
       DIRECTION OF NORMAL USED FOR PLOTTING DATA IN GSM: ( .930; .088;-.358)

*****  MP LOCATION IS: YEAR=1978; MONTH=10; DAY=21; TIME= 4.00 UT; OUTBOUND; R=12.0; LT= 945; LAT= 35.1
       MAGNETOSHEATH FTES:  1;  MAGNETOSPHERE FTES:  1
       SIGN OF MAGNETOSHEATH BL IS:  2( 1);  SIGN OF MAGNETOSHEATH BM IS:  1( 1)
       DIRECTION OF NORMAL USED FOR PLOTTING DATA IN GSM: ( .796;-.123; .593)

*****  MP LOCATION IS: YEAR=1978; MONTH=10; DAY=23; TIME= 1.25 UT; INBOUND; R=11.3; LT=1232; LAT=  2.4
       MAGNETOSHEATH FTES:  0;  MAGNETOSPHERE FTES:  0
       SIGN OF MAGNETOSHEATH BL IS:  2( 2);  SIGN OF MAGNETOSHEATH BM IS:  1( 1)
       DIRECTION OF NORMAL USED FOR PLOTTING DATA IN GSM: ( .997; .054; .054)

*****  MP LOCATION IS: YEAR=1978; MONTH=10; DAY=23; TIME=12.15 UT; OUTBOUND; R=11.5; LT= 959; LAT= 42.7
       MAGNETOSHEATH FTES:  1;  MAGNETOSPHERE FTES:  1
       SIGN OF MAGNETOSHEATH BL IS:  2( 1);  SIGN OF MAGNETOSHEATH BM IS:  1( 1)
       DIRECTION OF NORMAL USED FOR PLOTTING DATA IN GSM: ( .784;-.310; .523)

*****  MP LOCATION IS: YEAR=1978; MONTH=10; DAY=25; TIME=12.51 UT; INBOUND; R= 8.5; LT=1243; LAT= -5.6
       MAGNETOSHEATH FTES:  0;  MAGNETOSPHERE FTES:  0
       SIGN OF MAGNETOSHEATH BL IS:  2( 1);  SIGN OF MAGNETOSHEATH BM IS:  1( 1)
       DIRECTION OF NORMAL USED FOR PLOTTING DATA IN GSM: ( .966;-.159;-.208)

*****  MP LOCATION IS: YEAR=1978; MONTH=10; DAY=25; TIME=22.02 UT; OUTBOUND; R=11.1; LT= 954; LAT= 29.5
       MAGNETOSHEATH FTES:  0;  MAGNETOSPHERE FTES:  0
       SIGN OF MAGNETOSHEATH BL IS:  2( 2);  SIGN OF MAGNETOSHEATH BM IS:  1( 1)
       DIRECTION OF NORMAL USED FOR PLOTTING DATA IN GSM: ( .795;-.478; .374)

*****  MP LOCATION IS: YEAR=1978; MONTH=10; DAY=28; TIME= 8.21 UT; OUTBOUND; R=12.3; LT= 945; LAT= 42.7
       MAGNETOSHEATH FTES:  2;  MAGNETOSPHERE FTES:  1
       SIGN OF MAGNETOSHEATH BL IS:  2( 1);  SIGN OF MAGNETOSHEATH BM IS:  3( 3)
       DIRECTION OF NORMAL USED FOR PLOTTING DATA IN GSM: ( .689;-.357; .631)

*****  MP LOCATION IS: YEAR=1978; MONTH=10; DAY=30; TIME= 6.33 UT; INBOUND; R=10.0; LT=1216; LAT=   .4
       MAGNETOSHEATH FTES:  4;  MAGNETOSPHERE FTES:  2
       SIGN OF MAGNETOSHEATH BL IS:  2( 1);  SIGN OF MAGNETOSHEATH BM IS:  2( 2)
       DIRECTION OF NORMAL USED FOR PLOTTING DATA IN GSM: ( .914; .228;-.335)

*****  MP LOCATION IS: YEAR=1978; MONTH=11; DAY= 1; TIME=15.21 UT; INBOUND; R=10.8; LT=1201; LAT=  3.1
       MAGNETOSHEATH FTES:  0;  MAGNETOSPHERE FTES:  0
       SIGN OF MAGNETOSHEATH BL IS:  2( 2);  SIGN OF MAGNETOSHEATH BM IS:  1( 1)
       DIRECTION OF NORMAL USED FOR PLOTTING DATA IN GSM: ( .999;-.036; .001)

*****  MP LOCATION IS: YEAR=1978; MONTH=11; DAY= 4; TIME= 1.37 UT; INBOUND; R= 9.6; LT=1202; LAT=  1.1
       MAGNETOSHEATH FTES:  2;  MAGNETOSPHERE FTES:  0
       SIGN OF MAGNETOSHEATH BL IS:  1;  SIGN OF MAGNETOSHEATH BM IS:  3
       DIRECTION OF NORMAL USED FOR PLOTTING DATA IN GSM: (1.000;-.004;-.003)

*****  MP LOCATION IS: YEAR=1978; MONTH=11; DAY= 4; TIME=13.01 UT; OUTBOUND; R=12.8; LT= 906; LAT= 42.9
       MAGNETOSHEATH FTES:  1;  MAGNETOSPHERE FTES:  1
       SIGN OF MAGNETOSHEATH BL IS:  2( 1);  SIGN OF MAGNETOSHEATH BM IS:  1( 1)
       DIRECTION OF NORMAL USED FOR PLOTTING DATA IN GSM: ( .649;-.241; .721)

*****  MP LOCATION IS: YEAR=1978; MONTH=11; DAY= 6; TIME= 9.50 UT; INBOUND; R=10.8; LT=1146; LAT=  5.0
       MAGNETOSHEATH FTES:  0;  MAGNETOSPHERE FTES:  0
       SIGN OF MAGNETOSHEATH BL IS:  2( 3);  SIGN OF MAGNETOSHEATH BM IS:  1( 1)
       DIRECTION OF NORMAL USED FOR PLOTTING DATA IN GSM: ( .995;-.047;-.083)

*****  MP LOCATION IS: YEAR=1978; MONTH=11; DAY= 6; TIME=22.04 UT; OUTBOUND; R=12.4; LT= 813; LAT= 27.1
       MAGNETOSHEATH FTES:  0;  MAGNETOSPHERE FTES:  0
       SIGN OF MAGNETOSHEATH BL IS:  2( 2);  SIGN OF MAGNETOSHEATH BM IS:  3( 3)
       DIRECTION OF NORMAL USED FOR PLOTTING DATA IN GSM: ( .820;-.025; .571)

*****  MP LOCATION IS: YEAR=1978; MONTH=11; DAY= 6; TIME=21.14 UT; OUTBOUND; R=11.5; LT= 805; LAT= 28.1
       MAGNETOSHEATH FTES:  0;  MAGNETOSPHERE FTES:  0
       SIGN OF MAGNETOSHEATH BL IS:  2;  SIGN OF MAGNETOSHEATH BM IS:  1
       DIRECTION OF NORMAL USED FOR PLOTTING DATA IN GSM: ( .820;-.025; .571)

*****  MP LOCATION IS: YEAR=1978; MONTH=11; DAY=11; TIME= 4.53 UT; INBOUND; R= 9.3; LT=1137; LAT=  2.4
       MAGNETOSHEATH FTES:  2;  MAGNETOSPHERE FTES:  0
       SIGN OF MAGNETOSHEATH BL IS:  2;  SIGN OF MAGNETOSHEATH BM IS:  2
       DIRECTION OF NORMAL USED FOR PLOTTING DATA IN GSM: ( .938;-.184;-.294)
```

```
*****
MP LOCATION IS: YEAR=1978; MONTH=11; DAY=11; TIME=16.24 UT; OUTBOUND; R=12.0; LT= 902; LAT= 36.5
MAGNETOSHEATH FILES:  0;  MAGNETOSPHERE FILES:  0
SIGN OF MAGNETOSHEATH BL IS:  2;  SIGN OF MAGNETOSHEATH BM IS:  3
DIRECTION OF NORMAL USED FOR PLOTTING DATA IN GSM: ( .714;-.500; .490)
*****
MP LOCATION IS: YEAR=1978; MONTH=11; DAY=13; TIME=13.19 UT; INBOUND; R=11.6; LT=1112; LAT=  8.5
MAGNETOSHEATH FILES:  0;  MAGNETOSPHERE FILES:  1
SIGN OF MAGNETOSHEATH BL IS:  1;  SIGN OF MAGNETOSHEATH BM IS:  2
DIRECTION OF NORMAL USED FOR PLOTTING DATA IN GSM: ( .987;-.121; .106)
*****
MP LOCATION IS: YEAR=1978; MONTH=11; DAY=14; TIME= 4.02 UT; OUTBOUND; R=14.4; LT= 811; LAT= 33.4
MAGNETOSHEATH FILES:  0;  MAGNETOSPHERE FILES:  0
SIGN OF MAGNETOSHEATH BL IS:  2( 2);  SIGN OF MAGNETOSHEATH BM IS:  2( 2)
DIRECTION OF NORMAL USED FOR PLOTTING DATA IN GSM: ( .783;-.201; .589)
*****
MP LOCATION IS: YEAR=1978; MONTH=11; DAY=15; TIME=16.15 UT; INBOUND; R=17.5; LT=1022; LAT= 15.1
MAGNETOSHEATH FILES:  0;  MAGNETOSPHERE FILES:  0
SIGN OF MAGNETOSHEATH BL IS:  2;  SIGN OF MAGNETOSHEATH BM IS:  1
DIRECTION OF NORMAL USED FOR PLOTTING DATA IN GSM: ( .986;-.165; .026)
*****
MP LOCATION IS: YEAR=1978; MONTH=11; DAY=15; TIME=23.06 UT; INBOUND; R=11.4; LT=1056; LAT=  3.6
MAGNETOSHEATH FILES:  0;  MAGNETOSPHERE FILES:  0
SIGN OF MAGNETOSHEATH BL IS:  2( 2);  SIGN OF MAGNETOSHEATH BM IS:  2( 2)
DIRECTION OF NORMAL USED FOR PLOTTING DATA IN GSM: ( .986;-.165; .026)
*****
MP LOCATION IS: YEAR=1978; MONTH=11; DAY=16; TIME=19.43 UT; INBOUND; R=14.7; LT=1032; LAT=  8.2
MAGNETOSHEATH FILES:  0;  MAGNETOSPHERE FILES:  0
SIGN OF MAGNETOSHEATH BL IS:  2( 2);  SIGN OF MAGNETOSHEATH BM IS:  1( 1)
DIRECTION OF NORMAL USED FOR PLOTTING DATA IN GSM: ( .986;-.165; .026)
*****
MP LOCATION IS: YEAR=1978; MONTH=11; DAY=18; TIME=21.15 UT; OUTBOUND; R=14.1; LT= 739; LAT= 23.5
MAGNETOSHEATH FILES:  0;  MAGNETOSPHERE FILES:  0
SIGN OF MAGNETOSHEATH BL IS:  2( 2);  SIGN OF MAGNETOSHEATH BM IS:  1( 1)
DIRECTION OF NORMAL USED FOR PLOTTING DATA IN GSM: ( .926;-.711; .321)
*****
MP LOCATION IS: YEAR=1978; MONTH=11; DAY=20; TIME=20.08 UT; INBOUND; R= 8.2; LT=1114; LAT= -1.0
MAGNETOSHEATH FILES:  0;  MAGNETOSPHERE FILES:  0
SIGN OF MAGNETOSHEATH BL IS:  2( 2);  SIGN OF MAGNETOSHEATH BM IS:  1( 1)
DIRECTION OF NORMAL USED FOR PLOTTING DATA IN GSM: ( .943;-.189;-.276)
*****
MP LOCATION IS: YEAR=1978; MONTH=11; DAY=21; TIME= 7.11 UT; OUTBOUND; R=14.6; LT= 750; LAT= 40.4
MAGNETOSHEATH FILES:  1;  MAGNETOSPHERE FILES:  1
SIGN OF MAGNETOSHEATH BL IS:  1( 1);  SIGN OF MAGNETOSHEATH BM IS:  1( 1)
DIRECTION OF NORMAL USED FOR PLOTTING DATA IN GSM: ( .591;-.255; .765)
*****
MP LOCATION IS: YEAR=1978; MONTH=11; DAY=21; TIME= 4.45 UT; OUTBOUND; R=11.6; LT= 712; LAT= 36.0
MAGNETOSHEATH FILES:  0;  MAGNETOSPHERE FILES:  1
SIGN OF MAGNETOSHEATH BL IS:  1;  SIGN OF MAGNETOSHEATH BM IS:  1
DIRECTION OF NORMAL USED FOR PLOTTING DATA IN GSM: ( .591;-.255; .765)
*****
MP LOCATION IS: YEAR=1978; MONTH=11; DAY=23; TIME= 3.28 UT; INBOUND; R=10.8; LT=1034; LAT=  5.3
MAGNETOSHEATH FILES:  0;  MAGNETOSPHERE FILES:  2
SIGN OF MAGNETOSHEATH BL IS:  2( 2);  SIGN OF MAGNETOSHEATH BM IS:  1( 1)
DIRECTION OF NORMAL USED FOR PLOTTING DATA IN GSM: ( .993;-.088;-.077)
*****
MP LOCATION IS: YEAR=1978; MONTH=11; DAY=23; TIME=17.21 UT; OUTBOUND; R=14.3; LT= 722; LAT= 29.4
MAGNETOSHEATH FILES:  1;  MAGNETOSPHERE FILES:  0
SIGN OF MAGNETOSHEATH BL IS:  1( 1);  SIGN OF MAGNETOSHEATH BM IS:  2( 2)
DIRECTION OF NORMAL USED FOR PLOTTING DATA IN GSM: ( .880;-.449; .154)
*****
MP LOCATION IS: YEAR=1978; MONTH=11; DAY=25; TIME=15.30 UT; INBOUND; R= 7.0; LT=1108; LAT= -1.0
MAGNETOSHEATH FILES:  2;  MAGNETOSPHERE FILES:  2
SIGN OF MAGNETOSHEATH BL IS:  2( 1);  SIGN OF MAGNETOSHEATH BM IS:  1( 1)
DIRECTION OF NORMAL USED FOR PLOTTING DATA IN GSM: ( .995;-.089;-.037)
*****
MP LOCATION IS: YEAR=1978; MONTH=11; DAY=27; TIME=21.14 UT; INBOUND; R=12.1; LT=1002; LAT=  2.5
MAGNETOSHEATH FILES:  3;  MAGNETOSPHERE FILES:  0
SIGN OF MAGNETOSHEATH BL IS:  1( 1);  SIGN OF MAGNETOSHEATH BM IS:  3( 3)
DIRECTION OF NORMAL USED FOR PLOTTING DATA IN GSM: ( .929;-.370; .016)
*****
MP LOCATION IS: YEAR=1978; MONTH=11; DAY=27; TIME=21.51 UT; INBOUND; R=11.0; LT=1000; LAT=  1.4
MAGNETOSHEATH FILES:  0;  MAGNETOSPHERE FILES:  0
SIGN OF MAGNETOSHEATH BL IS:  1( 1);  SIGN OF MAGNETOSHEATH BM IS:  3( 3)
DIRECTION OF NORMAL USED FOR PLOTTING DATA IN GSM: ( .929;-.370; .016)
*****
MP LOCATION IS: YEAR=1978; MONTH=11; DAY=30; TIME= 7.13 UT; INBOUND; R=11.4; LT=1007; LAT= 10.9
MAGNETOSHEATH FILES:  0;  MAGNETOSPHERE FILES:  1
SIGN OF MAGNETOSHEATH BL IS:  2( 2);  SIGN OF MAGNETOSHEATH BM IS:  1( 1)
DIRECTION OF NORMAL USED FOR PLOTTING DATA IN GSM: ( .941;-.337;-.024)
*****
MP LOCATION IS: YEAR=1978; MONTH=12; DAY= 3; TIME= 7.07 UT; OUTBOUND; R=15.5; LT= 654; LAT= 36.7
MAGNETOSHEATH FILES:  0;  MAGNETOSPHERE FILES:  0
SIGN OF MAGNETOSHEATH BL IS:  2( 2);  SIGN OF MAGNETOSHEATH BM IS:  3( 3)
DIRECTION OF NORMAL USED FOR PLOTTING DATA IN GSM: ( .750;-.143; .646)
*****
MP LOCATION IS: YEAR=1978; MONTH=12; DAY= 5; TIME= 2.23 UT; INBOUND; R= 9.2; LT=1002; LAT=  -.5
MAGNETOSHEATH FILES:  0;  MAGNETOSPHERE FILES:  0
SIGN OF MAGNETOSHEATH BL IS:  2( 3);  SIGN OF MAGNETOSHEATH BM IS:  2( 2)
DIRECTION OF NORMAL USED FOR PLOTTING DATA IN GSM: ( .924;-.381;-.007)
*****
MP LOCATION IS: YEAR=1978; MONTH=12; DAY= 5; TIME=16.21 UT; OUTBOUND; R=14.4; LT= 630; LAT= 28.5
MAGNETOSHEATH FILES:  0;  MAGNETOSPHERE FILES:  3
SIGN OF MAGNETOSHEATH BL IS:  3;  SIGN OF MAGNETOSHEATH BM IS:  2
DIRECTION OF NORMAL USED FOR PLOTTING DATA IN GSM: ( .642;-.622; .447)
*****
MP LOCATION IS: YEAR=1978; MONTH=12; DAY= 8; TIME= 2.20 UT; OUTBOUND; R=15.0; LT= 623; LAT= 19.8
MAGNETOSHEATH FILES:  0;  MAGNETOSPHERE FILES:  0
SIGN OF MAGNETOSHEATH BL IS:  1;  SIGN OF MAGNETOSHEATH BM IS:  2
DIRECTION OF NORMAL USED FOR PLOTTING DATA IN GSM: ( .679;-.529; .379)
*****
MP LOCATION IS: YEAR=1978; MONTH=12; DAY=10; TIME=12.30 UT; OUTBOUND; R=15.6; LT= 622; LAT= 35.6
MAGNETOSHEATH FILES:  0;  MAGNETOSPHERE FILES:  0
SIGN OF MAGNETOSHEATH BL IS:  2( 3);  SIGN OF MAGNETOSHEATH BM IS:  2( 2)
DIRECTION OF NORMAL USED FOR PLOTTING DATA IN GSM: ( .625;-.625; .469)
*****
MP LOCATION IS: YEAR=1978; MONTH=12; DAY=12; TIME= 7.19 UT; INBOUND; R= 9.5; LT= 933; LAT=  7.5
MAGNETOSHEATH FILES:  1;  MAGNETOSPHERE FILES:  1
SIGN OF MAGNETOSHEATH BL IS:  2( 2);  SIGN OF MAGNETOSHEATH BM IS:  1( 1)
DIRECTION OF NORMAL USED FOR PLOTTING DATA IN GSM: ( .923;-.384;-.034)
*****
MP LOCATION IS: YEAR=1978; MONTH=12; DAY=12; TIME=19.02 UT; OUTBOUND; R=12.9; LT= 546; LAT= 19.0
MAGNETOSHEATH FILES:  1;  MAGNETOSPHERE FILES:  0
SIGN OF MAGNETOSHEATH BL IS:  2;  SIGN OF MAGNETOSHEATH BM IS:  1
DIRECTION OF NORMAL USED FOR PLOTTING DATA IN GSM: ( .276;-.649; .709)
*****
MP LOCATION IS: YEAR=1978; MONTH=12; DAY=14; TIME=14.58 UT; INBOUND; R=11.7; LT= 901; LAT=  7.8
MAGNETOSHEATH FILES:  0;  MAGNETOSPHERE FILES:  0
SIGN OF MAGNETOSHEATH BL IS:  2;  SIGN OF MAGNETOSHEATH BM IS:  1
DIRECTION OF NORMAL USED FOR PLOTTING DATA IN GSM: ( .921;-.361; .169)
*****
```

```
MP LOCATION IS: YEAR=1978; MONTH=12; DAY=15; TIME= 4.31 UT; OUTBOUND; R=13.1; LT= 537; LAT= 24.5
MAGNETOSHEATH FILES:  1;  MAGNETOSPHERE FILES:  1
SIGN OF MAGNETOSHEATH BL IS:  1( 1);  SIGN OF MAGNETOSHEATH BM IS:  1( 1)
DIRECTION OF NORMAL USED FOR PLOTTING DATA IN GSM: ( .464;-.774; .424)

*****

MP LOCATION IS: YEAR=1978; MONTH=12; DAY=15; TIME= 6.50 UT; OUTBOUND; R=13.5; LT= 557; LAT= 31.3
MAGNETOSHEATH FILES:  1;  MAGNETOSPHERE FILES:  1
SIGN OF MAGNETOSHEATH BL IS:  1( 1);  SIGN OF MAGNETOSHEATH BM IS:  3( 3)
DIRECTION OF NORMAL USED FOR PLOTTING DATA IN GSM: ( .464;-.778; .424)

*****

MP LOCATION IS: YEAR=1978; MONTH=12; DAY=17; TIME=14.03 UT; OUTBOUND; R=13.3; LT= 525; LAT= 30.8
MAGNETOSHEATH FILES:  0;  MAGNETOSPHERE FILES:  0
SIGN OF MAGNETOSHEATH BL IS:  2( 2);  SIGN OF MAGNETOSHEATH BM IS:  2( 2)
DIRECTION OF NORMAL USED FOR PLOTTING DATA IN GSM: ( .480;-.394; .267)

*****

MP LOCATION IS: YEAR=1978; MONTH=12; DAY=19; TIME= 8.59 UT; INBOUND; R=12.4; LT= 838; LAT= 12.9
MAGNETOSHEATH FILES:  1;  MAGNETOSPHERE FILES:  1
SIGN OF MAGNETOSHEATH BL IS:  1( 1);  SIGN OF MAGNETOSHEATH BM IS:  3( 3)
DIRECTION OF NORMAL USED FOR PLOTTING DATA IN GSM: ( .919;-.370; .062)

*****

MP LOCATION IS: YEAR=1978; MONTH=12; DAY=21; TIME=17.52 UT; INBOUND; R=12.1; LT= 826; LAT=  -.7
MAGNETOSHEATH FILES:  1;  MAGNETOSPHERE FILES:  1
SIGN OF MAGNETOSHEATH BL IS:  3( 3);  SIGN OF MAGNETOSHEATH BM IS:  1( 1)
DIRECTION OF NORMAL USED FOR PLOTTING DATA IN GSM: ( .794;-.607;-.101)

*****

MP LOCATION IS: YEAR=1978; MONTH=12; DAY=26; TIME=11.30 UT; INBOUND; R=13.7; LT= 756; LAT= 12.0
MAGNETOSHEATH FILES:  0;  MAGNETOSPHERE FILES:  0
SIGN OF MAGNETOSHEATH BL IS:  2( 2);  SIGN OF MAGNETOSHEATH BM IS:  2( 2)
DIRECTION OF NORMAL USED FOR PLOTTING DATA IN GSM: ( .765;-.630; .135)

*****

MP LOCATION IS: YEAR=1978; MONTH=12; DAY=26; TIME=12.15 UT; INBOUND; R=13.6; LT= 758; LAT= 11.8
MAGNETOSHEATH FILES:  3;  MAGNETOSPHERE FILES:  1
SIGN OF MAGNETOSHEATH BL IS:  1;  SIGN OF MAGNETOSHEATH BM IS:  1
DIRECTION OF NORMAL USED FOR PLOTTING DATA IN GSM: ( .765;-.630; .135)

*****

MP LOCATION IS: YEAR=1979; MONTH= 6; DAY=29; TIME= 6.51 UT; OUTBOUND; R=15.0; LT=1710; LAT=  8.0
MAGNETOSHEATH FILES:  1;  MAGNETOSPHERE FILES:  1
SIGN OF MAGNETOSHEATH BL IS:  3( 3);  SIGN OF MAGNETOSHEATH BM IS:  2( 2)
DIRECTION OF NORMAL USED FOR PLOTTING DATA IN GSM: ( .630; .745; .218)

*****

MP LOCATION IS: YEAR=1979; MONTH= 7; DAY= 3; TIME=22.25 UT; OUTBOUND; R=12.4; LT=1615; LAT= 25.7
MAGNETOSHEATH FILES:  1;  MAGNETOSPHERE FILES:  3
SIGN OF MAGNETOSHEATH BL IS:  3( 3);  SIGN OF MAGNETOSHEATH BM IS:  1( 1)
DIRECTION OF NORMAL USED FOR PLOTTING DATA IN GSM: ( .792; .455; .405)

*****

MP LOCATION IS: YEAR=1979; MONTH= 7; DAY= 5; TIME=11.01 UT; INBOUND; R=18.2; LT=1850; LAT=-15.8
MAGNETOSHEATH FILES:  2;  MAGNETOSPHERE FILES:  2
SIGN OF MAGNETOSHEATH BL IS:  1;  SIGN OF MAGNETOSHEATH BM IS:  1
DIRECTION OF NORMAL USED FOR PLOTTING DATA IN GSM: ( .697; .411;-.587)

*****

MP LOCATION IS: YEAR=1979; MONTH= 7; DAY= 6; TIME= 8.09 UT; OUTBOUND; R=12.8; LT=1420; LAT=  5.9
MAGNETOSHEATH FILES:  2;  MAGNETOSPHERE FILES:  2
SIGN OF MAGNETOSHEATH BL IS:  1( 1);  SIGN OF MAGNETOSHEATH BM IS:  1( 1)
DIRECTION OF NORMAL USED FOR PLOTTING DATA IN GSM: ( .788; .570; .233)

*****

MP LOCATION IS: YEAR=1979; MONTH= 7; DAY=10; TIME= 3.43 UT; INBOUND; R=19.0; LT=1823; LAT= -1.7
MAGNETOSHEATH FILES:  2;  MAGNETOSPHERE FILES:  2
SIGN OF MAGNETOSHEATH BL IS:  2;  SIGN OF MAGNETOSHEATH BM IS:  1
DIRECTION OF NORMAL USED FOR PLOTTING DATA IN GSM: ( .447; .893; .049)

*****

MP LOCATION IS: YEAR=1979; MONTH= 7; DAY=11; TIME= 3.48 UT; OUTBOUND; R=13.8; LT=1609; LAT= 14.4
MAGNETOSHEATH FILES:  2;  MAGNETOSPHERE FILES:  2
SIGN OF MAGNETOSHEATH BL IS:  3( 3);  SIGN OF MAGNETOSHEATH BM IS:  1( 1)
DIRECTION OF NORMAL USED FOR PLOTTING DATA IN GSM: ( .790; .549; .272)

*****

MP LOCATION IS: YEAR=1979; MONTH= 7; DAY=12; TIME=16.30 UT; INBOUND; R=17.0; LT=1829; LAT= -8.6
MAGNETOSHEATH FILES:  2;  MAGNETOSPHERE FILES:  0
SIGN OF MAGNETOSHEATH BL IS:  1;  SIGN OF MAGNETOSHEATH BM IS:  1
DIRECTION OF NORMAL USED FOR PLOTTING DATA IN GSM: ( .432; .899;-.067)

*****

MP LOCATION IS: YEAR=1979; MONTH= 7; DAY=12; TIME=19.08 UT; INBOUND; R=14.9; LT=1844; LAT= -2.2
MAGNETOSHEATH FILES:  2;  MAGNETOSPHERE FILES:  0
SIGN OF MAGNETOSHEATH BL IS:  1;  SIGN OF MAGNETOSHEATH BM IS:  1
DIRECTION OF NORMAL USED FOR PLOTTING DATA IN GSM: ( .432; .899;-.067)

*****

MP LOCATION IS: YEAR=1979; MONTH= 7; DAY=13; TIME= 3.12 UT; INBOUND; R=16.3; LT=1824; LAT= -5.0
MAGNETOSHEATH FILES:  0;  MAGNETOSPHERE FILES:  0
SIGN OF MAGNETOSHEATH BL IS:  2;  SIGN OF MAGNETOSHEATH BM IS:  2
DIRECTION OF NORMAL USED FOR PLOTTING DATA IN GSM: ( .692; .667;-.274)

*****

MP LOCATION IS: YEAR=1979; MONTH= 7; DAY=15; TIME=21.32 UT; OUTBOUND; R=12.8; LT=1536; LAT= 21.3
MAGNETOSHEATH FILES:  1;  MAGNETOSPHERE FILES:  3
SIGN OF MAGNETOSHEATH BL IS:  1( 1);  SIGN OF MAGNETOSHEATH BM IS:  2( 2)
DIRECTION OF NORMAL USED FOR PLOTTING DATA IN GSM: ( .813; .283; .509)

*****

MP LOCATION IS: YEAR=1979; MONTH= 7; DAY=16; TIME= 5.10 UT; OUTBOUND; R=10.8; LT=1517; LAT= 12.5
MAGNETOSHEATH FILES:  0;  MAGNETOSPHERE FILES:  3
SIGN OF MAGNETOSHEATH BL IS:  2;  SIGN OF MAGNETOSHEATH BM IS:  1
DIRECTION OF NORMAL USED FOR PLOTTING DATA IN GSM: ( .828; .342; .411)

*****

MP LOCATION IS: YEAR=1979; MONTH= 7; DAY=19; TIME=21.47 UT; INBOUND; R=16.3; LT=1807; LAT=   .7
MAGNETOSHEATH FILES:  0;  MAGNETOSPHERE FILES:  1
SIGN OF MAGNETOSHEATH BL IS:  1;  SIGN OF MAGNETOSHEATH BM IS:  2
DIRECTION OF NORMAL USED FOR PLOTTING DATA IN GSM: ( .475; .873;-.110)

*****

MP LOCATION IS: YEAR=1979; MONTH= 7; DAY=22; TIME= 4.58 UT; INBOUND; R=17.8; LT=1746; LAT=-11.4
MAGNETOSHEATH FILES:  1;  MAGNETOSPHERE FILES:  1
SIGN OF MAGNETOSHEATH BL IS:  3( 3);  SIGN OF MAGNETOSHEATH BM IS:  2( 2)
DIRECTION OF NORMAL USED FOR PLOTTING DATA IN GSM: ( .624; .704;-.340)

*****

MP LOCATION IS: YEAR=1979; MONTH= 7; DAY=23; TIME= 2.05 UT; OUTBOUND; R=13.3; LT=1519; LAT= 15.3
MAGNETOSHEATH FILES:  0;  MAGNETOSPHERE FILES:  0
SIGN OF MAGNETOSHEATH BL IS:  3( 3);  SIGN OF MAGNETOSHEATH BM IS:  1( 1)
DIRECTION OF NORMAL USED FOR PLOTTING DATA IN GSM: ( .761; .611; .218)

*****

MP LOCATION IS: YEAR=1979; MONTH= 7; DAY=24; TIME=15.07 UT; INBOUND; R=16.6; LT=1745; LAT=-15.0
MAGNETOSHEATH FILES:  1;  MAGNETOSPHERE FILES:  1
SIGN OF MAGNETOSHEATH BL IS:  3( 3);  SIGN OF MAGNETOSHEATH BM IS:  2( 2)
DIRECTION OF NORMAL USED FOR PLOTTING DATA IN GSM: ( .601; .761;-.244)

*****

MP LOCATION IS: YEAR=1979; MONTH= 7; DAY=25; TIME=10.24 UT; OUTBOUND; R=12.4; LT=1510; LAT=  1.5
MAGNETOSHEATH FILES:  0;  MAGNETOSPHERE FILES:  0
SIGN OF MAGNETOSHEATH BL IS:  2( 2);  SIGN OF MAGNETOSHEATH BM IS:  1( 1)
DIRECTION OF NORMAL USED FOR PLOTTING DATA IN GSM: ( .817; .568; .105)

*****

MP LOCATION IS: YEAR=1979; MONTH= 7; DAY=27; TIME= 2.26 UT; INBOUND; R=15.8; LT=1741; LAT= -7.9
MAGNETOSHEATH FILES:  2;  MAGNETOSPHERE FILES:  0
SIGN OF MAGNETOSHEATH BL IS:  1;  SIGN OF MAGNETOSHEATH BM IS:  2
DIRECTION OF NORMAL USED FOR PLOTTING DATA IN GSM: ( .554; .767;-.325)

*****
```

```
*****
MP LOCATION IS: YEAR=1979; MONTH= 7; DAY=27; TIME=16.42 UT; OUTBOUND; R= 8.4; LT=1416; LAT= 16.4
MAGNETOSHEATH_FTES:  0;  MAGNETOSPHERE_FTES:  0
SIGN OF MAGNETOSHEATH_BL IS:  2( 3);  SIGN OF MAGNETOSHEATH_BM IS:  1( 1)
DIRECTION OF NORMAL USED FOR PLOTTING DATA IN GSM: ( .997; .062; .043)

*****
MP LOCATION IS: YEAR=1979; MONTH= 7; DAY=30; TIME= 3.11 UT; OUTBOUND; R=10.1; LT=1425; LAT= 16.3
MAGNETOSHEATH_FTES:  2;  MAGNETOSPHERE_FTES:  2
SIGN OF MAGNETOSHEATH_BL IS:  2( 2);  SIGN OF MAGNETOSHEATH_BM IS:  1( 1)
DIRECTION OF NORMAL USED FOR PLOTTING DATA IN GSM: ( .967; .334; .370)

*****
MP LOCATION IS: YEAR=1979; MONTH= 8; DAY= 3; TIME= 7.55 UT; INBOUND; R=14.8; LT=1717; LAT=-25.2
MAGNETOSHEATH_FTES:  3;  MAGNETOSPHERE_FTES:  0
SIGN OF MAGNETOSHEATH_BL IS:  1( 1);  SIGN OF MAGNETOSHEATH_BM IS:  1( 3)
DIRECTION OF NORMAL USED FOR PLOTTING DATA IN GSM: ( .805; .465;-.368)

*****
MP LOCATION IS: YEAR=1979; MONTH= 8; DAY= 3; TIME=22.23 UT; OUTBOUND; R=10.5; LT=1406; LAT= 19.3
MAGNETOSHEATH_FTES:  0;  MAGNETOSPHERE_FTES:  0
SIGN OF MAGNETOSHEATH_BL IS:  2;  SIGN OF MAGNETOSHEATH_BM IS:  1
DIRECTION OF NORMAL USED FOR PLOTTING DATA IN GSM: ( .599; .241; .763)

*****
MP LOCATION IS: YEAR=1979; MONTH= 8; DAY= 5; TIME=13.35 UT; OUTBOUND; R=11.9; LT=1422; LAT= 17.4
MAGNETOSHEATH_FTES:  1;  MAGNETOSPHERE_FTES:  0
SIGN OF MAGNETOSHEATH_BL IS:  2( 1);  SIGN OF MAGNETOSHEATH_BM IS:  1( 1)
DIRECTION OF NORMAL USED FOR PLOTTING DATA IN GSM: ( .799; .356; .485)

*****
MP LOCATION IS: YEAR=1979; MONTH= 8; DAY= 5; TIME=15.00 UT; INBOUND; R=16.5; LT=1655; LAT=-21.9
MAGNETOSHEATH_FTES:  2;  MAGNETOSPHERE_FTES:  0
SIGN OF MAGNETOSHEATH_BL IS:  2;  SIGN OF MAGNETOSHEATH_BM IS:  1
DIRECTION OF NORMAL USED FOR PLOTTING DATA IN GSM: ( .564; .798;-.214)

*****
MP LOCATION IS: YEAR=1979; MONTH= 8; DAY= 5; TIME=17.20 UT; INBOUND; R=14.5; LT=1712; LAT=-16.6
MAGNETOSHEATH_FTES:  2;  MAGNETOSPHERE_FTES:  2
SIGN OF MAGNETOSHEATH_BL IS:  2( 2);  SIGN OF MAGNETOSHEATH_BM IS:  1( 1)
DIRECTION OF NORMAL USED FOR PLOTTING DATA IN GSM: ( .564; .798;-.214)

*****
MP LOCATION IS: YEAR=1979; MONTH= 8; DAY= 8; TIME=17.25 UT; OUTBOUND; R=11.0; LT=1405; LAT= 13.5
MAGNETOSHEATH_FTES:  0;  MAGNETOSPHERE_FTES:  0
SIGN OF MAGNETOSHEATH_BL IS:  1( 1);  SIGN OF MAGNETOSHEATH_BM IS:  1( 1)
DIRECTION OF NORMAL USED FOR PLOTTING DATA IN GSM: ( .951;-.060; .304)

MP LOCATION IS: YEAR=1979; MONTH= 8; DAY= 9; TIME=  .49 UT; INBOUND; R=16.2; LT=1652; LAT= -7.9
MAGNETOSHEATH_FTES:  3;  MAGNETOSPHERE_FTES:  3
SIGN OF MAGNETOSHEATH_BL IS:  1( 1);  SIGN OF MAGNETOSHEATH_BM IS:  1( 1)
DIRECTION OF NORMAL USED FOR PLOTTING DATA IN GSM: ( .812; .576;-.098)

*****
MP LOCATION IS: YEAR=1979; MONTH= 8; DAY=10; TIME=13.00 UT; INBOUND; R=13.8; LT=1651; LAT=-30.4
MAGNETOSHEATH_FTES:  0;  MAGNETOSPHERE_FTES:  2
SIGN OF MAGNETOSHEATH_BL IS:  1;  SIGN OF MAGNETOSHEATH_BM IS:  1
DIRECTION OF NORMAL USED FOR PLOTTING DATA IN GSM: ( .733; .440; .515)

*****
MP LOCATION IS: YEAR=1979; MONTH= 8; DAY=11; TIME= 3.15 UT; OUTBOUND; R=11.6; LT=1401; LAT= 13.8
MAGNETOSHEATH_FTES:  0;  MAGNETOSPHERE_FTES:  1
SIGN OF MAGNETOSHEATH_BL IS:  2( 2);  SIGN OF MAGNETOSHEATH_BM IS:  2( 2)
DIRECTION OF NORMAL USED FOR PLOTTING DATA IN GSM: ( .867; .368; .335)

*****
MP LOCATION IS: YEAR=1979; MONTH= 8; DAY=13; TIME=  .23 UT; INBOUND; R=11.7; LT=1708; LAT=-13.7
MAGNETOSHEATH_FTES:  0;  MAGNETOSPHERE_FTES:  0
SIGN OF MAGNETOSHEATH_BL IS:  2( 2);  SIGN OF MAGNETOSHEATH_BM IS:  2( 2)
DIRECTION OF NORMAL USED FOR PLOTTING DATA IN GSM: ( .668; .720;-.189)

*****
MP LOCATION IS: YEAR=1979; MONTH= 8; DAY=15; TIME= 7.13 UT; INBOUND; R=14.3; LT=1628; LAT=-27.2
MAGNETOSHEATH_FTES:  0;  MAGNETOSPHERE_FTES:  1
SIGN OF MAGNETOSHEATH_BL IS:  2( 2);  SIGN OF MAGNETOSHEATH_BM IS:  2( 2)
DIRECTION OF NORMAL USED FOR PLOTTING DATA IN GSM: ( .741; .537;-.402)

*****
MP LOCATION IS: YEAR=1979; MONTH= 8; DAY=15; TIME=23.08 UT; OUTBOUND; R=12.8; LT=1348; LAT= 15.7
MAGNETOSHEATH_FTES:  1;  MAGNETOSPHERE_FTES:  3
SIGN OF MAGNETOSHEATH_BL IS:  1( 1);  SIGN OF MAGNETOSHEATH_BM IS:  2( 2)
DIRECTION OF NORMAL USED FOR PLOTTING DATA IN GSM: ( .962; .368; .227)

*****
MP LOCATION IS: YEAR=1979; MONTH= 8; DAY=17; TIME=18.14 UT; INBOUND; R=12.6; LT=1639; LAT=-18.7
MAGNETOSHEATH_FTES:  2;  MAGNETOSPHERE_FTES:  3
SIGN OF MAGNETOSHEATH_BL IS:  2( 1);  SIGN OF MAGNETOSHEATH_BM IS:  2( 2)
DIRECTION OF NORMAL USED FOR PLOTTING DATA IN GSM: ( .630; .723;-.266)

*****
MP LOCATION IS: YEAR=1979; MONTH= 8; DAY=18; TIME= 7.39 UT; OUTBOUND; R=11.9; LT=1349; LAT=  8.5
MAGNETOSHEATH_FTES:  0;  MAGNETOSPHERE_FTES:  1
SIGN OF MAGNETOSHEATH_BL IS:  2;  SIGN OF MAGNETOSHEATH_BM IS:  2
DIRECTION OF NORMAL USED FOR PLOTTING DATA IN GSM: ( .846; .497; .191)

*****
MP LOCATION IS: YEAR=1979; MONTH= 8; DAY=20; TIME= 3.13 UT; INBOUND; R=13.0; LT=1625; LAT=-19.0
MAGNETOSHEATH_FTES:  0;  MAGNETOSPHERE_FTES:  0
SIGN OF MAGNETOSHEATH_BL IS:  2( 2);  SIGN OF MAGNETOSHEATH_BM IS:  2( 2)
DIRECTION OF NORMAL USED FOR PLOTTING DATA IN GSM: ( .738; .569;-.402)

*****
MP LOCATION IS: YEAR=1979; MONTH= 8; DAY=20; TIME=14.02 UT; OUTBOUND; R= 7.9; LT=1305; LAT= 18.8
MAGNETOSHEATH_FTES:  0;  MAGNETOSPHERE_FTES:  0
SIGN OF MAGNETOSHEATH_BL IS:  2( 2);  SIGN OF MAGNETOSHEATH_BM IS:  1( 1)
DIRECTION OF NORMAL USED FOR PLOTTING DATA IN GSM: ( .918; .195; .346)

*****
MP LOCATION IS: YEAR=1979; MONTH= 8; DAY=22; TIME=13.58 UT; INBOUND; R=11.3; LT=1619; LAT=-32.8
MAGNETOSHEATH_FTES:  0;  MAGNETOSPHERE_FTES:  0
SIGN OF MAGNETOSHEATH_BL IS:  1;  SIGN OF MAGNETOSHEATH_BM IS:  3
DIRECTION OF NORMAL USED FOR PLOTTING DATA IN GSM: ( .686; .592;-.424)

*****
MP LOCATION IS: YEAR=1979; MONTH= 8; DAY=23; TIME= 2.20 UT; OUTBOUND; R=11.9; LT=1321; LAT= 15.3
MAGNETOSHEATH_FTES:  0;  MAGNETOSPHERE_FTES:  0
SIGN OF MAGNETOSHEATH_BL IS:  2( 2);  SIGN OF MAGNETOSHEATH_BM IS:  2( 2)
DIRECTION OF NORMAL USED FOR PLOTTING DATA IN GSM: ( .919; .301; .254)

*****
MP LOCATION IS: YEAR=1979; MONTH= 8; DAY=23; TIME= 3.41 UT; OUTBOUND; R=13.3; LT=1335; LAT= 11.8
MAGNETOSHEATH_FTES:  1;  MAGNETOSPHERE_FTES:  0
SIGN OF MAGNETOSHEATH_BL IS:  2( 2);  SIGN OF MAGNETOSHEATH_BM IS:  1( 1)
DIRECTION OF NORMAL USED FOR PLOTTING DATA IN GSM: ( .919; .301; .254)

*****
MP LOCATION IS: YEAR=1979; MONTH= 8; DAY=24; TIME=23.11 UT; INBOUND; R=11.6; LT=1620; LAT=-15.0
MAGNETOSHEATH_FTES:  1;  MAGNETOSPHERE_FTES:  0
SIGN OF MAGNETOSHEATH_BL IS:  2;  SIGN OF MAGNETOSHEATH_BM IS:  2
DIRECTION OF NORMAL USED FOR PLOTTING DATA IN GSM: ( .749; .619;-.234)

*****
MP LOCATION IS: YEAR=1979; MONTH= 8; DAY=27; TIME= 8.24 UT; INBOUND; R=11.9; LT=1549; LAT=-33.2
MAGNETOSHEATH_FTES:  2;  MAGNETOSPHERE_FTES:  3
SIGN OF MAGNETOSHEATH_BL IS:  2( 1);  SIGN OF MAGNETOSHEATH_BM IS:  1( 1)
DIRECTION OF NORMAL USED FOR PLOTTING DATA IN GSM: ( .850; .507;-.146)

*****
MP LOCATION IS: YEAR=1979; MONTH= 8; DAY=27; TIME=20.03 UT; OUTBOUND; R=10.5; LT=1259; LAT= 18.9
MAGNETOSHEATH_FTES:  1;  MAGNETOSPHERE_FTES:  1
SIGN OF MAGNETOSHEATH_BL IS:  2( 3);  SIGN OF MAGNETOSHEATH_BM IS:  1( 1)
DIRECTION OF NORMAL USED FOR PLOTTING DATA IN GSM: ( .798; .121; .590)

*****
MP LOCATION IS: YEAR=1979; MONTH= 8; DAY=29; TIME=14.18 UT; INBOUND; R=10.3; LT=1612; LAT=-21.4
MAGNETOSHEATH_FTES:  2;  MAGNETOSPHERE_FTES:  0
SIGN OF MAGNETOSHEATH_BL IS:  1( 1);  SIGN OF MAGNETOSHEATH_BM IS:  2( 2)
DIRECTION OF NORMAL USED FOR PLOTTING DATA IN GSM: ( .776; .360;-.517)
```

```
*****
MP LOCATION IS: YEAR=1979; MONTH= 8; DAY=30; TIME= 4.59 UT; OUTBOUND; R=10.0; LT=1250; LAT= 18.3
MAGNETOSHEATH_FTES:  1;  MAGNETOSPHERE_FTES:  1
SIGN OF MAGNETOSHEATH_BL IS:  1( 1);  SIGN OF MAGNETOSHEATH_BM IS:  2( 2)
DIRECTION OF NORMAL USED FOR PLOTTING DATA IN GSM: ( .961; .152; .231)
*****
MP LOCATION IS: YEAR=1979; MONTH= 9; DAY= 1; TIME=15.03 UT; OUTBOUND; R=10.9; LT=1254; LAT= 16.2
MAGNETOSHEATH_FTES:  1;  MAGNETOSPHERE_FTES:  1
SIGN OF MAGNETOSHEATH_BL IS:  2( 2);  SIGN OF MAGNETOSHEATH_BM IS:  1( 1)
DIRECTION OF NORMAL USED FOR PLOTTING DATA IN GSM: ( .930;-.001; .369)
*****
MP LOCATION IS: YEAR=1979; MONTH= 9; DAY= 3; TIME=12.31 UT; INBOUND; R=11.9; LT=1515; LAT=-32.5
MAGNETOSHEATH_FTES:  2;  MAGNETOSPHERE_FTES:  0
SIGN OF MAGNETOSHEATH_BL IS:  1( 1);  SIGN OF MAGNETOSHEATH_BM IS:  1( 1)
DIRECTION OF NORMAL USED FOR PLOTTING DATA IN GSM: ( .766; .383;-.525)
*****
MP LOCATION IS: YEAR=1979; MONTH= 9; DAY= 4; TIME=  .45 UT; OUTBOUND; R=11.4; LT=1232; LAT= 18.9
MAGNETOSHEATH_FTES:  0;  MAGNETOSPHERE_FTES:  0
SIGN OF MAGNETOSHEATH_BL IS:  2( 2);  SIGN OF MAGNETOSHEATH_BM IS:  1( 1)
DIRECTION OF NORMAL USED FOR PLOTTING DATA IN GSM: ( .900;-.249; .359)
*****
MP LOCATION IS: YEAR=1979; MONTH= 9; DAY= 5; TIME=21.29 UT; INBOUND; R=12.4; LT=1525; LAT=-15.0
MAGNETOSHEATH_FTES:  0;  MAGNETOSPHERE_FTES:  2
SIGN OF MAGNETOSHEATH_BL IS:  2( 2);  SIGN OF MAGNETOSHEATH_BM IS:  1( 1)
DIRECTION OF NORMAL USED FOR PLOTTING DATA IN GSM: ( .772; .599;-.212)
*****
MP LOCATION IS: YEAR=1979; MONTH= 9; DAY= 6; TIME=10.05 UT; OUTBOUND; R=11.3; LT=1253; LAT= 16.1
MAGNETOSHEATH_FTES:  1;  MAGNETOSPHERE_FTES:  0
SIGN OF MAGNETOSHEATH_BL IS:  1;  SIGN OF MAGNETOSHEATH_BM IS:  2
DIRECTION OF NORMAL USED FOR PLOTTING DATA IN GSM: ( .945; .038; .325)
*****
MP LOCATION IS: YEAR=1979; MONTH= 9; DAY= 8; TIME= 8.24 UT; INBOUND; R=10.6; LT=1504; LAT=-33.5
MAGNETOSHEATH_FTES:  2;  MAGNETOSPHERE_FTES:  2
SIGN OF MAGNETOSHEATH_BL IS:  1( 1);  SIGN OF MAGNETOSHEATH_BM IS:  1( 1)
DIRECTION OF NORMAL USED FOR PLOTTING DATA IN GSM: ( .640; .264;-.722)
*****
MP LOCATION IS: YEAR=1979; MONTH= 9; DAY= 8; TIME=18.31 UT; OUTBOUND; R=10.1; LT=1210; LAT= 21.8
MAGNETOSHEATH_FTES:  1;  MAGNETOSPHERE_FTES:  1
SIGN OF MAGNETOSHEATH_BL IS:  1( 1);  SIGN OF MAGNETOSHEATH_BM IS:  1( 1)
DIRECTION OF NORMAL USED FOR PLOTTING DATA IN GSM: ( .827;-.058; .559)
*****
MP LOCATION IS: YEAR=1979; MONTH= 9; DAY=10; TIME=18.02 UT; INBOUND; R=10.2; LT=1518; LAT=-23.6
MAGNETOSHEATH_FTES:  2;  MAGNETOSPHERE_FTES:  2
SIGN OF MAGNETOSHEATH_BL IS:  1( 1);  SIGN OF MAGNETOSHEATH_BM IS:  1( 1)
DIRECTION OF NORMAL USED FOR PLOTTING DATA IN GSM: ( .844; .387;-.371)
*****
MP LOCATION IS: YEAR=1979; MONTH= 9; DAY=11; TIME= 4.11 UT; OUTBOUND; R=10.6; LT=1213; LAT= 21.4
MAGNETOSHEATH_FTES:  1;  MAGNETOSPHERE_FTES:  1
SIGN OF MAGNETOSHEATH_BL IS:  1( 1);  SIGN OF MAGNETOSHEATH_BM IS:  1( 1)
DIRECTION OF NORMAL USED FOR PLOTTING DATA IN GSM: ( .902; .126; .412)
*****
MP LOCATION IS: YEAR=1979; MONTH= 9; DAY=13; TIME= 3.05 UT; INBOUND; R=10.8; LT=1503; LAT=-21.9
MAGNETOSHEATH_FTES:  2;  MAGNETOSPHERE_FTES:  0
SIGN OF MAGNETOSHEATH_BL IS:  1( 2);  SIGN OF MAGNETOSHEATH_BM IS:  1( 1)
DIRECTION OF NORMAL USED FOR PLOTTING DATA IN GSM: ( .750; .452;-.483)
*****
MP LOCATION IS: YEAR=1979; MONTH= 9; DAY=13; TIME=13.11 UT; OUTBOUND; R=10.2; LT=1217; LAT= 22.5
MAGNETOSHEATH_FTES:  0;  MAGNETOSPHERE_FTES:  0
SIGN OF MAGNETOSHEATH_BL IS:  1( 1);  SIGN OF MAGNETOSHEATH_BM IS:  1( 1)
DIRECTION OF NORMAL USED FOR PLOTTING DATA IN GSM: ( .995; .034; .104)
*****
MP LOCATION IS: YEAR=1979; MONTH= 9; DAY=15; TIME=22.03 UT; OUTBOUND; R= 9.2; LT=1124; LAT= 24.7
MAGNETOSHEATH_FTES:  0;  MAGNETOSPHERE_FTES:  0
SIGN OF MAGNETOSHEATH_BL IS:  3( 3);  SIGN OF MAGNETOSHEATH_BM IS:  2( 2)
DIRECTION OF NORMAL USED FOR PLOTTING DATA IN GSM: ( .851; .081; .519)
*****
MP LOCATION IS: YEAR=1979; MONTH= 9; DAY=17; TIME=23.42 UT; INBOUND; R= 7.8; LT=1523; LAT=-22.9
MAGNETOSHEATH_FTES:  2;  MAGNETOSPHERE_FTES:  2
SIGN OF MAGNETOSHEATH_BL IS:  1( 1);  SIGN OF MAGNETOSHEATH_BM IS:  2( 2)
DIRECTION OF NORMAL USED FOR PLOTTING DATA IN GSM: ( .771; .321;-.365)
*****
MP LOCATION IS: YEAR=1979; MONTH= 9; DAY=18; TIME= 5.50 UT; OUTBOUND; R= 7.0; LT=1119; LAT= 33.6
MAGNETOSHEATH_FTES:  1;  MAGNETOSPHERE_FTES:  1
SIGN OF MAGNETOSHEATH_BL IS:  1( 1);  SIGN OF MAGNETOSHEATH_BM IS:  1( 3)
DIRECTION OF NORMAL USED FOR PLOTTING DATA IN GSM: ( .724;-.249; .643)
*****
MP LOCATION IS: YEAR=1979; MONTH= 9; DAY=20; TIME= 7.22 UT; INBOUND; R=10.5; LT=1417; LAT=-28.3
MAGNETOSHEATH_FTES:  0;  MAGNETOSPHERE_FTES:  1
SIGN OF MAGNETOSHEATH_BL IS:  2( 2);  SIGN OF MAGNETOSHEATH_BM IS:  2( 2)
DIRECTION OF NORMAL USED FOR PLOTTING DATA IN GSM: ( .765; .272;-.548)
*****
MP LOCATION IS: YEAR=1979; MONTH= 9; DAY=22; TIME=16.35 UT; INBOUND; R=10.8; LT=1417; LAT=-22.8
MAGNETOSHEATH_FTES:  0;  MAGNETOSPHERE_FTES:  0
SIGN OF MAGNETOSHEATH_BL IS:  2( 2);  SIGN OF MAGNETOSHEATH_BM IS:  3( 3)
DIRECTION OF NORMAL USED FOR PLOTTING DATA IN GSM: ( .926; .133;-.353)

*****
MP LOCATION IS: YEAR=1979; MONTH= 9; DAY=23; TIME= 2.59 UT; OUTBOUND; R=10.3; LT=1124; LAT= 25.2
MAGNETOSHEATH_FTES:  1;  MAGNETOSPHERE_FTES:  1
SIGN OF MAGNETOSHEATH_BL IS:  1( 3);  SIGN OF MAGNETOSHEATH_BM IS:  1( 1)
DIRECTION OF NORMAL USED FOR PLOTTING DATA IN GSM: ( .899;-.141; .402)
*****
MP LOCATION IS: YEAR=1979; MONTH= 9; DAY=25; TIME= 2.03 UT; INBOUND; R=10.5; LT=1420; LAT=-20.0
MAGNETOSHEATH_FTES:  2;  MAGNETOSPHERE_FTES:  2
SIGN OF MAGNETOSHEATH_BL IS:  1( 1);  SIGN OF MAGNETOSHEATH_BM IS:  1( 1)
DIRECTION OF NORMAL USED FOR PLOTTING DATA IN GSM: ( .893; .101;-.439)
*****
MP LOCATION IS: YEAR=1979; MONTH= 9; DAY=25; TIME=12.57 UT; OUTBOUND; R=11.1; LT=1147; LAT= 26.2
MAGNETOSHEATH_FTES:  0;  MAGNETOSPHERE_FTES:  0
SIGN OF MAGNETOSHEATH_BL IS:  2( 2);  SIGN OF MAGNETOSHEATH_BM IS:  1( 1)
DIRECTION OF NORMAL USED FOR PLOTTING DATA IN GSM: ( .912;-.051; .408)
*****
MP LOCATION IS: YEAR=1979; MONTH= 9; DAY=29; TIME=19.30 UT; INBOUND; R=12.2; LT=1349; LAT=-14.3
MAGNETOSHEATH_FTES:  0;  MAGNETOSPHERE_FTES:  0
SIGN OF MAGNETOSHEATH_BL IS:  1;  SIGN OF MAGNETOSHEATH_BM IS:  1
DIRECTION OF NORMAL USED FOR PLOTTING DATA IN GSM: ( .953; .231;-.197)
*****
MP LOCATION IS: YEAR=1979; MONTH= 9; DAY=29; TIME=18.24 UT; INBOUND; R=13.4; LT=1338; LAT=-13.5
MAGNETOSHEATH_FTES:  0;  MAGNETOSPHERE_FTES:  2
SIGN OF MAGNETOSHEATH_BL IS:  1( 3);  SIGN OF MAGNETOSHEATH_BM IS:  1( 1)
DIRECTION OF NORMAL USED FOR PLOTTING DATA IN GSM: ( .953; .231;-.197)
*****
MP LOCATION IS: YEAR=1979; MONTH= 9; DAY=30; TIME= 8.00 UT; OUTBOUND; R=11.3; LT=1131; LAT= 28.1
MAGNETOSHEATH_FTES:  1;  MAGNETOSPHERE_FTES:  1
SIGN OF MAGNETOSHEATH_BL IS:  1( 3);  SIGN OF MAGNETOSHEATH_BM IS:  2( 2)
DIRECTION OF NORMAL USED FOR PLOTTING DATA IN GSM: ( .919;-.091; .383)
*****
MP LOCATION IS: YEAR=1979; MONTH=10; DAY= 5; TIME= 4.15 UT; OUTBOUND; R=13.2; LT=1105; LAT= 24.8
MAGNETOSHEATH_FTES:  0;  MAGNETOSPHERE_FTES:  0
SIGN OF MAGNETOSHEATH_BL IS:  2( 2);  SIGN OF MAGNETOSHEATH_BM IS:  2( 2)
DIRECTION OF NORMAL USED FOR PLOTTING DATA IN GSM: ( .919;-.194; .343)
*****
```

```
...
     MP LOCATION IS: YEAR=1979; MONTH=10; DAY= 7; TIME= 2.22 UT; INBOUND; R= 8.7; LT=1349; LAT=-20.5
     MAGNETOSHEATH FILE:  2;  MAGNETOSPHERE FILE:  0
     SIGN OF MAGNETOSHEATH BL IS:  1( 2);  SIGN OF MAGNETOSHEATH BM IS:  2( 1)
     DIRECTION OF NORMAL USED FOR PLOTTING DATA IN GSM: ( .928; .299;-.223)
*****
     MP LOCATION IS: YEAR=1979; MONTH=10; DAY= 7; TIME=11.21 UT; OUTBOUND; R=10.5; LT=1103; LAT= 34.0
     MAGNETOSHEATH FILE:  1;  MAGNETOSPHERE FILE:  1
     SIGN OF MAGNETOSHEATH BL IS:  1( 3);  SIGN OF MAGNETOSHEATH BM IS:  1( 1)
     DIRECTION OF NORMAL USED FOR PLOTTING DATA IN GSM: ( .891;-.153; .427)
*****
     MP LOCATION IS: YEAR=1979; MONTH=10; DAY= 9; TIME=10.50 UT; INBOUND; R= 9.8; LT=1304; LAT=-23.1
     MAGNETOSHEATH FILE:  2;  MAGNETOSPHERE FILE:  2
     SIGN OF MAGNETOSHEATH BL IS:  2( 2);  SIGN OF MAGNETOSHEATH BM IS:  1
     DIRECTION OF NORMAL USED FOR PLOTTING DATA IN GSM: ( .540; .020;-.764)
*****
     MP LOCATION IS: YEAR=1979; MONTH=10; DAY=11; TIME=16.45 UT; INBOUND; R=13.9; LT=1247; LAT=-10.4
     MAGNETOSHEATH FILE:  0;  MAGNETOSPHERE FILE:  0
     SIGN OF MAGNETOSHEATH BL IS:  2( 2);  SIGN OF MAGNETOSHEATH BM IS:  1( 1)
     DIRECTION OF NORMAL USED FOR PLOTTING DATA IN GSM: ( .272; .935;-.224)
*****
     MP LOCATION IS: YEAR=1979; MONTH=10; DAY=12; TIME= 6.45 UT; OUTBOUND; R=11.8; LT=1043; LAT= 31.9
     MAGNETOSHEATH FILE:  1;  MAGNETOSPHERE FILE:  1
     SIGN OF MAGNETOSHEATH BL IS:  1;  SIGN OF MAGNETOSHEATH BM IS:  1
     DIRECTION OF NORMAL USED FOR PLOTTING DATA IN GSM: ( .799;-.330; .503)
*****
     MP LOCATION IS: YEAR=1979; MONTH=10; DAY=12; TIME= 7.07 UT; OUTBOUND; R=12.0; LT=1048; LAT= 32.0
     MAGNETOSHEATH FILE:  0;  MAGNETOSPHERE FILE:  0
     SIGN OF MAGNETOSHEATH BL IS:  2( 2);  SIGN OF MAGNETOSHEATH BM IS:  1( 1)
     DIRECTION OF NORMAL USED FOR PLOTTING DATA IN GSM: ( .799;-.330; .503)
*****
     MP LOCATION IS: YEAR=1979; MONTH=10; DAY=14; TIME=14.30 UT; OUTBOUND; R= 9.3; LT=1006; LAT= 38.0
     MAGNETOSHEATH FILE:  1;  MAGNETOSPHERE FILE:  1
     SIGN OF MAGNETOSHEATH BL IS:  1( 1);  SIGN OF MAGNETOSHEATH BM IS:  2( 2)
     DIRECTION OF NORMAL USED FOR PLOTTING DATA IN GSM: ( .685;-.131; .716)
*****
     MP LOCATION IS: YEAR=1979; MONTH=10; DAY=16; TIME=13.25 UT; INBOUND; R=11.7; LT=1234; LAT=-14.0
     MAGNETOSHEATH FILE:  0;  MAGNETOSPHERE FILE:  0
     SIGN OF MAGNETOSHEATH BL IS:  2;  SIGN OF MAGNETOSHEATH BM IS:  2
     DIRECTION OF NORMAL USED FOR PLOTTING DATA IN GSM: ( .940; .134;-.257)
*****
     MP LOCATION IS: YEAR=1979; MONTH=10; DAY=17; TIME= 2.26 UT; OUTBOUND; R=13.1; LT=1007; LAT= 25.4
     MAGNETOSHEATH FILE:  0;  MAGNETOSPHERE FILE:  0
     SIGN OF MAGNETOSHEATH BL IS:  2;  SIGN OF MAGNETOSHEATH BM IS:  2
     DIRECTION OF NORMAL USED FOR PLOTTING DATA IN GSM: ( .902;-.076; .424)
*****
     MP LOCATION IS: YEAR=1979; MONTH=10; DAY=18; TIME=22.12 UT; INBOUND; R=12.5; LT=1235; LAT= -8.8
     MAGNETOSHEATH FILE:  4;  MAGNETOSPHERE FILE:  2
     SIGN OF MAGNETOSHEATH BL IS:  2( 1);  SIGN OF MAGNETOSHEATH BM IS:  2( 2)
     DIRECTION OF NORMAL USED FOR PLOTTING DATA IN GSM: ( .877; .304;-.371)
*****
     MP LOCATION IS: YEAR=1979; MONTH=10; DAY=18; TIME=19.50 UT; INBOUND; R=14.2; LT=1222; LAT= -6.6
     MAGNETOSHEATH FILE:  0;  MAGNETOSPHERE FILE:  0
     SIGN OF MAGNETOSHEATH BL IS:  2;  SIGN OF MAGNETOSHEATH BM IS:  2
     DIRECTION OF NORMAL USED FOR PLOTTING DATA IN GSM: ( .877; .304;-.371)
*****
     MP LOCATION IS: YEAR=1979; MONTH=10; DAY=18; TIME=19.00 UT; INBOUND; R=14.9; LT=1217; LAT= -5.7
     MAGNETOSHEATH FILE:  0;  MAGNETOSPHERE FILE:  0
     SIGN OF MAGNETOSHEATH BL IS:  2( 2);  SIGN OF MAGNETOSHEATH BM IS:  2( 2)
     DIRECTION OF NORMAL USED FOR PLOTTING DATA IN GSM: ( .877; .304;-.371)
*****
     MP LOCATION IS: YEAR=1979; MONTH=10; DAY=19; TIME=13.00 UT; OUTBOUND; R=13.6; LT=1030; LAT= 32.0
     MAGNETOSHEATH FILE:  0;  MAGNETOSPHERE FILE:  0
     SIGN OF MAGNETOSHEATH BL IS:  2( 2);  SIGN OF MAGNETOSHEATH BM IS:  2( 3)
     DIRECTION OF NORMAL USED FOR PLOTTING DATA IN GSM: ( .938;-.081; .340)
*****
     MP LOCATION IS: YEAR=1979; MONTH=10; DAY=21; TIME= 7.52 UT; INBOUND; R=11.7; LT=1218; LAT=-11.8
     MAGNETOSHEATH FILE:  2;  MAGNETOSPHERE FILE:  2
     SIGN OF MAGNETOSHEATH BL IS:  1;  SIGN OF MAGNETOSHEATH BM IS:  1
     DIRECTION OF NORMAL USED FOR PLOTTING DATA IN GSM: ( .974; .041;-.214)
*****
     MP LOCATION IS: YEAR=1979; MONTH=10; DAY=21; TIME=19.24 UT; OUTBOUND; R=11.0; LT= 924; LAT= 28.2
     MAGNETOSHEATH FILE:  1;  MAGNETOSPHERE FILE:  1
     SIGN OF MAGNETOSHEATH BL IS:  1( 1);  SIGN OF MAGNETOSHEATH BM IS:  3( 3)
     DIRECTION OF NORMAL USED FOR PLOTTING DATA IN GSM: ( .870;-.126; .477)
*****
     MP LOCATION IS: YEAR=1979; MONTH=10; DAY=23; TIME=16.40 UT; INBOUND; R=12.2; LT=1214; LAT= -9.5
     MAGNETOSHEATH FILE:  2;  MAGNETOSPHERE FILE:  2
     SIGN OF MAGNETOSHEATH BL IS:  1( 1);  SIGN OF MAGNETOSHEATH BM IS:  1( 1)
     DIRECTION OF NORMAL USED FOR PLOTTING DATA IN GSM: ( .975;-.039; .221)
*****
     MP LOCATION IS: YEAR=1979; MONTH=10; DAY=24; TIME= 4.33 UT; OUTBOUND; R=11.1; LT= 932; LAT= 34.4
     MAGNETOSHEATH FILE:  1;  MAGNETOSPHERE FILE:  1
     SIGN OF MAGNETOSHEATH BL IS:  1;  SIGN OF MAGNETOSHEATH BM IS:  1
     DIRECTION OF NORMAL USED FOR PLOTTING DATA IN GSM: ( .743;-.362; .563)
*****
     MP LOCATION IS: YEAR=1979; MONTH=10; DAY=24; TIME= 6.30 UT; OUTBOUND; R=12.2; LT= 953; LAT= 35.1
     MAGNETOSHEATH FILE:  1;  MAGNETOSPHERE FILE:  1
     SIGN OF MAGNETOSHEATH BL IS:  1( 1);  SIGN OF MAGNETOSHEATH BM IS:  1( 1)
     DIRECTION OF NORMAL USED FOR PLOTTING DATA IN GSM: ( .743;-.362; .563)
*****
     MP LOCATION IS: YEAR=1979; MONTH=10; DAY=26; TIME=16.06 UT; OUTBOUND; R=12.4; LT= 930; LAT= 32.0
     MAGNETOSHEATH FILE:  1;  MAGNETOSPHERE FILE:  1
     SIGN OF MAGNETOSHEATH BL IS:  1( 3);  SIGN OF MAGNETOSHEATH BM IS:  1( 1)
     DIRECTION OF NORMAL USED FOR PLOTTING DATA IN GSM: ( .771;-.326; .548)
*****
     MP LOCATION IS: YEAR=1979; MONTH=10; DAY=28; TIME=13.02 UT; INBOUND; R=10.3; LT=1202; LAT=-12.2
     MAGNETOSHEATH FILE:  2;  MAGNETOSPHERE FILE:  2
     SIGN OF MAGNETOSHEATH BL IS:  2( 1);  SIGN OF MAGNETOSHEATH BM IS:  1( 1)
     DIRECTION OF NORMAL USED FOR PLOTTING DATA IN GSM: ( .809;-.181;-.559)
*****
     MP LOCATION IS: YEAR=1979; MONTH=10; DAY=28; TIME=23.18 UT; OUTBOUND; R=10.6; LT= 942; LAT= 26.3
     MAGNETOSHEATH FILE:  1;  MAGNETOSPHERE FILE:  1
     SIGN OF MAGNETOSHEATH BL IS:  1;  SIGN OF MAGNETOSHEATH BM IS:  1
     DIRECTION OF NORMAL USED FOR PLOTTING DATA IN GSM: ( .744;-.539; .393)
*****
     MP LOCATION IS: YEAR=1979; MONTH=10; DAY=29; TIME= 1.35 UT; OUTBOUND; R=13.1; LT= 910; LAT= 25.2
     MAGNETOSHEATH FILE:  0;  MAGNETOSPHERE FILE:  1
     SIGN OF MAGNETOSHEATH BL IS:  2( 1);  SIGN OF MAGNETOSHEATH BM IS:  1( 1)
     DIRECTION OF NORMAL USED FOR PLOTTING DATA IN GSM: ( .744;-.539; .393)
*****
     MP LOCATION IS: YEAR=1979; MONTH=10; DAY=31; TIME= 9.57 UT; OUTBOUND; R=12.1; LT= 930; LAT= 40.2
     MAGNETOSHEATH FILE:  1;  MAGNETOSPHERE FILE:  1
     SIGN OF MAGNETOSHEATH BL IS:  1;  SIGN OF MAGNETOSHEATH BM IS:  1
     DIRECTION OF NORMAL USED FOR PLOTTING DATA IN GSM: ( .708;-.241; .664)
*****
     MP LOCATION IS: YEAR=1979; MONTH=11; DAY= 4; TIME=17.13 UT; INBOUND; R=10.9; LT=1140; LAT= -8.8
     MAGNETOSHEATH FILE:  2;  MAGNETOSPHERE FILE:  2
     SIGN OF MAGNETOSHEATH BL IS:  2( 1);  SIGN OF MAGNETOSHEATH BM IS:  1( 1)
     DIRECTION OF NORMAL USED FOR PLOTTING DATA IN GSM: ( .996;-.092;-.141)
*****
     MP LOCATION IS: YEAR=1979; MONTH=11; DAY= 5; TIME= 6.30 UT; OUTBOUND; R=13.4; LT= 904; LAT= 35.4
     MAGNETOSHEATH FILE:  0;  MAGNETOSPHERE FILE:  0
     SIGN OF MAGNETOSHEATH BL IS:  2( 2);  SIGN OF MAGNETOSHEATH BM IS:  3( 3)
     DIRECTION OF NORMAL USED FOR PLOTTING DATA IN GSM: ( .742;-.468; .479)
*****
```

```
*****
MP LOCATION IS: YEAR=1979; MONTH=11; DAY= 9; TIME=14.05 UT; INBOUND; R= 8.0; LT=1145; LAT=-14.0
MAGNETOSHEATH_FTES:  2;  MAGNETOSPHERE_FTES:  0
SIGN OF MAGNETOSHEATH_BL IS:  1( 1);  SIGN OF MAGNETOSHEATH_BM IS:  1( 1)
DIRECTION OF NORMAL USED FOR PLOTTING DATA IN GSM: ( .804;-.117;-.582)

*****
MP LOCATION IS: YEAR=1979; MONTH=11; DAY=10; TIME=  .50 UT; OUTBOUND; R=13.0; LT= 913; LAT= 22.9
MAGNETOSHEATH_FTES:  0;  MAGNETOSPHERE_FTES:  0
SIGN OF MAGNETOSHEATH_BL IS:  2( 2);  SIGN OF MAGNETOSHEATH_BM IS:  2( 2)
DIRECTION OF NORMAL USED FOR PLOTTING DATA IN GSM: ( .769;-.547; .281)

*****
MP LOCATION IS: YEAR=1979; MONTH=11; DAY=11; TIME=22.55 UT; INBOUND; R= 8.8; LT=1142; LAT=-12.8
MAGNETOSHEATH_FTES:  0;  MAGNETOSPHERE_FTES:  0
SIGN OF MAGNETOSHEATH_BL IS:  2( 2);  SIGN OF MAGNETOSHEATH_BM IS:  2( 2)
DIRECTION OF NORMAL USED FOR PLOTTING DATA IN GSM: ( .798;-.129;-.589)

*****
MP LOCATION IS: YEAR=1979; MONTH=11; DAY=14; TIME= 6.04 UT; INBOUND; R=11.7; LT=1056; LAT= -3.6
MAGNETOSHEATH_FTES:  2;  MAGNETOSPHERE_FTES:  1
SIGN OF MAGNETOSHEATH_BL IS:  1;  SIGN OF MAGNETOSHEATH_BM IS:  2
DIRECTION OF NORMAL USED FOR PLOTTING DATA IN GSM: ( .962;-.265;-.065)

*****
MP LOCATION IS: YEAR=1979; MONTH=11; DAY=15; TIME= 2.02 UT; OUTBOUND; R=18.1; LT= 835; LAT= 18.1
MAGNETOSHEATH_FTES:  0;  MAGNETOSPHERE_FTES:  0
SIGN OF MAGNETOSHEATH_BL IS:  2( 2);  SIGN OF MAGNETOSHEATH_BM IS:  2( 1)
DIRECTION OF NORMAL USED FOR PLOTTING DATA IN GSM: ( .864;-.494; .270)

*****
MP LOCATION IS: YEAR=1979; MONTH=11; DAY=16; TIME=16.59 UT; INBOUND; R= 9.8; LT=1106; LAT= -9.0
MAGNETOSHEATH_FTES:  2;  MAGNETOSPHERE_FTES:  2
SIGN OF MAGNETOSHEATH_BL IS:  1( 1);  SIGN OF MAGNETOSHEATH_BM IS:  2( 2)
DIRECTION OF NORMAL USED FOR PLOTTING DATA IN GSM: ( .940;-.216;-.264)

*****
MP LOCATION IS: YEAR=1979; MONTH=11; DAY=17; TIME= 5.03 UT; OUTBOUND; R=13.0; LT= 753; LAT= 31.8
MAGNETOSHEATH_FTES:  1;  MAGNETOSPHERE_FTES:  1
SIGN OF MAGNETOSHEATH_BL IS:  1;  SIGN OF MAGNETOSHEATH_BM IS:  1
DIRECTION OF NORMAL USED FOR PLOTTING DATA IN GSM: ( .721;-.543; .429)

*****
MP LOCATION IS: YEAR=1979; MONTH=11; DAY=17; TIME= 5.55 UT; OUTBOUND; R=13.9; LT= 805; LAT= 33.2
MAGNETOSHEATH_FTES:  0;  MAGNETOSPHERE_FTES:  0
SIGN OF MAGNETOSHEATH_BL IS:  2( 2);  SIGN OF MAGNETOSHEATH_BM IS:  1( 1)
DIRECTION OF NORMAL USED FOR PLOTTING DATA IN GSM: ( .721;-.543; .429)

*****
MP LOCATION IS: YEAR=1979; MONTH=11; DAY=18; TIME=23.01 UT; INBOUND; R=13.7; LT=1029; LAT= -5.2
MAGNETOSHEATH_FTES:  0;  MAGNETOSPHERE_FTES:  0
SIGN OF MAGNETOSHEATH_BL IS:  2( 2);  SIGN OF MAGNETOSHEATH_BM IS:  1( 1)
DIRECTION OF NORMAL USED FOR PLOTTING DATA IN GSM: ( .954;-.212;-.212)

*****
MP LOCATION IS: YEAR=1979; MONTH=11; DAY=21; TIME=10.35 UT; INBOUND; R=11.2; LT=1034; LAT= -1.0
MAGNETOSHEATH_FTES:  1;  MAGNETOSPHERE_FTES:  0
SIGN OF MAGNETOSHEATH_BL IS:  1( 1);  SIGN OF MAGNETOSHEATH_BM IS:  3( 3)
DIRECTION OF NORMAL USED FOR PLOTTING DATA IN GSM: ( .937;-.291;-.195)

*****
MP LOCATION IS: YEAR=1979; MONTH=11; DAY=22; TIME=19.57 UT; INBOUND; R=22.2; LT= 848; LAT=  7.7
MAGNETOSHEATH_FTES:  0;  MAGNETOSPHERE_FTES:  0
SIGN OF MAGNETOSHEATH_BL IS:  2( 2);  SIGN OF MAGNETOSHEATH_BM IS:  1( 1)
DIRECTION OF NORMAL USED FOR PLOTTING DATA IN GSM: ( .927;-.344; .142)

*****
MP LOCATION IS: YEAR=1979; MONTH=11; DAY=22; TIME=23.47 UT; INBOUND; R=22.1; LT= 858; LAT=  4.4
MAGNETOSHEATH_FTES:  1;  MAGNETOSPHERE_FTES:  0
SIGN OF MAGNETOSHEATH_BL IS:  2( 2);  SIGN OF MAGNETOSHEATH_BM IS:  1( 1)
DIRECTION OF NORMAL USED FOR PLOTTING DATA IN GSM: ( .879;-.730; .077)

*****
MP LOCATION IS: YEAR=1979; MONTH=11; DAY=23; TIME=  .59 UT; INBOUND; R=22.0; LT= 902; LAT=  5.0
MAGNETOSHEATH_FTES:  0;  MAGNETOSPHERE_FTES:  0
SIGN OF MAGNETOSHEATH_BL IS:  2( 3);  SIGN OF MAGNETOSHEATH_BM IS:  1( 1)
DIRECTION OF NORMAL USED FOR PLOTTING DATA IN GSM: ( .866;-.464;-.186)

*****
```